January 2022

Evaluation Of CO2 Enhanced Oil Recovery In Unconventional Reservoirs

Nidhal Badrouchi

EVALUATION OF CO_2 ENHANCED OIL RECOVERY IN UNCONVENTIONAL RESERVOIRS

by

Nidhal Badrouchi

Bachelor of Science, National School of Engineering of Gabes, Tunisia, 2013

Master of Engineering, University of North Dakota, USA, 2019

A dissertation

Submitted to the Graduate Faculty

of the

University of North Dakota

in partial fulfillment of the requirements

for the degree of

Doctor of Philosophy

Grand Forks, North Dakota

August

2022

This thesis, submitted by Nidhal Badrouchi in partial fulfillment of the requirements for the Degree of Doctor of Philosophy in Petroleum Engineering from the University of North Dakota, has been read by the Faculty Advisory Committee under whom the work has been done and is hereby approved.

_____

Dr. Vamegh Rasouli

_____

Dr. Hui Pu

_____

Dr. Kegang Ling

_____

Dr. Minou Rabiei

_____

Dr. Kouhyar Tavakolian

This thesis is being submitted by the appointed advisory committee as having met all of the requirements of the School of Graduate Studies at the University of North Dakota and is hereby approved.

_____

Chris Nelson

Dean of the School of Graduate Studies

_____

PERMISSION

Title Evaluation of CO_2 Enhanced Oil Recovery in Unconventional Reservoirs

Department Petroleum Engineering

Degree Doctor of Philosophy

In presenting this thesis in partial fulfillment of the requirements for a graduate degree from the University of North Dakota, I agree that the library of this University shall make it freely available for inspection. I further agree that permission for extensive copying for scholarly purposes may be granted by the professor who supervised my thesis work or, in his absence, by the Chairperson of the department or the dean of the School of Graduate Studies. It is understood that any copying or publication or other use of this thesis or part thereof for financial gain shall not be allowed without my written permission. It is also understood that due recognition shall be given to me and to the University of North Dakota in any scholarly use which may be made of any material in my thesis.

Nidhal Badrouchi

Date

ACKNOWLEDGMENTS

I wish to express my sincere appreciation to my advisor, Profs. Vamegh Rasouli and Hui Pu for their guidance and support during my time in the PhD program at the University of North Dakota. I would like to extend my appreciation to the committee members, Dr. Kegang Ling, Dr. Minou Rabiei, and Dr. Kouhyar Tavakolian. I acknowledge the financial support of the North Dakota Industry Commission during the beginning of my research program (NDIC).

DEDICATIONS

I dedicate this work to my family. They were and will always be my source of inspiration and motivation. To my father, mother, sister, and brothers. To my supportive beautiful wife and my son YASSIN.

Abstract

The recent advances in horizontal drilling and hydraulic fracturing have enabled a profitable oil and gas recovery from unconventional geologic plays. The Bakken is one of the largest oil-bearing tight formations in North America, with an estimated original oil in place of 600 billion barrels; however, only a small fraction (7% to 12%) of this oil is recoverable using currently available technologies.

CO_2 injection can be an effective technique to enhance the oil recovery from unconventional reservoirs. It can assist with extracting residual oil and overcoming injectivity problems in tight formations. Previous CO_2 enhanced oil recovery (EOR) pilot tests performed in the Bakken Formation indicated that cyclic CO_2 injection might be a promising technique for enhanced oil recovery; however, no clear consensus has been reached, and the reported results have revealed that CO_2 EOR mechanisms in unconventional reservoirs are still poorly understood. This study addresses the knowledge gap related to CO_2 EOR in unconventional reservoirs, investigates the side effects of CO_2 injection, and compares the EOR performance of different gases to determine the optimum EOR scheme in tight formations.

We investigated and analyzed the effects of different parameters on CO_2 performance using samples from the Middle Bakken member and Three Forks Formation. The factors studied include CO_2 Huff-n-Puff (HnP) injection parameters, sample size, water presence within the fractures, and the volume of CO_2 in contact with the rock matrix during the HnP experiments.

The injected CO_2 can interact with the *in-situ* reservoir fluids and rock minerals, which can impact and alter several reservoir attributes. The potential changes in rock wettability, pore size

distribution, and effective porosity before and after exposure to CO_2 were evaluated. The results indicate that CO_2 can alter wettability and increase the hydrophilicity of the rock. The nuclear magnetic resonance spectroscopy technique was used to determine fluid distribution before and after CO_2 injection. The results confirm that carbonic acid can dissolve portions of the dolomite, calcite, and feldspar in the rock and create new micro- and nanopores.

We compared the EOR performance of CO_2 and hydrocarbon gases to determine the most effective gases. Then we introduced a novel gas EOR scheme to boost oil mobilization and achieve higher recovery factors.

Content

List of Figures

List of Tables

Chapter 1

CO_2 EOR in Unconventional Plays

1.1 Introduction

Oil production from tight reservoirs became possible and economically efficient after the development of hydraulic fracturing and horizontal drilling. The U.S. Energy Information Administration estimated in 2019 that 63% of the total U.S crude oil production is from tight oil resources [1]. The Bakken is one of the largest oil-bearing tight formations in North America, with an estimated original oil in place (OOIP) of 300 to 900 billion barrels [2,3]; however, long-term stable oil production from tight formations in ND is becoming a challenge [4,5]. Horizontal wells drilled in targeted formations have decline rates higher than 80% over the first three years of their production lives. Depletion drive is the current primary oil production mechanism in the Bakken [6–9], which recovers approximately 8% to 12 % of the OOIP [10,11]. There is an immense volume of residual oil in unconventional reservoirs; therefore, any incremental production improvement could dramatically increase recoverable oil, extend the life of unconventional

reservoirs, and contribute to greater energy independence and security. Each 1% increase in the oil recovery factor could result in revenues of $128 to $720 billion with an estimated oil price of $80 per barrel [12]; therefore, it is crucial to evaluate the potential of EOR techniques in the Bakken and understand their application to other tight formations.

Different techniques have been successfully implemented to improve oil recovery in conventional reservoirs. CO_2 flooding, in particular, has demonstrated tremendous success over the past four decades [13]. The poor reservoir quality in the Bakken has limited the number of appropriate enhanced oil recovery techniques. Previous water injection pilot tests revealed that fluid injectivity is the primary concern due to very low matrix permeability [14]. Gas injection pilot tests revealed that injectivity is not a concern in Bakken; however, gas flooding in densely fractured unconventional reservoirs may result in early breakthrough, resulting in poor performance [15]. CO_2 can be injected at different cycles using the HnP technique to mitigate these issues [16,17]. Each CO_2 HnP cycle consists of three phases: 1) injecting CO_2 into the reservoir via the well, or around the core sample in the case of laboratory experiments, 2) pausing injection to close the system, which allows the injected CO_2 to soak for a given period, and 3) opening the system for production (see Fig. **1.1**).

CO_2 EOR techniques have been extensively studied, well understood, and successfully applied over the last four decades to conventional reservoirs; however, the evaluation of their applicability to unconventional reservoirs began in the last decade [17]. The assessment of CO_2 EOR potential in tight formations is still in the preliminary stage compared to conventional reservoirs, and the recovery mechanisms are still poorly understood[18–20]. Todd et al. [14] discussed the results of CO_2 EOR pilot tests in the Bakken, which revealed that the simulation studies in the literature were too optimistic, and the previous core-scale injection tests overestimated CO_2 potential. These pilot-

scale results indicate that CO_2 EOR mechanisms in shale formations are not well understood, demonstrating the need for further evaluation efforts [14,15].

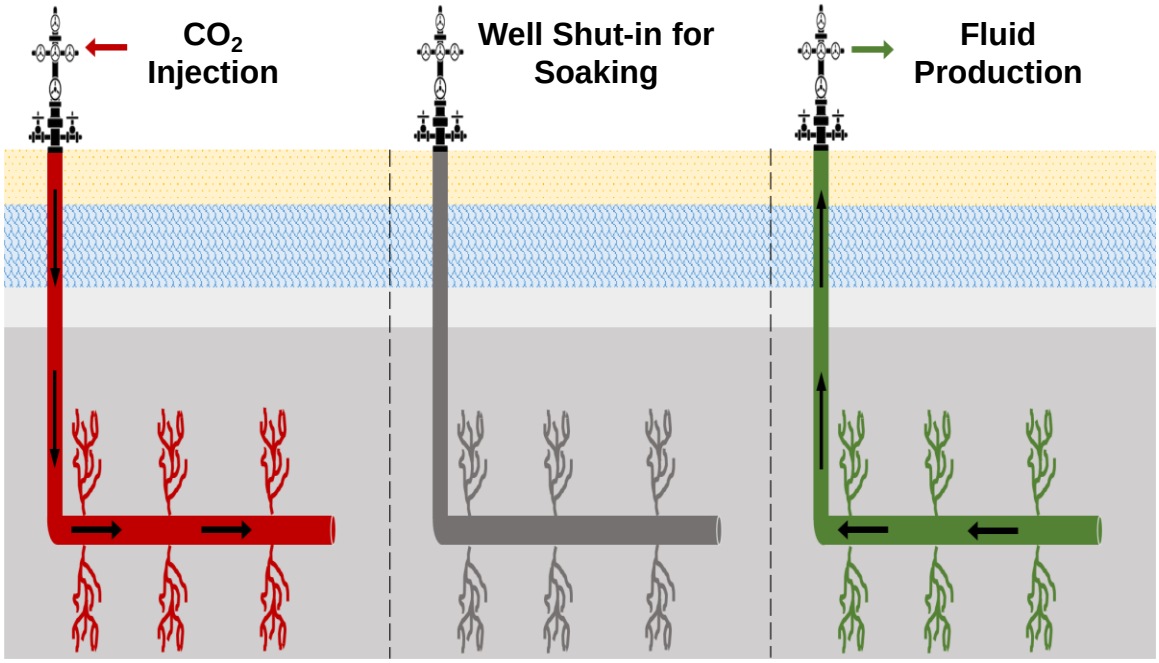

Fig. 1.1. Schematic of CO_2 Huff-n-Puff injection

1.2 Objectives

As mentioned above, the immense volume of residual oil in Bakken is a strong motivation to perform EOR studies. Therefore, the overall goal of this study is to evaluate the performance of CO_2 injection in Bakken oil reservoirs. The detailed objectives of this work can be summarized as followings:

1. Comprehensive review of existing literature on CO_2 injection in tight formations. This includes laboratory experiments, numerical simulations, and field pilot tests.
2. Evaluate the effect of injection pressure, soaking time, and the number of injection cycles using CO_2 HnP under typical reservoir conditions.

3. Perform a parametric study to investigate the effect of multiple parameters on CO_2 EOR performance and oil recovery from ultra-tight core samples. The parameters that will be investigated include the sample size, HnP schedule, water presence, CO_2 volume to exposed rock surface, and a comparison of CO_2 flooding vs HnP.
4. Investigate the possible side effects of CO_2 injection on different reservoir attributes, which might result after the interactions of the injected CO_2 with minerals present in the reservoir rock.
5. Evaluate the EOR performance of CO_2 and different hydrocarbon gases by comparing the Minimum Miscibility Pressure (MMP), capacity to dissolve oil, and molecular weight selectivity. Introduce a novel EOR scheme by combining CO_2 and hydrocarbon gases.

1.3 Methodology

The following approaches will be used to accomplish the objectives of this project.

1. Retrieve representative oil and rock samples from the targeted formations.
2. Characterize the reservoir sections of interest and determine the reservoir properties using representative oil and rock samples. This includes a detailed PVT study of the obtained oil sample and evaluation of porosity, permeability, and mineralogical composition of the rock samples.
3. Prepare the experimental setup to perform CO_2 HnP tests and conduct several CO_2 injection experiments.
4. Use the X-Ray Diffraction technique to determine the mineralogical composition of the selected samples and identify the possible chemical reaction between the injected CO_2 and the existing rock minerals.

5. Use the Nuclear Magnetic Resonance (NMR) technique to identify the fluid distribution in the samples before and after CO_2.
6. Measure the contact angle to identify the change of the wettability state of the rock sample after CO_2 exposure.
7. Use the data in the literature to compare the EOR performance of different gas EOR agents and select the most promising ones. Perform multiple cyclic injection tests using those gases to measure the oil recovery. Then, combine the selected gases in one injection scheme to improve the EOR performance.

1.4 Significance

Any incremental production improvement in Bakken could dramatically increase the oil recovery. In fact, due to the large volume of residual oil in Bakken, each 1% increase in the oil recovery factor could result in revenues of $128 to $720 billion with an estimated oil price of $80 per barrel. This study addresses the knowledge gap related to CO_2 EOR in unconventional reservoirs and the lack of understanding of the mechanisms that control the oil recovery. The obtained results will aid industry and academia in their understanding of CO_2 EOR performance in tight formations and contribute to designing an optimum CO_2 injection solution that will unlock billions of barrels of residual oil in unconventional reservoirs.

The results of this research study will present multifold novelties, including the followings:

1. In this project, we have addressed the gap between the results of the recent pilot tests and previous research studies in the Bakken.
2. A thorough parametric study was conducted to examine and understand the effects of key parameters on CO_2 EOR using representative samples from the Middle Bakken Member (MB) and the Three Forks Formation (TF).

3. The side effects of CO_2 injection on different reservoir attributes in Bakken, as will be presented in this study, were evaluated and discussed to enlighten future EOR projects.
4. This research project includes a comparison of the EOR performance of multiple gases (CO_2, methane, ethane, propane, and rich gas mixture) using available data in the literature and our lab experiments. A novel gas EOR scheme is introduced, which can help further increase the oil recovery.
5. The results and discussions included in this study can be used to improve the understanding of oil recovery mechanisms using gas injection in unconventional reservoirs.
6. Practical recommendations and suggestions that are proposed in this study contribute to designing an optimum EOR solution to unlock billions of barrels of residual oil.

1.5 Thesis structure

This thesis consists of eight chapters

Chapter 1 is an introduction to the project. A brief overview of CO_2 EOR and injection techniques in unconventional reservoirs is given. We also listed the objectives, methodology, and significance of this study.

Chapter 2 includes an overview of the Bakken Petroleum System and a literature review of the previous numerical simulation, experimental work, and field pilot tests performed in Bakken.

Chapter 3 details the methodology we followed, and the different materials used in this study. The description of the different experimental designs and the methods used are presented in this section.

Chapter 4 presents the optimization of the injection parameters, using CO_2 HnP injection scheme, which include the injection pressure, soaking time, and number of injection cycles.

Chapter 5 discusses the effect of water presence, sample size, injection scheme, and fracture size on CO_2 performance in tight formations.

In Chapter 6 the effect of CO_2 injection on different reservoir properties in MB and TF, as wettability, pore size distribution, and porosity will be investigated.

Chapter 7 presents the comparison of EOR performance of CO_2 and different hydrocarbon gases. A novel injection scheme that consists of combining the most promising gases will be introduced.

In Chapter 8 a summary of the findings from this study will be presented along with some recommendations and future studies that can be carried out.

1.6 Summary

This chapter introduced the need for EOR techniques in Bakken. It was highlighted that recent field CO_2 injection pilot tests indicated that oil recovery mechanisms using CO_2 injection in unconventional reservoirs are still in the primary stage, demonstrating the need for further evaluation efforts. Also, it was mentioned that can HnP injection scheme can help overcome the challenges related to continuous injection in poor quality reservoirs, which may result in early CO2 breakthrough and inefficient oil displacement.

Also, in this Chapter, a summary of the main objectives of this research, the methodology which will be implemented, distinguished aspects of this study and the structure of this thesis were presented.

In the next Chapter, an overview of the Bakken petroleum system and a review of the literature will be presented to give a background to CO_2 EOR techniques in Bakken and unconventional in general.

Chapter 2

Literature Review

In this Chapter, we present an overview of the Bakken Petroleum System (BPS), a review of the CO_2 EOR studies in tight formations, and a review of the field EOR pilot tests conducted in Bakken. The chapter is divided into three sections related to BPS overview, previous research work, field pilot tests.

2.1 Overview of the Bakken Petroleum System

The Bakken is one of the largest oil-bearing tight formations in North America that covers parts of the United States in Montana and North Dakota and parts of Saskatchewan and Manitoba in Canada [21] (Fig. 2.1). Oil was initially discovered in the Bakken in 1951, but with a very limited production capacity before a tremendous oil production increase took place in 2006 (Fig. 2.2). The Bakken petroleum system is composed of: The Upper Bakken Shale member (UBS), Middle Bakken Member, Lower Bakken Shale member (LBS), and the Three Forks (Fig. 2.3). The UBS and LBS members constitute the source rocks, whereas the middle member and the underlying

Three Forks formation are the oil reservoir units, and they are both classified as unconventional reservoirs [22,23].

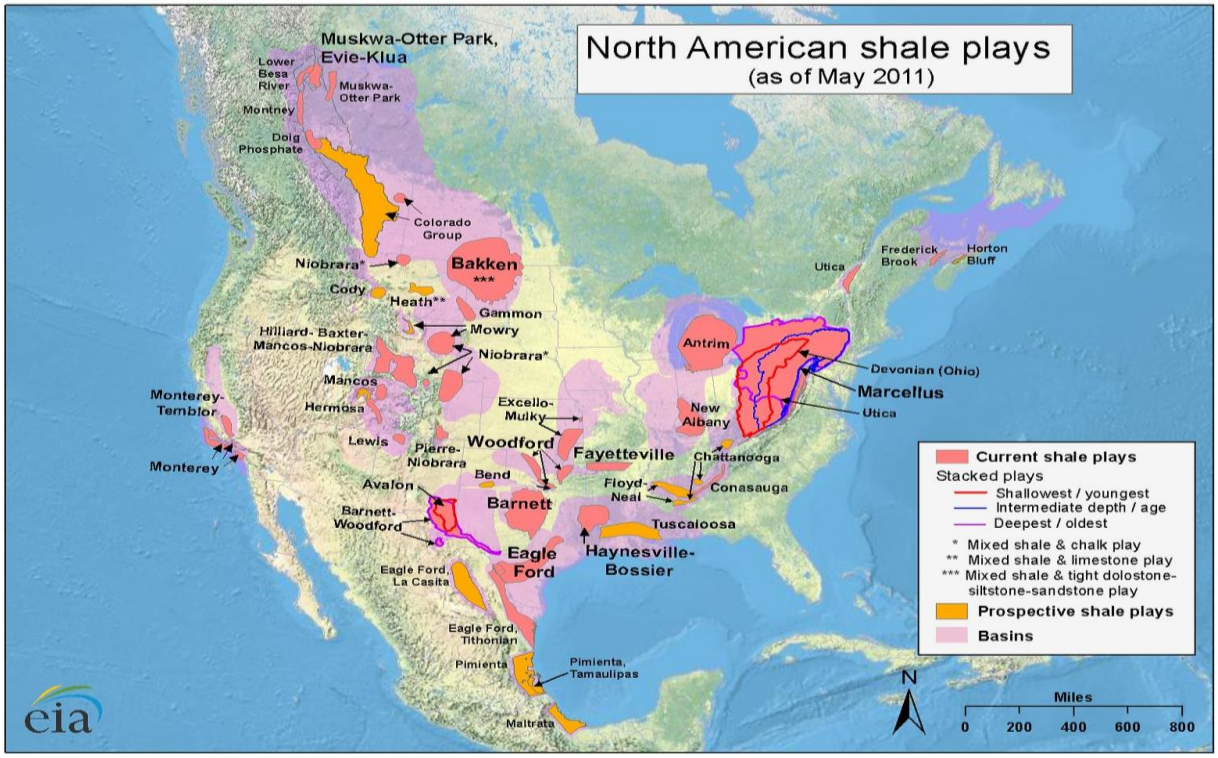

Fig. 2.1. North America shale resource plays [24]

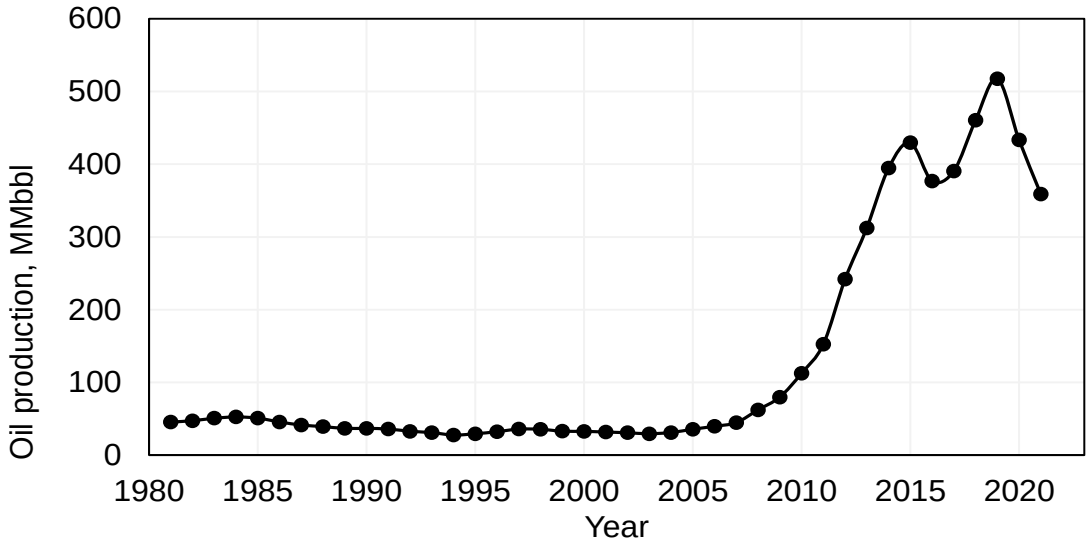

Fig. 2.2. North Dakota oil production history [25]

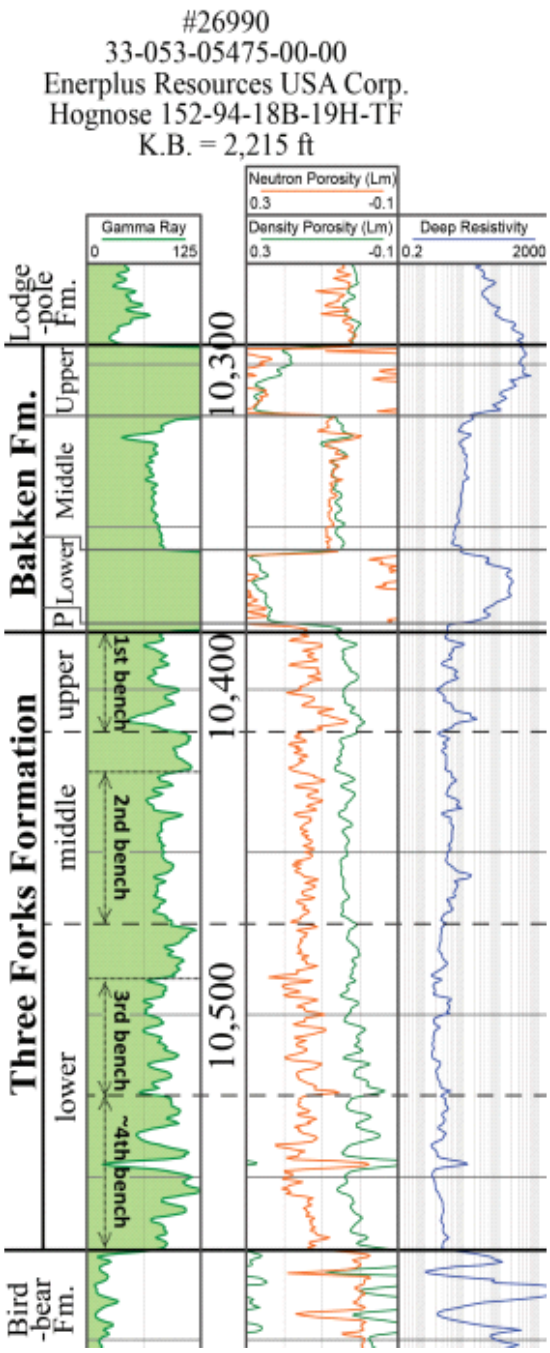

Fig. 2.3. Typical well logs for the Bakken petroleum system showing both Three Forks and Bakken formations [22]

The middle member was the main target for oil production until 2012 when some operators started drilling and completing in the Three Forks Formation, And they started to consider it as a prospective unconventional reservoir [22,23]. Both formations are characterized by low

permeability and porosity, so they are considered as ultra-tight formations. The average porosity is somewhere between 4% and 8%, while the permeability is in a micro- and nano-Darcy range [3]. The Middle Bakken formation consists of clastic and carbonate rocks, while Three Forks is formed of interbedded dolomitic mudstone and silty dolostone [21]. OOIP estimations varies from 300 to 900 billion barrels [10]; however, after the primary recovery the oil recovery factor is typically less than 12% of the OOIP [10,11].

2.2 CO_2 EOR Research Progress in Unconventional Oil Reservoirs

The technology for CO_2 EOR in tight oil plays is still in the early stages of development compared to conventional reservoirs [26]. Usually, every technology goes through three main stages, which are conceptualization, proof of concept, then implementation. At present, specifically in Bakken, EOR methods are in the early phase of proof of concept (see Fig. 2.4). In this section, we present a review the progress of CO_2 EOR-related work in the literature.

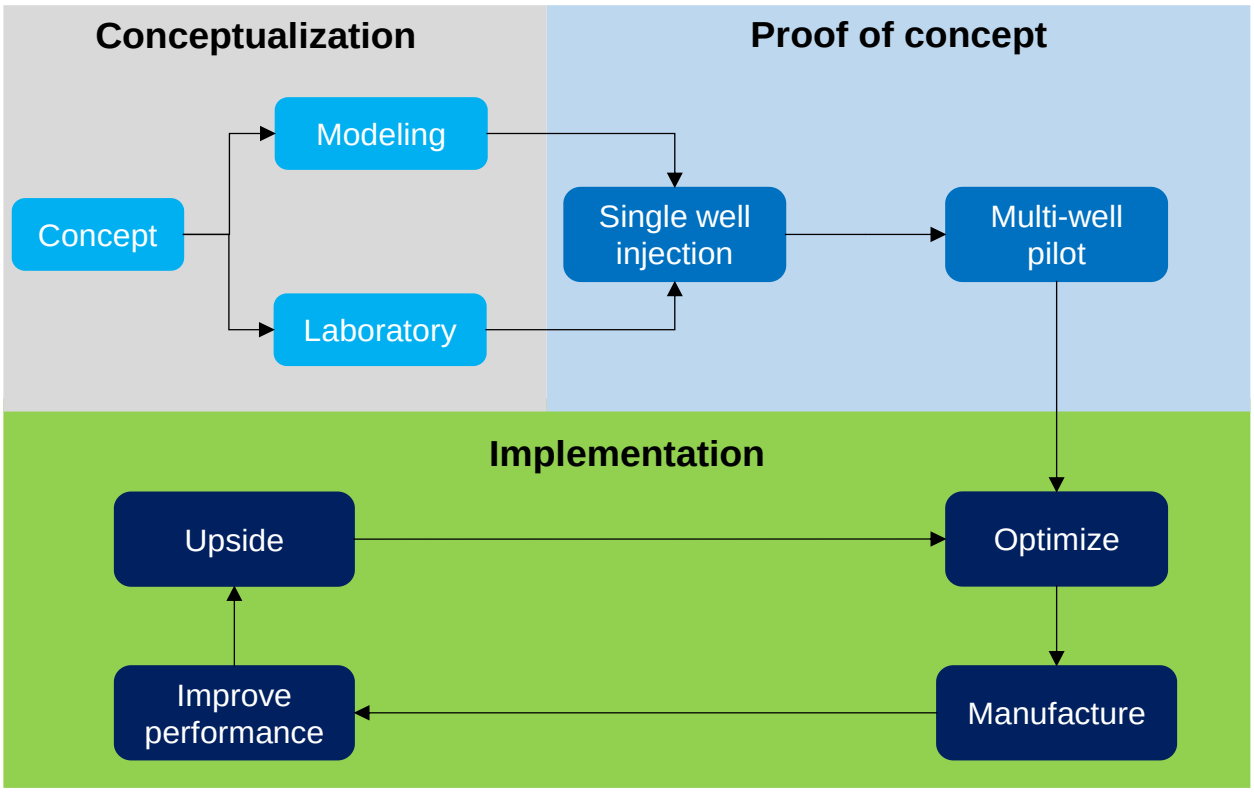

Fig. 2.4. Road map for EOR in Unconventional plays [27]

2.2.1 Miscible VS immiscible CO_2 injection

The miscibility conditions between the injected gas and the reservoir crude can be a fundamental parameter that controls the success of gas EOR applications in unconventional reservoirs. Some studies compared miscible and immiscible CO_2 EOR using tight rock samples; however, the results are contradictory in the literature.

Gamadi et al. [28] used two samples of 1.5 in diameter and 2 in length retrieved from Eagle Ford and Mancos shale. They used synthetic oil (C10-C13 Isoalkanes) to saturate the samples. They conducted experiments using a huff-and-puff scheme at 95°F and at pressures of 1500, 2500, and 3500 psi. The soak times varied from 6 to 48 hours. They reported recovery factors up to 95% and concluded that miscibility had a significant impact on oil recovery. They also found that the

recovery factor increases with pressure and soak time; however, they reported that injecting CO_2 at a pressure higher than the MMP does not result in an additional recovery.

Song and Yang [29] performed CO_2 HnP experiments at immiscible (1015 psi), near-miscible (1350 psi), and miscible (2030 psi) conditions. The authors reported that the samples were collected from the Bakken formation of southern Saskatchewan without specifying which member or lithology. Also, the dimensions of the samples were not reported. The experiments were conducted at 145.4°F. For each cycle, CO_2 was injected at constant pressure for 3 h, the system soaked for 6h, then the production lasted for 1h. A total of six cycles were performed for each scenario. The total oil recovery was 48%, 63%, and 61% for immiscible, near-miscible, and miscible conditions, respectively. No discussions were provided to explain the oil recovery drop at miscible conditions. The authors indicated that increasing the pressure above MMP does not result in higher oil recovery. It is important to mention that the tested plugs had porosity and permeability ranging from 18 to 23% and 0.2 to 0.8 mD, respectively, which might not be representative for ultra-low permeability and porosity of the characteristic of shale reservoirs.

Contrarily, other studies showed that increasing the pressure above MMP lead to higher recovery factors. Hawthorne et al. conducted several CO_2 HnP experiments using rock samples from MB and LBS. LBS samples were crushed and sieved to obtain 0.04 to 0.12 in size rock cuttings, and MB rods were drilled from the original core slabs rods using a 0.5 in diameter drill bit. The injection tests were performed at a temperature of 213 °F. Production fractions were collected after every hour, for the first seven hours of soaking time, then another fraction was collected at the end of 24 hours of soaking. Methylene chloride solution was used to capture the produced hydrocarbons. The CO_2 HnP tests were conducted at three injection pressures of 1494, 2495, and 5000 psi to represent immiscible, miscible, and above MMP conditions. The ultimate oil recovery

factor values for MB rods were 30% (immiscible), 82% (miscible), and 97% (above miscible), and 3% (immiscible), 14% (miscible), and 40% (above miscible) for the LBS samples. These results suggest that increasing the pressure above MMP results in a tremendous increase in oil recovery.

Similarly, Tovar et al. [30] and Adel et al. [31] studied the effect of injection pressure on CO_2 EOR performance using tight rock samples. They concluded that increasing the pressure above MMP results in higher recovery factors. They indicated the injection pressure strongly influence the recovery factor, and increasing the injection pressure above MMP result in incremental oil recovery.

These contradictory observations in the literature set the need for further evaluation efforts of CO_2 EOR performance under representative reservoir conditions.

2.2.2 Proposed CO_2 EOR mechanisms

Tovar et al. [32,33] coupled CO_2 HnP tests with Computed Tomography (CT) to investigate the oil recovery mechanism in shale oil reservoirs. They used a high-resolution medical CT-scanner to interpret CO_2 penetration into the rock matrix based on CT number change. CO_2 permeation of the rock matrix results in a change of the density throughout the rock sample during the soaking period, which is correlated to the CT number change. The analysis of the CT images and produced oil characteristics suggested that oil vaporization into the injected CO_2 is the governing mechanism of oil production.

Alfarge et al. [34,35] investigated CO_2-EOR mechanisms using HnP in shale oil reservoirs based on history matching results. They used numerical simulation and history matched CO_2 HnP experiments and field pilot tests that were performed in Bakken. They indicated that molecular diffusion is the governing mechanism that controls oil recovery in shale oil reservoirs and CO_2-diffusivity level dictates the success of CO_2-EOR project in shale formations.

Zhang et al. [36] used core scale simulation and CO_2 HnP experiments to unveil CO_2 EOR mechanisms in tight formations. They used samples from Eagle Ford shale to perform five CO_2 HnP tests at a temperature of 170°F and pressure values of 1400, 1800, 2500, 3000, and 3500 psi. The experimental results were used to history match the core scale model and obtain the diffusion coefficient of CO_2. A pseudo-ternary diagram was built for CO_2-oil system using Peng-Robinson EOS. Based on the observations from core-scale simulation and ternary diagram analysis, the authors indicated that multi-contact miscibility and vaporizing gas drive are the dominant mechanisms. Also, they compared CO_2 HnP results with Nitrogen injection at 5000 psi. At such pressure, N_2 is immiscible with the crude oil and has the same diffusion coefficient as CO_2. No oil was displaced from the rock matrix using N_2 injection. These results indicated that diffusion has a minor role in improving oil recovery in unconventional liquid reservoirs compared to multi-contact miscibility.

Hawthorne et al. [37] proposed a conceptual mechanism for CO_2 EOR in tight fractured formations. As presented in Fig. 2.5, the proposed mechanistic of oil displacement using CO_2 HnP consists of the following four steps: 1) during the initial injection, CO_2 fills the fracture space, 2) CO_2 begins to permeate the rock via pressure gradient and starts swelling the oil in the rock matrix, 3) as CO_2 permeation continues, swelling and viscosity reduction of the trapped oil will lead it to migrate from the rock matrix toward the fracture, and 4) The pressure equalizes throughout the rock, and molecular diffusion of hydrocarbons becomes the dominating process.

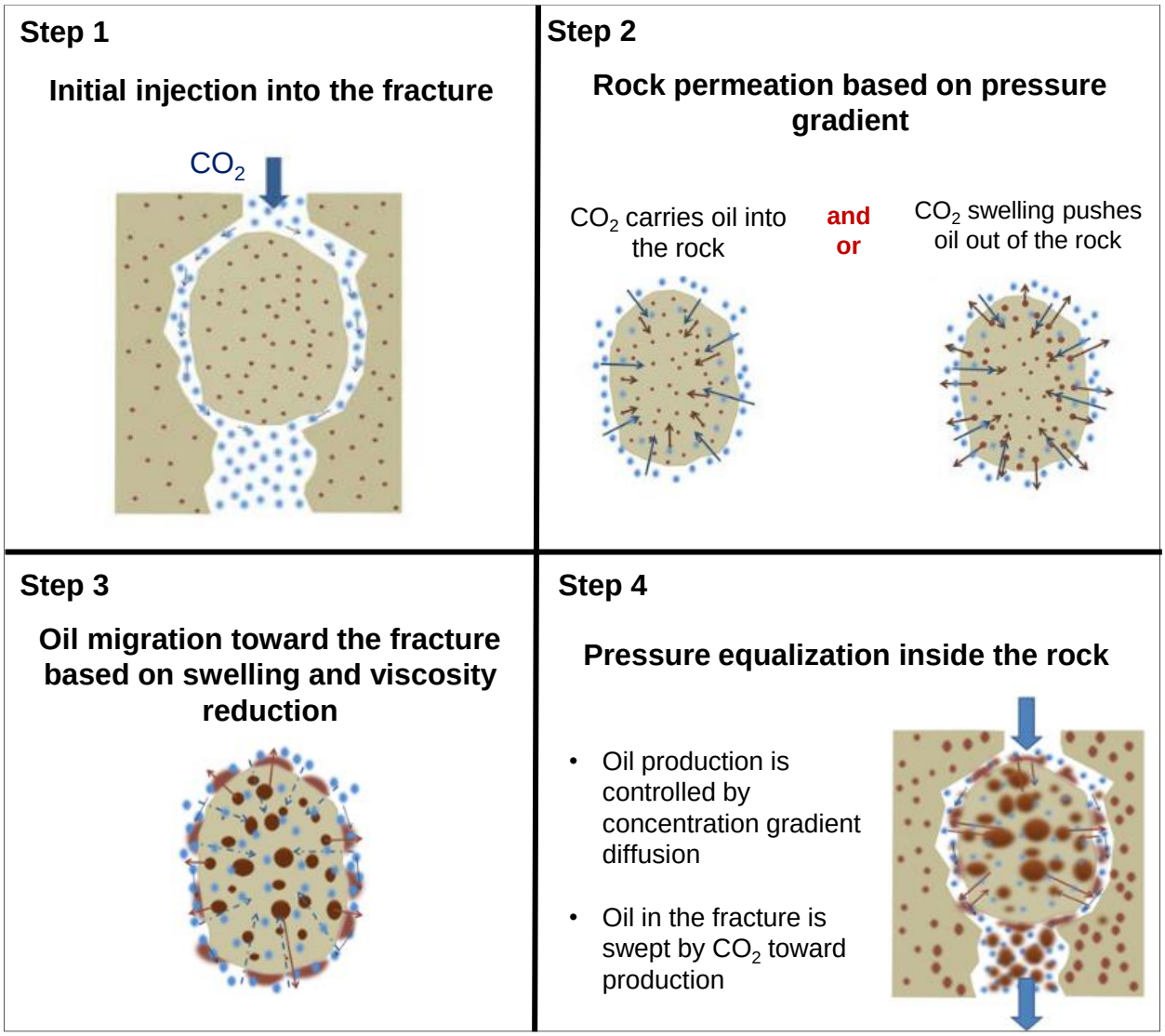

Fig. 2.5. Conceptual steps for oil mobilization using CO_2 injection in tight fractured formations (modified from [37])

2.2.3 CO_2 EOR potential estimation in Bakken

2.2.3.1 Experimental work

Compared to other shale oil plays, very few experimental studies were performed to estimate the CO_2 capacity to recover oil from Bakken oil reservoirs.

Tovar et al. [32] evaluated the performance of cyclic CO_2 injection using four preserved sidewall cores that were initially saturated with crude. The cores had a diameter of 1 in and a length of 1.5,

1.4,1.4, and 1.3 in. The authors did not report the specific location of the selected samples. The CO_2 was injected at a temperature of 150°F and pressure values of 1600 psi and 3000 psi. They opted to test the samples as received and without any intervention that might alter the properties of the cores; therefore, the petrophysical properties of the samples were unknown. They assumed different values for the porosity (0.3% and 0.6%) and water saturation (0% and 30%). Based on different porosity and water saturation scenarios, the estimated oil recovery factor values varied from 18 to 55%. The absence of an accurate measurement of the residual oil volume in the tested samples resulted in high uncertainty in recovery factor estimations.

Jin et al. [38,39] collected 21 preserved small samples from LBS, MB, UBS, and TF. They performed cyclic CO_2 injection experiments at 230°F. The LBS and UBS were represented using 0.04 to 0.12 in size rock cuttings. For the TF and MB, they drilled 0.4 in diameter and 1.5 in length cylindrical rods. The injection pressure was maintained at 5000 psi, and oil fractions were collected every hour for the first seven hours of the test. After 24 hours of exposure, the rock was crushed and extracted with methylene chloride to collect the remaining oil. The tests yielded very high recovery factors. After only seven hours of CO_2 exposure, they recovered almost 90% of the oil from the MB and TF rods, and the ultimate recoveries after 24 hours were between 95 and 100%. The ultimate oil recovery factors for UBS and LBS samples were around 60%.

Another experimental study that evaluated the oil recovery using CO_2 injection into Bakken rock samples was performed by Song and Yang [40]. They used rock samples from the Bakken formation of southern Saskatchewan. Using CO_2 HnP at 145°F and 2030 psi, they measured a recovery factor of 60 % of the OOIP after 6 hours of soaking. The permeability of the samples used in this test was around 0.8 mD, and the porosity was above 20%, which might represent the characteristics of ultra-tight formations and unconventional reservoirs.

2.2.3.2 Modeling studies

Table 1 illustrates different numerical simulation studies that evaluated the performance of CO_2 injection in Bakken. Most of the studies confirmed the viability of CO_2 EOR and estimated an oil recovery factor between 10 and 35%.

Table 1 Review of CO_2 EOR simulation studies in Bakken

Authors	Model	Simulator	EOR technique	Recovery Factor (RF)
Chen [41]	Single porosity	IMEX	CO_2 flooding and water flooding	7200 days of primary production + 30 cycles of CO_2 injection, each cycle includes: 200 days of injection and 200 days of production: **RF=25.5%** 3600 days of primary production and 60 years of CO_2 flooding production: **RF=15%** 10-year primary production and 60 years of water flooding: **RF=11.9%** 10-year primary production and 60 years of cyclic water flooding: **RF=11.03%** 70 years of water flooding production: **RF=11.05%**
Pu and Hoffman [42]	Single porosity	IMEX	CO_2, WAG, separator gas, lean gas	30-year recovery factor: WAG: **RF=22.74%** CO_2: **RF=24.59%** Separator gas: **RF=26.32%** Lean gas: **RF=22.28%**
Fai et al. [43]	Single porosity	Compositional simulator	Gas injection	1-year recovery factor: 100% CO_2: **RF=33%** 75% CO_2 + 25% C1: **RF=36%** 50% CO_2 + 50% C1: **RF=42%** 50% CO_2 + 25% C1 + 25% C2: **RF=42%**
Chen et al. [44]	Single porosity	UT-COMP	CO_2 huff 'n' puff	Step 1: 300 days of primary recovery; production at 3,000 psi Step 2: 30 days of CO_2 injection at 4,000 psi

				Step 3: 10/20 days of well shut-in (**W**) Step 4: 100 days of production at 3,000 psi Step 5: Repeat Steps 2 through 4 until 1,000 days **W**=10: **RF= 6%** **W**=20: **RF= 6%**
Sanchez [45]	Single porosity	GEM	CO_2/CO_2-enriched gas huff 'n' puff	1/30/100 days of soaking, with 30 days of injection and 200 days of production: **RF= 17%** Effect of the number of cycles: 2 cycles: **RF=16.3%** 5 cycles: **RF=17.3%** 8 cycles: **RF=17.8%**
Yu et al. [46]	Single porosity	GEM	CO_2 huff-n-puff	30 years Recovery Factor (RF) and Incremental Recovery Factor (IRF) Effect of number of fractures by stage 1 fracture/stage: **RF=15.8%** **IRF=4%** 2 fractures/stage: **RF=20%** **IRF=6.2%** 3 fractures/stage: **RF=20%** **IRF=5.2%** 4 fractures/stage: **RF=22%** **IRF=5.3%** Effect of Injection rate: 0 Mscf/day: **RF=12.5%** 50 Mscf/day: **RF=16%** 500 Mscf/day: **RF=24%**
Yu et al. [47]	Single porosity	GEM	CO_2 huff-n-puff	30 years Recovery Factor (RF) and Incremental Recovery Factor (IRF) Effect of number of cycles: 0 cycles: **RF=20%** 1 cycle: **RF=22%** 2 cycles: **RF=23.5%** 3 cycles: **RF=24%**

				Effect of fracture half-length: 110 ft: **RF= 16.5%**, **IRF=0%** 210 ft: **RF=22%**, **IRF=2%** 310 ft: **RF= 26%**, **IRF=3%**
Sun et al. [48]	Unstructured Discrete fracture network	In-house	CO_2 huff-n-puff	Initial reservoir pressure: 3000 psi. Effect of producer BHP: 1000 psi: **IRF=10%** 1300 psi: **IRF=3.56%** 1550 psi: **IRF=1.57%** 2000 psi: **IRF=1.68%**
Alharthy et al. [49]	Dual porosity and dual perm	GEM	NGL/CO_2 huff-n-puff	Experiment: The experiments recovered 90% oil from several Middle Bakken cores and nearly 40% from Lower Bakken cores. Simulation: Primary depletion: **RF=7.5%** Effect of CO_2 injection rate and soaking time: Injection: 200 Mscf/D; soaking: 15 days: **RF=12%** Injection: 200 Mscf/D; soaking: 30 days: **RF=12%** Injection: 400 Mscf/D; soaking: 15 days: **RF=14.5%** Injection: 400 Mscf/D; soaking: 30 days: **RF=14.5%** Effect of molecular diffusion: CO_2 injection without diffusion: **RF=11%** CO_2 injection with diffusion: **RF=11.5%** NGL injection without diffusion: **RF=12%** NGL injection with diffusion: **RF=12.5%**

2.2.4 Limitations of previous CO_2 EOR studies

Experimental work is fundamental to understanding and evaluating the performance of any new EOR technology in the oil and gas industry. The main limitations of most of the previous CO_2 EOR experimental studies can be summarized as follows:

- Several CO_2 injection tests were conducted under non-realistic reservoir conditions.
- Multiple studies used non-representative oil and rock samples as synthetic oil or rock samples with relatively high porosity and permeability.
- Most of the previous lab work studies used very small samples, which might not represent the heterogeneity in the formation and the complexity of fluid flow mechanistic in tight formations.

Also, there is no agreement in the literature regarding the oil mechanisms using CO_2 injection in unconventional plays. Some studies indicated that concentration driven molecular diffusion is the key mechanism, while others concluded that it had a minimal effect on oil recovery in tight formations.

Despite the considerable amount of modeling work related to the Bakken EOR [18,19,36,50–53], such results need to be viewed with cautious optimism for the following reasons:

- Modeling programs have been developed primarily for conventional reservoirs and may not adequately address the additional complexities of a “tight oil” reservoir.
- Numerical models rely on relatively simple and non-realistic assumptions, which can affect their capacity to capture the multiple phases, complexities, and heterogeneities of a “real” reservoir situation.

CO_2 EOR modeling in unconventional reservoirs such as the Bakken requires the input of additional variables to adequately address the complexities of the reservoir.

2.3 Previous EOR Pilot Tests in Bakken

Several EOR pilot tests were performed in Bakken using water and gas injection. The objectives included testing the injectivity into the sub-millidarcy reservoir rocks and evaluating the performance of different EOR agents. Table 2 lists the different EOR pilot tests that were performed in the U.S portion of the Bakken and reported to public domain.

Table 2 List of EOR pilot tests performed in the U.S portion of the Bakken

Well ID	Operator	Formation	Test year	Injected fluid	Avg. inj. rate	Max. inj. Pres. (psi)	Cum. Inj. Volume	Type
#9660	Meridian	UBS	1994	Water	200 bpd	5000	13082 bbl	Flood
#16713	EOG	MB	2008	CO_2	580 bpd	1500	30.7 MMscf	HnP
#17170	EOG	MB	2012	Water	1500 bpd	4000	38177 bbl	HnP
#16986	EOG	MB	2014	Water / Produced gas	1500 Mscfd	5000	88.7 MMscf	Flood
#24779	Whiting	MB	2014	CO_2	500 Mscfd	3500	3.4 MMscf	Flood
#11413	XTO	MB	2017	CO_2	9 gpm	9480	1.7 MMscf	HnP
#32937	Hess	MB	2017	C3	105 Mscfd	5500	20 MMscf	-

2.3.1 Water injection tests

An early EOR pilot test was performed in 1994 by Meridian Oil Company. The operator used an existing horizontal well drilled into the UBS to test freshwater injection. The selected well was in production status before converting it to water injector to evaluate the feasibility of water flood in the Bakken shale. The injection began on March 8, 1994, for 50 days with an average injection rate of 200 bpd. On April 27, 1994, the well was shut-in for approximately 1-2 months to evaluate its performance. The monitored data were not reported, and the test was found to be unsuccessful (NDIC, well file 9660).

Another water injection test was conducted in 2012 by EOG Resources, Inc. They used a fractured horizontal well that was taken off production on April 22, 2012, then converted it to an injector for water flood. The injection operations started on May 3, 2012, using a HnP schedule with 30-day injection and 10-day soaking. Well returned to production on June 21, 2012, until October 12, 2012. A second injection cycle was performed from October 12, 2012, to November 11, 2012. The well returned to production on December 25, 2012. The test was deemed uneconomical, and the operator declared no intention to continue on water injection (NDIC, well file 17170).

2.3.2 CO_2 injection tests

In 2008, EOG Resources used a fractured horizontal well to perform HnP injection test using food-grade CO_2. The selected well was actively producing from the MB before starting the injection. The operating company was licensed for only one HnP injection scheme with 30 days of injection and 60 days of soaking. The injection started on September 15, 2008, until October 14, 2008, with a cumulative injection volume of 30.7 MMscf of CO_2. After 11 days of injection, CO_2 breakthrough was detected in an offset well located over a mile away from the injector. The operator continued the injection and completed the planned 30 days injection period. Then the well was shut-in for 50 days and reopened for production on December 3, 2008. The production history is presented in Fig. 2.6. The well was allowed to naturally flow for the first six months of the producing life. At this point, the well had a cumulative oil production of 133,152 bbl of oil before the decision was made to place the well on artificial lift using an electronic submersible pump. Right after injection, a slight increase in oil production was observed; however, it quickly declined after one month (see Fig. 2.6).

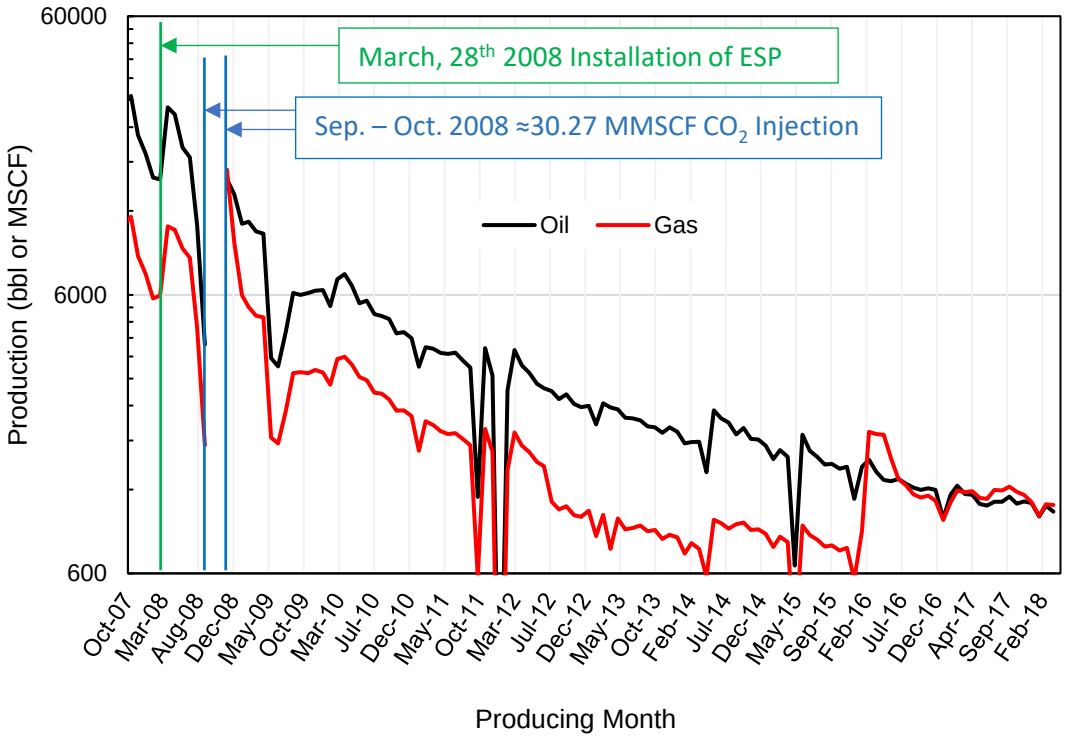

Fig. 2.6. Oil production history of well # 16713 (data from NDIC website under well file #16713)

In 2014, Whiting Oil & Gas Corporation used a vertical non-fractured well completed in the MB to conduct a CO_2 injection test. The objective of the test was to evaluate the injectivity of CO_2 into the MB rock matrix. They planned to conduct one HnP cycle with an injection period of 20 days and an average injection flow rate of 500 Mscf per day. The production records of MB wells located within a quarter-mile radius were monitored (Red circle in Fig. 2.7). Also, to further understand the potential for CO_2 propagation into the underlying Three Forks formation, three TF producers were also monitored for increased CO_2 production (green rectangles in Fig. 2.7).

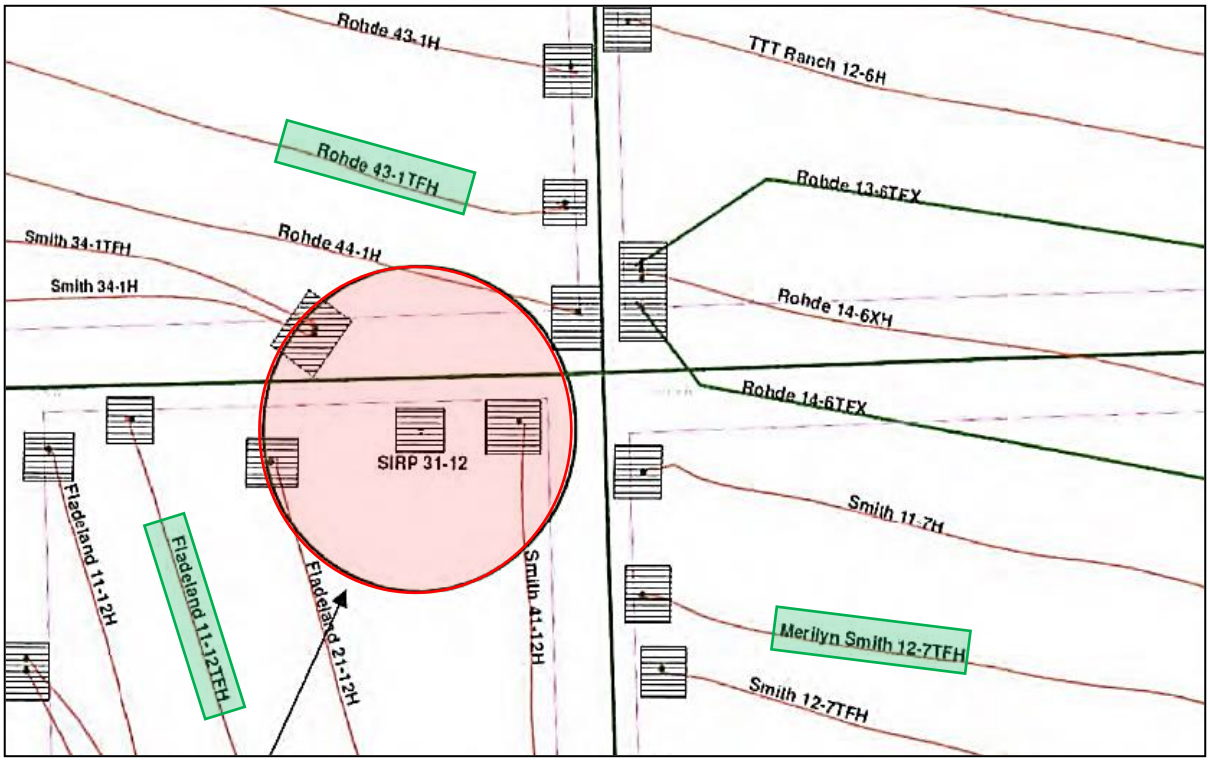

Fig. 2.7. Well 24779 quarter-mile radius of interest in monitoring Bakken CO_2 production changes during CO_2 injection (NDIC, well file 24779)

The test started on February 2, 2014, and after four days, the injection was ceased due to a CO_2 breakthrough that was detected in the offset MB well Fladeland 21-12H. The test was stopped, and only a small volume of CO_2 was injected. No substantial influence was observed on oil production from the offset MB wells. Whiting stated that the test was “less than optimal” and would re-evaluate the injection operation before attempting another field trial with CO_2 EOR in the Bakken. Another CO_2 pilot test in a vertical MB well was performed by XTO and the EERC in 2017. Similar to the test performed by Whiting Corporation, the objective was to evaluate the injectivity of CO_2 into a non-stimulated reservoir volume. The test was motivated by the results of previous numerical simulations and experiments that showed a recovery factor of nearly 100% after CO_2 injection. They performed one HnP cycle with four days of injection and a soak period of 15 days.

A total of 1.7 MMscf of CO_2 was injected into the MB. After soaking, the well flowed to produce 9 bbl of oil over the first 45 minutes, then stopped. The hydrocarbon composition was analyzed, and the results suggested that CO_2 successfully penetrated and displaced oil from the rock matrix.

2.3.3 Hydrocarbons gas injection tests

A produced gas pilot test performed by EOG Resources was conducted in 2014. They used a horizontal well producing from the MB. The well was first taken off production on March 30, 2012, and converted to an injection well on April 6, 2012, for produced water flood pilot project. The produced water injection continued until February 17, 2014, and the well returned to production in March 2014. There are no available details on the injection schedule or the outcome of the water flood test. On June 27, 2014, the well was used to inject a mixture of field gas and produced water. The injected produced gas consisted mainly of nitrogen, methane, ethane, and propane with a mole percent of 10.3, 52, 19, and 12.7%, respectively. The test goal was to evaluate the technical feasibility and production performance results after injecting produced gas into the MB for the purpose of secondary recovery. The mixture of water and gas was used to manage the surface injection pressure, increase the viscosity of the injected steam to manage the gas mobility in the fracture system, and build system pressure with less gas volume. It appeared that there was no communication with the production well, and the injection ended on August 16, 2014.

In 2017, Hess conducted an EOR pilot test to evaluate propane injection. They used a vertical hydraulically fractured well that was producing from the MB. The test plan state that propane will be injected in the vertical fractured well and four offset wells were monitored to track oil and gas production changes. The injection scheme was not clearly stated; however, based on the injection and pressure data, the test was conducted for approximately one year and a half and consisted of

two propane injection cycles (see Fig. 2.8). Fig. 2.9 presents the oil production of the offset wells monitored during this pilot test.

After two months of injection, one offset well had a sharp increase of oil production from 22 to 54 bbl per operated day. The production gradually decreased to stabilize at the previous baseline. Hess considered this test as a demonstration of the feasibility of miscible EOR in Bakken, while requiring further evaluation for future larger-scale tests.

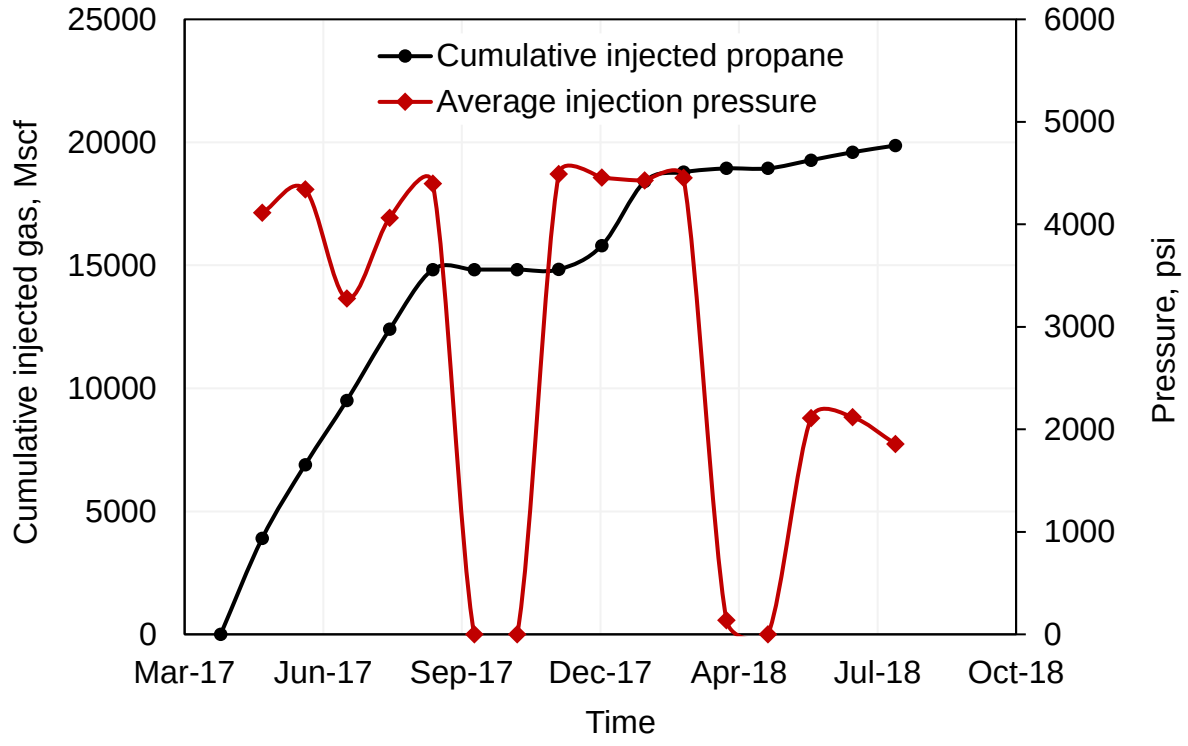

Fig. 2.8. Hess pilot test cumulative injected gas and injection pressure history (data from NDIC website under well file #32937)

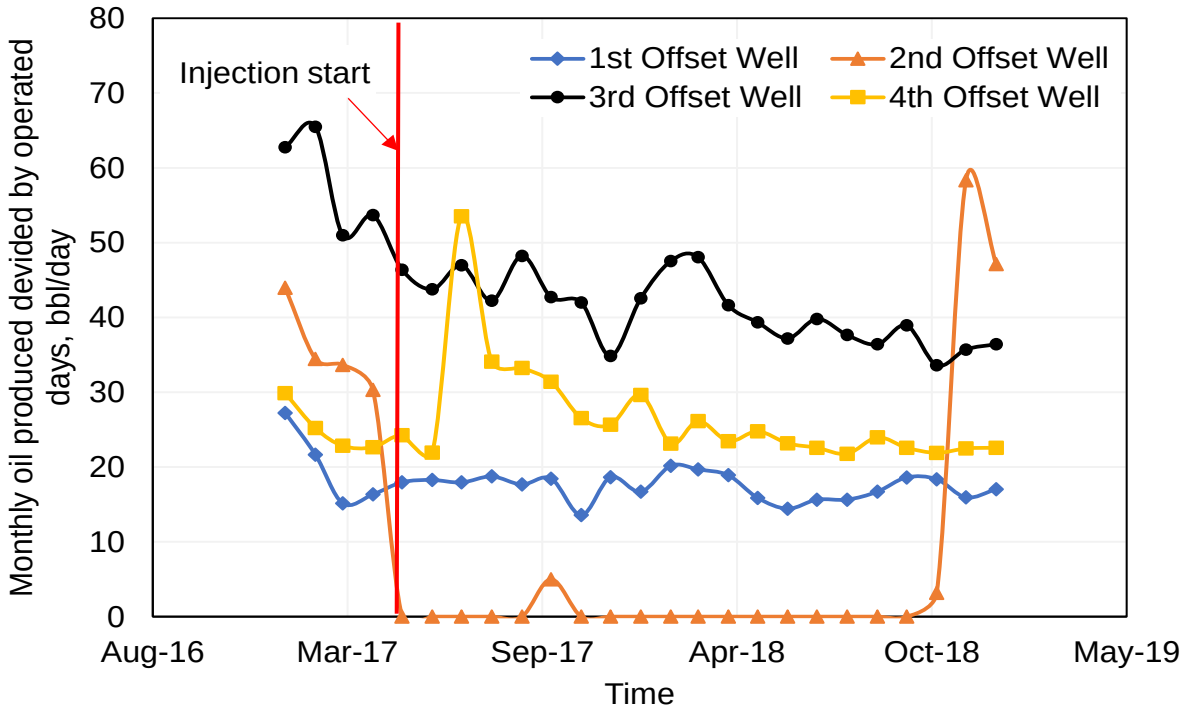

Fig. 2.9. Offset well production during propane pilot test performed by Hess (data from NDIC website under well file #32937)

2.3.4 Lessons learned from pilot scale EOR tests

The main lessons that can be learned from the previous pilot tests can be summarized as follow:

- Both water injection tests (fresh water and produced water) confirmed the non-viability of this technique in Bakken due to the low injectivity.
- The pilot-scale injections were performed separately with little to no collaboration between the operating companies. Better coordination in the future can reduce the cost and lead to obtaining more valuable outcomes.
- The results of CO_2 injection pilot tests revealed that the simulation studies in the literature were too optimistic, and the previous core-scale injection tests overestimated CO_2 potential.

- Some tests had promising outcomes; however, no clear consensus has been reached. The reported results have revealed that CO_2 EOR mechanisms in unconventional reservoirs are still poorly understood.
- Almost all the gas EOR pilot tests were concluded with a recommendation of further evaluation of oil recovery mechanisms under miscible EOR conditions.

2.4 Summary

In this Chapter, we presented an overview of the BPS and a review of the previous CO_2 EOR research studies in tight formations. Also, we summarized and discussed the results of previous pilot-scale EOR tests in Bakken. It was mentioned that the results of various CO_2 EOR experimental studies were highly variable. Furthermore, the injection tests that were conducted in the Bakken between 2008 and 2014 did not produce the same robust results as some of the previous modeling and laboratory work.

Also, it was indicated that further CO_2 EOR evaluation efforts are required to bridge the gap between the results of previous research studies and field pilot tests.

In the next Chapter, we present the samples used to represent the oil producing units in Bakken and describe the different experimental designs used in this study.

Chapter 3

Experimental Designs

In this Chapter, we present the methods and materials used in this study. The properties of the samples used in this study are presented in this section. Also, a description of the different equipment used for the experimental work is provided. This Chapter comprises of two sections related to materials and experimental setups description.

3.1 Materials

3.1.1 Sampling location

In five out of the seven EOR pilot tests performed by different operators in the U.S portion of the Bakken, the selected wells are located in Mountrail County, ND (see Fig. 3.1). This highlights the interests of operating companies in that region of the basin. To be able to compare and correlate

our experimental results with the outcomes of the field pilot tests, two wells located in Mountrail County, ND were selected for sampling in this study (see Fig. 3.1).

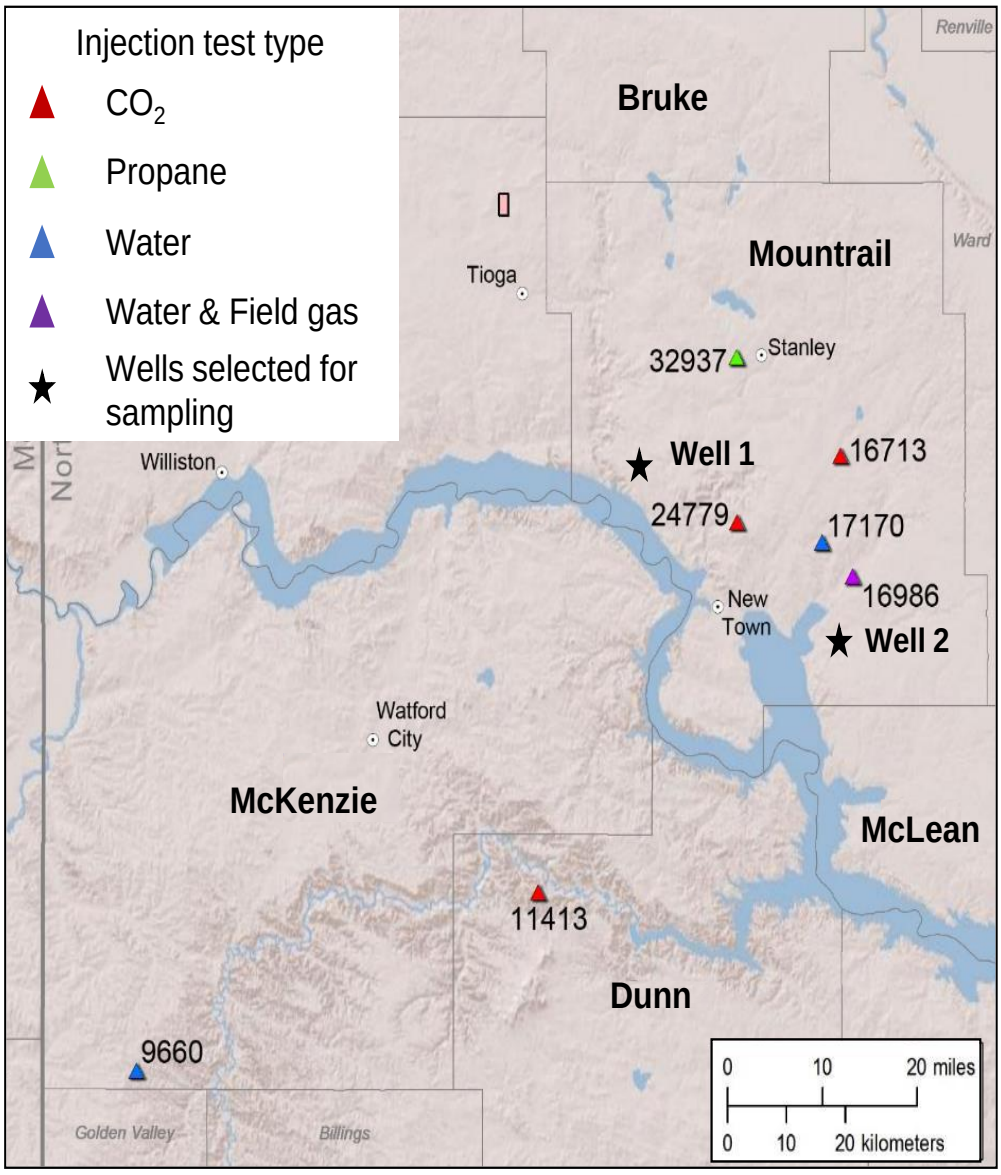

Fig. 3.1 Map location of the wells used for EOR pilot Bakken and the wells selected for sampling in this study

It is important to mention that the availability of well-data in the public domain and the availability of core samples in the targeted reservoir intervals had a major impact on wells selection in this study. Table 3 lists the producing units of both wells and the corresponding cumulative production.

Table 3 producing units and production data of the wells selected for sampling

Well ID	Well NDIC number	Field	Producing unit	Cum oil production (bbl)	Cum water production (bbl)	Gas production (Mscf)
Well 1	25688	Robinson Lake	Middle Bakken Member	270,886	420,943	313,447
Well 2	18101	Parshall	Three Forks Formation	258,922	114,018	164,572

3.1.2 Samples

3.1.2.1 Rock samples

A total of 20 rock samples were retrieved from both wells for the different experiments performed in this study. The samples were drilled from both Middle Bakken Member and the Three Forks Formation. The properties of the tested rock samples will be presented in each corresponding Chapter.

3.1.2.2 Oil properties

Crude oil samples were collected from each sampled well. Table 4 illustrates the reservoir conditions and the properties of Bakken crude oil. PVT analysis was performed to measure the different properties of a bottomhole oil sample retrieved from a similar location of the selected wells. A detailed PVT analysis of a Bakken crude oil sample is included in Appendix A.

Table 4 Bakken crude oil properties and reservoir conditions

Reservoir temperature (°F)	213
Reservoir pressure (psi)	6555
Oil density at reservoir conditions (g/cc)	0.668
API gravity (°)	39.3
Viscosity at reservoir conditions (cp)	0.37
Bubble point pressure (psi)	2198
Formation Volume Factor at reservoir conditions	1.609

3.2 Experimental Setups

3.2.1 Samples preparation

Depending on the experimental design, some samples were tested as-received while others were cleaned then re-saturated. After drilling the plugs from the original core slab, cleaning and drying were performed following the recommended best practice of McPhee et al. [54]. Samples saturation with oil was performed at reservoir pressure and temperature (see Table 4). The schematic of the saturation setup used in this work is illustrated in Fig. 3.2. The apparatus can withstand a pressure of 10,000 psi and a temperature of 315 °F. It is composed of a vacuum pump, a saturation chamber equipped with a pressure gauge, a floating piston accumulator, a water syringe pump, and an air bath thermostat that keeps the saturation process at a constant temperature.

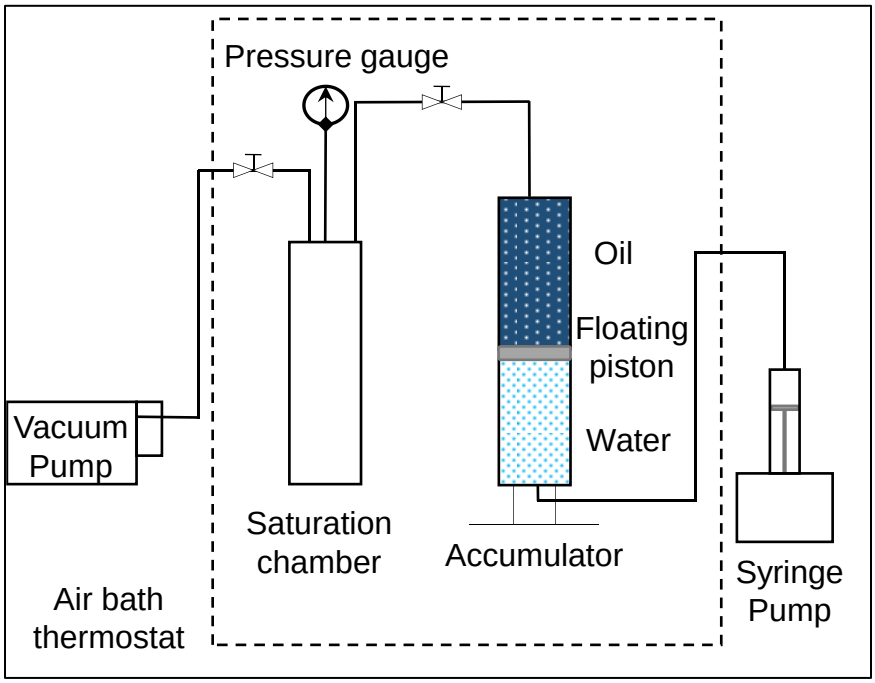

Fig. 3.2 Schematic of the saturation setup

3.2.2 Mineralogical composition

The bulk mineralogical composition of two MB and two TF samples was examined using X-ray diffraction (XRD). The samples were crushed and pulverized to be analyzed with a RIGAKU Smartlab XRD equipment and results were interpreted with a PDXL software. Each sample was analyzed at 5 degrees to 90 degrees, two theta (5º-90º 2θ) in order to identify the entire mineral assemblage and distributions.

3.2.3 CO_2 injection

Fig. 3.3 illustrates the experimental setup used to run the CO_2 Huff-n-Puff experiments. It consists of two floating piston accumulators used to pressurize CO_2, where each piston is connected to a water syringe pump, a Hassler-type core holder with a maximum pressure of 10,000 psi connected to a pressure transducer that monitors the CO_2 injection pressure, a back pressure regulator, an air bath thermostat, and a data acquisition system.

The OOIP and the recovered oil volume are expected to be very small for samples with very low porosity. The produced oil might be smaller than the dead-volume of the experimental setup. Therefore, we recommend using the difference in core weights to accurately determine the recovery factor. We measured the core weight difference before and after saturation to determine the OOIP before each injection cycle (Equation (1)). We then measured the core weight after CO_2 injection and calculated the oil recovery factor using Equation (2).

$$OOIP = W_2 - W_1 \quad (1)$$

$$RF = \frac{W_3 - W_2}{OOIP} \times 100\% \quad (2)$$

Where $OOIP$ is the original oil in place, W_1, W_2, and W_3 are the core weights before saturation, after saturation, and after CO_2 injection, respectively, and RF is the oil recovery factor.

We used the same apparatus with a modified core holder assembly for CO_2 flooding experiments (Fig. 3.4). The core sample was placed in a rubber sleeve and a manual pump was used to apply a confining pressure, which was 500 psi higher than the desired injection pressure to prevent CO_2 slippage between the core and the sleeve. The backpressure regulator (BPR) was used to control the injection pressure during the flooding process. The produced oil volume was collected in a graduated pipette and recorded over time.

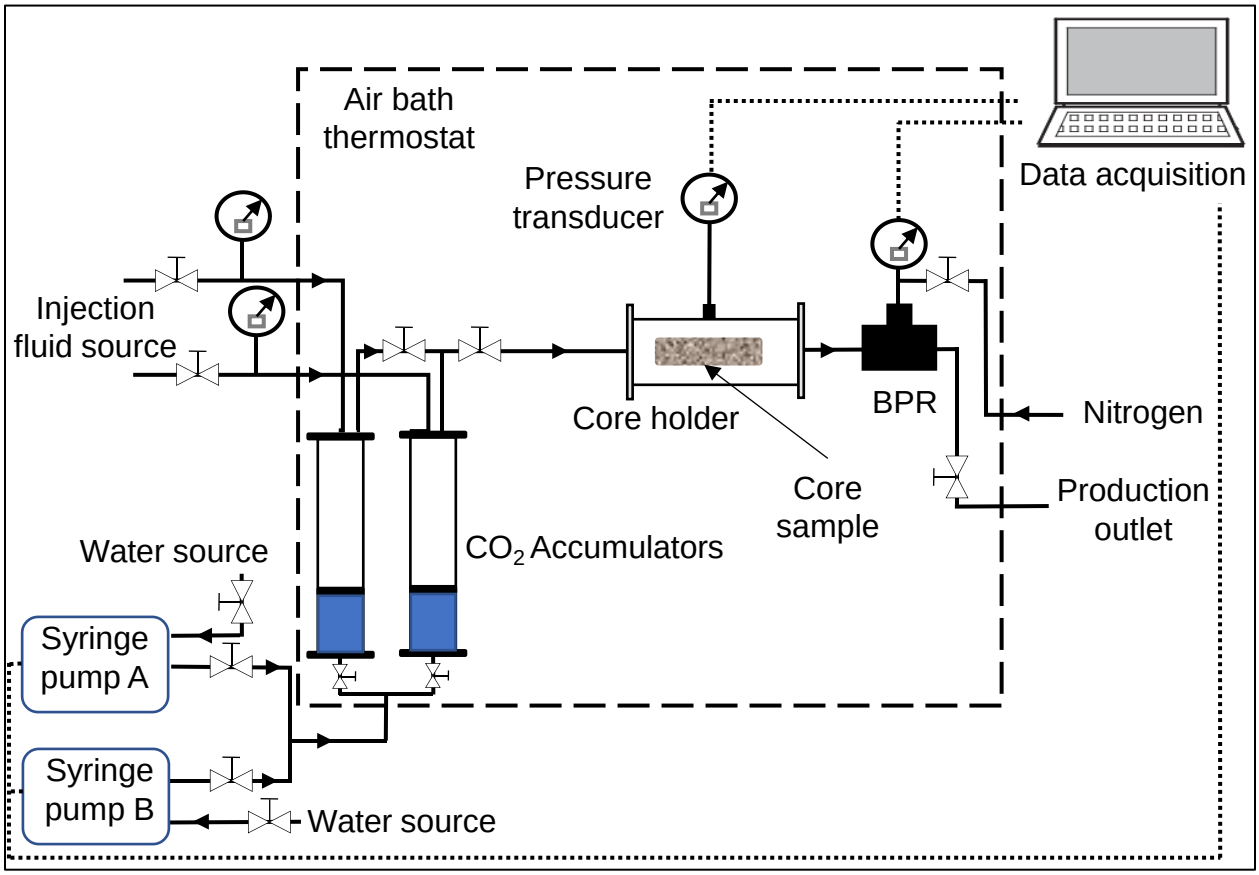

Fig. 3.3 Schematic of the CO_2 injection experimental design

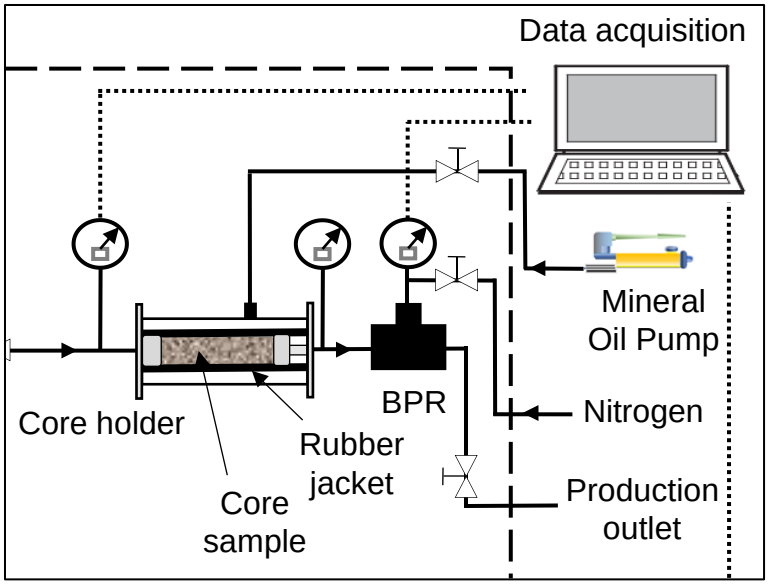

Fig. 3.4 Schematic of the core holder assembly for HnP in fractured samples and CO_2 flooding experiments

3.2.4 Wettability

Fig. 3.5 depicts the schematic of the Core Lab IFT-10 model we used in our experiments, which was designed to measure both interfacial tension and contact angle under high pressure, up to 10,000 psi, and high temperature, up to 315°F. The key components of this apparatus are a manual pump, two floating piston accumulators used to pressurize and inject the surrounding phase and the droplet phase, a visual cell in which we placed the core chunk and injected the fluids, a thermocouple to set the desired temperature, a camera with a light source, and a PC with droplet image analysis software.

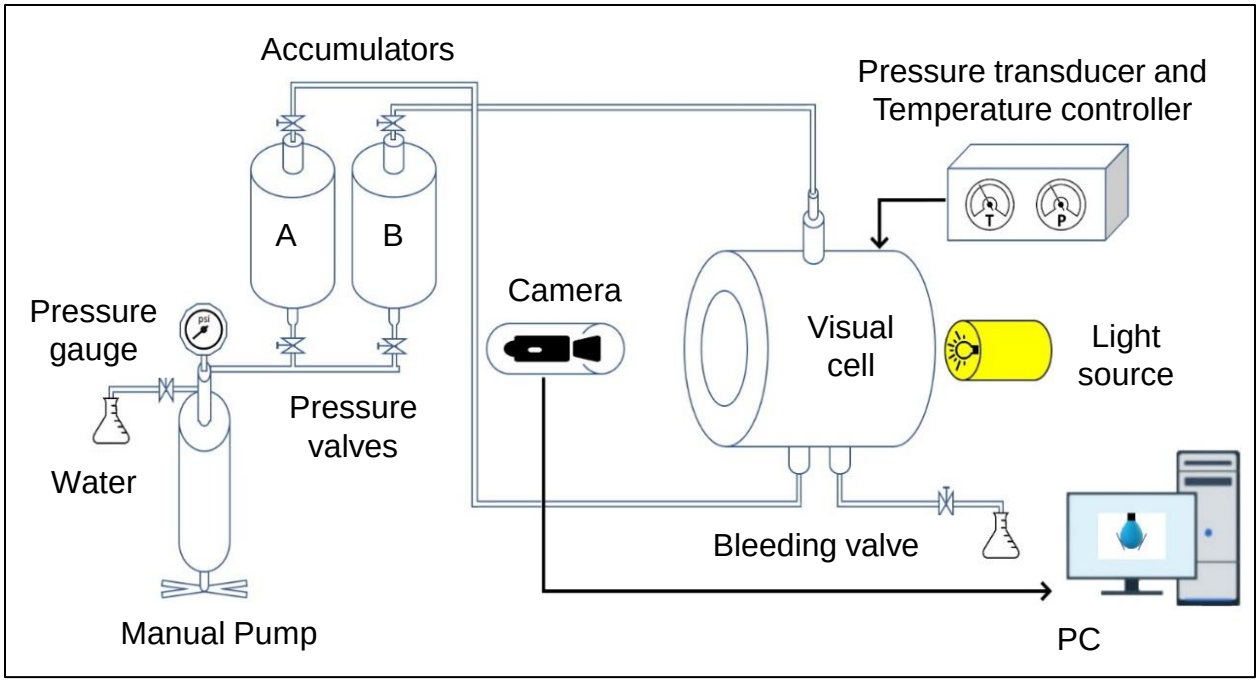

Fig. 3.5 Schematic of the contact angle measurement equipment

3.2.5 Nuclear Magnetic Resonance

Nuclear magnetic resonance (NMR) was used to characterize pore fluid distribution within the rocks. An Oxford Instruments GeoSpec2 core analyzer coupled with Green Imaging Technology software was used to acquire the NMR transverse relaxation measurements. Porosity geometry and pore sizes distribution were acquired from NMR transverse relaxation (T_2) analysis. NMR T_2 results were used to estimate pore size distributions and to classify them into micropore, mesopore, and macropore, based on unconventional T_2 cut-off.

3.3 Summary

In this Chapter, we presented the sampling location and depicted the different experimental designs used in this study.

In the next Chapter we present the evaluation of the effect of cyclic CO_2 injection parameters on oil recovery from MB and TF samples.

Chapter 4

Optimization of CO_2 Huff-n-Puff Parameters

Several research studies and pilot tests reported that the Huff-n-Puff injection technique helps overcome the limitations of continuous gas injection in gas EOR applications in unconventional reservoirs. As described in the previous chapters, the HnP cycle consists of three fundamental steps: 1) gas injection to reach a set downhole pressure, 2) shut-in period to allow the injected gas to soak, and 3) reopening for production. Therefore, in cyclic injection, a single well is used to perform a preset number of HnP cycles.

In this Chapter, we evaluate the effect of CO_2 Huff-n-Puff injection parameters (injection pressure, soaking time, and the number of cycles) on oil recovery using MB and TF rock samples. We first introduce the methodology used in this work, then present and discuss the experimental results

obtained using different injection pressures and multiple soaking times. Finally, the effect of increasing the number of cycles on oil recovery is investigated and discussed.

4.1 Methodology

Four rock samples were selected to represent the target formations in Mountrail County, ND. They were retrieved from two different wells in Parshall and Robinson Lake fields. Two samples from each well were collected to represent the Middle Bakken member and Three Forks formation, respectively. The oil samples were also collected from the same location of the selected wells. The properties of the selected rock samples are listed in Table 5.

Table 5 Properties of rock samples used to investigate the effect of CO_2 HnP parameters

Sample ID	Well	Formation	Diameter (in)	Length (in)	Porosity (%)	Permeability (mD)
MB#1	W1	Middle Bakken	1	3.8	2.6	0.005
TF#1	W1	Three Forks	1	4	8.21	0.178
MB#2	W2	Middle Bakken	1	4	7	0.0017
TF#2	W2	Three Forks	1	3.25	8.3	1.83

Fluid properties and interactions can be strongly affected by temperature. All CO_2 injection and saturation experiments were performed at the actual reservoir temperature of 213 °F. The experimental setup used to conduct CO_2 HnP experiments is illustrated in Fig. 3.3.

In this part of the study, we performed several CO_2 injection tests to evaluate the effect of injection pressure, soaking time, and the number of HnP cycles on oil recovery from MB and TF rock samples. The rock samples were initially cleaned and saturated with crude oil. After each experiment, the tested rock plugs were re-cleaned and re-saturated with oil before starting the next

CO_2 injection test. First, the samples MB#1 and TF#1 were used to measure the oil recovery after CO_2 HnP using a soaking time of 24 hours and different injection pressures of 880, 1500, 3300, 3750, and 4500 psi. The same samples were used to assess the effect of soaking time on oil recovery. Five HnP tests were performed at the same injection pressure of 3750 psi and soaking times of 3, 10, 17, 31, and 38 hours. After selecting the optimum injection pressure and soaking time, the samples MB#1, MB#2, TF#1, and TF#2 were re-cleaned re-saturated and to conduct six successive CO_2 HnP cycles for each sample.

4.2 Effect of Injection Pressure

Different studies have estimated the CO_2 MMP in the Bakken, and the values can vary from 2600 to 3300 psi, depending on the location of the oil sample used and the measuring method [3,35,55,56]. Fig. 4.1 presents the measured oil recovery factor using CO_2 HnP below, Near, and above MMP.

The tests performed at 880 psi and 1500 psi are considered below MMP and yielded recovery factors of 5.3% and 12.4% for the MB sample and 6.8% and 19.2% for the TF sample, respectively. CO_2 injection at miscible conditions is represented using an injection pressure of 3300 psi, which resulted in recovering 23.9% from the MB sample and 35.7% from the TF sample. To study the effect of increasing the pressure above MMP, CO_2 was injected at 3750 psi and 4500 psi, which tremendously increased the oil recovery to 41.2% and 46.1% for the MB sample and 48.4% and 57.9% for the TF sample, respectively.

Our results indicate that the injection pressure considerably impacts oil mobilization in tight formations. Also, it highlights the importance of achieving miscibility between CO_2 and reservoir fluids. Furthermore, the results suggest that increasing the pressure above MMP leads to incremental oil recovery. Previous experimental studies performed on Eagle Ford and Barnett

shales reported similar observations [30,31,33]. The authors indicated that increasing the pressure above MMP can promote the vaporizing gas drive mechanism and multiple contact miscibility. Menzie [57] performed oil CO_2 multi-exposure experiments at different pressure conditions and found that increasing the injection pressure leads to increasing the capacity of CO_2 to dissolve oil. Another possible explanation is the increase of the contribution of viscous forces to oil recovery when the injection pressure is increased above MMP. It enables CO_2 to sweep more pore volume and promotes its access to the micro-pores, which are the most dominant in this type of rock.

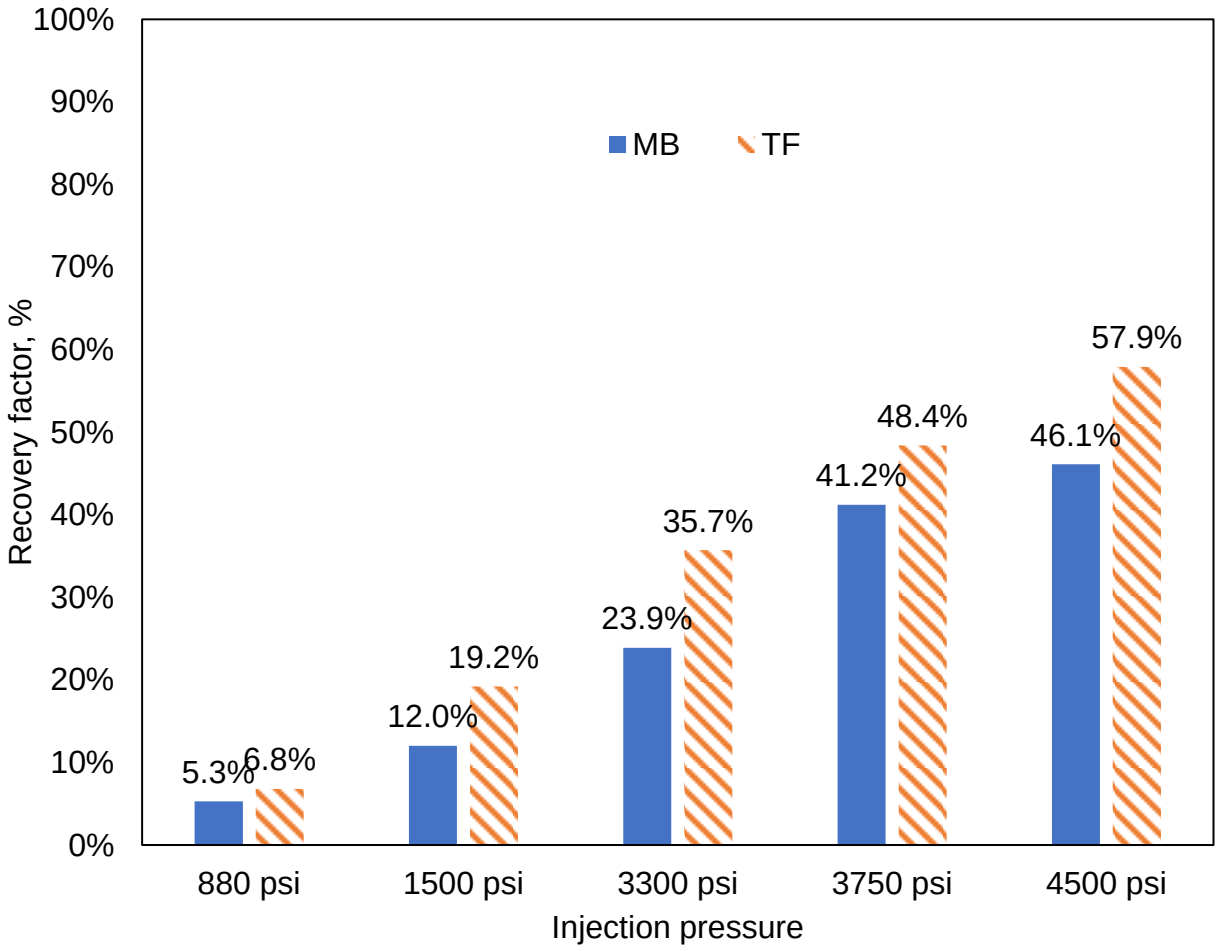

Fig. 4.1 Recovery factors of MB and TF samples after on CO_2 HnP cycle at different injection pressures and using the same soaking period of 24 hours

4.3 Effect of Soaking Time

There are different concepts proposed in the literature to describe the oil recovery mechanism in tight formations; however, it is clear that the injected CO_2 could not permeate a rock matrix with nano-Darcy permeability via convective flux [58,59]. Several researchers suggested that concentration-driven molecular diffusion can control the oil recovery at some stages of oil mobilization using CO_2 injection [58,60–63]. Thereby, the soaking time during a HnP injection is a key parameter that needs to be optimized. Fig. 4.2 presents the oil recovery factors from MB and TF samples after a CO_2 HnP cycle at 3750 psi and different soaking times.

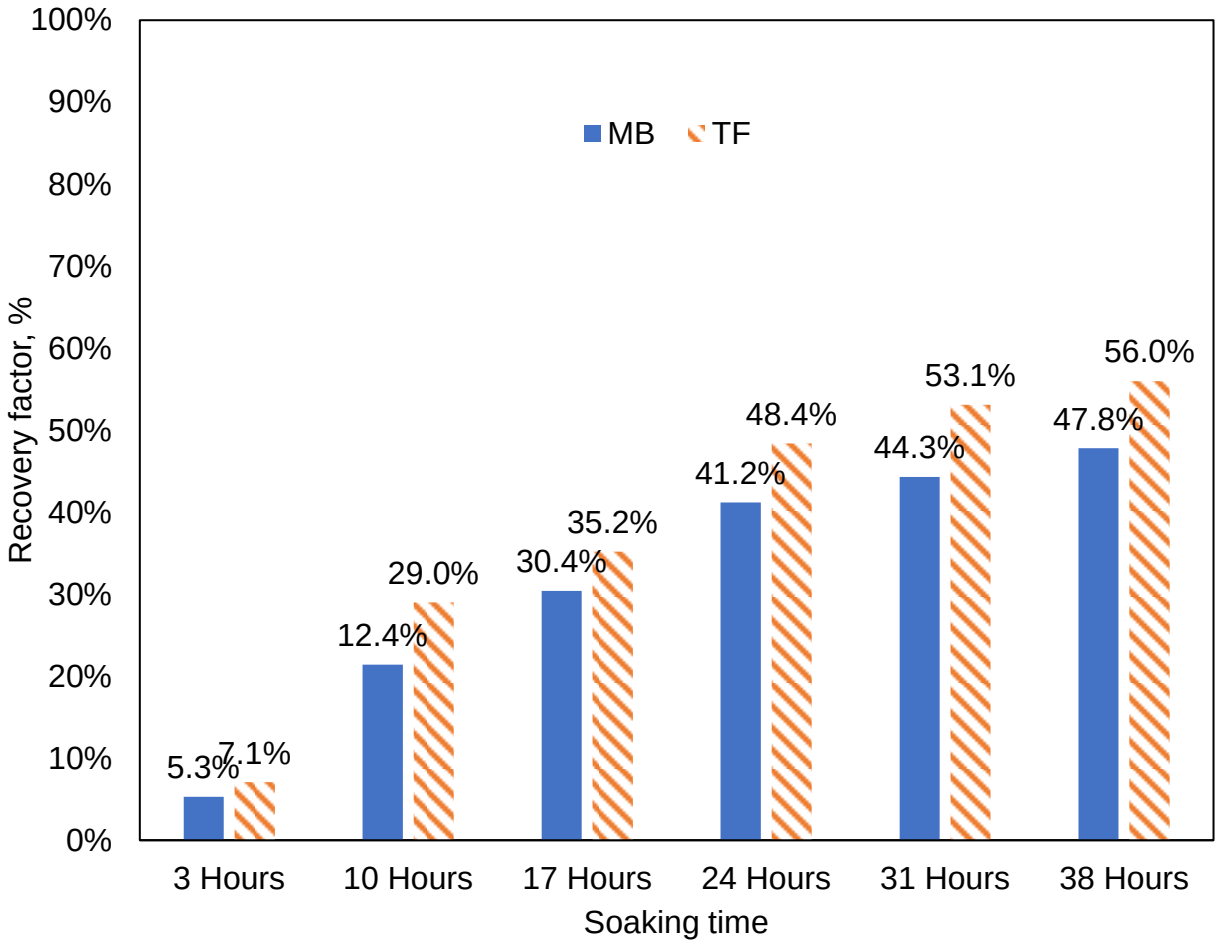

Fig. 4.2 Recovery factors of MB and TF samples after one CO_2 HnP cycle at different soaking periods and using the same injection pressure of 3750 psi

The results clearly suggest that increasing the soaking time to a specific threshold can exceedingly increase the oil recovery from ultra-tight rock samples. For a soaking time of 3, 10, 17, 24, 31, and 38 hours CO_2 recovered 5.3, 12.4, 30.4, 41.2, 44.3, 47.8% of the OOIP for the MB sample and 7.1, 29.0, 35.2, 48.4, 53.1, and 56.0% for the TF sample, respectively.

Increasing the soaking time from 3 to 24 hours resulted in an incremental oil recovery of 35.9% and 41.3 % of the OOIP from the MB and TF samples, respectively, which reflects the kinetics of molecular diffusion that is known as a relatively slow process. Nevertheless, increasing the soaking time beyond 24 hours did not result in remarkable additional oil recovery. Only 6.6% and 7.6% of the OOIP were incrementally recovered by increasing the soaking time from 24 to 38 hours. These results indicate that the concentration gradient between the sample surface and near-surface zone decreases drastically after approximately 24 hours of soaking, which slows further the CO_2 diffusion in the rock, and consequently reduces the oil recovery efficiency.

4.4 Effect of Number of Injection Cycles

After identifying the optimum injection pressure and soaking time for CO_2 HnP in MB and TF samples, we studied the performance of multicyclic CO_2 injection by performing six successive HnP cycles for each MB and TF sample. Prior to CO_2 injection tests, all the rock samples were cleaned and re-saturated with oil. Fig. 4.3 illustrates the cumulative oil recovery factors after six CO_2 HnP cycles performed at 3750 psi and 24 hours of soaking for each cycle. As mentioned above, all the experiments were performed at the reservoir temperature of 213°F. The ultimate oil recovery factors after the sixth cycle for the samples MB#1, MB#2, TF#1, and TF#2 were 61.3, 64.8, 73.0, and 68.3%, respectively. The permeability of the TF samples is two to three degrees of

magnitude higher than the MB samples, which might explain the slightly larger oil recovery factors obtained for those samples.

The results show that the oil recovery performance of the injected CO_2 diminishes after each cycle and the oil recovery curves exhibit a plateau after the second cycle for all the tested samples. Most of the cyclic CO_2 injection studies in the literature reported similar observations, where the CO_2 oil recovery capacity significantly decreases after each HnP cycle [16,28,32,37–39,64,65]. The equilibrium partitioning mechanism controls oil solubility in the injected gas, and the dissolved oil concentration in the gas-dominated phase diminishes after each sequential exposure to the injected CO_2. This fundamental limitation of cyclic CO_2 injection will be further discussed in Chapter 7.

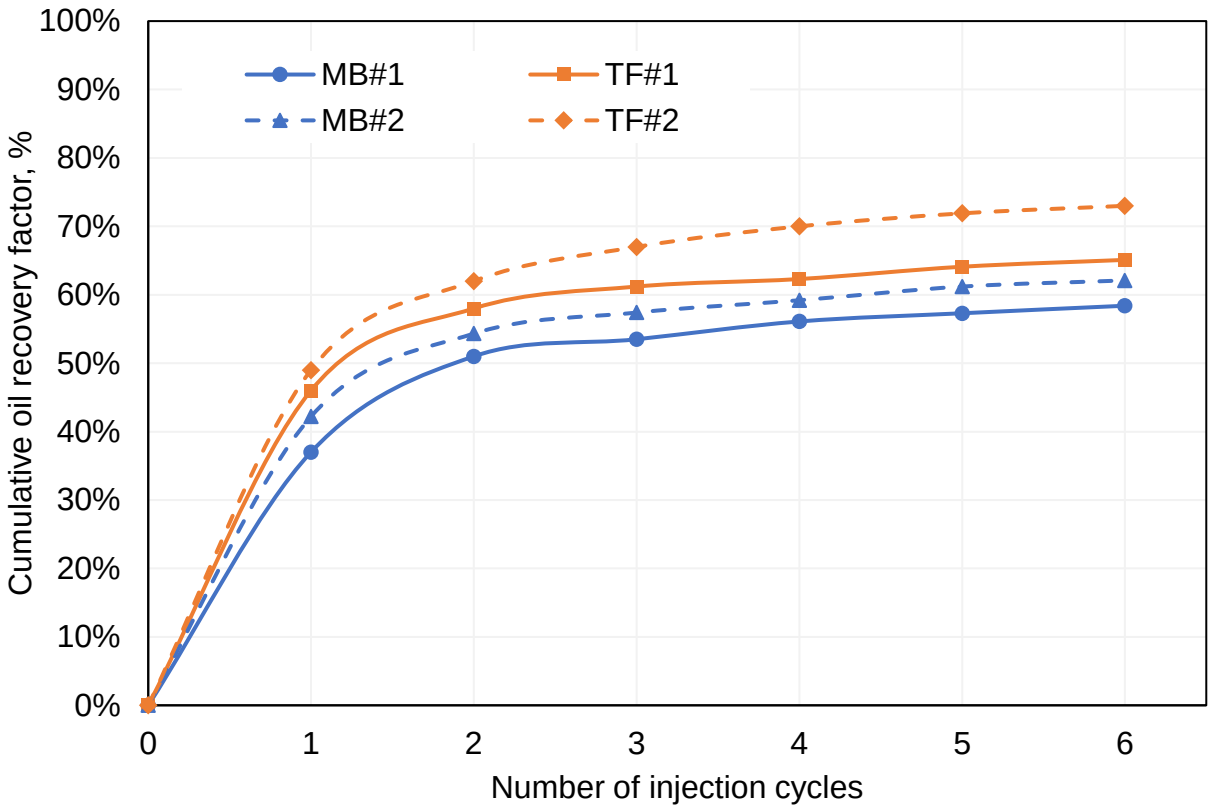

Fig. 4.3 Cumulative oil recovery factors of MB and TF samples after six successive CO_2 HnP cycles at 3750 psi and 24 hours soaking

4.5 Summary

The effect of injection pressure and soaking time was evaluated in this Chapter. The experimental results showed that increasing the injection pressure above MMP can help recover more oil from tight rock samples. Also, a soaking time of 24 hours was determined as the optimum value for one CO_2 HnP cycle using MB and TF samples. The results of multicyclic CO_2 injection indicate that the CO_2 performance decreases drastically after the second HnP cycle.

In the next Chapter, we present the results of the experimental parametric study that was conducted to understand the effect of different parameters on oil recovery using CO_2 HnP.

Chapter 5

Experimental Parametric Study in The Bakken

Very little work has been performed to investigate the difference between field results and the antecedent simulation and experimental studies despite the disappointing results from the different CO_2 pilot tests in the Bakken. Alfarge et al. [34] investigated oil recovery delay after CO_2 pilot tests in unconventional reservoirs by combining production data analysis for different pilot tests with numerical simulation to identify the controlling mechanisms of oil recovery. The authors determined that molecular diffusion is the governing mechanism in shale formations, which causes a delayed response in incremental oil recovery after CO_2 injection. To the best of our knowledge no previous work has examined the effect of water presence in the fractures, nor the effect of fracture size on CO_2 performance in tight formations, even though these effects are key factors in hydraulically fractured unconventional reservoirs. In this Chapter, we have addressed the gap

between the results of the recent pilot tests and previous research studies in the Bakken by conducting an extensive parametric study to examine and understand the effects of a series of key parameters, such as sample size, water presence, fracture size, and CO_2 injection scheme, on CO_2 EOR in unconventional reservoirs.

5.1 Methodology

To expand our understanding of CO_2 performance in MB and TF, in this study, we examined the effect of other parameters on oil recovery by comparing the recovery factor obtained after each experiment. Table 6 lists the properties of the core plugs used in this study. Fig. 5.1 and Fig. 5.2 illustrate the experimental workflow used to perform the parametric study. We cut two plugs with different dimensions from the same Middle Bakken core slab: MB#3 and MB#4 (Fig. 5.1). Similarly, TF#3 and TF#4 were cut from the same Three Forks core.

Table 6 Properties of rock samples used in the CO_2 parametric study

Sample Number	Formation/Member	Length (in)	Diameter (in)	Porosity (%)	Permeability (md)
MB#3	Middle Bakken	3.35	1.0	4	0.001
MB#4	Middle Bakken	3.35	1.5	4	0.001
TF#3	Three Forks	3.35	1.0	5	0.930
TF#4	Three Forks	3.35	1.5	5	0.930
MB#5	Middle Bakken	3.00	1.5	4	0.006
TF#5	Three Forks	3.00	1.5	9	1.040

MB#3 and MB#4 were placed simultaneously in the core holder after cleaning and saturation, then we performed one CO_2 HnP cycle to determine the recovery factor. The same steps were repeated

to measure the oil recovery for TF#3 and TF#4. We compared the recovery factors obtained in this step to examine the effect of sample size on CO_2 performance.

The MB and TF samples with the highest recovery factor after Test (I) were re-saturated then placed in the core holder. We filled 30% of the fracture space, or the void volume in the core holder, with Bakken brine collected from the field before injecting CO_2. We compared the recovery factors measured after Test (II) with the previous experiment to investigate the effect of water-presence in the fracture space.

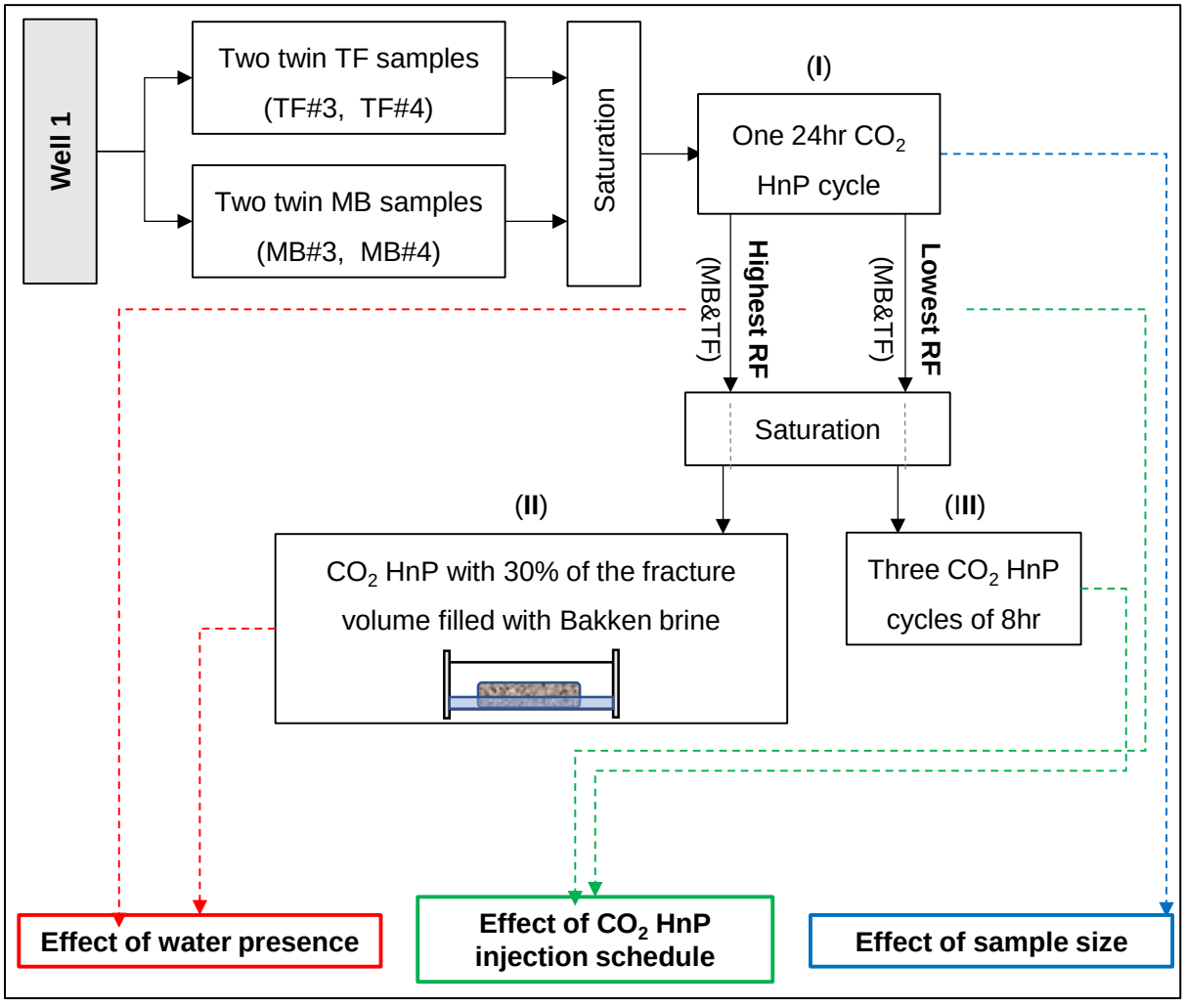

Fig. 5.1 Experimental workflow schematic part 1: investigation of the effects of sample size, water presence, and CO_2 HnP injection schedule

We present the experimental workflow of the second part of this parametric study in Fig. 5.2. CO_2 was injected in relatively large volumes around samples to simulate fracture/matrix systems in almost all previous HnP shale experiments that can be found in the literature [20]. Large amounts of CO_2 around the sample surface might not represent the conditions in unconventional reservoirs, where the fracture volume limits the amount of CO_2 that can sweep and interact with the rock matrix during the EOR process. Therefore, we examined the effect of reducing the CO_2 volume that surrounds the sample during the HnP experiment.

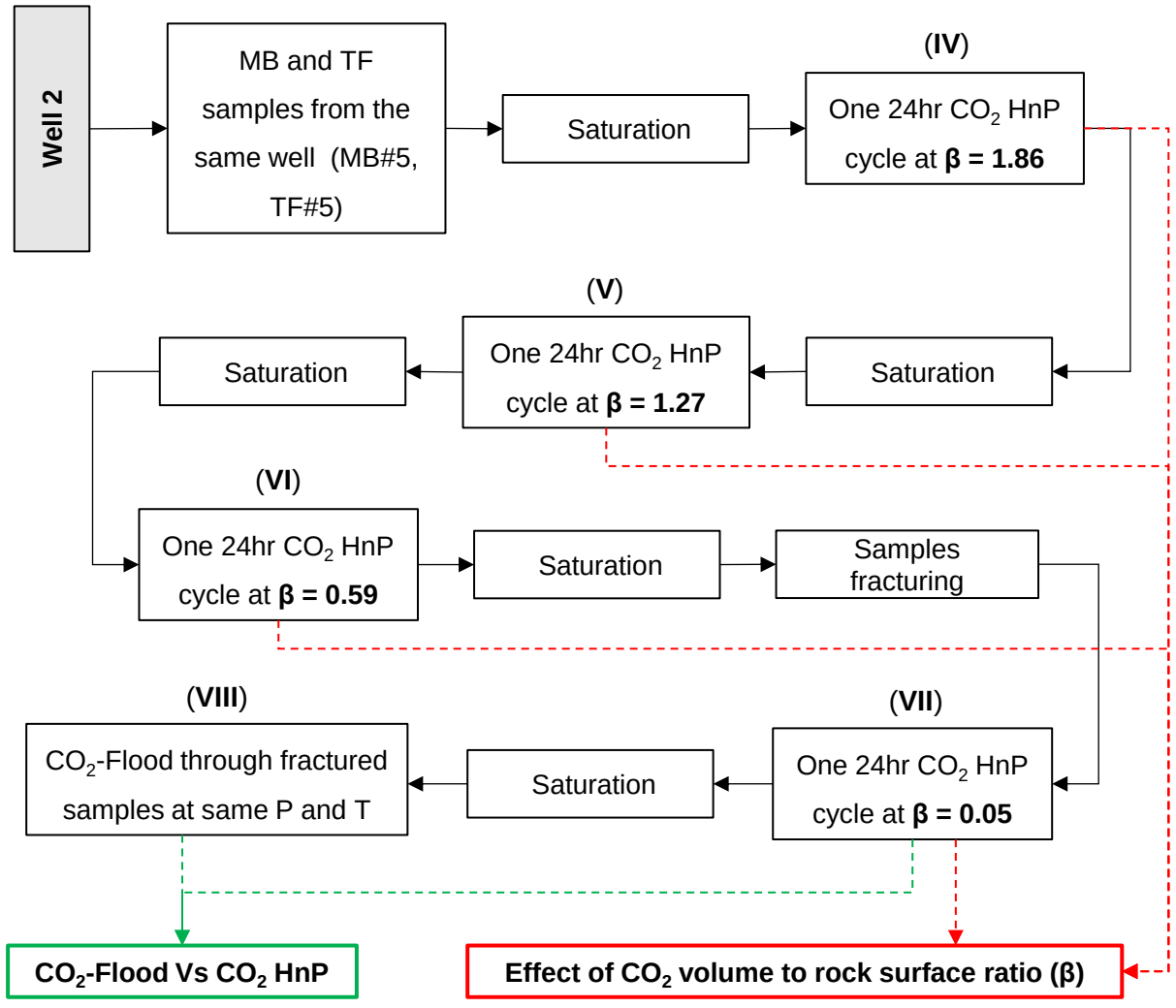

Fig. 5.2 Experimental workflow schematic part 2: investigation of the effect of CO_2 volume to rock surface ratio and comparing CO_2 flood to CO_2 HnP

We used the ratio of the volume available in the core chamber for the permeation of CO_2 into the rock matrix to the rock sample surface, or the Beta ratio (β), as an indicator for each experiment. The samples MB#5 and TF#5 were cut from the MB and TF core slabs of the second well, respectively. Each sample was subjected to one CO_2 HnP cycle with a soaking time of 24 hours (Test (IV)) after cleaning and saturation. We continued to reduce the Beta ratio and subject the cores to a CO_2 HnP cycle to measure the recovery factor for Tests (V) and (VI) (Fig. 5.2). We then fractured the rock samples (see Fig. 5.3) to reach a lower value of the Beta ratio. The oil recovery factors for CO_2 HnP (Test (VII)) and CO_2 flooding (Test (VIII)) were measured and compared. HnP and continuous flooding tests were performed at the same temperature, injection pressure, and CO_2 exposure time.

Fig. 5.3 Photos of the fractured MB#5 and TF#5 samples

5.2 Effect of Sample Size

Unconventional reservoirs are typically characterized by ultra-small pore sizes [66,67], which may lead to the assumption that small samples can represent the pore sizes distribution. Reducing the experimental time and targeting a quicker oil recovery response are other reasons to use samples with relatively small sizes for CO_2 EOR experimental studies in tight formations [37,39].

Jin et al. [39] measured the oil recovery factor using CO_2 HnP for MB and TF samples with similar properties to those used in this study. The tested cores had a bulk volume of 3.8 cc, and the recovery factor was measured after seven hours of soaking time with an injection pressure of 5,000 psi. Hawthorne et al. [37] used the same experimental parameters to test Middle Bakken cores with three different sizes and shapes: cylindrical rods (3.14 cc), square rods (2.43 cc), and small rock

chips (0.24 cc). We used twin samples with bulk volumes of, 97.01 cc and 43.11 cc, from each target formation to investigate the effect of sample size and measured the recovery factor after one CO_2 HnP at 3,750 psi and 24 hours of soaking. Fig. 5.4 illustrates the recovery factor under similar conditions for the MB and TF samples, including the cores tested in this study and results found in the literature.

MB#3 had a recovery factor of 59.8%, while MB#4 had a factor of 35.5% after soaking for 24 hours. We recovered 68.5% from the smaller TF sample, TF#3, and 54.6% from TF#4. Jin et al. [39] obtained recovery factors of 81.5% and 95% for MB and TF cores, respectively, with seven hours of soaking time. Hawthorn et al. (2013) had high oil recovery factors of 87%, 91%, and 97% for MB samples with bulk volumes of 3.14 cc, 2.4 cc, and 0.24 cc, respectively, with the same soaking time. The results indicate that the use of smaller samples leads to an overestimation of CO_2 performance in the lab. The portion of the oil adsorbed on the core surface might be higher than the oil volume imbibed in the pores after saturation for samples with relatively small bulk volumes, such as chicklets or small diameter rods, which explains previous lab results that reported high recovery factors after just a few hours of CO_2 exposure.

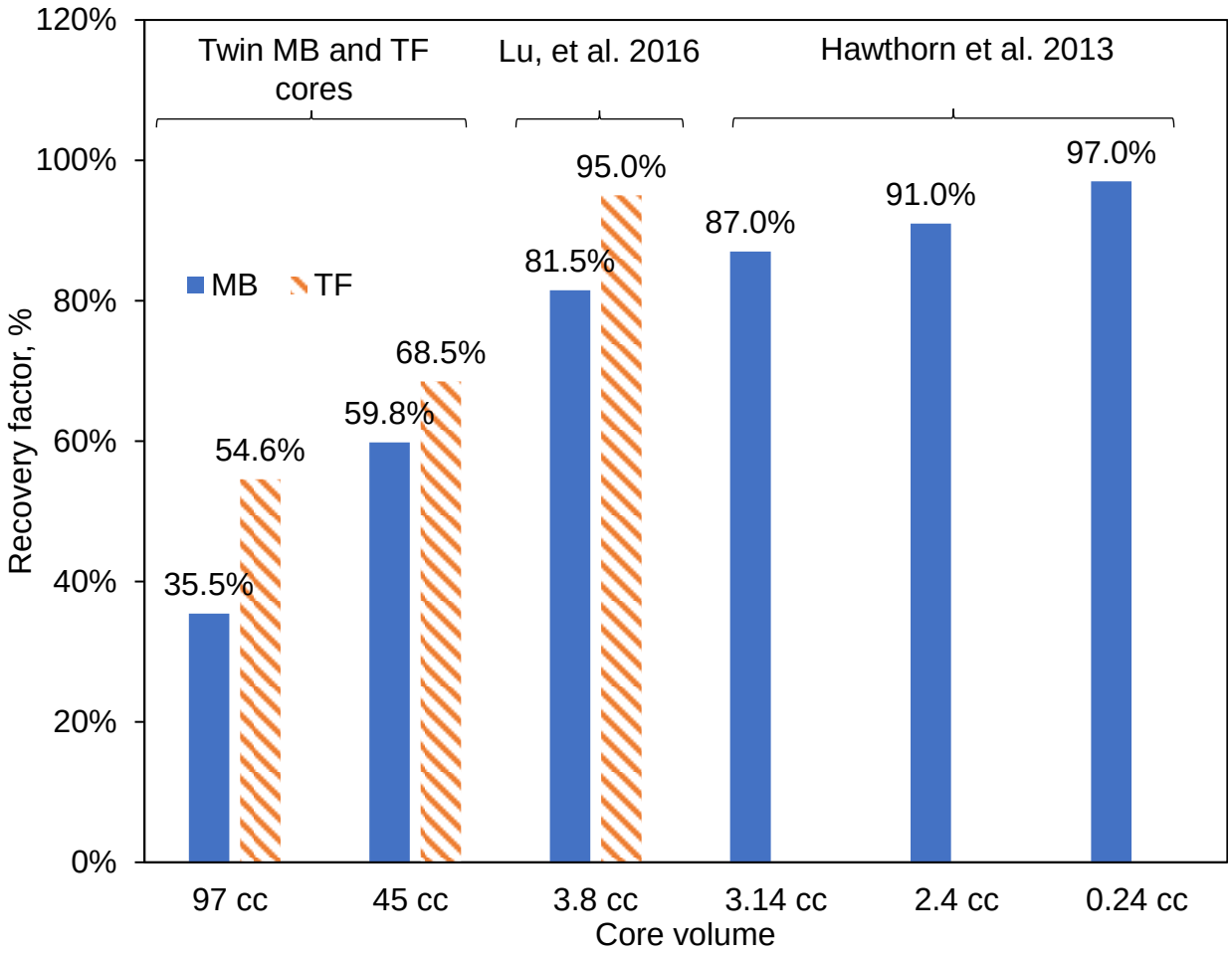

Fig. 5.4 Oil recovery factors for MB and TF samples of different sizes

5.3 Effect of CO_2 HnP Injection Schedule

We used samples MB#4 and TF#4, which had the lowest recovery factors after the previous injection test, for Test (II) to investigate the effect of changing the injection schedule on CO_2 HnP performance. MB#4 and TF#4 had recovery factors of 35.5% and 54.6%, respectively, after one HnP cycle with 24 hours of soaking time. The samples were re-saturated, then subjected to three successive HnP cycles each with eight hours of soaking time.

The solid blue line curve in Fig. 5.5 represents the recovery factor for MB#4 after one HnP cycle with 24 hours of soaking time, and the dashed blue line represents the recovery factor after HnP

cycles with eight hours of soaking in CO_2. CO_2 HnP yielded a recovery of 28% after the first eight hours, then after the second and third cycles the recovery increased to 36% and 45%, respectively. 54.6% was recovered from sample TF#4 after one cycle with 24 hours of soaking (solid orange line), while the recovery factor after the first, second, and third HnP cycles, with eight hours of soaking, were 41%, 56%, and 71%, respectively (dashed orange line).

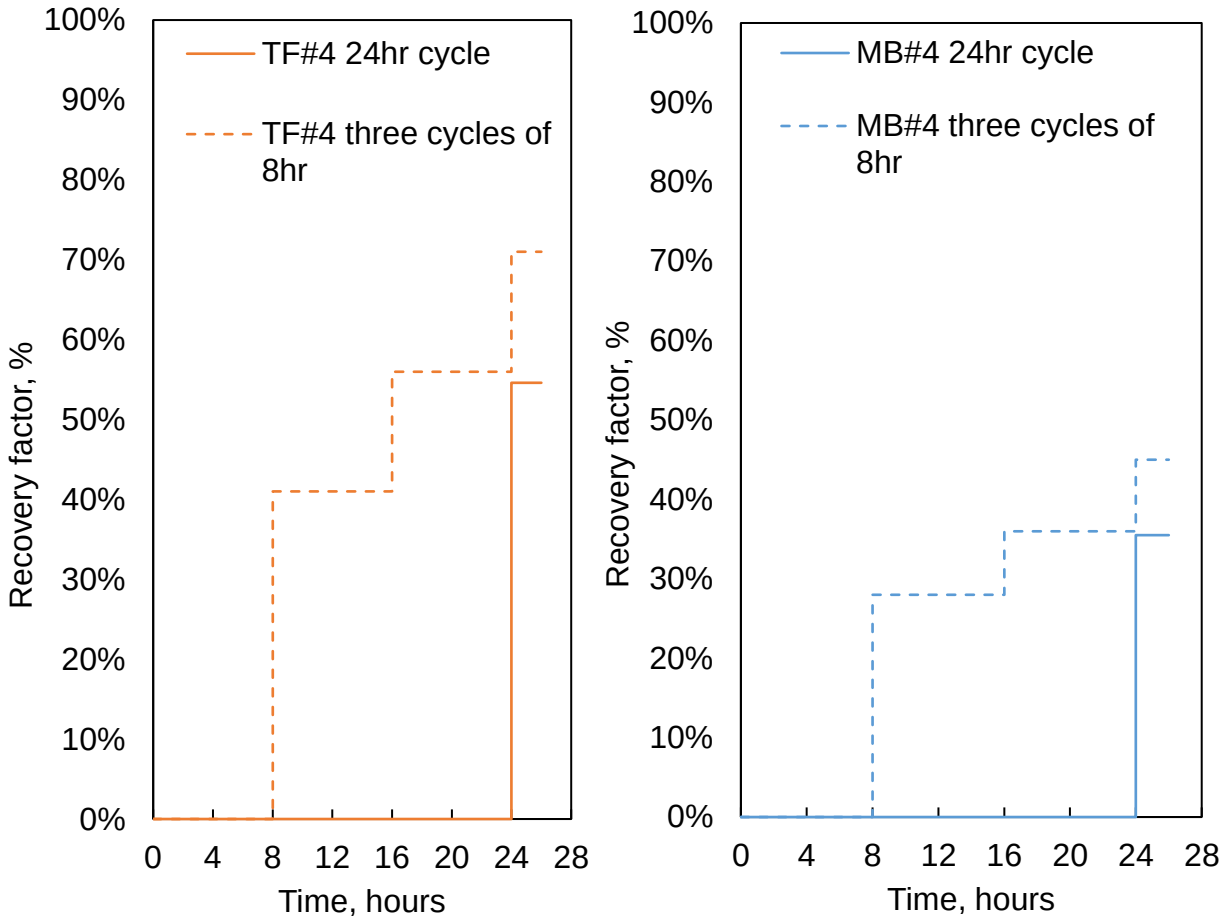

Fig. 5.5 Oil recovery factors for MB#4 (right) and TF#4 (left) after one CO_2 HnP with 24 hours of soaking (solid lines) and three cycles with eight hours of soaking time (dashed line).

The total CO_2 exposure time was the same for Tests (I) and (II); however, Test (II) was subdivided into three different cycles, resulting in recovering 9.5% more oil for sample MB#4 and 16.4% for TF#4 compared to the one soaking cycle of 24 hours in Test (I).

Several researchers reported that diffusion is the primary mechanism for oil recovery using CO_2 injection in tight formations [35,59,63,68,69]. Our results suggest that the pressure gradient drives the rock permeation of the injected CO_2 in the early stages of the soaking period, causing the rock to swell and mobilizing some of the oil toward the bulk CO_2 surrounding the sample. The CO_2 pressure gradient subsequently declines, and concentration gradient diffusion drives oil production from the pores into the fractures filled with CO_2. Molecular diffusion is a slow process and becomes slower as the concentration gradient gets smaller once a portion of the oil is extracted near the fracture. Splitting the 24 hours of soaking into three HnP cycles, that were eight hours long each, resulted in exposing the rock to new pressure and concentration gradients. This new exposure allowed us to recover more oil compared to the oil recovered when the core was allowed to soak in CO_2 for 24 hours, where diffusion drove the oil production for an extended period at a slow rate.

5.4 Effect of Water Presence

Different factors may contribute to an increase of the water cut in Bakken wells, such as expanding the production area, which leads to drilling wells in regions with relatively higher water saturation, and massive fracturing activities. We simulated the accumulation of the mobile water in the lower portion of the fracture that may occur in such reservoirs for Experiment (III). We performed a CO_2 HnP test using samples MB#3 and TF#3, which had the highest recovery factor after Experiment (I). We filled a portion of the fracture space, or void volume, with formation brine before starting CO_2 injection after loading the sample in the core holder.

The results presented in Fig. 5.6 indicate that the oil recovery factor for MB#3 decreased from 59.8% in Test (I) to 18.6% when brine was present in the fracture, and from 68.5% to 39.8% for the Three Forks sample TF#3. The significant decrease in oil recovery indicates that water

presence can severely impact CO_2 EOR performance. The water accumulating in the fracture can cover a portion of the rock and impede its contact with the injected gas, reducing oil recovery.

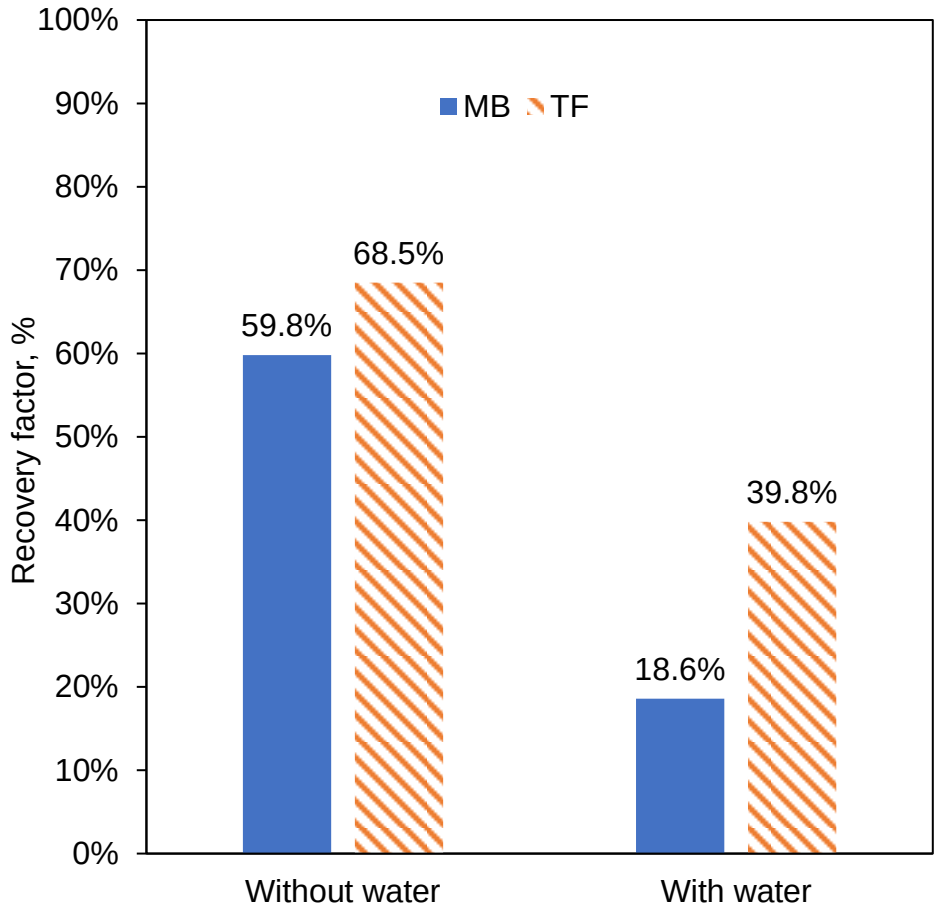

Fig. 5.6 Oil recovery factors for MB#3 and TF#3 with and without water presence

5.5 Effect of CO_2 Volume to the Exposed Rock Surface

The common practice in CO_2 HnP lab studies consists of placing a core sample in a vessel to inject a certain amount of CO_2 specified by the design of the apparatus in use. In tight formations, the rock matrix is characterized by an ultralow permeability, and the injected fluid is limited to the volume of the fractures to permeate the rock surfaces; therefore, the CO_2 abundance around the sample can be an important parameter that affects the reliability of the experimental results. We

continued to reduce the void volume in the core chamber for Experiments (IV) through (VI) to evaluate the impact of reducing the CO_2 volume surrounding the sample with cyclic injection experiments. At the final stage, in experiment (VII), we created a longitudinal fracture through the sample to reach lower volume to surface ratios and simulate the reservoir conditions (see Fig. 5.3). Fig. 5.7 presents the change in oil recovery for samples MB#5 and TF#5 at different β values. The results indicate that reducing β after each experiment resulted in decreased CO_2 performance in the same samples. The recovery factor of the TF plug was 56%, 49.7%, 35.1%, and 25.7% for CO_2 volume to rock surface ratios of 1.86, 1.27, 0.6, and 0.05, respectively. The oil recovery for the MB sample was also negatively impacted, and the recovery factor decreased from 35.5% to 31.3%, 23%, and 13.6% for the same β ratios used in the TF sample experiments.

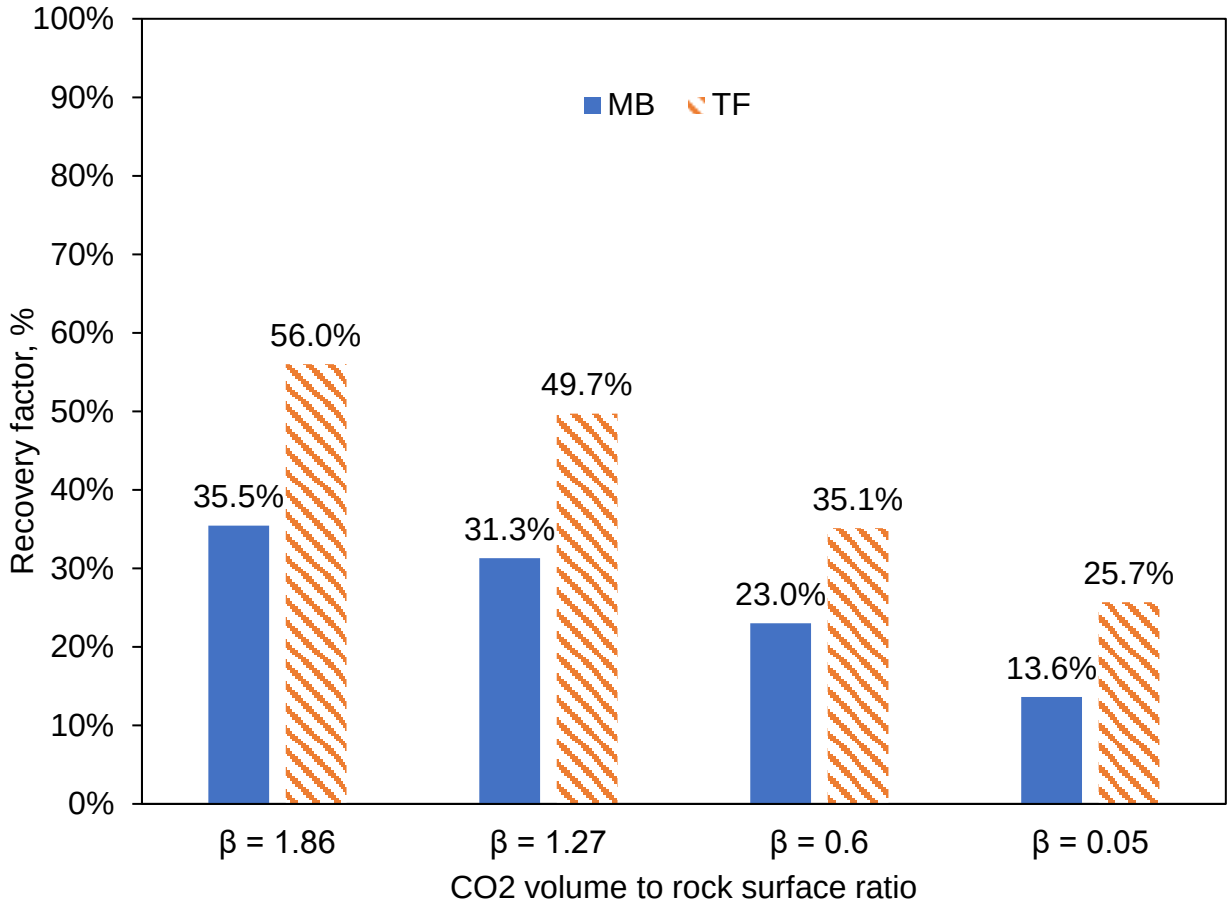

Fig. 5.7 Oil recovery factors with different CO_2 volume to exposed rock surface ratios for the MB#5 and TF#5 samples

This test illustrates that the performance of a CO_2 EOR application is related to the amount of CO_2 that can permeate the rock sample and interact with the fluids in place, which is consistent with the results of previous experiments in this study. Reducing the volume of CO_2 in contact with the rock surface while keeping the same injection pressure in each scenario will have two main consequences: 1) quicker depletion of the CO_2 concentration gradient that leads to a less effective molecular diffusion, and 2) less CO_2 to maintain the pressure in the fracture, which limits the contribution of viscous forces to CO_2 imbibition and oil mobilization.

The outcomes of this test suggest that the standard experimental procedure used to evaluate cyclic injection, which consists of submerging the core sample into a relatively large volume of CO_2 [28,37,38,65,70], can lead to optimistic results and an oil recovery overestimation.

5.6 CO_2 Flooding Vs HnP in Fractured Samples

CO_2 flooding in consolidated MB and TF samples can be very challenging and impossible in some cores. In this work, it was possible to perform a CO_2 flood experiment and compare the results with the previous HnP test for the same samples after they were fractured during Test (VII).

The results displayed in Fig. 5.8 indicate that HnP outperforms the flooding technique in both MB and TF fractured plugs. The recovery factor for the fractured TF and MB samples after CO_2 HnP was 25.7% and 13.6%, respectively. We recovered 13.1% and 5.2% of the OOIP during the CO_2 flood test for the TF and MB samples, respectively, after re-saturating them. The high contrast in permeability between the fractures and rock matrix in both samples causes poor sweep and displacement efficiency. A CO_2 breakthrough was detected during the flood experiment: after 15 minutes for the MB sample and 38 minutes for the TF sample. On the other hand, the HnP injection schedule provided more time for the injected CO_2 to permeate the rock matrix.

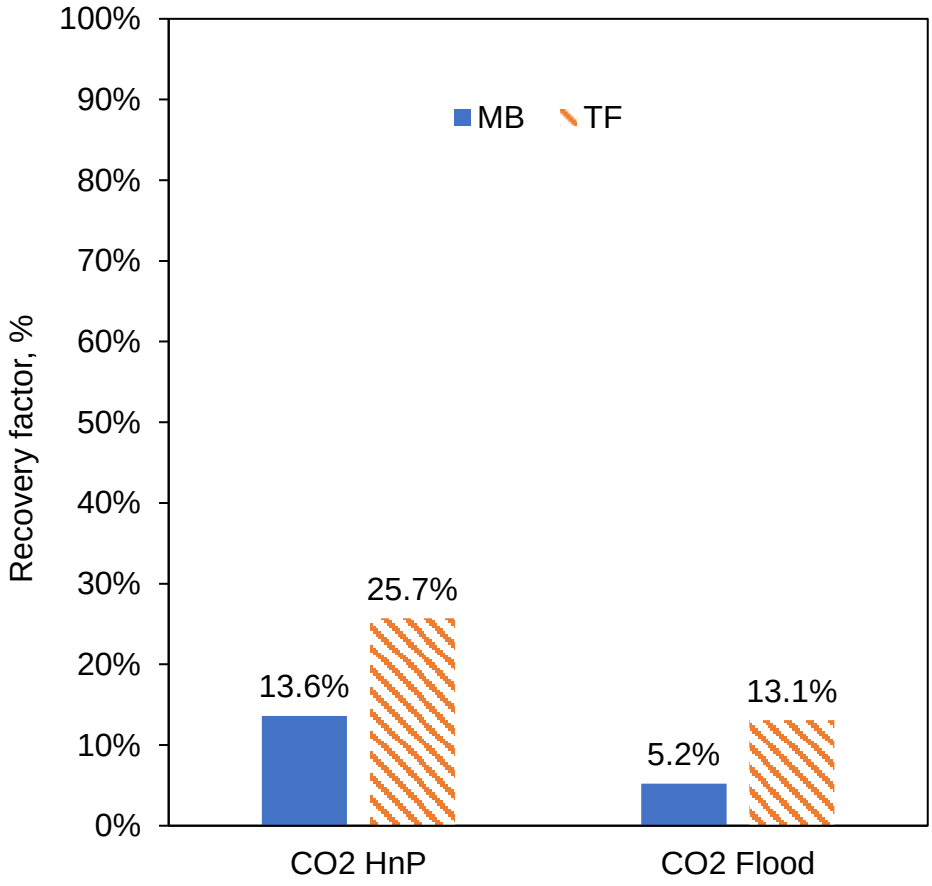

Fig. 5.8 Oil recovery factors after CO_2 HnP and flood through fractured MB and TF samples

5.7 Summary

We evaluated the effects of different parameters on oil recovery using CO_2 injection experiments in Middle Bakken and Three Forks samples. This comprehensive study provides a better understanding of how to enhance oil recovery in the Bakken effectively. Several observations were revealed by the experimental results, which could be used to enlighten future EOR design:

- The size of the tested samples has an important impact on EOR experiments. The selection of smaller samples can lead to overestimating the potential of CO_2 EOR and oil recovery. We recommend using samples that are large enough to represent fluid flow in the reservoir and represent its heterogeneity.

- Splitting one HnP cycle into three successive cycles allowed us to recover 10 % and 17% more oil from the same MB and TF samples, respectively. These results suggest that both viscous forces and molecular diffusion control oil recovery. The pressure gradient initially pushes CO_2 into larger pores and promotes its penetration, then diffusion controls oil extraction toward the bulk CO_2 volume surrounding the rock.
- Water accumulated in the fracture can impede the contact between CO_2 and the reservoir rock, which results in reduced oil recovery. Water presence significantly impacted CO_2 performance: the measured recovery factor decreased from 59.8% to 18.6% for the MB sample and from 68.5% to 39.8% for the TF sample.
- The ratio of the volume surrounding the sample to the sample surface needs to be considered carefully and should represent reservoir conditions for cyclic injection experiments in tight samples. The experimental results indicated that submerging a core sample in a relatively large CO_2 volume can overestimate subsequent oil recovery.
- It became possible to test a CO_2 flooding scheme and compare its performance to HnP under similar conditions using fractured tight formation samples. Cyclic injection outperformed the flooding process, which was limited by low sweep efficiency and early breakthrough.

In the next Chapter, we present the effect of CO_2 injection on different reservoir attributes in unconventional plays.

Chapter 6

Evaluation of CO_2 Injection Side Effects

This Chapter aims to provide insight into property alteration in unconventional reservoirs that might occur due to CO_2 injection and to improve the understanding of those mechanisms. We present the evaluation of the potential side effects of CO_2 injection related to rock wettability, pore size distribution, and effective porosity. Two Middle Bakken (MB) and two Three Forks (TF) formation samples were tested to investigate changes in rock wettability, Pore Size Distribution (PSD), and effective porosity before and after exposure to CO_2. We used the contact angle technique to measure the wettability state with and without CO_2 exposure. The Nuclear Magnetic Resonance (NMR) spectroscopy technique was used to determine fluid distribution before and after CO_2 injection.

6.1 Background

As depicted in previous Chapters, CO_2 injection can assist with extracting residual oil and overcoming injectivity problems in tight formations [71]; however, its interactions with the *in-situ* reservoir fluids and rock minerals can affect some reservoir attributes and must be evaluated. The interaction of the injected CO_2 with the oil in place can result in asphaltene precipitation, which can cause pore plugging and reduce reservoir permeability [72,73]. Some chemical reactions may also occur when CO_2 is in contact with brine and rock minerals [74]. The possible reactions that can take place in water-containing oil reservoirs include [74–80]:

$$CO_2+H_2O \leftrightarrow H_2CO_3 \quad (1)$$

$$H_2CO_3 \leftrightarrow H^+ + HCO_3^- \quad (2)$$

$$2H^+ + CaMg(CO_3)_2(\text{dolomite}) \leftrightarrow Mg^{2+} + Ca^{2+} + 2HCO_3^- \quad (3)$$

$$H^+ + CaCO_3(\text{Calcite}) \leftrightarrow Ca^{2+} + HCO_3^- \quad (4)$$

$$2KAlSi_3O_8(\text{Potash feldspar}) + 2H^+ + 9H_2O \rightarrow Al_2Si_2O_5(OH)_4(\text{Kaolinite}) + 2k^+ + 4H_4SiO_4 \quad (5)$$

$$2NaAlSi_3O_8(\text{Albite}) + 3H_2O + 2CO_2 \rightarrow Al_2Si_2O_5(OH)_4 + 4SiO_2 + 2Na^+ + 2HCO_3^- \quad (6)$$

$$CaAlSi_3O_8(\text{Anorthite}) + H_2CO_3 + H_2O \rightarrow CaCO_3 + Al_2Si_2O_5(OH)_4 \quad (7)$$

The injected CO_2 can dissolve into the formation brine and form a weak acid solution (Equation (1)), which will decompose into bicarbonate and hydrogen ions (Equation (2)). The acid solution can dissolve some of the existing minerals (Equations (3) to (7)) such as dolomite, calcite, and feldspar. New pores may be created as a result of these reactions, and others might be plugged by formed precipitates, such as carbonate and kaolinite [79,80].

Previous studies have been conducted to evaluate possible CO_2-induced petrophysical property changes in oil reservoirs. The impact of these CO_2-rock-fluid interactions on oil reservoir attributes

can vary based on the characteristics of the reservoir of interest, the tested oil's properties, and the experimental conditions. Contradictory results have been reported: some studies reported that CO_2 can negatively affect the petrophysical properties of the reservoir [76,78,79,81–83], while others observed an improvement in porosity and permeability [77,80,84–88].

Numerous studies have been performed to evaluate the effect of CO_2 injection and asphaltene deposition on rock permeability, however, the CO_2 induced changes of wettability, PSD, and effective porosity are seldomly discussed. Very little research has been performed to investigate those changes in unconventional plays compared to conventional reservoirs, and no previous work has investigated the side effects of CO_2 injection into the Bakken to the best of our knowledge.

An alteration of the wettability state can have a huge impact on oil displacement in the reservoir [89,90]. A change of the PSD or the porosity can impact future field development plans and needs to be assessed in advance. Thus, a thorough understanding of the side effects of CO_2 injection on those parameters is fundamental for evaluating the performance of CO_2 EOR applications. In this work, we compared the wettability state of the rock before and after CO_2 exposure, and investigated the possible changes in fluid distribution and PSD after CO_2 Huff-n-Puff (HnP). Since there is no agreement in the literature regarding the effect of CO_2 injection on the pore volume of the rock, we evaluated the porosity changes before and after CO_2 exposure using representative MB and TF rock samples. This study aims to provide insight into property alteration in unconventional reservoirs that might occur due to CO_2 injection and improve the understanding of those mechanisms. The reported results help understand the potential side effects of CO_2 injection in tight formations and can be used to enlighten future EOR projects.

6.2 Methodology

6.2.1 Materials

We retrieved two twin MB and TF samples (MB#6, MB#6*, TF#6, and TF#6*) from the first well. We used one more MB and TF sample (MB#7 and TF#7) from the second well for experiment repeatability purposes. The brine and dead oil samples were collected from each sampled well. Table 7 lists the properties of the cores as received. We cut two identical disc-shaped chunks (Ca. 1*1*0.3 cm) from each sample for the contact angle measurements, denoted as MB#6c1, MB#6c2, MB#7c1, MB#7c2, TF#6c1, TF#6c2, TF#7c1, and TF#7c2.

We used the X-Ray Diffraction (XRD) technique to determine the mineralogical composition of each sample so we could analyze the results of the experiments performed in this study and understand the effect of the CO_2 reactions with the core minerals. The XRD results, summarized in Table 8, indicate that carbonate minerals such as calcite and dolomite, feldspar, quartz, and clays are the dominant minerals in our samples. The MB samples have a higher calcite content than dolomite, while the latter is the primary component of both TF samples.

Table 7 Properties of rock samples used to investigate CO_2 injection side effects

Sample ID	Formation	Length (in)	Diameter (in)	Permeability (mD)	Oil Saturation (%)	Water Saturation (%)
MB#6 / MB#6*	Middle Bakken	4.0	1.0	0.009	30.8	28.4
TF#6 / TF#6*	Three Forks	4.2	1.0	0.130	30.9	26.4
MB#7	Middle Bakken	4.2	1.0	0.002	51.5	22.7
TF#7	Three Forks	4.0	1.0	0.183	59.9	11.4

Table 8 Mineralogical composition of the MB and TF samples

Sample ID	Calcite (%)	Dolomite (%)	Feldspar (%)	Clays (%)	Anhydrite (%)	Quartz (%)	Pyrite (%)
MB#6	20.20	8.43	13.80	7.30	10.90	37.42	2.00
TF#6	1.10	53.00	0.40	23.00	1.00	19.80	3.40
MB#7	48.90	10.80	14.70	3.53	1.30	20.63	0.10
TF#7	2.60	46.30	21.70	5.60	6.00	17.60	0.73

6.2.2 Wettability assessment

Wettability is a reservoir attribute that defines the degree of adhesion of a fluid to the rock surface when other immiscible fluids are present, dictating the tendency of that fluid to occupy smaller pores and how much rock surface it can contact [91]; therefore, it is an important parameter that can control fluid flow and distribution in the reservoir, and its evaluation is critical for the success of any EOR technique. Several methods have been proposed to determine wettability, including USBM, Amott cell, and contact angle [91–93]. The wettability state can be determined directly by measuring the contact angle of a brine droplet on a rock surface using the contact angle method, which makes it the most appropriate technique for unconventional reservoirs due to ultralow permeability and porosity; therefore, we used this method to determine the wettability state of the MB and TF samples. Different contact angle thresholds have been proposed in the literature to determine the wetting state. We adopted the repartition in carbonate reservoirs introduced by Chilingar and Yen [94] for our experiments (see Fig. 6.1). The rock can be considered water-wet

if the contact angle of a brine droplet is between 0° and 80°, mixed-wet for values between 80° and 100°, and oil-wet when the contact angle is higher than 100°.

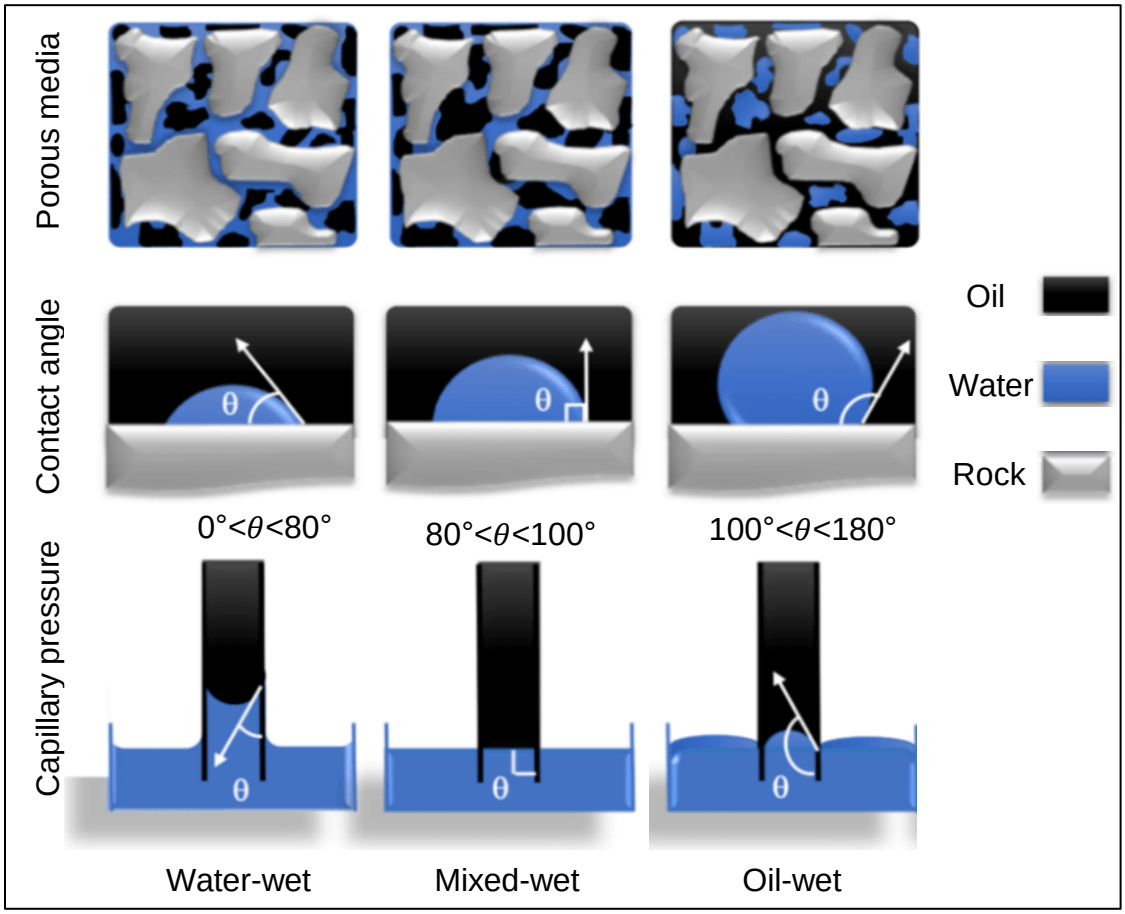

Fig. 6.1 Display of the different wettability states based on the contact angle of a water droplet (modified based on [95])

The apparatus used to measure the contact angle at different experimental conditions is presented in Fig. 3.5.

6.2.2.1 Oil brine rock system

We placed the samples MB#6c1, TF#6c1, MB#7c1, and TF#7c1 in the visual cell at the beginning of the experiment. Oil was then injected to fill the chamber and displace the existing air. The temperature was set to match the reservoir temperature of 213°F, and the system was allowed to

stabilize. The pressure was set to approximately 3,800 psi, and the brine was steadily injected through a capillary needle to generate a droplet on the rock surface, which was then allowed to stabilize before taking the final contact angle measurement. Instead of taking the contact angle measurement at a preset time, we used a different approach to ensure the stabilization of the system. The bubble shape was monitored, and the contact angle was measured every 30 minutes. The contact angle was considered stable when there was no variance among the last three values, and the final measurement was acquired.

6.2.2.2 CO_2 brine oil-saturated-rock system

We pre-saturated the samples MB#6c2, TF#6c2, MB#7c2, and TF#7c2 with oil before placing each one of them in the visual cell for this set of experiments. We then injected CO_2 into the cell and evacuated the existing air. We used the same procedure for the oil-brine system to increase the temperature to 213°F, the pressure to 3,800 psi, and generate the brine droplet on the rock surface. Several contact angle measurements were taken before obtaining the final value to make sure the system stabilized.

6.2.3 Nuclear magnetic resonance technique

Nuclear Magnetic Resonance is a technique used to detect the distribution of pore fluids in a porous media. Nuclear magnetic resonance can occur due to the oscillating magnetic field when hydrogen-containing fluids are exposed to a static magnetic field [96]. The measured transverse time (T_2) is generally affected by bulk relaxation, diffusion in magnetic gradients, and surface relaxation [96,97]; however, the diffusion relaxation can be neglected in tight formations, and the surface relaxation is correlated with the specific area of the core, which represents the ratio of the surface of the pore to the total pore volume of the sample. Transverse relaxation time T_2 is expressed as [80,98]:

$$\frac{1}{T_2}=\frac{1}{T_{2B}}+\frac{1}{T_{2S}}=\frac{1}{T_{2B}}+\rho\frac{S}{V} \qquad (8)$$

where T_2 is the transverse relaxation time (ms), T_{2B} is the transverse relaxation time due to bulk relaxation, T_{2S} is the transverse relaxation time due to surface relaxation, ρ is the relaxation rate (μm/ms), and $\frac{S}{V}$ represents the surface to volume ratio of the pore system (1/μm).

The NMR results can be used to evaluate the movable fluid porosity in low permeability reservoirs and determine the distribution of pore size across the samples. The relationship between the pore radius and T_2 spectrum can be defined as [99]:

$$r=CT_2 \qquad (9)$$

where r is the pore throat radius (μm), and C is a dimensionless proportional constant that should be determined to convert the T_2 spectrum to pore distribution.

The pore sizes can be classified into three categories: micro, meso, and macro using the unified pore size classification proposed by Zdravkov et al. [100]. The pores are considered of a macro, meso, and micro size when the pore diameter (d) >50nm, 50>d>3nm, and d < 3nm, respectively.

6.2.3.1 PSD before and after CO_2 injection

An Oxford Instruments GeoSpec2 core analyzer coupled with Green Imaging Technology software was used to acquire the NMR transverse relaxation measurements. The MB#6, TF#6, MB#7, TF#7 samples were saturated with oil and placed in the NMR instrument to measure the T_2 spectrum and determine the fluid distribution in the core. We then performed one CO_2 HnP cycle for each plug. The sample was placed in the NMR machine again to evaluate the PSD change after CO_2 injection.

6.2.3.2 Effective porosity measurement

Samples MB#6* and TF#6* were cleaned and saturated with brine to measure the change in effective porosity, then saturated with oil under high pressure to ensure that each core was 100% saturated. More details regarding the core preparation and saturation procedure can be found in our previous publications [101,102]. The cores were placed in the NMR machine to determine the initial effective porosity after saturation, then we performed a CO_2 injection cycle followed by re-saturation. The core was placed into the NMR instrument to measure the effective porosity after one HnP cycle (24 hours of soaking). The process was repeated, and four injection cycles followed by re-saturation were performed for each sample. We used the same procedure to remeasure effective porosity. These experiments are costly and are relatively time-consuming; therefore, we only tested one sample each from MB and TF.

6.3 Wettability Alteration Due to CO_2 Exposure

Fig. 6.2 and Fig. 6.3 illustrate the results of the contact angle experiments performed on the MB and TF samples with and without CO_2 exposure. The contact angle of the brine droplet submerged in oil and introduced on the MB samples MB#6c1 and MB#7c1 was 134° and 133°, respectively (Fig. 6.2 (A) and Fig. 6.3 (A)). The contact angle was 143° and 142° for the TF samples TF#6c1 and TF#7c1, respectively. These results demonstrate that both reservoirs can be characterized as oil-wet to strongly oil-wet prior to CO_2 exposure (see reservoir wettability classification in Fig. 6.1).

Fig. 6.2 (B) and Fig. 6.3 (B) illustrate that the contact angle of the brine droplet on the oil-saturated MB samples MB#6c2 and MB#7c2 dropped to 69° and 85°, respectively, after CO_2 exposure. The contact angle was 82° and 89° for the TF samples TF#6c2 and TF#7c2, respectively. These results indicate that CO_2 increased the hydrophilicity of the MB and TF samples and shifted the wettability from strongly oil-wet towards neutral- and water-wet.

Chen et al. [103] observed a contact angle shift when they introduced an oil droplet on calcite substrates in non-carbonated and carbonated brine solutions. They observed that the system became more water-wet using the carbonated brine.

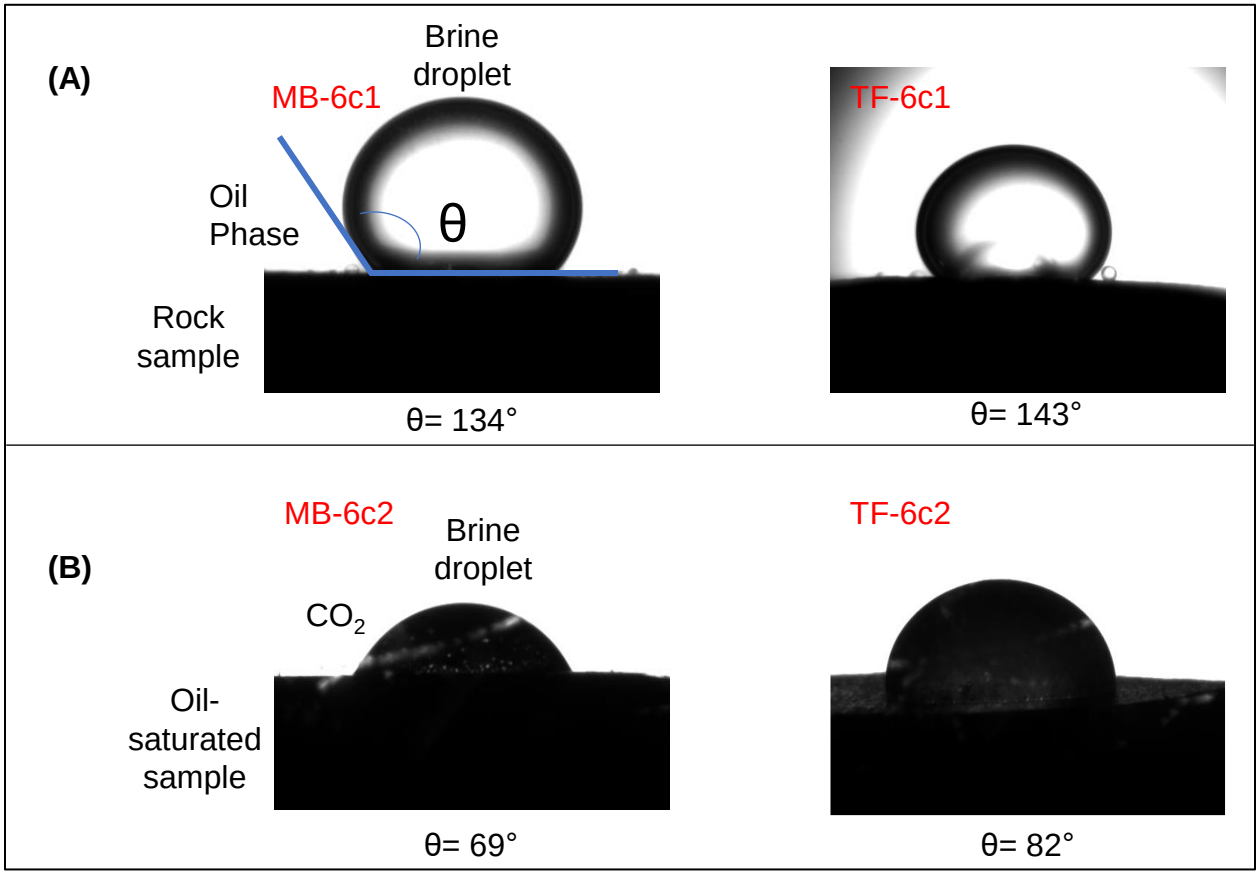

Fig. 6.2 Contact angle measurements in MB and TF samples from the first well, (A) oil/brine/rock system, and (B) CO_2/brine/oil-saturated-rock

Teklu et al. [104] used a seawater/oil/Three-Forks-sample system and found that the rock's wettability preference switched from oil-wet to water-wet when they used a mixture of seawater and CO_2. The contact angle measurements can yield important observations and determine the reservoir sample's wettability state under different conditions; however, it may not capture the complexity of the surface-fluid interactions. Closer examinations of the complex nature of wettability are needed to better understand the CO_2-induced wettability shift. Chen et al. [103]

developed a geochemical model, which coupled CO_2 dissolution, mineral dissolution, and oil and calcite surface chemistry to understand how dissolved CO_2 increases hydrophilicity. They used a quantitative measure of electrostatic attraction named the Bond Product Sum (BPS) to reflect the electrostatic force change between fluid-fluid and fluid-rock interfaces with and without CO_2. The authors determined that the BPS change after carbonate-calcite equilibrium can increase hydrophilicity, which explains the dramatic drop of the contact angle. Another possible reason for the increase of the hydrophilicity, is the CO_2 capacity to dissolve the hydrocarbons. Considering the pressure and temperature conditions of our test CO_2 is in the supercritical state, and it can dissolve the oil in place, thereby rendering the surface of the rock sample more water-wet. Adel et al., 2018 and Tovar et al., 2018 showed that CO_2 can volatilize a large portion of the hydrocarbons via gas drive mechanism. Hawthorne and Miller, 2020 indicated that when CO_2 is injected at miscible conditions, it can dissolve large volumes of the oil in place. The capacity of supercritical CO_2 to dissolve the crude oil from the interstitial pores of the rock matrix has been proven in several studies [8,29,31,106]. Displacing the oil from the rock surface toward the CO_2-dominated phase via molecular diffusion or vaporizing gas drive will expose more pores to the brine bubble, which might explain the increase of hydrophilicity after CO_2 exposure.

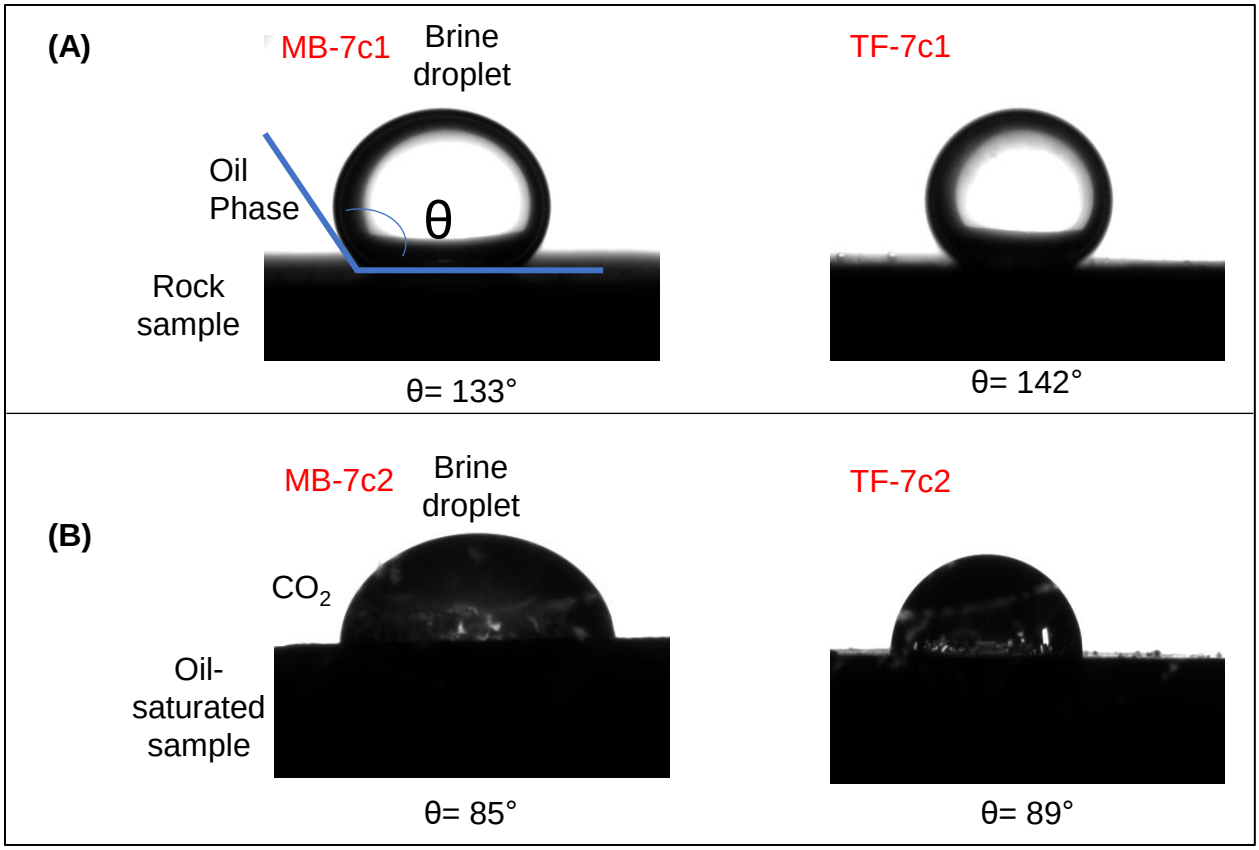

Fig. 6.3 Contact angle measurements in MB and TF samples from the second well, (A) oil/brine/rock system, and (B) CO_2/brine/oil-saturated-rock

6.4 T_2 Spectrum Change After CO_2 Injection

The NMR technique can be used to detect the distribution of hydrogen-containing fluids in a reservoir rock sample that contains water and hydrocarbons. The generated data can then be used to determine the movable fluid porosity in low-permeability reservoirs and evaluate the pore size distribution. Fig. 6.4 and Fig. 6.5 depict the T_2 spectrum of the saturated MB and TF samples before and after one CO_2 HnP cycle. The difference in the areas below the curves before and after CO_2 injection, the straight lines and squared lines, reflect the total amount of displaced fluids after the HnP cycle.

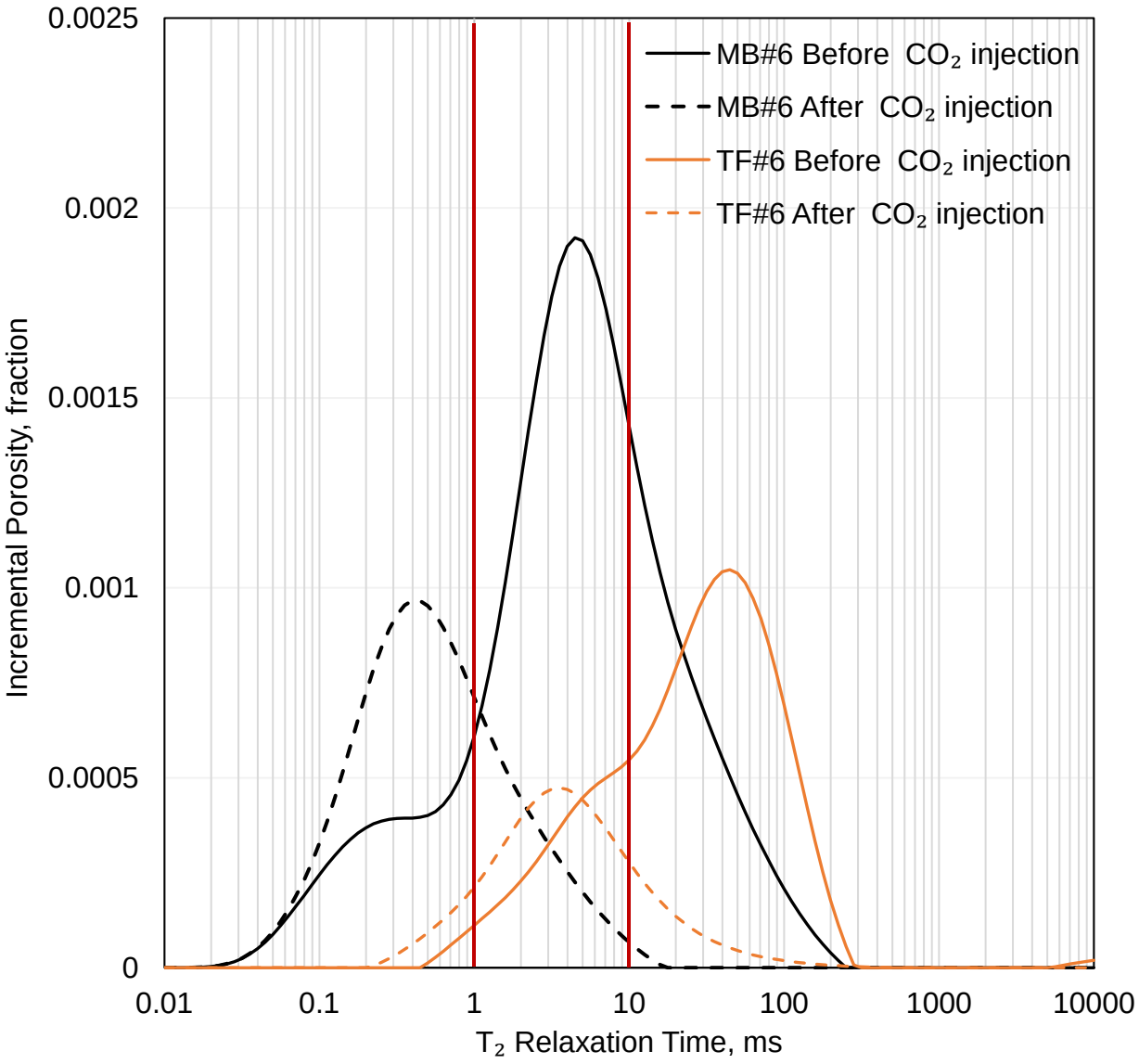

Fig. 6.4 Incremental porosity vs. T_2 Relaxation, straight black line: sample MB#6 before CO_2 injection, black-squared line: sample MB#6 after one CO_2 HnP cycle, straight orange line: sample TF#6 before CO_2 injection, orange-squared line: sample TF#6 after one CO_2 HnP cycle

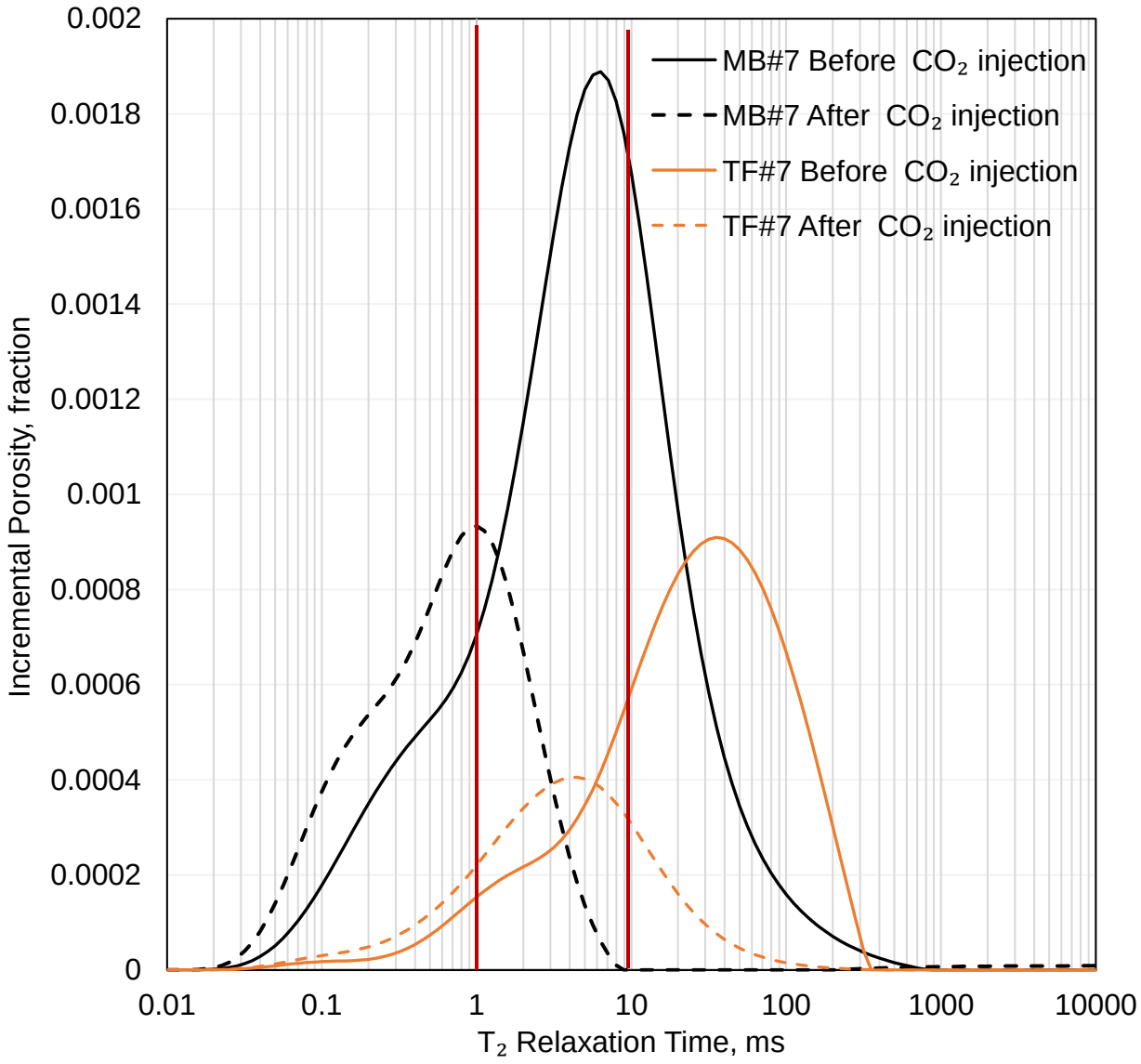

Fig. 6.5 Incremental porosity vs. T_2 Relaxation, straight black line: sample MB#7 before CO_2 injection, black-squared line: sample MB#7 after one CO_2 HnP cycle, straight orange line: sample TF#7 before CO_2 injection, orange-squared line: sample TF#7 after one CO_2 HnP cycle

All curves shifted towards smaller T_2 values after CO_2 exposure. The curve shift reflects a PSD change, and new small pore volumes were detected after CO_2 injection. We used the T_2 cutoff repartition of the different pore sizes adopted by Onwumelu et al. [67] to analyze the PSD change and partition the micro-, meso-, and macro-porosity in the Bakken samples (see Fig. 6.6).

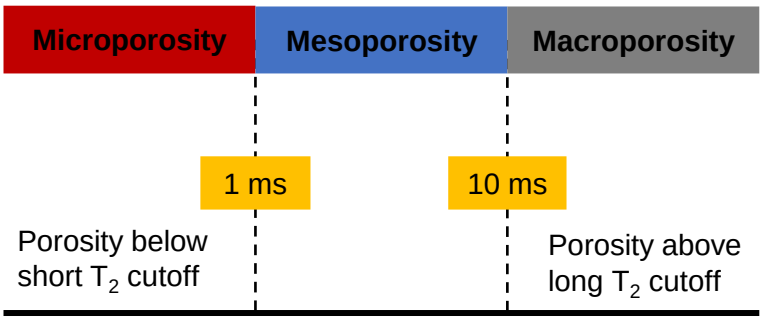

Fig. 6.6 NMR porosity partitioning in Bakken samples based on T_2 cutoffs (modified based on [67])

We calculated the percentage of each porosity type, before and after the CO_2 test, by summing the incremental porosity that falls between the corresponding T_2 cutoffs and dividing it by the initial cumulative porosity when the core was 100% saturated. Fig. 6.7 illustrates the PSD changes in our samples based on the NMR data before and after the HnP cycle. Nearly all of the fluids in the macropores were displaced and the macro-porosity decreased from 26% to 0.2 % for MB#6, 15% to 3% for MB#7, 73% to 7% for TF#6, and 27% to 1% for TF#7 after CO_2 injection. The mesopore distribution decreased for samples MB#6, MB#7, and TF#7 by 44%, 37%, and 21%, respectively. We expect that CO_2 will displace a portion of the fluids in place and "clean" some pores. Those empty pores will not be detected in the NMR after the injection test, explaining the decrease in macro- and meso-porosity; however, the meso-porosity of sample TF#7 increased by 2% after CO_2 exposure and the total volume of the micropores increased for all tested samples. The micro-porosity increased by 14%, 25%, 3%, and 8% for samples MB#6, MB#7, TF#6, and TF#7, respectively. The initial NMR results before CO_2 injection reflect the total pore volume initially saturated with brine and hydrocarbons. The increase in micro-porosity after CO_2 HnP is the result of pushing a portion of the fluids in place toward those pores instead of displacing it toward the fracture volume.

The XRD results (Table 8) indicate that calcite and dolomite are the primary mineral constituents of our samples. The acid solution generated from the reaction of the injected CO_2 with the brine in the core can dissolve some of those minerals, resulting in the creation of new tiny-pore volumes (Equations (1(1) through (7)).

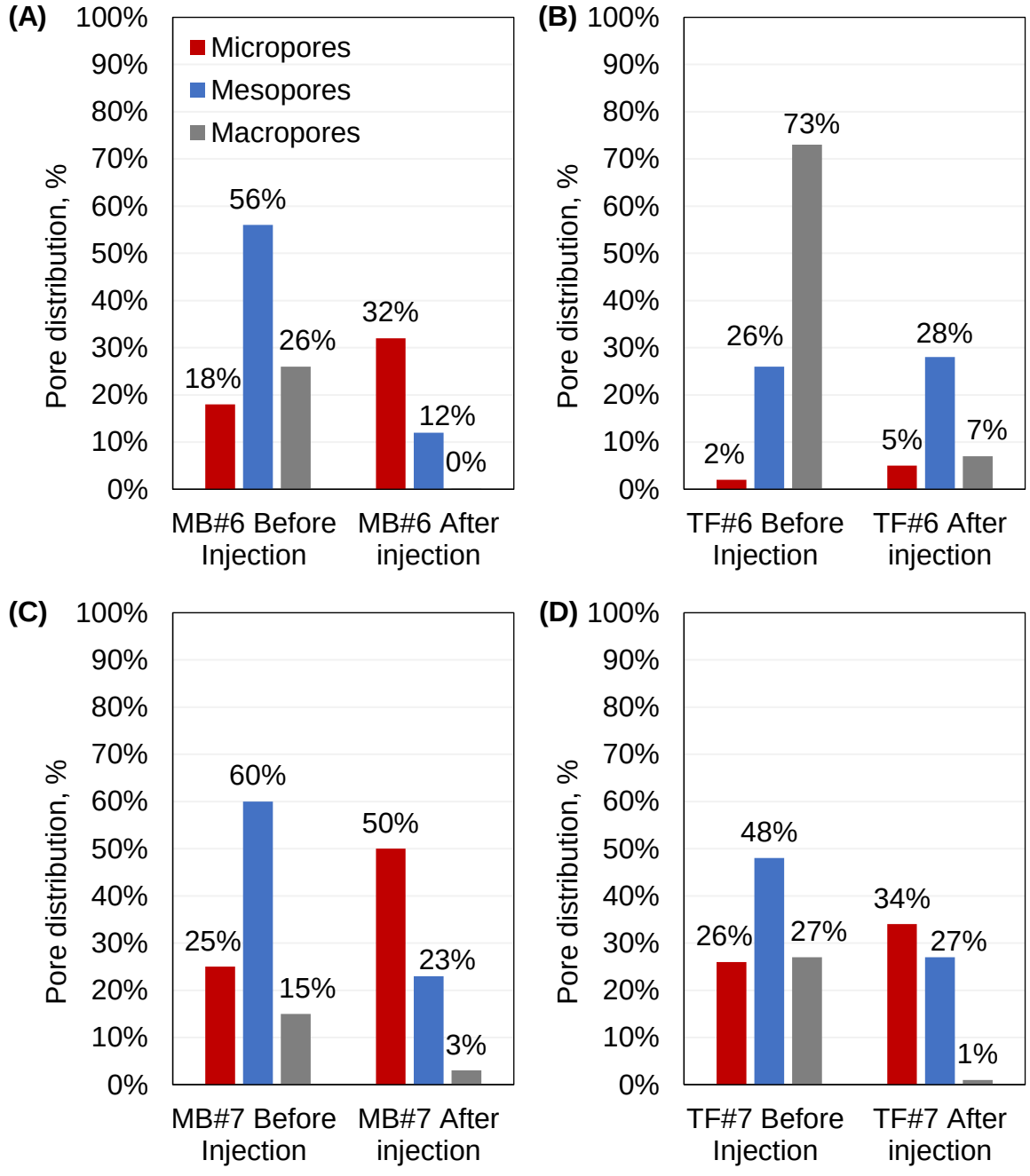

Fig. 6.7 Distribution of pore sizes before and after one CO_2 HnP, (A): MB#6, (B): TF#6, (C): MB#7, (D) TF#7

The "new" pores must be filled with hydrogen-containing fluids to be detected in the NMR, which confirms that the injected CO_2 displaced a portion of the reservoir fluids toward the rock matrix. A closer examination using a high-resolution Computed Tomography Scanner (CT-Scan) is recommended to characterize the pore microstructure change after CO_2 exposure better, even though the NMR results were very informative.

6.5 Variation of Effective Porosity After CO_2 HnP

We used the NMR technique to determine the initial cumulative porosity of each sample after cleaning and saturation with oil and brine. Four CO_2 HnP cycles were performed, and the core was re-saturated with oil after each cycle to remeasure the effective porosity before the next injection test. Fig. 6.8 illustrates the effective porosity changes after multiple CO_2 HnP cycles. The effective porosity of the MB sample was reduced from 5.3% to 4.8%, 4.4%, 4.2, and 3.8% after the 1^{st}, 2^{nd}, 3^{rd}, and 4^{th} injection cycles, respectively. The TF samples' effective porosity was reduced from 7.6% to 7%, 6.9 %, 6.7%, and 6.3%. Equations (5),(6), and (7) describe the different precipitates, kaolinite and calcite, that can form when dissolved CO_2 reacts with the core minerals; therefore, the minerals on the pore walls can react with carbonic acid to form precipitates, reducing pore volume. These precipitates may consequently plug some of the pore volumes, resulting in a decrease of the total pore volume of the core. Moreover, the alternative change of the effective stress induced by cyclic CO_2 injection can result in damaging a portion of the pore volume.

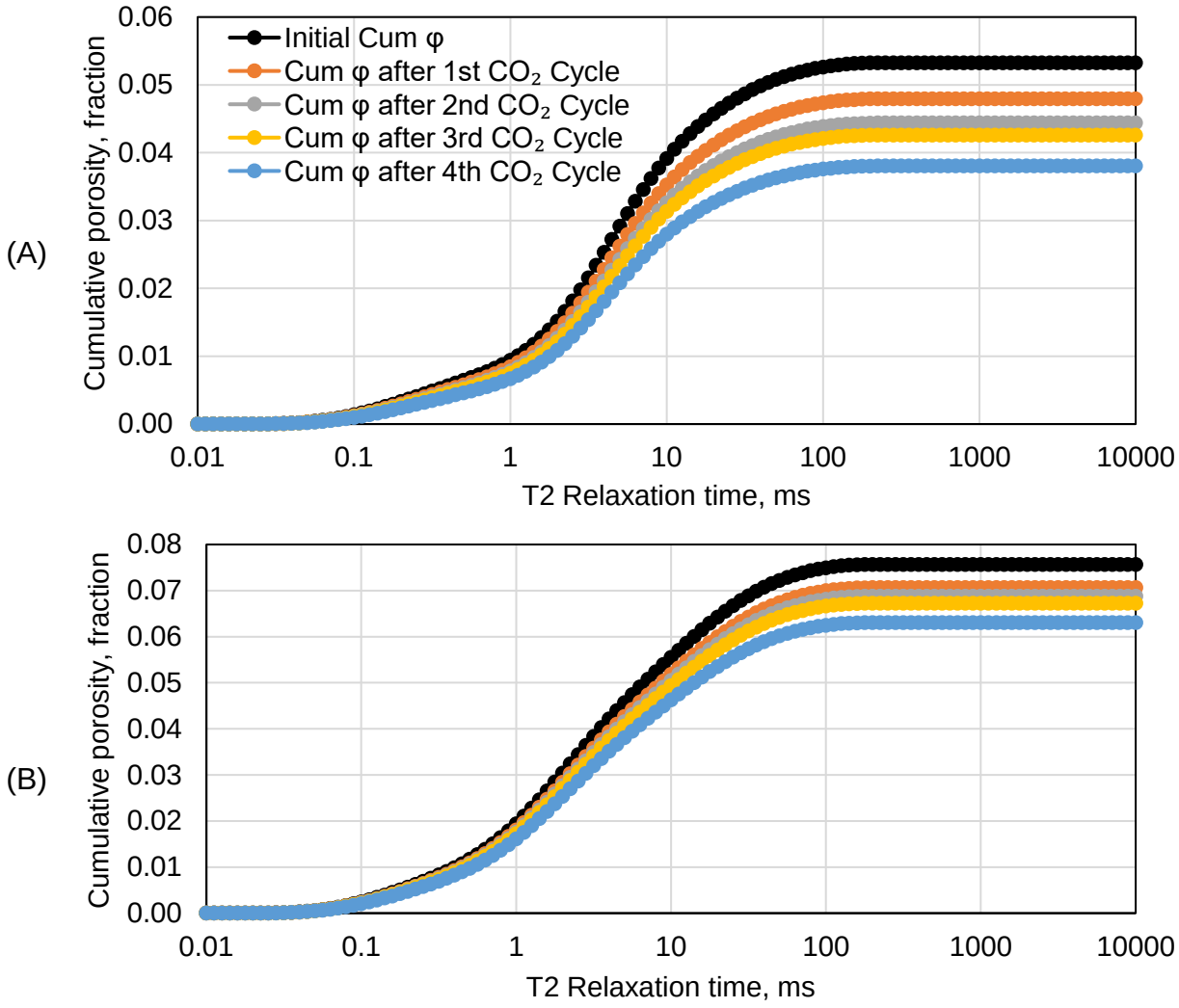

Fig. 6.8 Change in cumulative porosity (Cum φ) after each CO_2 HnP cycle, (A): MB#6*, (B): TF#6*

6.6 Summary

We investigated the different side effects that could result from CO_2 exposure in the Middle Bakken member and the Three Forks formation to optimize the prediction and management of CO_2 EOR and storage operations in unconventional reservoirs. We evaluated the CO_2-induced wettability shift using the contact angle method and the NMR technique to investigate pore size distribution and effective porosity changes before and after CO_2 HnP. The findings can be summarized as follows:

- The contact angle measurements indicate that MB and TF samples were originally strongly oil-wet. CO_2 exposure resulted in a rock hydrophilicity increase. When we used a CO_2/brine oil-saturated-rock system, the tested sample wettability preference became mix-wet to water-wet.
- The NMR results indicated a change in T_2 spectrum before and after CO_2 injection. The curve shifted towards small transverse time values after CO_2 injection, reflecting the PSD changes caused by the interaction of injected CO_2 with some minerals present in the tested cores.
- The microporosity increased in all samples, indicating that new tiny pores can be created after the dissolution of calcite and dolomite into the carbonic acid that forms when CO_2 is in contact with formation brine.
- The increase of the micropores volume after CO_2 HnP indicated that some hydrocarbons were displaced towards the small pores of rock sample, which might complicate their recovery in the future.
- CO_2 chemical reactions with rock minerals can form precipitates that block a portion of the existing pore volume. The effective porosity decreased by 28.7% for the MB sample and 16.6% for the TF sample after four CO_2 HnP cycles.

In the next Chapter, we compare the EOR performance of CO_2 and several hydrocarbon gases. Also, a combination of different gases into one EOR scheme is discussed.

Chapter 7

Novel EOR Scheme Using CO_2 and Hydrocarbon Gases

In this Chapter, we introduce a novel EOR scheme by alternating the type of the injected gas in each cycle to further improve the EOR performance of cyclic gas injection in tight formations. A comparison of the performance of multiple gases is presented based on the MMP, capacity to vaporize oil hydrocarbons, and molecular weight selectivity of each gas. After selecting the most promising gases, we present the results of several HnP injection tests that were performed to compare the oil recovery factor using MB and TF rock samples. Then the results are compared with a HnP test that was performed by combing CO_2 and hydrocarbon gases.

7.1 Background and Motivations

In 2019, 19% of the produced gas from the Bakken was flared due to the inadequate pipeline and production infrastructure, resulting in the emission of about 1.5 million metric tons of CO_2 equivalents [107]. The mutual goals of increasing oil production and reducing the emission of greenhouse gases have led to growing interest in gas EOR, which are epitomized in several pilot-scale injection tests in Bakken. These pilot tests suggested that gas injection can help overcome the injectivity concern in Bakken, and it is a promising solution to enhance oil recovery. The results also showed that gas flooding in densely fractured unconventional reservoirs might result in an early breakthrough, resulting in poor performance [15] . Cyclic injection scheme so-called Huff and Puff (HnP) method can be used to mitigate these issues [16,29]. In a HnP scheme, the gas is injected into the reservoir until reaching a predesigned pressure. After that, the well is shut-in to allow the injected gas to soak for a given period, the system is opened for production [101]. The common HnP procedure consists of repeating the same steps for a set number of cycles using the same gas. Although cyclic injection can help overcome continuous flooding challenges in unconventional reservoirs, the injected gas capacity to mobilize crude oil hydrocarbons decreases tremendously after each cycle. Regardless of the type of gas used, previous simulation and experimental studies that evaluated the HnP technique under realistic reservoir conditions indicated that oil production reaches a plateau at a relatively low cumulative recovery factor after a few cycles [108]. Both results in the literature and our study show that CO_2 capacity to recover oil diminishes after each cycle and becomes less and less efficient.

As presented in Fig. 4.3, the results of multicyclic CO_2 injection showed a tremendous decrease in the CO_2 performance after a few HnP cycles. After the second cycle, only 7% OOIP, on average, was incrementally recovered for samples MB#1 and TF#1, respectively. The oil recovery curve exhibited a plateau after the first two cycles for all the samples we tested. Similar observations can

be found elsewhere in the literature. For example, Adel et al. [31] performed seven successive CO_2 HnP tests using rock samples from the Eagle Ford shale. Fig. 7.1 presents the oil recovery factor for each cycle using an injection pressure of 3500 psi and a soaking time of 10 hours. The results show that 25% of the OOIP was recovered after the first cycle and only 6% after the second cycle. The oil recovery decreased continuously after each cycle to reach less than 1% after the seventh cycle.

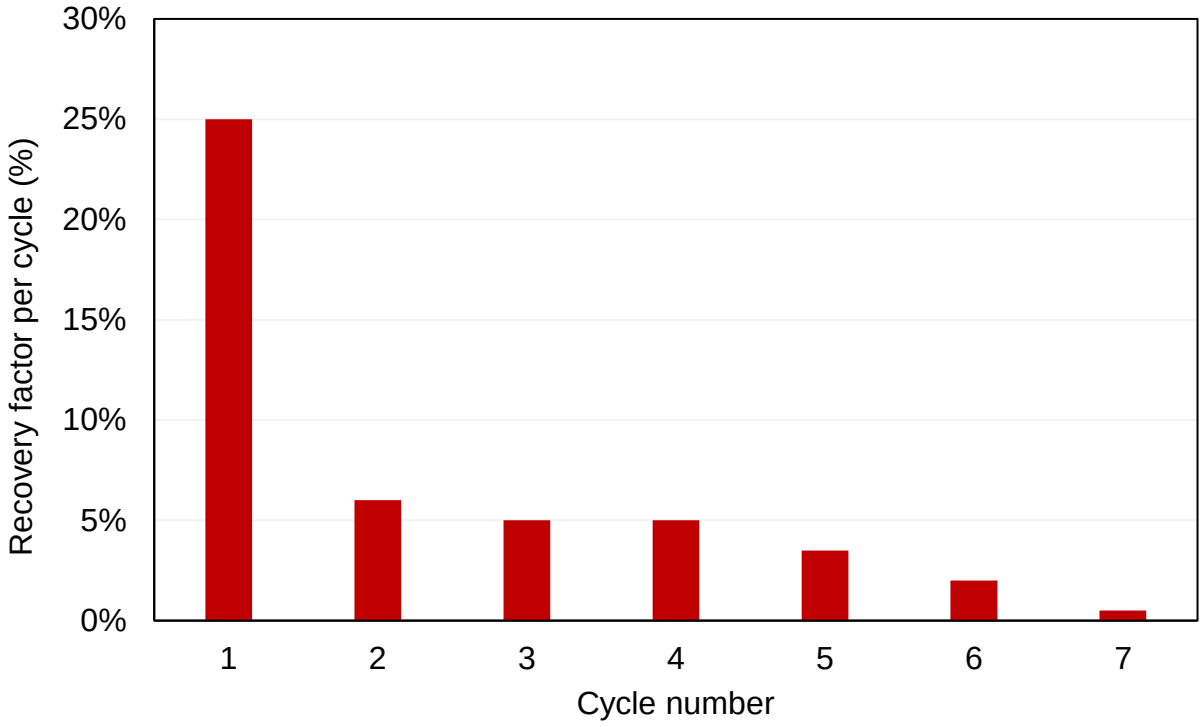

Fig. 7.1 Recovery factor per cycle during CO_2 HnP on Eagle Ford shale core plug at 3500 psi and soaking time of 10 hours ([31])

Menzie [57] and Hawthorne and Miller [106] performed oil gas multi-exposure experiments using different gases to investigate crude oil hydrocarbons mobilization by vaporizing gas drive. The tests were performed by partially filling a chamber with crude oil then the tested gas was injected to reach the desired pressure. After reaching equilibrium, the gas-dominated phase was collected

to measure the dissolved oil, and a new injection cycle took place. Both studies indicated that the equilibrium partitioning mechanism controls oil solubility in the injected gas, and the dissolved oil concentration in the gas-dominated phase diminishes after each sequential exposure. These findings help understand the tremendous decrease of oil mobilization efficiency after each HnP cycle.

Alternating the type of the injected gas after each cycle can be a solution to boost the oil recovery and hydrocarbons mobilization using cyclic injection in tight formations. Although several studies evaluated the performance of different gases separately, combining them into one EOR scheme is seldom discussed. In this work, we used the data available in the literature to compare the EOR performance of CO_2 and multiple gas hydrocarbons (methane, ethane, propane, and produced gas mixture). After determining the most effective gases, several HnP tests were conducted to measure their oil recovery limit. Then we introduced a novel gas EOR scheme to boost oil mobilization and achieve higher recovery factors.

7.2 Evaluation of Different Gases

As stated in the previous sections, the oil recovery mechanisms in tight formations are different than EOR floods in highly permeable reservoirs [15,16,29]. Oil recovery using gas injection in conventional reservoirs relies on viscosity reduction after mixture with the injected gas, oil swelling, and generating a stable oil-gas front [13,57]. For unconventional reservoirs, molecular diffusion driven by the concentration gradient seems to control the oil recovery [35,60,109]; therefore, the success of gas EOR applications relies on the ability of the injected gas to mix with the reservoir fluids, efficiently dissolve the residual oil in the interstitial pores, and displace the hydrocarbons toward the fractures.

7.2.1 Minimum miscibility pressure

In the previous Chapters, we indicated that reaching miscible conditions between the injected gas and the reservoir fluids is crucial for gas EOR applications in tight formations. Different gases can be used for miscible EOR processes, which include CO_2, methane, ethane, propane, and produced rich gas. Hawthorne et al. [110] used the vanishing interfacial tension technique to measure the Minimum Miscibility Pressure (MMP) of those gases with MB and TF crude oil samples. The produced rich gas was simulated by mixing methane, ethane, and propane with a composition of 69.5%, 21%, and 9.5%, respectively. The results presented in Table 9 show that the gases can be arranged based on their MMP values from highest to lowest as follow: methane, CO_2, produced gas, ethane, and propane.

It has been shown that increasing the injection pressure above the MMP can result in an incremental oil recovery [33,101]; therefore, the gases with lower MMP requirements limit the need to over-pressure the reservoir and are expected to have better EOR performances at relatively low reservoir pressures.

Table 9 MMP values of different gases with MB and TF crude oil

Solvent	Methane	CO_2	Ethane	Propane	Produced gas
MMP with MB crude oil (psi)	4238	2521	1330	554	2435
MMP with TF crude oil (psi)	4461	2696	1453	614	2345

7.2.2 Oil solubility in different gases

The capacity of the injected gas to dissolve crude oil is an important parameter that needs to be evaluated in order to compare the EOR performance of different gases. Harthorne and Miller [105] used oil-gas contact experiments to measure Bakken crude oil solubility in the gases listed in Table 9. A visual cell was filled with 10 ml of Bakken crude oil. Then the test gas was injected in the remaining 10 ml through the oil sample at different pressures of 1450 psi (below MMP), 3000 psi

(near MMP), and 5000 psi (above MMP). The system was allowed to equilibrate then the upper gas-dominated phase was collected and analyzed. The steps were repeated until four sequential injections were performed for each gas. Methane and produced gas had the poorest performance at all pressure conditions. At 5000 psi, the oil solubility expressed in mg of dissolved oil per ml of injected gas for methane, produced gas, CO_2, ethane, and propane was 67 mg/ml, 145 mg/ml, 254, mg/ml, 228 mg/ml, and 277 mg/ml, respectively. The results showed that CO_2, ethane, and propane had the highest capacity to dissolve Bakken crude oil at all pressure conditions; therefore, only these three gases will be considered in this work.

7.2.3 Molecular weight selectivity

Another important characteristic of the gas EOR agent is its Molecular Weight Selectivity (MWS), which needs to be considered to design an appropriate EOR scheme for the targeted formation. The MWS can be defined as the bias of the injected gas to dissolve and mobilize hydrocarbons within a specific molecular weight window. Hawthorne et al. [105,111,112] compared the MWS of different gases using gas-oil contact experiments and HnP injection tests. They used oil and rock samples retrieved from a similar location to our rock and oil samples. Fig. 7.2 shows the similarity between the composition of our Bakken oil sample (black line) and the oil sample they used in their experiments (blue line). The same carbon numbers are present in our oil sample with similar compositions.

In a first step, Hawthorne et al. [105] evaluated the viscosity change after sequential exposure to different gases. The test consists of filling a 20 ml cell with 10 ml of Bakken crude oil then injecting the test gas from the bottom of the cell at 5000 psi and 230°F. The fresh oil viscosity was 2.2 cp, and the change of the Bakken crude oil viscosity after contact with the gases selected in this study is presented in Fig. 7.3.

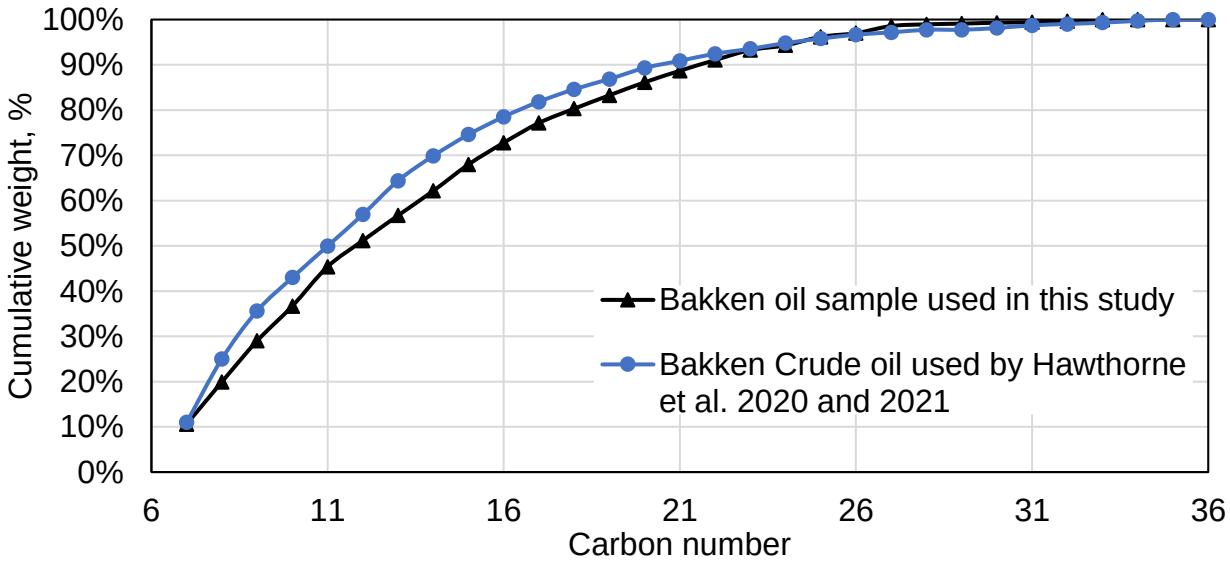

Fig. 7.2 Oil composition of the crude oil sample used in our work (black line) and the oil samples used by Hawthorne et al. 2020 and 2021([105,111]) to study the MWS of different gases.

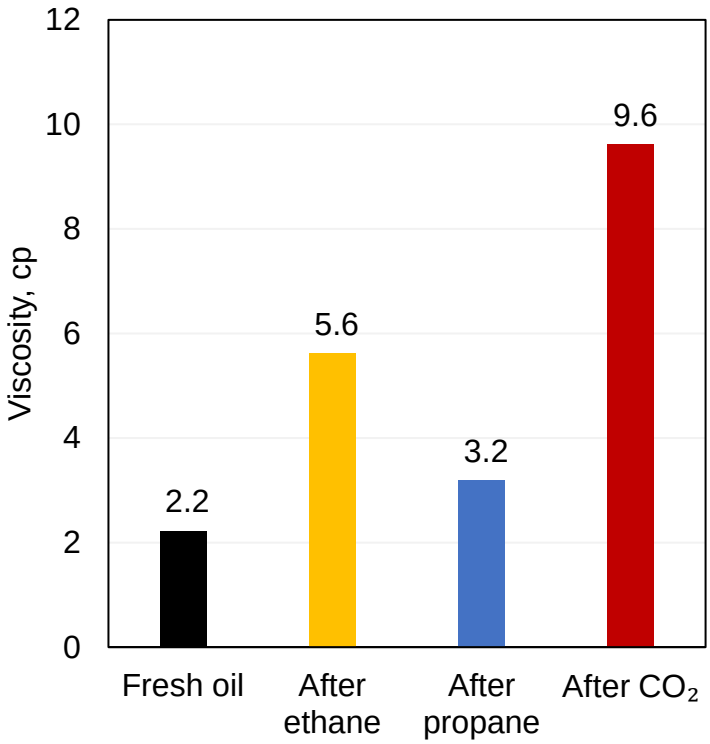

Fig. 7.3 Bakken oil viscosity change after exposure to CO_2, ethane, and propane [105]

Changes in the oil viscosity after contact with the injected gas are directly related to the changes in hydrocarbon distribution. The increase of oil viscosity to 9.6 cp after CO_2 injection reflects the high selectivity of CO_2 towards Light Weight Hydrocarbons (LWH). The oil that was exposed to ethane had a viscosity of 5.6 cp, which indicates that ethane has a larger MWS window than CO_2 that includes LWC and Medium Weight Components (MWC). Also, the results suggest that propane has the most uniform MWS. The oil viscosity after propane injection was 3.2 cp which is the closest value to the original viscosity of the Bakken crude oil.

In a recent study, Hawthorn et al. [111] performed a series of HnP tests using MB rock samples and analyzed the composition of the displaced oil using Gas Chromatography (GC). Fig. 7.4 depicts the recoveries of C8, C16, C22, and C28 after CO_2, ethane, and propane HnP injection tests using an injection pressure of 5000 psi, temperature of 230°F, and 24 hours of soaking. The results of these tests confirm the findings of oil viscosity change (Fig. 7.3). CO_2 recovered 98.0, 66.7, and 13.0 % of the C8, C16, and C22 fractions in the crude oil, respectively. Also, the GC results show that the oil displaced by CO_2 didn't contain any C28 faction, which confirms the CO_2 bias against higher molecular weight hydrocarbons. After ethane injection, 96.0, 85.7, 66.8, and 27.6% of the C8, C16, C22, and C28 fractions were recovered from the rock sample, respectively. As expected, propane had the most uniform recovery and displaced 95.0, 75.0, 60.0, and 40.0% of the C8, C16, C22, and C28 fractions, respectively.

In conclusion, CO_2 recovered the highest amount of LWH and couldn't mobilize Heavy Weight Hydrocarbons (HWH). Ethane had the best performance in recovering MWH, and the MWS of propane covers the widest range of hydrocarbons.

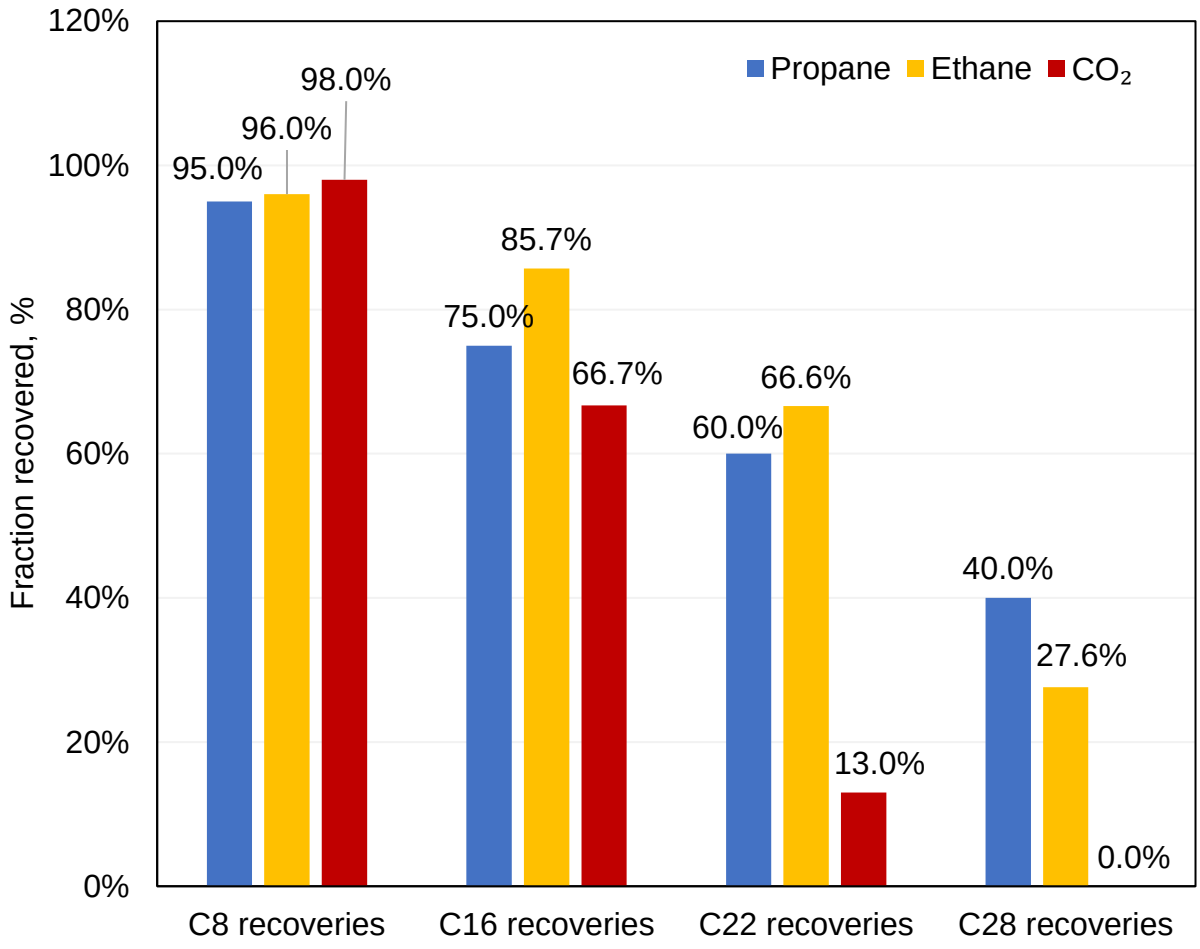

Fig. 7.4 Recoveries of C8, C16, C22, and C28 from MB rock samples after 24 h exposure to CO_2, ethane, and propane ([111])

7.3 Comparing EOR Performance of CO_2, Ethane, and Propane

As discussed in the previous sections of this Chapter, CO_2, ethane, and propane are the most promising gases for EOR in tight formations. Hawthorne et al. [111] compared the oil recovery performance of these gases using cylindrical MB rods (0.44 in diameter * 1.75 in length) and LBS rock cuttings (see Fig. 7.5). They performed HnP tests at different pressures, including 1500, 2500, and 5000 psi. In this study, we focus on comparing the EOR performance above MMP. Fig. 7.6

presents the oil recovery factors from the MB rods after cyclic injection of CO_2, ethane, and propane at 5000 psi.

Fig. 7.5 Geometries of the rock samples used by Hawthorn et al. [111] for gas HnP experiments, 0.44 in diameter * 1.75 in length rods to represent the MB (left) and 0.04-0.13 in cuttings for the LBS (right)

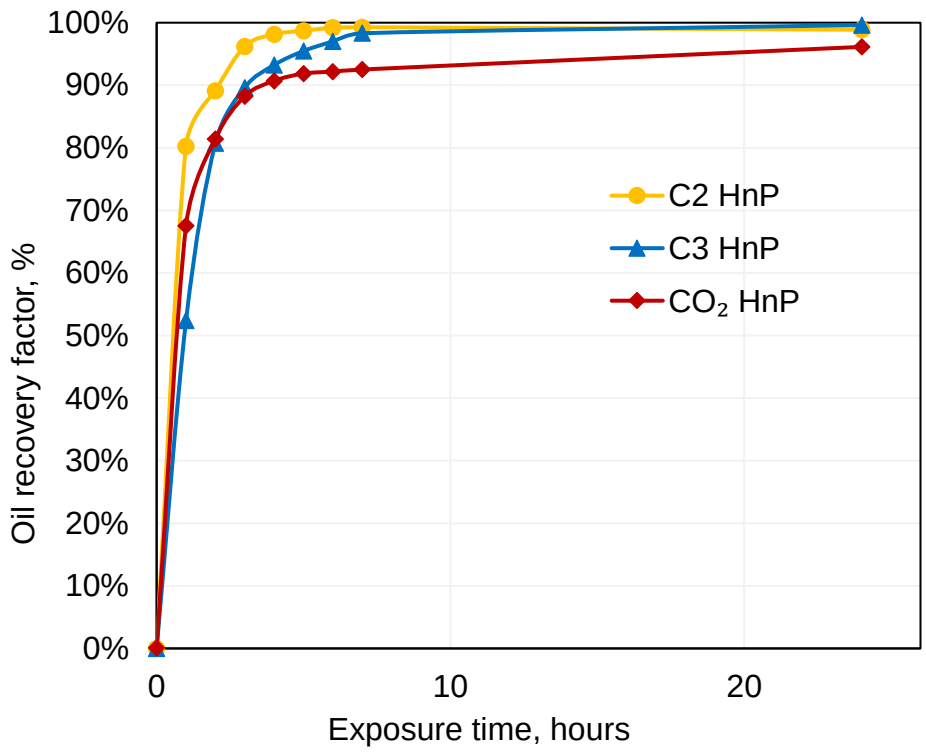

Fig. 7.6 Oil recovery from MB rods after CO_2 (red line), ethane (yellow line), and propane (blue line) HnP at 5000 psi and 230°F

The reported results didn't clearly display the difference between the tested gases. In fact, the usage of very small rock samples resulted in recovering over 90% of the OOIP after two to three hours of soaking for all the gases. Therefore, we used larger MB and TF samples to compare the oil recovery of each gas using multicyclic injection at typical reservoir conditions. Four twin MB and four twin TF rock samples (1.5 in diameter * 4 in length) were selected for this study. The permeability and porosity of the MB and TF samples were 0.009 mD, 6.4%, 0.145 mD, and 8.4%, respectively. After cleaning and saturating the rock samples, we first performed two CO_2 HnP cycles using an injection pressure of 4000 psi, a temperature of 213 °F, and a soaking time of 24 hours. As expected (see section 7.1), the results illustrated in Fig. 7.7 show that the EOR performance of all the tested gases diminishes after each cycle and the oil recovery reaches a

plateau after a few HnP cycles. The oil recovery after the second cycle of CO_2 injection was 32.3% and 38.1% for the TF and MB samples, respectively. However, the ultimate oil recovery factor after six HnP cycles was 38.3% and 44.7% for the TF and MB samples, respectively. For ethane and propane injection, the oil recovery factor after the second cycle was 34.0% and 38.9% for the MB samples and 41.5% and 48.1% for the TF samples, respectively. Similar to CO_2 HnP, the incremental oil recovery from the second to the sixth cycle of ethane and propane injections was between 6 and 8% of the OOIP for the MB and TF samples.

To overcome this limitation, we proposed an EOR scheme that consists of alternating the test gas based on the MWS. We first injected CO_2 for its preference to dissolve and mobilize the light hydrocarbons. Then, ethane injection was performed to efficiently mobilize the medium-weight components, followed by propane injection to displace the remaining heavy hydrocarbons. After cleaning and saturating the rock samples, we first performed two HnP cycles using CO_2, followed by two ethane and propane cycles. All the tests were performed at similar experimental conditions of 4000 psi, 213°F, and 24 hours of soaking.

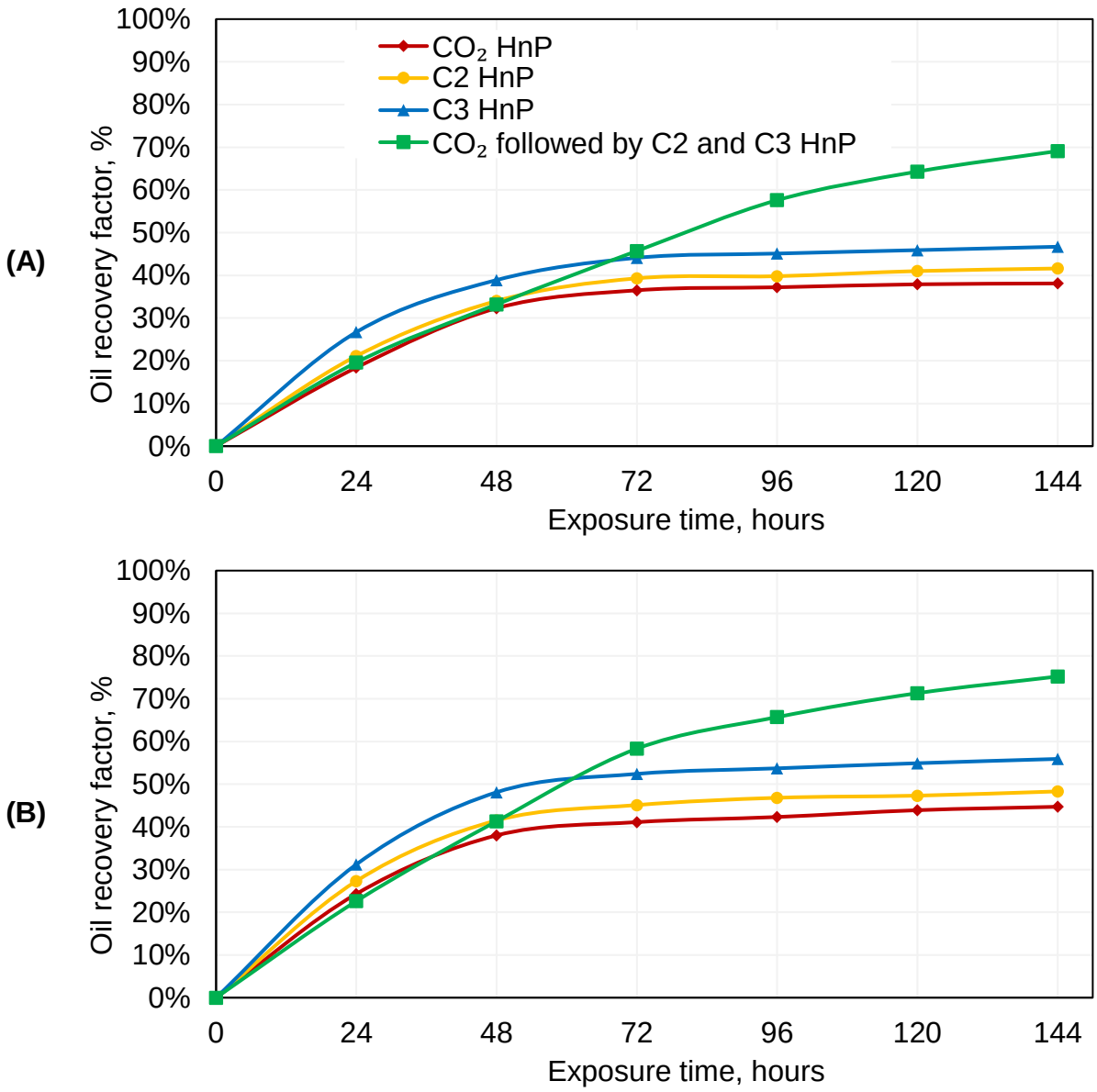

Fig. 7.7 Oil recoveries from MB samples (A) and TF samples (B) using CO_2, ethane and propane

The green line curves in Fig. 7.7 (A) and (B) represent the oil recovery using the alternating gas injection method in MB and TF samples, respectively. Alternating the injection gas resulted in an incremental oil recovery of 31.2, 27.5, and 22.4 % of the OOIP from the MB sample compared to multicyclic injection of CO_2, ethane, and propane, respectively. Similarly, 24.4, 20.8, and 13.2% of the OOIP were incrementally recovered from the TF sample compared to CO_2, ethane, and

propane HnP, respectively. The composition of the oil in the interstitial pores changes after gas injection; therefore, alternating the type of the injected gas can help mobilize most of the hydrocarbons in place better than re-injecting the same gas for multiple cycles.

7.4 Summary

In this Chapter, we compared the EOR performance of CO_2 and gas hydrocarbons then evaluated the oil recoveries using multicyclic and alternating gas injection schemes. The findings can be summarized as follow:

- In cyclic gas injection, the capacity of the injected gas capacity to mobilize crude oil hydrocarbons decreases tremendously after each cycle. The equilibrium partitioning mechanism controls oil solubility in the injected gas, and the dissolved oil concentration in the gas-dominated phase diminishes after each sequential exposure.
- The ability of the injected gas to reach the miscibility with the reservoir fluids, efficiently dissolve the residual oil in the interstitial pores, and displace the hydrocarbons toward the fractures are important factors for the success of gas EOR applications in unconventional reservoirs.
- CO_2, ethane, and propane had the lowest MMP with Bakken crude oil compared to methane and produced rich gas mixture. Also, Oil-gas contact experiments showed that CO_2, ethane, and propane dissolved the highest volumes of hydrocarbons from Bakken oil.
- The GC analysis of the oil displaced using CO_2, ethane, and propane suggested that CO_2 can efficiently displace the light hydrocarbons, while ethane has a better performance in mobilizing the medium weight components, and propane has the most uniform recovery and the best performance in recovering the heavy hydrocarbons.

- Multicyclic injection tests in MB and TF rock samples showed that using an injection pressure of 4000 psi and a soaking time of 24 hours, all the three gases had similar EOR performance.
- Each gas can dissolve and mobilize hydrocarbons within a specific molecular weight window; therefore, alternating the type of the injected gas based on their MWS instead of multicyclic injection of the same gas led to increasing the oil recovery.

Chapter 8

Conclusions and Recommendations

The main conclusions driven from this work are summarizedin the first section of this Chapter and the second section presents some of the future work that is recommended as continuation of this study.

8.1 Conclusions

In this study, we evaluated the performance of CO_2 EOR in unconventional reservoirs. We first studied the influence of HnP injection parameters on oil recovery using representative MB and TF rock and fluid samples. Then, we investigated the gap between the results of CO_2 EOR field tests and the antecedent research studies. We conducted an extensive parametric study to examine and understand the effects of a series of key parameters, such as sample size, water presence, fracture size, and CO_2 injection scheme, on CO_2 EOR in unconventional reservoirs. After that, we studied the potential side effects of CO_2 injection in tight formations and evaluated the possible CO_2-induced alteration of reservoir properties. The effect of CO_2 injection on rock wettability, pore size

distribution, and effective porosity was assessed and discussed. Finally, we compared the EOR performance of CO_2 and different hydrocarbon gases to determine the most promising gases. Then the selected gases were combined into one EOR scheme to overcome the oil recovery limits of multicyclic gas injection.

The main findings of this work can be summarized as follow:

- Increasing the injection pressure above MMP can help recover more oil from tight rock samples and the results of multicyclic CO_2 injection indicate that the CO_2 performance decreases drastically after the second HnP cycle.
- The size of the tested samples has an important impact on EOR experiments. The selection of smaller samples can lead to overestimating the potential of CO_2 EOR and oil recovery. We recommend using samples that are large enough to represent fluid flow in the reservoir and represent its heterogeneity.
- The results suggest that both viscous forces and molecular diffusion control the oil recovery. The pressure gradient initially pushes CO_2 into larger pores and promotes its penetration, then diffusion controls oil extraction toward the bulk CO_2 volume surrounding the rock.
- Water accumulated in the fracture can impede the contact between CO_2 and the reservoir rock, which results in reduced oil recovery.
- Submerging a core sample in a relatively large CO_2 volume can result in overestimating the oil recovery. The ratio of the volume surrounding the sample to the sample surface areas needs to be considered carefully and should represent reservoir conditions for cyclic injection experiments in tight samples.

- Using fractured tight formation samples, cyclic injection outperformed the flooding process, which was limited by low sweep efficiency and early breakthrough.
- The contact angle measurements indicate that MB and TF samples were originally strongly oil-wet. CO_2 exposure resulted in a rock hydrophilicity increase. When we used a CO_2/oil/brine system, the tested sample wettability preference became mix-wet to water-wet.
- The NMR results indicated a change in T_2 spectrum before and after CO_2 injection. The curve shifted towards small transverse time values after CO_2 injection, reflecting the PSD changes caused by the interaction of injected CO_2 with some minerals present in the tested cores.
- The microporosity increased in all samples, indicating that new tiny pores can be created after the dissolution of calcite and dolomite into the carbonic acid when CO_2 is in contact with formation brine.
- The increase of the micropore volumes after CO_2 HnP indicated that some hydrocarbons were displaced towards the small pores of rock sample, which might complicate their recovery in the future.
- CO_2 chemical reactions with rock minerals can form precipitates that block a portion of the existing pore volume, which might result in decreasing the effective porosity after CO_2 exposure.
- In cyclic gas injection, the capacity of the injected gas capacity to mobilize crude oil hydrocarbons decreases tremendously after each cycle. The equilibrium partitioning mechanism controls oil solubility in the injected gas, and the dissolved oil concentration in the gas-dominated phase diminishes after each sequential exposure.

- The ability of the injected gas to reach the miscibility with the reservoir fluids, efficiently dissolving the residual oil in the interstitial pores, and displacing the hydrocarbons toward the fractures are important factors for the success of gas EOR applications in unconventional reservoirs.
- CO_2, ethane, and propane had the lowest MMP with Bakken crude oil compared to methane and produced rich gas mixture. Also, Oil-gas contact experiments showed that CO_2, ethane, and propane dissolved the highest volumes of hydrocarbons from Bakken oil.
- The GC analysis of the oil displaced using CO_2, ethane, and propane suggested that CO_2 can efficiently displace the light hydrocarbons, while ethane has a better performance in mobilizing the medium weight components, and propane has the most uniform recovery and the best performance in recovering the heavy hydrocarbons.
- Each gas can dissolve and mobilize hydrocarbons within a specific molecular weight window; therefore, alternating the type of the injected gas based on their MWS instead of multicyclic injection of the same gas led to increasing the oil recovery.

8.2 Recommendations

Below are some recommendations for future gas EOR related work in unconventional reservoirs:

- Coupling the gas injection experiments with CT-scanner or NMR measurements can help understand gas penetration into the rock matrix.
- The CO_2-induced pore structure change can be further investigated using SEM and CT-scan images comparison before and after CO_2 exposure.

- The experimental results can be used to calibrate analytical models and numerical simulations for a better prediction performance of EOR applications in tight formations in the future.
- A mixture of different gases such as CO_2 and hydrocarbon gases can be studied and compared to pure gas injection results. We recommend measuring the MMP of different mixtures and analyze the produced oil composition using different gas mixtures.

Appendix

Compositional Analysis of Bakken Bottomhole Sample

Component	MW	Flashed Gas		Flashed Liquid		Reservoir Fluid	
	g/mol	wt%	mole %	wt%	mole %	wt%	mole %
CO_2	44.01	0.55	0.39	0.00	0.00	0.13	0.24
H_2S	34.08	0.00	0.00	0.00	0.00	0.00	0.00
N_2	28.01	2.88	3.19	0.00	0.00	0.65	1.98
C_1	16.04	23.35	45.26	0.00	0.00	5.29	28.14
C_2	30.07	20.31	21.01	0.00	0.00	4.60	13.04
C_3	44.10	22.86	16.13	0.27	1.06	5.39	10.41
i-C_4	58.12	3.51	1.88	0.14	0.42	0.90	1.32
n-C_4	58.12	12.33	6.60	0.86	2.57	3.46	5.07
i-C_5	72.15	3.01	1.30	0.63	1.52	1.17	1.38
n-C_5	72.15	4.48	1.93	1.31	3.15	2.03	2.39
C_6	84.00	3.15	1.17	2.88	5.96	2.94	2.98
Mcyclo-C_5	84.16	0.72	0.27	1.04	2.15	0.97	0.98
Benzene	78.11	0.07	0.03	0.09	0.20	0.08	0.09
Cyclo-C_6	84.16	0.20	0.07	0.39	0.81	0.35	0.35
C_7	100.21	1.43	0.45	4.70	8.15	3.96	3.37
Mcyclo-C_6	98.19	0.22	0.07	1.06	1.88	0.87	0.75
Toluene	92.14	0.08	0.03	0.33	0.62	0.27	0.25
C_8	114.23	0.55	0.15	5.97	9.04	4.74	3.54
C_2-Benzene	106.17	0.02	0.01	0.26	0.43	0.21	0.16
m&p-Xylene	106.17	0.03	0.01	0.61	1.00	0.48	0.38
o-Xylene	106.17	0.01	0.00	0.20	0.33	0.16	0.13
C_9	128.26	0.18	0.04	4.73	6.41	3.70	2.46
C_{10}	134.00	0.05	0.01	5.80	7.52	4.50	2.86
C_{11}	147.00	0.01	0.00	4.89	5.78	3.79	2.19
C_{12}	161.00	0.00	0.00	4.68	5.05	3.62	1.92

C_{13}	175.00	0.00	0.00	4.59	4.56	3.55	1.73
C_{14}	190.00	0.00	0.00	3.98	3.64	3.08	1.38
C_{15}	206.00	0.00	0.00	3.96	3.34	3.06	1.27
C_{16}	222.00	0.00	0.00	3.53	2.76	2.73	1.05
C_{17}	237.00	0.00	0.00	3.30	2.42	2.55	0.92
C_{18}	251.00	0.00	0.00	3.10	2.15	2.40	0.81
C_{19}	263.00	0.00	0.00	2.99	1.98	2.31	0.75
C_{20}	275.00	0.00	0.00	2.67	1.69	2.07	0.64
C_{21}	291.00	0.00	0.00	2.51	1.50	1.94	0.57
C_{22}	305.00	0.00	0.00	2.32	1.32	1.80	0.50
C_{23}	318.00	0.00	0.00	2.14	1.17	1.66	0.44
C_{24}	331.00	0.00	0.00	1.98	1.04	1.53	0.39
C_{25}	345.00	0.00	0.00	1.86	0.94	1.44	0.36
C_{26}	359.00	0.00	0.00	1.70	0.82	1.31	0.31
C_{27}	374.00	0.00	0.00	1.67	0.78	1.29	0.29
C_{28}	388.00	0.00	0.00	1.53	0.69	1.18	0.26
C_{29}	402.00	0.00	0.00	1.43	0.62	1.11	0.23
C_{30+}	532.59	0.00	0.00	13.90	4.53	10.73	1.72

Single Stage Flash of Bottomhole Sample Standard Conditions (15 psia and 60.0 °F)

GOR (SCF/STB)	STO API Gravity (API)	Measured STO Density (g/cm^3)	Vapor Gravity
1037	39.3	0.828	1.074

Gas Chromatogram of Flashed Liquid

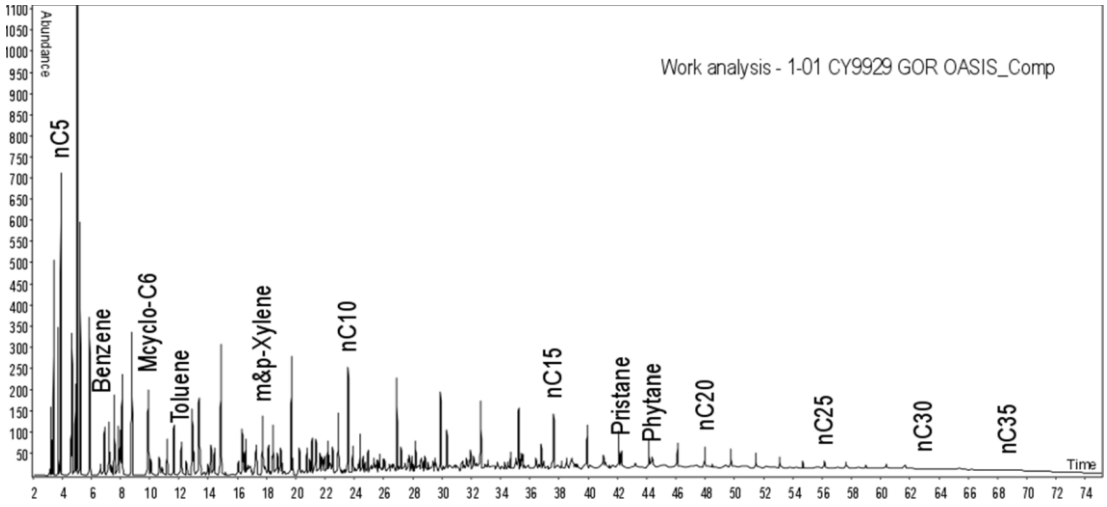

Fluid Properties at Reservoir Conditions

Density	0.668	g/cm^3
Viscosity	0.29	cP
Formation Volume Factor (B_o)	1.609	vol/vol
Oil Compressibility Coefficient (C_o)	12.425	10^{-6}/psia

Fluid Properties at Saturation Conditions

Bubble Point Pressure	2198	psia
Density	0.623	g/cm^3
Viscosity[1]	0.19	cP
Formation Volume Factor (B_o)	1.724	vol/vol
Oil Compressibility (C_o)	19.132	10-6/psia
Solution GOR	1184	SCF/STB

Stock Tank Fluid Properties

Density	0.828	g/cm3
API Gravity	39.3	API

References

[1] U.S. Energy Information Administration. How much shale (tight) oil is produced in the United States? Freq Asked Quest 2019. https://www.eia.gov/tools/faqs/faq.php?id=847&t=6 (accessed May 18, 2020).

[2] Flannery J. Integrated analysis of the Bakken petroleum system, US Williston Basin 2006.

[3] Kurtoglu B. Integrated Reservoir Characterization and Modeling in Support of Enhanced Oil Recovery for Bakken. Colorado School of Mines, 2013.

[4] Wang L, Yu W. Mechanistic simulation study of gas Puff and Huff process for Bakken tight oil fractured reservoir. Fuel 2019;239:1179–93. https://doi.org/https://doi.org/10.1016/j.fuel.2018.11.119.

[5] Hejazi SH, Assef Y, Tavallali M, Popli A. Cyclic CO2-EOR in the Bakken Formation: Variable cycle sizes and coupled reservoir response effects. Fuel 2017;210:758–67. https://doi.org/10.1016/j.fuel.2017.08.084.

[6] Yang J, Wang X, Peng X, Du Z, Zeng F. Experimental studies on CO2 foam performance in the tight cores. J Pet Sci Eng 2019;175:1136–49. https://doi.org/10.1016/j.petrol.2019.01.029.

[7] Smith SA, Kurz B, Sorensen J, Beddoe C, Mibeck B, Azenkeng A, et al. Laboratory Investigation of CO2 Injectivity and Adsorption Potential Within the Bakken Formation. SPE/AAPG/SEG Unconv Resour Technol Conf 2019. https://doi.org/10.15530/urtec-2019-967.

[8] Wang L, Yu W. Mechanistic simulation study of gas Puff and Huff process for Bakken tight oil fractured reservoir. Fuel 2019;239:1179–93. https://doi.org/10.1016/j.fuel.2018.11.119.

[9] Yu W, Lashgari HR, Wu K, Sepehrnoori K. CO2 injection for enhanced oil recovery in Bakken tight oil reservoirs. Fuel 2015;159:354–63. https://doi.org/10.1016/j.fuel.2015.06.092.

[10] Dechongkit P, Prasad M. Recovery Factor and Reserves Estimation in the Bakken Petroleum System (Analysis of the Antelope, Sanish and Parshall fields). Can Unconv Resour Conf 2011:15. https://doi.org/10.2118/149471-MS.

[11] Clark AJ. Determination of Recovery Factor in the Bakken Formation, Mountrail County, ND. SPE Annu Tech Conf Exhib 2009. https://doi.org/10.2118/133719-STU.

[12] Tang X, Zhang J, Wang X, Yu B, Ding W, Xiong J, et al. Shale characteristics in the southeastern Ordos Basin, China: Implications for hydrocarbon accumulation conditions and the potential of continental shales. Int J Coal Geol 2014;128:32–46.

[13] Aryana SA, Barclay C, Liu S. North Cross Devonian Unit - A Mature Continuous CO2 Flood Beyond 200% HCPV Injection. SPE Annu Tech Conf Exhib 2014. https://doi.org/10.2118/170653-MS.

[14] Todd HB, Evans JG. Improved Oil Recovery IOR Pilot Projects in the Bakken Formation. SPE Low Perm Symp 2016. https://doi.org/10.2118/180270-MS.
[15] Alfarge D, Wei M, Bai B, Alsaba M. Lessons learned from IOR pilots in Bakken formation by using numerical simulation. J Pet Sci Eng 2018;171:1–15. https://doi.org/10.1016/j.petrol.2018.07.025.
[16] Wan T, Yu Y, Sheng JJ. Experimental and numerical study of the EOR potential in liquid-rich shales by cyclic gas injection. J Unconv Oil Gas Resour 2015;12:56–67. https://doi.org/10.1016/j.juogr.2015.08.004.
[17] Alfarge D, Wei M, Bai B. Data analysis for CO2-EOR in shale-oil reservoirs based on a laboratory database. J Pet Sci Eng 2018;162:697–711. https://doi.org/10.1016/j.petrol.2017.10.087.
[18] Lashgari HR, Sun A, Zhang T, Pope GA, Lake LW. Evaluation of carbon dioxide storage and miscible gas EOR in shale oil reservoirs. Fuel 2019;241:1223–35. https://doi.org/10.1016/j.fuel.2018.11.076.
[19] Pankaj P, Mukisa H, Solovyeva I, Xue H. Enhanced Oil Recovery in Eagle Ford: Opportunities Using Huff-n-Puff Technique in Unconventional Reservoirs. SPE Liq Basins Conf - North Am 2018. https://doi.org/10.2118/191780-MS.
[20] Jia B, Tsau JS, Barati R. A review of the current progress of CO2 injection EOR and carbon storage in shale oil reservoirs. Fuel 2019;236:404–27. https://doi.org/10.1016/j.fuel.2018.08.103.
[21] Mba K, Prasad M. Mineralogy and its contribution to anisotropy and kerogen stiffness variations with maturity in the Bakken Shales. SEG Annu Meet 2010. https://doi.org/doi:10.1190/1.3513383.
[22] Nesheim TO. Examination of downward hydrocarbon charge within the Bakken-Three Forks petroleum system – Williston Basin, North America. Mar Pet Geol 2019;104:346–60. https://doi.org/10.1016/j.marpetgeo.2019.03.016.
[23] Gaswirth SB, Marra KR. U.S. Geological Survey 2013 assessment of undiscovered resources in the Bakken and Three Forks Formations of the U.S. Williston basin province. Am Assoc Pet Geol Bull 2015;99:639–60. https://doi.org/10.1306/08131414051.
[24] U.S. Energy Information Administration. Maps: Oil and Gas Exploration, Resources, and Production - Energy Information Administration 2011. https://www.eia.gov/maps/maps.htm (accessed February 16, 2022).
[25] U.S. Energy Information Administration. North Dakota Field Production of Crude Oil 2015. http://www.eia.gov/dnav/pet/hist/LeafHandler.ashx?n=PET&s=MCRFPND1&f=M (accessed February 16, 2022).
[26] Sorensen J, Hawthorne SB, Jin L, A.Torres J, Bosshart NW, Azzolina NA, et al. Bakken CO2 Storage and Enhanced Recovery Program. 2015.
[27] Irena Agalliu;Curtis Smith;Mohammad, Tavallali;Min, Rao; Stephen, Adams;Aube, Montero; Leslie, Levesque;Cody, Coughlin;Dennis, Yang;Shawn G. CO2 EOR Potential in North Dakota. 2016.
[28] Gamadi TD, Sheng JJ, Soliman MY, Menouar H, Watson MC, Emadibaladehi H. An Experimental Study of Cyclic CO2 Injection to Improve Shale Oil Recovery. SPE Improv Oil Recover Symp 2014. https://doi.org/10.2118/169142-MS.
[29] Song C, Yang D. Experimental and numerical evaluation of CO2 huff-n-puff processes in Bakken formation. Fuel 2017;190:145–62. https://doi.org/10.1016/j.fuel.2016.11.041.

[30] Tovar FD, Barrufet MA, Schechter DS. Gas Injection for EOR in Organic Rich Shale. Part I: Operational Philosophy. SPE Improv Oil Recover Conf 2018:25. https://doi.org/10.2118/190323-MS.
[31] Adel IA, Tovar FD, Zhang F, Schechter DS. The Impact of MMP on Recovery Factor During CO2 – EOR in Unconventional Liquid Reservoirs. SPE Annu Tech Conf Exhib 2018:D021S022R004. https://doi.org/10.2118/191752-MS.
[32] Tovar FD, Eide O, Graue A, Schechter DS. Experimental Investigation of Enhanced Recovery in Unconventional Liquid Reservoirs using CO2: A Look Ahead to the Future of Unconventional EOR. SPE Unconv Resour Conf 2014. https://doi.org/10.2118/169022-MS.
[33] Tovar FD, Barrufet MA, Schechter DS. Gas Injection for EOR in Organic Rich Shales. Part II: Mechanisms of Recovery. SPE/AAPG/SEG Unconv Resour Technol Conf 2018. https://doi.org/10.15530/URTEC-2018-2903026.
[34] Alfarge D, Wei M, Bai B. CO2-EOR mechanisms in huff-n-puff operations in shale oil reservoirs based on history matching results. Fuel 2018;226:112–20. https://doi.org/https://doi.org/10.1016/j.fuel.2018.04.012.
[35] Alfarge D, Wei M, Bai B, Almansour A. Effect of Molecular-Diffusion Mechanism on CO2 Huff-n-Puff Process in Shale-Oil Reservoirs. SPE Kingdom Saudi Arab Annu Tech Symp Exhib 2017. https://doi.org/10.2118/188003-MS.
[36] Zhang F, Adel IA, Saputra IWR, Chen W, Schechter DS. Numerical Investigation to Understand the Mechanisms of CO2 EOR in Unconventional Liquid Reservoirs. SPE Annu Tech Conf Exhib 2019. https://doi.org/10.2118/196019-MS.
[37] Hawthorne SB, Gorecki CD, Sorensen JA, Steadman EN, Harju JA, Melzer S. Hydrocarbon Mobilization Mechanisms from Upper, Middle, and Lower Bakken Reservoir Rocks Exposed to CO2. SPE Unconv Resour Conf Canada 2013. https://doi.org/10.2118/167200-MS.
[38] Jin L, Hawthorne S, Sorensen J, Pekot L, Kurz B, Smith S, et al. Advancing CO2 enhanced oil recovery and storage in unconventional oil play—Experimental studies on Bakken shales. Appl Energy 2017;208:171–83. https://doi.org/10.1016/j.apenergy.2017.10.054.
[39] Jin L, Sorensen JA, Hawthorne SB, Smith SA, Bosshart NW, Burton-Kelly ME, et al. Improving Oil Transportability Using CO2 in the Bakken System – A Laboratory Investigation. SPE Int Conf Exhib Form Damage Control 2016. https://doi.org/10.2118/178948-MS.
[40] Song C, Yang D. Performance Evaluation of CO2 Huff-n-puff Processes in Tight Oil Formations. SPE Unconv Resour Conf Canada 2013:SPE-167217-MS. https://doi.org/10.2118/167217-MS.
[41] Chen K. Evaluation of EOR Potential By Gas and Water Flooding in Shale Oil Reservoirs. Texas Tech University, 2013.
[42] Pu W, Hoffman T. EOS Modeling and Reservoir Simulation Study of Bakken Gas Injection Improved Oil Recovery in the Elm Coulee Field, Montana. Proc. 2nd Unconv. Resour. Technol. Conf., Tulsa, OK, USA: American Association of Petroleum Geologists; 2014. https://doi.org/10.15530/urtec-2014-1922538.
[43] Fai-Yengo VA, Rahnema H, Alfi M. Impact of Light Component Stripping During CO2 Injection in Bakken Formation. Proc. 2nd Unconv. Resour. Technol. Conf., Tulsa, OK, USA: American Association of Petroleum Geologists; 2014. https://doi.org/10.15530/urtec-

2014-1922932.
[44] Chen C, Balhoff M, Mohanty KK. Effect of Reservoir Heterogeneity on Primary Recovery and CO2 Huff 'n' Puff Recovery in Shale-Oil Reservoirs. SPE Reserv Eval Eng 2014;17:404–13. https://doi.org/10.2118/164553-PA.
[45] Sanchez-Rivera D. Reservoir simulation and optimization of CO2 Huff-and-Puff operations in the Bakken Shale. The University of Texas at Austin, 2014.
[46] Yu W, Lashgari H, Sepehrnoori K. Simulation Study of CO2 Huff-n-Puff Process in Bakken Tight Oil Reservoirs. SPE West. North Am. Rocky Mt., vol. 2, Denver, Colorado: SPE; 2014. https://doi.org/10.2118/169575-MS.
[47] Yu W, Lashgari HR, Wu K, Sepehrnoori K. CO2 injection for enhanced oil recovery in Bakken tight oil reservoirs. Fuel 2015;159:354–63. https://doi.org/10.1016/j.fuel.2015.06.092.
[48] Sun J, Zou A, Sotelo E, Schechter D. Numerical simulation of CO2 huff-n-puff in complex fracture networks of unconventional liquid reservoirs. J Nat Gas Sci Eng 2016;31:481–92. https://doi.org/10.1016/j.jngse.2016.03.032.
[49] Alharthy N, Teklu T, Kazemi H, Graves R, Hawthorne S, Braunberger J, et al. Enhanced oil recovery in liquid-rich shale reservoirs: Laboratory to field. SPE Reserv Eval Eng 2018;21:137–59. https://doi.org/10.2118/175034-pa.
[50] Yu W, Lashgari H, Sepehrnoori K. Simulation Study of CO2 Huff-n-Puff Process in Bakken Tight Oil Reservoirs. SPE West North Am Rocky Mt Jt Meet 2014:16. https://doi.org/10.2118/169575-MS.
[51] Kim TH, Cho J, Lee KS. Modeling of CO2 Flooding and Huff and Puff Considering Molecular Diffusion and Stress-Dependent Deformation in Tight Oil Reservoir. SPE Eur Featur 79th EAGE Conf Exhib 2017. https://doi.org/10.2118/185783-MS.
[52] Song C, Yang D. Performance Evaluation of CO2 Huff-n-Puff Processes in Tight Oil Formations. SPE Unconv Resour Conf Canada 2013. https://doi.org/10.2118/167217-MS.
[53] Joslin K, Abraham AM, Thaker T, Pathak V, Kumar A. Viability of EOR Processes in the Bakken Under Geological and Economic Uncertainty. SPE Canada Unconv Resour Conf 2018. https://doi.org/10.2118/189779-MS.
[54] McPhee C, Reed J, Zubizarreta I. Chapter 4 - Core Sample Preparation. In: McPhee C, Reed J, Zubizarreta IBT-D in PS, editors. Core Anal., vol. 64, Elsevier; 2015, p. 135–79. https://doi.org/10.1016/B978-0-444-63533-4.00004-4.
[55] Sorensen JA, Braunberger JR, Liu G, Smith SA, Hawthorne SA, Steadman EN, et al. Characterization and Evaluation of the Bakken Petroleum System for CO2 Enhanced Oil Recovery. SPE/AAPG/SEG Unconv Resour Technol Conf 2015. https://doi.org/10.15530/URTEC-2015-2169871.
[56] Adekunle O, Hoffman BT. Minimum Miscibility Pressure Studies in the Bakken. SPE Improv Oil Recover Symp 2014:SPE-169077-MS. https://doi.org/10.2118/169077-MS.
[57] Holm LW, Josendal VA. Mechanisms of Oil Displacement By Carbon Dioxide. JPT, J Pet Technol 1974;26:1427–38. https://doi.org/10.2118/4736-PA.
[58] Eide Ø, Fernø MA, Alcorn Z, Graue A. Visualization of Carbon Dioxide Enhanced Oil Recovery by Diffusion in Fractured Chalk. SPE J 2016;21:112–20. https://doi.org/10.2118/170920-PA.
[59] Sun R, Yu W, Xu F, Pu H, Miao J. Compositional simulation of CO2 Huff-n-Puff process in Middle Bakken tight oil reservoirs with hydraulic fractures. Fuel 2019;236:1446–57.

https://doi.org/10.1016/j.fuel.2018.09.113.
[60] Eide O, Ersland G, Brattekas B, Haugen A, Graue A, Ferno M. CO2 EOR by Diffusive Mixing in Fractured Reservoirs. Petrophysics 2015;56:23–31.
[61] Wang L, Yu W. Gas Huff and Puff Process in Eagle Ford Shale: Recovery Mechanism Study and Optimization. SPE Oklahoma City Oil Gas Symp 2019. https://doi.org/10.2118/195185-MS.
[62] Song Y-Q, Kausik R. NMR application in unconventional shale reservoirs – A new porous media research frontier. Prog Nucl Magn Reson Spectrosc 2019;112–113:17–33. https://doi.org/https://doi.org/10.1016/j.pnmrs.2019.03.002.
[63] Moh DY, Zhang H, Wang S, Yin X, Qiao R. Soaking in CO2 huff-n-puff: A single-nanopore scale study. Fuel 2022;308:122026. https://doi.org/10.1016/j.fuel.2021.122026.
[64] Peng X, Wang Y, Diao Y, Zhang L, Yazid IM, Ren S. Experimental investigation on the operation parameters of carbon dioxide huff-n-puff process in ultra low permeability oil reservoirs. J Pet Sci Eng 2019;174:903–12. https://doi.org/10.1016/j.petrol.2018.11.073.
[65] Mohammad RS, Zhang S, Zhao X, Lu S. An Experimental Study of Cyclic CO2-Injection Process in Unconventional Tight Oil Reservoirs. Oil Gas Res 2018;04:1–9. https://doi.org/10.4172/2472-0518.1000150.
[66] Liu K, Ostadhassan M, Zhou J, Gentzis T, Rezaee R. Nanoscale pore structure characterization of the Bakken shale in the USA. Fuel 2017;209:567–78. https://doi.org/10.1016/j.fuel.2017.08.034.
[67] Onwumelu C, Nordeng S, Adeyilola A, Nwachukwu F, Azenkeng A, Smith S. Microscale Pore Characterization of Bakken Formation. 53rd US Rock Mech Symp 2019:10.
[68] Chen C, Gu M. Investigation of cyclic CO2 huff-and-puff recovery in shale oil reservoirs using reservoir simulation and sensitivity analysis. Fuel 2017;188:102–11. https://doi.org/10.1016/j.fuel.2016.10.006.
[69] Tang M, Zhao H, Ma H, Lu S, Chen Y. Study on CO2 huff-n-puff of horizontal wells in continental tight oil reservoirs. Fuel 2017;188:140–54. https://doi.org/10.1016/j.fuel.2016.10.027.
[70] Pu W, Wei B, Jin F, Li Y, Jia H, Liu P, et al. Experimental investigation of CO2 huff-n-puff process for enhancing oil recovery in tight reservoirs. Chem Eng Res Des 2016;111:269–76. https://doi.org/10.1016/j.cherd.2016.05.012.
[71] Yu W, Lashgari HR, Wu K, Sepehrnoori K. CO2 injection for enhanced oil recovery in Bakken tight oil reservoirs. Fuel 2015;159:354–63. https://doi.org/https://doi.org/10.1016/j.fuel.2015.06.092.
[72] Fakher S, Imqam A. Asphaltene precipitation and deposition during CO2 injection in nano shale pore structure and its impact on oil recovery. Fuel 2019;237:1029–39. https://doi.org/10.1016/j.fuel.2018.10.039.
[73] Mullins O, Sheu E, Hammami A, Marshall A. Asphaltenes, Heavy Oils, and Petroleomics. 2007. https://doi.org/10.1007/0-387-68903-6.
[74] Fatah A, Mahmud H Ben, Bennour Z, Hossain M, Gholami R. Effect of supercritical CO2 treatment on physical properties and functional groups of shales. Fuel 2021;303:121310. https://doi.org/https://doi.org/10.1016/j.fuel.2021.121310.
[75] Sanguinito S, Goodman A, Tkach M, Kutchko B, Culp J, Natesakhawat S, et al. Quantifying dry supercritical CO2-induced changes of the Utica Shale. Fuel 2018;226:54–64. https://doi.org/https://doi.org/10.1016/j.fuel.2018.03.156.

[76] Shiraki R, Dunn TL. Experimental study on water–rock interactions during CO2 flooding in the Tensleep Formation, Wyoming, USA. Appl Geochemistry 2000;15:265–79. https://doi.org/10.1016/S0883-2927(99)00048-7.
[77] Khather M, Saeedi A, Rezaee R, Noble RRP, Gray D. Experimental investigation of changes in petrophysical properties during CO2 injection into dolomite-rich rocks. Int J Greenh Gas Control 2017;59:74–90. https://doi.org/10.1016/j.ijggc.2017.02.007.
[78] Hemme C, van Berk W. Change in cap rock porosity triggered by pressure and temperature dependent CO2–water–rock interactions in CO2 storage systems. Petroleum 2017;3:96–108. https://doi.org/10.1016/j.petlm.2016.11.010.
[79] Saeedi A, Delle Piane C, Esteban L, Xie Q. Flood characteristic and fluid rock interactions of a supercritical CO2, brine, rock system: South West Hub, Western Australia. Int J Greenh Gas Control 2016;54:309–21. https://doi.org/10.1016/j.ijggc.2016.09.017.
[80] Zhao J, Wang P, Zhang Y, Ye L, Shi Y. Influence of CO2 injection on the pore size distribution and petrophysical properties of tight sandstone cores using nuclear magnetic resonance. Energy Sci Eng 2020;8. https://doi.org/10.1002/ese3.663.
[81] Bacci G, Korre A, Durucan S. An experimental and numerical investigation into the impact of dissolution/precipitation mechanisms on CO2 injectivity in the wellbore and far field regions. Int J Greenh Gas Control 2011;5:579–88. https://doi.org/10.1016/j.ijggc.2010.05.007.
[82] Soroush S, Pourafshary P, Vafaie-Sefti M. A Comparison of Asphaltene Deposition in Miscible and Immiscible Carbon Dioxide Flooding in Porous Media. SPE EOR Conf Oil Gas West Asia 2014:10. https://doi.org/10.2118/169657-MS.
[83] Srivastava RK, Huang SS. Asphaltene Deposition During CO2 Flooding: A Laboratory Assessment. SPE Prod Oper Symp 1997:19. https://doi.org/10.2118/37468-MS.
[84] Jin C, Liu L, Li Y, Zeng R. Capacity assessment of CO2 storage in deep saline aquifers by mineral trapping and the implications for Songliao Basin, Northeast China. Energy Sci Eng 2017;5:81–9. https://doi.org/10.1002/ese3.151.
[85] Gharbi O, Bijeljic B, Boek E, Blunt MJ. Changes in Pore Structure and Connectivity Induced by CO2 Injection in Carbonates: A Combined Pore-Scale Approach. Energy Procedia 2013;37:5367–78. https://doi.org/10.1016/j.egypro.2013.06.455.
[86] Rosenbauer RJ, Koksalan T, Palandri JL. Experimental investigation of CO2–brine–rock interactions at elevated temperature and pressure: Implications for CO2 sequestration in deep-saline aquifers. Fuel Process Technol 2005;86:1581–97. https://doi.org/10.1016/j.fuproc.2005.01.011.
[87] Zhu W, Ma Q, Song Z, Lin J, Li M, Li B. The effect of injection pressure on the microscopic migration characteristics by CO 2 flooding in heavy oil reservoirs. Energy Sources, Part A Recover Util Environ Eff 2019:1–9. https://doi.org/10.1080/15567036.2019.1644399.
[88] Ross GD, Todd AC, Tweedie JA. The effect of simulated CO2 flooding on the permeability of reservoir rocks. Enhanc Oil Recover Elsevier, Amsterdam 1981:351–66.
[89] Haghighi OM, Zargar G, Khaksar Manshad A, Ali M, Takassi MA, Ali JA, et al. Effect of Environment-Friendly Non-Ionic Surfactant on Interfacial Tension Reduction and Wettability Alteration; Implications for Enhanced Oil Recovery. Energies 2020;13. https://doi.org/10.3390/en13153988.
[90] Nazarahari MJ, Manshad AK, Ali M, Ali JA, Shafiei A, Sajadi SM, et al. Impact of a novel biosynthesized nanocomposite (SiO2@Montmorilant@Xanthan) on wettability shift and

interfacial tension: Applications for enhanced oil recovery. Fuel 2021;298:120773. https://doi.org/https://doi.org/10.1016/j.fuel.2021.120773.
[91] Anderson WG. Wettability Literature Survey- Part 1: Rock/Oil/Brine Interactions and the Effects of Core Handling on Wettability. J Pet Technol 1986;38:1125–44. https://doi.org/10.2118/13932-PA.
[92] McPhee C, Reed J, Zubizarreta I. Chapter 7 - Wettability and Wettability Tests. In: McPhee C, Reed J, Zubizarreta IBT-D in PS, editors. Core Anal., vol. 64, Elsevier; 2015, p. 313–45. https://doi.org/10.1016/B978-0-444-63533-4.00007-X.
[93] Anderson W. Wettability Literature Survey- Part 2: Wettability Measurement. J Pet Technol 1986;38:1246–62. https://doi.org/10.2118/13933-PA.
[94] Chilingar G V, Yen TF. Some notes on wettability and relative permeabilities of carbonate reservoir rocks, II. Energy Sources 1983;7:67–75.
[95] Mousavi Moghadam A, Baghban Salehi M. Enhancing hydrocarbon productivity via wettability alteration: a review on the application of nanoparticles. Rev Chem Eng 2019;35:531–63. https://doi.org/doi:10.1515/revce-2017-0105.
[96] McPhee C, Reed J, Zubizarreta I. Chapter 11 - Nuclear Magnetic Resonance (NMR). In: McPhee C, Reed J, Zubizarreta IBT-D in PS, editors. Core Anal., vol. 64, Elsevier; 2015, p. 655–69. https://doi.org/10.1016/B978-0-444-63533-4.00011-1.
[97] Coates GR, Peveraro RCA, Hardwick A, Roberts D. The Magnetic Resonance Imaging Log Characterized by Comparison With Petrophysical Properties and Laboratory Core Data. SPE Annu Tech Conf Exhib 1991. https://doi.org/10.2118/22723-MS.
[98] Gao H, Liu Y, Zhang Z, Niu B, Li H. Impact of Secondary and Tertiary Floods on Microscopic Residual Oil Distribution in Medium-to-High Permeability Cores with NMR Technique. Energy & Fuels 2015;29:4721–9. https://doi.org/10.1021/acs.energyfuels.5b00394.
[99] Fang T, Zhang L, Liu N, Zhang L, Wang W, Yu L, et al. Quantitative characterization of pore structure of the Carboniferous–Permian tight sandstone gas reservoirs in eastern Linqing depression by using NMR technique. Pet Res 2018;3:110–23. https://doi.org/10.1016/j.ptlrs.2018.06.003.
[100] Zdravkov B, Čermák J, Šefara M, Janků J. Pore classification in the characterization of porous materials: A perspective. Open Chem 2007;5:385–95. https://doi.org/doi:10.2478/s11532-007-0017-9.
[101] Badrouchi N, Badrouchi F, Tomomewo OS, Pu H. Experimental Investigation of CO2-EOR Viability in Tight Formations: Mountrail County Case Study. 54th US Rock Mech Symp 2020.
[102] Badrouchi N, Pu H, Smith S, Badrouchi F. Evaluation of CO2 enhanced oil recovery in unconventional reservoirs: Experimental parametric study in the Bakken. Fuel 2022;312:122941. https://doi.org/https://doi.org/10.1016/j.fuel.2021.122941.
[103] Chen Y, Sari A, Xie Q, Brady P V, Hossain MM, Saeedi A. Electrostatic Origins of CO2-Increased Hydrophilicity in Carbonate Reservoirs. Sci Rep 2018;8:17691. https://doi.org/10.1038/s41598-018-35878-3.
[104] Teklu TW, Alameri W, Graves RM, Kazemi H, AlSumaiti AM. Low-salinity water-alternating-CO2 EOR. J Pet Sci Eng 2016;142:101–18. https://doi.org/10.1016/j.petrol.2016.01.031.
[105] Hawthorne SB, Miller DJ. Comparison of CO2 and Produced Gas Hydrocarbons to

Dissolve and Mobilize Bakken Crude Oil at 10.3, 20.7, and 34.5 MPa and 110 °C. Energy & Fuels 2020;34:10882–93. https://doi.org/10.1021/acs.energyfuels.0c02112.
[106] Hawthorne SB, Miller DJ. A comparison of crude oil hydrocarbon mobilization by vaporization gas drive into methane, ethane, and carbon dioxide at 15.6 MPa and 42 °C. Fuel 2019;249:392–9. https://doi.org/https://doi.org/10.1016/j.fuel.2019.03.118.
[107] North Dakota Drilling and Production Statistics 2012. https://www.dmr.nd.gov/oilgas/stats/statisticsvw.asp (accessed January 28, 2022).
[108] Mahzari P, Mitchell TM, Jones AP, Oelkers EH, Striolo A, Iacoviello F, et al. Novel laboratory investigation of huff-n-puff gas injection for shale oils under realistic reservoir conditions. Fuel 2021;284:118950. https://doi.org/https://doi.org/10.1016/j.fuel.2020.118950.
[109] Eide, Fernø MA, Karpyn Z, Haugen Å, Graue A. CO2 injections for enhanced oil recovery visualized with an industrial CT-scanner. 17th Eur Symp Improv Oil Recover IOR 2013 - Saint Petersburg, Russ Fed 2013. https://doi.org/10.3997/2214-4609.20142641.
[110] Hawthorne SB, Miller DJ, Grabanski CB, Jin L. Experimental Determinations of Minimum Miscibility Pressures Using Hydrocarbon Gases and CO2 for Crude Oils from the Bakken and Cut Bank Oil Reservoirs. Energy & Fuels 2020;34:6148–57. https://doi.org/10.1021/acs.energyfuels.0c00570.
[111] Hawthorne SB, Grabanski CB, Jin L, Bosshart NW, Miller DJ. Comparison of CO2 and Produced Gas Hydrocarbons to Recover Crude Oil from Williston Basin Shale and Mudrock Cores at 10.3, 17.2, and 34.5 MPa and 110 °C. Energy & Fuels 2021;35:6658–72. https://doi.org/10.1021/acs.energyfuels.1c00412.
[112] Hawthorne SB, Miller DJ, Jin L, Azzolina NA, Hamling JA, Gorecki CD. Lab and Reservoir Study of Produced Hydrocarbon Molecular Weight Selectivity during CO2 Enhanced Oil Recovery. Energy & Fuels 2018;32:9070–80. https://doi.org/10.1021/acs.energyfuels.8b01645.

Name: Nidhal Badrouchi

Degree: Doctor of Philosophy

This document, submitted in partial fulfillment of the requirements for the degree from the University of North Dakota, has been read by the Faculty Advisory Committee under whom the work has been done and is hereby approved.

DocuSigned by:
Vamegh Rasouli
0EB956E8C9C9456...
Vamegh Rasouli

DocuSigned by:
Hui Pu
C63B8AB854E4448...
Hui Pu

DocuSigned by:
Minou Rabiei
DB5B8BA42D59466...
Minou Rabiei

DocuSigned by:
Kegang Ling
AE10F7CCAFC7487...
Kegang Ling

DocuSigned by:
Dr. Kouhyar Tavakolian
A24D898B29D94B8...
Kouhyar Tavakolian

This document is being submitted by the appointed advisory committee as having met all the requirements of the School of Graduate Studies at the University of North Dakota and is hereby approved.

DocuSigned by:
Chris Nelson
2E0AF088C7334O3...
Chris Nelson
Dean of the School of Graduate Studies

6/8/2022
Date

PERMISSION

Title Evaluation of CO_2 Enhanced Oil Recovery in Unconventional Reservoirs

Department Petroleum Engineering

Degree Doctor of Philosophy

In presenting this thesis in partial fulfillment of the requirements for a graduate degree from the University of North Dakota, I agree that the library of this University shall make it freely available for inspection. I further agree that permission for extensive copying for scholarly purposes may be granted by the professor who supervised my thesis work or, in his absence, by the Chairperson of the department or the dean of the School of Graduate Studies. It is understood that any copying or publication or other use of this thesis or part thereof for financial gain shall not be allowed without my written permission. It is also understood that due recognition shall be given to me and to the University of North Dakota in any scholarly use which may be made of any material in my thesis.

Nidhal Badrouchi

Date

ACKNOWLEDGMENTS

I wish to express my sincere appreciation to my advisor, Profs. Vamegh Rasouli and Hui Pu for their guidance and support during my time in the PhD program at the University of North Dakota. I would like to extend my appreciation to the committee members, Dr. Kegang Ling, Dr. Minou Rabiei, and Dr. Kouhyar Tavakolian. I acknowledge the financial support of the North Dakota Industry Commission during the beginning of my research program (NDIC).

DEDICATIONS

I dedicate this work to my family. They were and will always be my source of inspiration and motivation. To my father, mother, sister, and brothers. To my supportive beautiful wife and my son YASSIN.

Abstract

The recent advances in horizontal drilling and hydraulic fracturing have enabled a profitable oil and gas recovery from unconventional geologic plays. The Bakken is one of the largest oil-bearing tight formations in North America, with an estimated original oil in place of 600 billion barrels; however, only a small fraction (7% to 12%) of this oil is recoverable using currently available technologies.

CO_2 injection can be an effective technique to enhance the oil recovery from unconventional reservoirs. It can assist with extracting residual oil and overcoming injectivity problems in tight formations. Previous CO_2 enhanced oil recovery (EOR) pilot tests performed in the Bakken Formation indicated that cyclic CO_2 injection might be a promising technique for enhanced oil recovery; however, no clear consensus has been reached, and the reported results have revealed that CO_2 EOR mechanisms in unconventional reservoirs are still poorly understood. This study addresses the knowledge gap related to CO_2 EOR in unconventional reservoirs, investigates the side effects of CO_2 injection, and compares the EOR performance of different gases to determine the optimum EOR scheme in tight formations.

We investigated and analyzed the effects of different parameters on CO_2 performance using samples from the Middle Bakken member and Three Forks Formation. The factors studied include CO_2 Huff-n-Puff (HnP) injection parameters, sample size, water presence within the fractures, and the volume of CO_2 in contact with the rock matrix during the HnP experiments.

The injected CO_2 can interact with the *in-situ* reservoir fluids and rock minerals, which can impact and alter several reservoir attributes. The potential changes in rock wettability, pore size

distribution, and effective porosity before and after exposure to CO_2 were evaluated. The results indicate that CO_2 can alter wettability and increase the hydrophilicity of the rock. The nuclear magnetic resonance spectroscopy technique was used to determine fluid distribution before and after CO_2 injection. The results confirm that carbonic acid can dissolve portions of the dolomite, calcite, and feldspar in the rock and create new micro- and nanopores.

We compared the EOR performance of CO_2 and hydrocarbon gases to determine the most effective gases. Then we introduced a novel gas EOR scheme to boost oil mobilization and achieve higher recovery factors.

Content

List of Figures

List of Tables

Chapter 1

CO_2 EOR in Unconventional Plays

1.1 Introduction

Oil production from tight reservoirs became possible and economically efficient after the development of hydraulic fracturing and horizontal drilling. The U.S. Energy Information Administration estimated in 2019 that 63% of the total U.S crude oil production is from tight oil resources [1]. The Bakken is one of the largest oil-bearing tight formations in North America, with an estimated original oil in place (OOIP) of 300 to 900 billion barrels [2,3]; however, long-term stable oil production from tight formations in ND is becoming a challenge [4,5]. Horizontal wells drilled in targeted formations have decline rates higher than 80% over the first three years of their production lives. Depletion drive is the current primary oil production mechanism in the Bakken [6–9], which recovers approximately 8% to 12 % of the OOIP [10,11]. There is an immense volume of residual oil in unconventional reservoirs; therefore, any incremental production improvement could dramatically increase recoverable oil, extend the life of unconventional

reservoirs, and contribute to greater energy independence and security. Each 1% increase in the oil recovery factor could result in revenues of $128 to $720 billion with an estimated oil price of $80 per barrel [12]; therefore, it is crucial to evaluate the potential of EOR techniques in the Bakken and understand their application to other tight formations.

Different techniques have been successfully implemented to improve oil recovery in conventional reservoirs. CO_2 flooding, in particular, has demonstrated tremendous success over the past four decades [13]. The poor reservoir quality in the Bakken has limited the number of appropriate enhanced oil recovery techniques. Previous water injection pilot tests revealed that fluid injectivity is the primary concern due to very low matrix permeability [14]. Gas injection pilot tests revealed that injectivity is not a concern in Bakken; however, gas flooding in densely fractured unconventional reservoirs may result in early breakthrough, resulting in poor performance [15]. CO_2 can be injected at different cycles using the HnP technique to mitigate these issues [16,17]. Each CO_2 HnP cycle consists of three phases: 1) injecting CO_2 into the reservoir via the well, or around the core sample in the case of laboratory experiments, 2) pausing injection to close the system, which allows the injected CO_2 to soak for a given period, and 3) opening the system for production (see Fig. **1.1**).

CO_2 EOR techniques have been extensively studied, well understood, and successfully applied over the last four decades to conventional reservoirs; however, the evaluation of their applicability to unconventional reservoirs began in the last decade [17]. The assessment of CO_2 EOR potential in tight formations is still in the preliminary stage compared to conventional reservoirs, and the recovery mechanisms are still poorly understood[18–20]. Todd et al. [14] discussed the results of CO_2 EOR pilot tests in the Bakken, which revealed that the simulation studies in the literature were too optimistic, and the previous core-scale injection tests overestimated CO_2 potential. These pilot-

scale results indicate that CO_2 EOR mechanisms in shale formations are not well understood, demonstrating the need for further evaluation efforts [14,15].

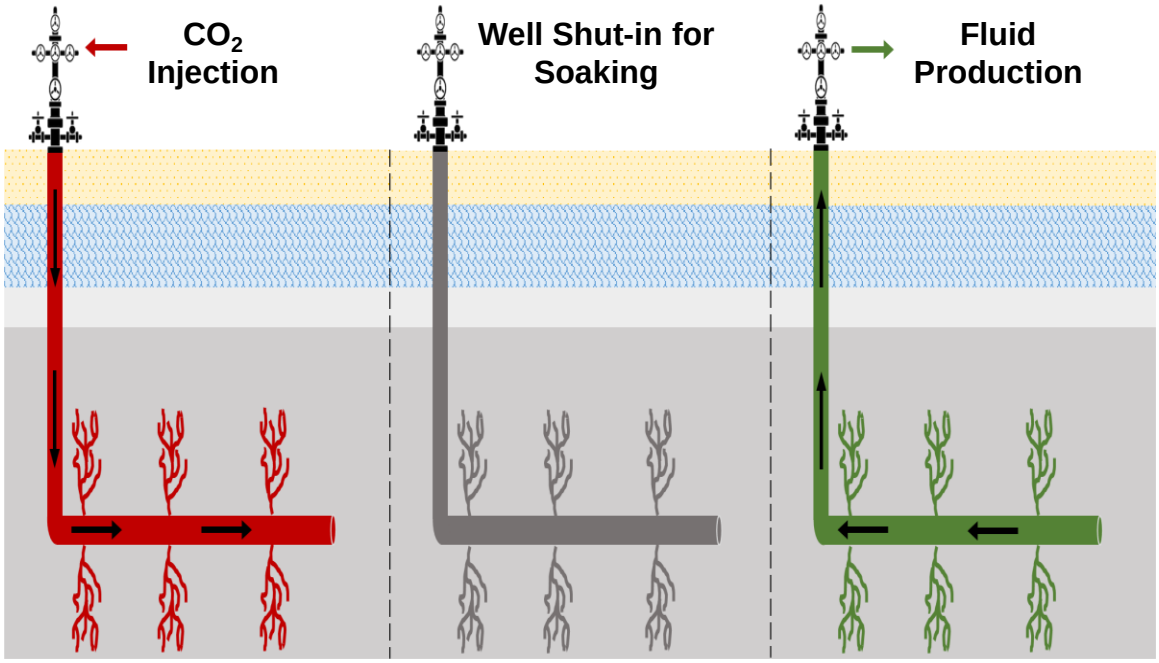

Fig. 1.1. Schematic of CO_2 Huff-n-Puff injection

1.2 Objectives

As mentioned above, the immense volume of residual oil in Bakken is a strong motivation to perform EOR studies. Therefore, the overall goal of this study is to evaluate the performance of CO_2 injection in Bakken oil reservoirs. The detailed objectives of this work can be summarized as followings:

1. Comprehensive review of existing literature on CO_2 injection in tight formations. This includes laboratory experiments, numerical simulations, and field pilot tests.
2. Evaluate the effect of injection pressure, soaking time, and the number of injection cycles using CO_2 HnP under typical reservoir conditions.

3. Perform a parametric study to investigate the effect of multiple parameters on CO_2 EOR performance and oil recovery from ultra-tight core samples. The parameters that will be investigated include the sample size, HnP schedule, water presence, CO_2 volume to exposed rock surface, and a comparison of CO_2 flooding vs HnP.
4. Investigate the possible side effects of CO_2 injection on different reservoir attributes, which might result after the interactions of the injected CO_2 with minerals present in the reservoir rock.
5. Evaluate the EOR performance of CO_2 and different hydrocarbon gases by comparing the Minimum Miscibility Pressure (MMP), capacity to dissolve oil, and molecular weight selectivity. Introduce a novel EOR scheme by combining CO_2 and hydrocarbon gases.

1.3 Methodology

The following approaches will be used to accomplish the objectives of this project.

1. Retrieve representative oil and rock samples from the targeted formations.
2. Characterize the reservoir sections of interest and determine the reservoir properties using representative oil and rock samples. This includes a detailed PVT study of the obtained oil sample and evaluation of porosity, permeability, and mineralogical composition of the rock samples.
3. Prepare the experimental setup to perform CO_2 HnP tests and conduct several CO_2 injection experiments.
4. Use the X-Ray Diffraction technique to determine the mineralogical composition of the selected samples and identify the possible chemical reaction between the injected CO_2 and the existing rock minerals.

5. Use the Nuclear Magnetic Resonance (NMR) technique to identify the fluid distribution in the samples before and after CO_2.
6. Measure the contact angle to identify the change of the wettability state of the rock sample after CO_2 exposure.
7. Use the data in the literature to compare the EOR performance of different gas EOR agents and select the most promising ones. Perform multiple cyclic injection tests using those gases to measure the oil recovery. Then, combine the selected gases in one injection scheme to improve the EOR performance.

1.4 Significance

Any incremental production improvement in Bakken could dramatically increase the oil recovery. In fact, due to the large volume of residual oil in Bakken, each 1% increase in the oil recovery factor could result in revenues of $128 to $720 billion with an estimated oil price of $80 per barrel. This study addresses the knowledge gap related to CO_2 EOR in unconventional reservoirs and the lack of understanding of the mechanisms that control the oil recovery. The obtained results will aid industry and academia in their understanding of CO_2 EOR performance in tight formations and contribute to designing an optimum CO_2 injection solution that will unlock billions of barrels of residual oil in unconventional reservoirs.

The results of this research study will present multifold novelties, including the followings:

1. In this project, we have addressed the gap between the results of the recent pilot tests and previous research studies in the Bakken.
2. A thorough parametric study was conducted to examine and understand the effects of key parameters on CO_2 EOR using representative samples from the Middle Bakken Member (MB) and the Three Forks Formation (TF).

3. The side effects of CO_2 injection on different reservoir attributes in Bakken, as will be presented in this study, were evaluated and discussed to enlighten future EOR projects.
4. This research project includes a comparison of the EOR performance of multiple gases (CO_2, methane, ethane, propane, and rich gas mixture) using available data in the literature and our lab experiments. A novel gas EOR scheme is introduced, which can help further increase the oil recovery.
5. The results and discussions included in this study can be used to improve the understanding of oil recovery mechanisms using gas injection in unconventional reservoirs.
6. Practical recommendations and suggestions that are proposed in this study contribute to designing an optimum EOR solution to unlock billions of barrels of residual oil.

1.5 Thesis structure

This thesis consists of eight chapters

Chapter 1 is an introduction to the project. A brief overview of CO_2 EOR and injection techniques in unconventional reservoirs is given. We also listed the objectives, methodology, and significance of this study.

Chapter 2 includes an overview of the Bakken Petroleum System and a literature review of the previous numerical simulation, experimental work, and field pilot tests performed in Bakken.

Chapter 3 details the methodology we followed, and the different materials used in this study. The description of the different experimental designs and the methods used are presented in this section.

Chapter 4 presents the optimization of the injection parameters, using CO_2 HnP injection scheme, which include the injection pressure, soaking time, and number of injection cycles.

Chapter 5 discusses the effect of water presence, sample size, injection scheme, and fracture size on CO_2 performance in tight formations.

In Chapter 6 the effect of CO_2 injection on different reservoir properties in MB and TF, as wettability, pore size distribution, and porosity will be investigated.

Chapter 7 presents the comparison of EOR performance of CO_2 and different hydrocarbon gases. A novel injection scheme that consists of combining the most promising gases will be introduced.

In Chapter 8 a summary of the findings from this study will be presented along with some recommendations and future studies that can be carried out.

1.6 Summary

This chapter introduced the need for EOR techniques in Bakken. It was highlighted that recent field CO_2 injection pilot tests indicated that oil recovery mechanisms using CO_2 injection in unconventional reservoirs are still in the primary stage, demonstrating the need for further evaluation efforts. Also, it was mentioned that can HnP injection scheme can help overcome the challenges related to continuous injection in poor quality reservoirs, which may result in early CO2 breakthrough and inefficient oil displacement.

Also, in this Chapter, a summary of the main objectives of this research, the methodology which will be implemented, distinguished aspects of this study and the structure of this thesis were presented.

In the next Chapter, an overview of the Bakken petroleum system and a review of the literature will be presented to give a background to CO_2 EOR techniques in Bakken and unconventional in general.

Chapter 2

Literature Review

In this Chapter, we present an overview of the Bakken Petroleum System (BPS), a review of the CO_2 EOR studies in tight formations, and a review of the field EOR pilot tests conducted in Bakken. The chapter is divided into three sections related to BPS overview, previous research work, field pilot tests.

2.1 Overview of the Bakken Petroleum System

The Bakken is one of the largest oil-bearing tight formations in North America that covers parts of the United States in Montana and North Dakota and parts of Saskatchewan and Manitoba in Canada [21] (Fig. 2.1). Oil was initially discovered in the Bakken in 1951, but with a very limited production capacity before a tremendous oil production increase took place in 2006 (Fig. 2.2). The Bakken petroleum system is composed of: The Upper Bakken Shale member (UBS), Middle Bakken Member, Lower Bakken Shale member (LBS), and the Three Forks (Fig. 2.3). The UBS and LBS members constitute the source rocks, whereas the middle member and the underlying

Three Forks formation are the oil reservoir units, and they are both classified as unconventional reservoirs [22,23].

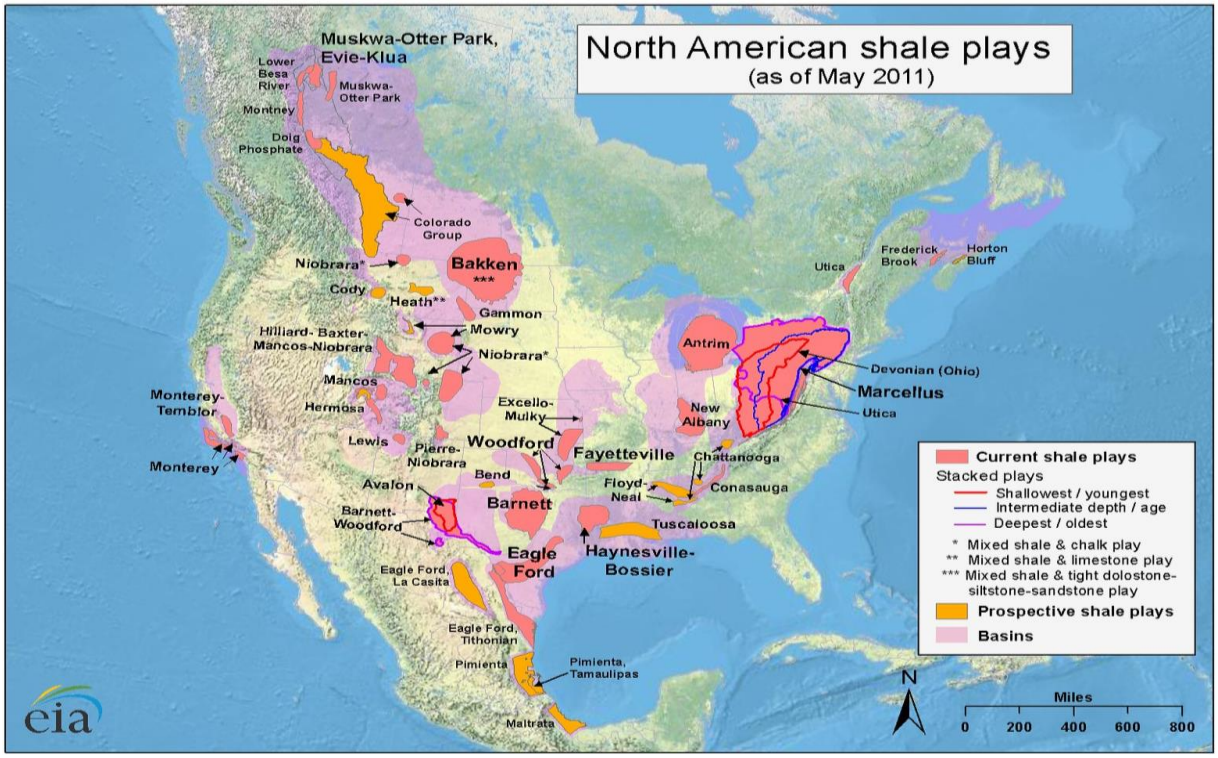

Fig. 2.1. North America shale resource plays [24]

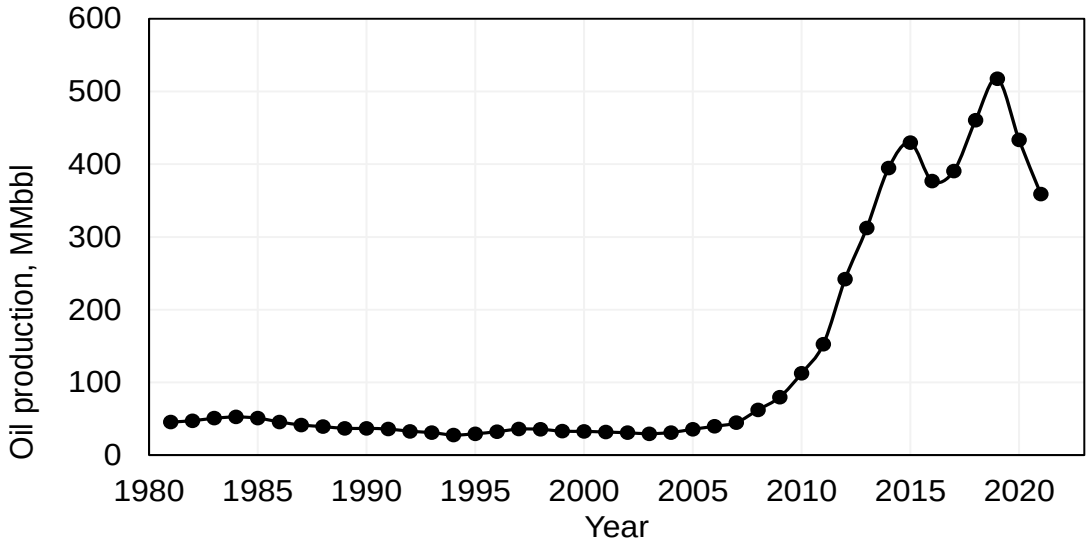

Fig. 2.2. North Dakota oil production history [25]

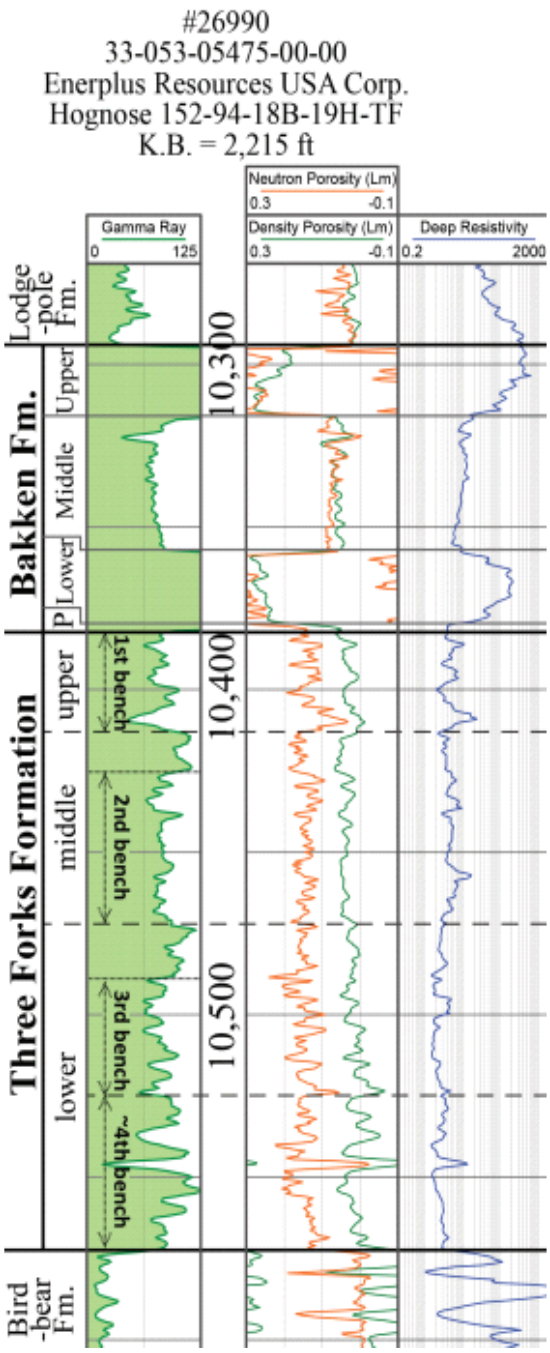

Fig. 2.3. Typical well logs for the Bakken petroleum system showing both Three Forks and Bakken formations [22]

The middle member was the main target for oil production until 2012 when some operators started drilling and completing in the Three Forks Formation, And they started to consider it as a prospective unconventional reservoir [22,23]. Both formations are characterized by low

permeability and porosity, so they are considered as ultra-tight formations. The average porosity is somewhere between 4% and 8%, while the permeability is in a micro- and nano-Darcy range [3]. The Middle Bakken formation consists of clastic and carbonate rocks, while Three Forks is formed of interbedded dolomitic mudstone and silty dolostone [21]. OOIP estimations varies from 300 to 900 billion barrels [10]; however, after the primary recovery the oil recovery factor is typically less than 12% of the OOIP [10,11].

2.2 CO_2 EOR Research Progress in Unconventional Oil Reservoirs

The technology for CO_2 EOR in tight oil plays is still in the early stages of development compared to conventional reservoirs [26]. Usually, every technology goes through three main stages, which are conceptualization, proof of concept, then implementation. At present, specifically in Bakken, EOR methods are in the early phase of proof of concept (see Fig. 2.4). In this section, we present a review the progress of CO_2 EOR-related work in the literature.

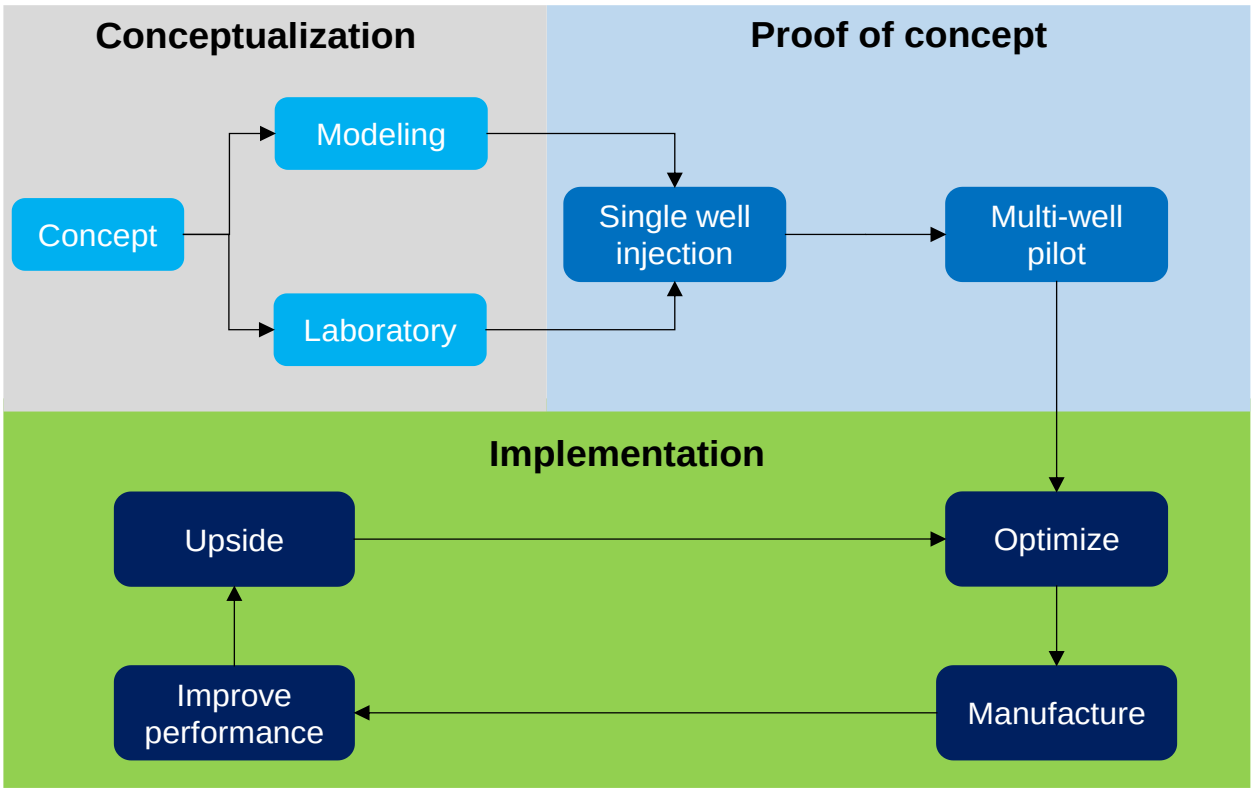

Fig. 2.4. Road map for EOR in Unconventional plays [27]

2.2.1 Miscible VS immiscible CO_2 injection

The miscibility conditions between the injected gas and the reservoir crude can be a fundamental parameter that controls the success of gas EOR applications in unconventional reservoirs. Some studies compared miscible and immiscible CO_2 EOR using tight rock samples; however, the results are contradictory in the literature.

Gamadi et al. [28] used two samples of 1.5 in diameter and 2 in length retrieved from Eagle Ford and Mancos shale. They used synthetic oil (C10-C13 Isoalkanes) to saturate the samples. They conducted experiments using a huff-and-puff scheme at 95°F and at pressures of 1500, 2500, and 3500 psi. The soak times varied from 6 to 48 hours. They reported recovery factors up to 95% and concluded that miscibility had a significant impact on oil recovery. They also found that the

recovery factor increases with pressure and soak time; however, they reported that injecting CO_2 at a pressure higher than the MMP does not result in an additional recovery.

Song and Yang [29] performed CO_2 HnP experiments at immiscible (1015 psi), near-miscible (1350 psi), and miscible (2030 psi) conditions. The authors reported that the samples were collected from the Bakken formation of southern Saskatchewan without specifying which member or lithology. Also, the dimensions of the samples were not reported. The experiments were conducted at 145.4°F. For each cycle, CO_2 was injected at constant pressure for 3 h, the system soaked for 6h, then the production lasted for 1h. A total of six cycles were performed for each scenario. The total oil recovery was 48%, 63%, and 61% for immiscible, near-miscible, and miscible conditions, respectively. No discussions were provided to explain the oil recovery drop at miscible conditions. The authors indicated that increasing the pressure above MMP does not result in higher oil recovery. It is important to mention that the tested plugs had porosity and permeability ranging from 18 to 23% and 0.2 to 0.8 mD, respectively, which might not be representative for ultra-low permeability and porosity of the characteristic of shale reservoirs.

Contrarily, other studies showed that increasing the pressure above MMP lead to higher recovery factors. Hawthorne et al. conducted several CO_2 HnP experiments using rock samples from MB and LBS. LBS samples were crushed and sieved to obtain 0.04 to 0.12 in size rock cuttings, and MB rods were drilled from the original core slabs rods using a 0.5 in diameter drill bit. The injection tests were performed at a temperature of 213 °F. Production fractions were collected after every hour, for the first seven hours of soaking time, then another fraction was collected at the end of 24 hours of soaking. Methylene chloride solution was used to capture the produced hydrocarbons. The CO_2 HnP tests were conducted at three injection pressures of 1494, 2495, and 5000 psi to represent immiscible, miscible, and above MMP conditions. The ultimate oil recovery

factor values for MB rods were 30% (immiscible), 82% (miscible), and 97% (above miscible), and 3% (immiscible), 14% (miscible), and 40% (above miscible) for the LBS samples. These results suggest that increasing the pressure above MMP results in a tremendous increase in oil recovery.

Similarly, Tovar et al. [30] and Adel et al. [31] studied the effect of injection pressure on CO_2 EOR performance using tight rock samples. They concluded that increasing the pressure above MMP results in higher recovery factors. They indicated the injection pressure strongly influence the recovery factor, and increasing the injection pressure above MMP result in incremental oil recovery.

These contradictory observations in the literature set the need for further evaluation efforts of CO_2 EOR performance under representative reservoir conditions.

2.2.2 Proposed CO_2 EOR mechanisms

Tovar et al. [32,33] coupled CO_2 HnP tests with Computed Tomography (CT) to investigate the oil recovery mechanism in shale oil reservoirs. They used a high-resolution medical CT-scanner to interpret CO_2 penetration into the rock matrix based on CT number change. CO_2 permeation of the rock matrix results in a change of the density throughout the rock sample during the soaking period, which is correlated to the CT number change. The analysis of the CT images and produced oil characteristics suggested that oil vaporization into the injected CO_2 is the governing mechanism of oil production.

Alfarge et al. [34,35] investigated CO_2-EOR mechanisms using HnP in shale oil reservoirs based on history matching results. They used numerical simulation and history matched CO_2 HnP experiments and field pilot tests that were performed in Bakken. They indicated that molecular diffusion is the governing mechanism that controls oil recovery in shale oil reservoirs and CO_2-diffusivity level dictates the success of CO_2-EOR project in shale formations.

Zhang et al. [36] used core scale simulation and CO_2 HnP experiments to unveil CO_2 EOR mechanisms in tight formations. They used samples from Eagle Ford shale to perform five CO_2 HnP tests at a temperature of 170°F and pressure values of 1400, 1800, 2500, 3000, and 3500 psi. The experimental results were used to history match the core scale model and obtain the diffusion coefficient of CO_2. A pseudo-ternary diagram was built for CO_2-oil system using Peng-Robinson EOS. Based on the observations from core-scale simulation and ternary diagram analysis, the authors indicated that multi-contact miscibility and vaporizing gas drive are the dominant mechanisms. Also, they compared CO_2 HnP results with Nitrogen injection at 5000 psi. At such pressure, N_2 is immiscible with the crude oil and has the same diffusion coefficient as CO_2. No oil was displaced from the rock matrix using N_2 injection. These results indicated that diffusion has a minor role in improving oil recovery in unconventional liquid reservoirs compared to multi-contact miscibility.

Hawthorne et al. [37] proposed a conceptual mechanism for CO_2 EOR in tight fractured formations. As presented in Fig. 2.5, the proposed mechanistic of oil displacement using CO_2 HnP consists of the following four steps: 1) during the initial injection, CO_2 fills the fracture space, 2) CO_2 begins to permeate the rock via pressure gradient and starts swelling the oil in the rock matrix, 3) as CO_2 permeation continues, swelling and viscosity reduction of the trapped oil will lead it to migrate from the rock matrix toward the fracture, and 4) The pressure equalizes throughout the rock, and molecular diffusion of hydrocarbons becomes the dominating process.

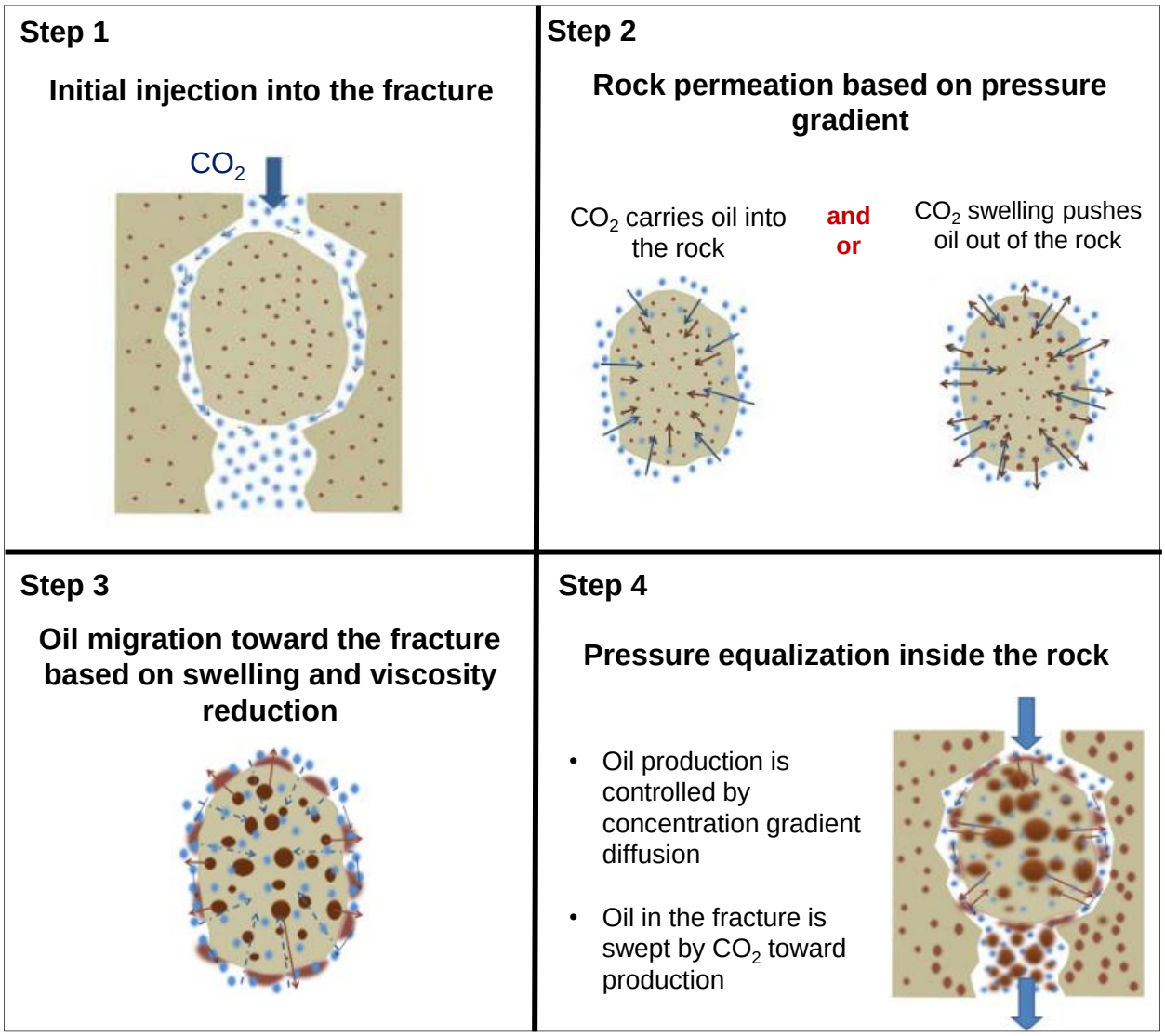

Fig. 2.5. Conceptual steps for oil mobilization using CO_2 injection in tight fractured formations (modified from [37])

2.2.3 CO_2 EOR potential estimation in Bakken

2.2.3.1 Experimental work

Compared to other shale oil plays, very few experimental studies were performed to estimate the CO_2 capacity to recover oil from Bakken oil reservoirs.

Tovar et al. [32] evaluated the performance of cyclic CO_2 injection using four preserved sidewall cores that were initially saturated with crude. The cores had a diameter of 1 in and a length of 1.5,

1.4,1.4, and 1.3 in. The authors did not report the specific location of the selected samples. The CO_2 was injected at a temperature of 150°F and pressure values of 1600 psi and 3000 psi. They opted to test the samples as received and without any intervention that might alter the properties of the cores; therefore, the petrophysical properties of the samples were unknown. They assumed different values for the porosity (0.3% and 0.6%) and water saturation (0% and 30%). Based on different porosity and water saturation scenarios, the estimated oil recovery factor values varied from 18 to 55%. The absence of an accurate measurement of the residual oil volume in the tested samples resulted in high uncertainty in recovery factor estimations.

Jin et al. [38,39] collected 21 preserved small samples from LBS, MB, UBS, and TF. They performed cyclic CO_2 injection experiments at 230°F. The LBS and UBS were represented using 0.04 to 0.12 in size rock cuttings. For the TF and MB, they drilled 0.4 in diameter and 1.5 in length cylindrical rods. The injection pressure was maintained at 5000 psi, and oil fractions were collected every hour for the first seven hours of the test. After 24 hours of exposure, the rock was crushed and extracted with methylene chloride to collect the remaining oil. The tests yielded very high recovery factors. After only seven hours of CO_2 exposure, they recovered almost 90% of the oil from the MB and TF rods, and the ultimate recoveries after 24 hours were between 95 and 100%. The ultimate oil recovery factors for UBS and LBS samples were around 60%.

Another experimental study that evaluated the oil recovery using CO_2 injection into Bakken rock samples was performed by Song and Yang [40]. They used rock samples from the Bakken formation of southern Saskatchewan. Using CO_2 HnP at 145°F and 2030 psi, they measured a recovery factor of 60 % of the OOIP after 6 hours of soaking. The permeability of the samples used in this test was around 0.8 mD, and the porosity was above 20%, which might represent the characteristics of ultra-tight formations and unconventional reservoirs.

2.2.3.2 Modeling studies

Table 1 illustrates different numerical simulation studies that evaluated the performance of CO_2 injection in Bakken. Most of the studies confirmed the viability of CO_2 EOR and estimated an oil recovery factor between 10 and 35%.

Table 1 Review of CO_2 EOR simulation studies in Bakken

Authors	Model	Simulator	EOR technique	Recovery Factor (RF)
Chen [41]	Single porosity	IMEX	CO_2 flooding and water flooding	7200 days of primary production + 30 cycles of CO_2 injection, each cycle includes: 200 days of injection and 200 days of production: **RF=25.5%** 3600 days of primary production and 60 years of CO_2 flooding production: **RF=15%** 10-year primary production and 60 years of water flooding: **RF=11.9%** 10-year primary production and 60 years of cyclic water flooding: **RF=11.03%** 70 years of water flooding production: **RF=11.05%**
Pu and Hoffman [42]	Single porosity	IMEX	CO_2, WAG, separator gas, lean gas	30-year recovery factor: WAG: **RF=22.74%** CO_2: **RF=24.59%** Separator gas: **RF=26.32%** Lean gas: **RF=22.28%**
Fai et al. [43]	Single porosity	Compositional simulator	Gas injection	1-year recovery factor: 100% CO_2: **RF=33%** 75% CO_2 + 25% C1: **RF=36%** 50% CO_2 + 50% C1: **RF=42%** 50% CO_2 + 25% C1 + 25% C2: **RF=42%**
Chen et al. [44]	Single porosity	UT-COMP	CO_2 huff 'n' puff	Step 1: 300 days of primary recovery; production at 3,000 psi Step 2: 30 days of CO_2 injection at 4,000 psi

				Step 3: 10/20 days of well shut-in (**W**) Step 4: 100 days of production at 3,000 psi Step 5: Repeat Steps 2 through 4 until 1,000 days **W**=10: **RF= 6%** **W**=20: **RF= 6%**
Sanchez [45]	Single porosity	GEM	CO_2/CO_2-enriched gas huff 'n' puff	1/30/100 days of soaking, with 30 days of injection and 200 days of production: **RF= 17%** Effect of the number of cycles: 2 cycles: **RF=16.3%** 5 cycles: **RF=17.3%** 8 cycles: **RF=17.8%**
Yu et al. [46]	Single porosity	GEM	CO_2 huff-n-puff	30 years Recovery Factor (RF) and Incremental Recovery Factor (IRF) Effect of number of fractures by stage 1 fracture/stage: **RF=15.8%** **IRF=4%** 2 fractures/stage: **RF=20%** **IRF=6.2%** 3 fractures/stage: **RF=20%** **IRF=5.2%** 4 fractures/stage: **RF=22%** **IRF=5.3%** Effect of Injection rate: 0 Mscf/day: **RF=12.5%** 50 Mscf/day: **RF=16%** 500 Mscf/day: **RF=24%**
Yu et al. [47]	Single porosity	GEM	CO_2 huff-n-puff	30 years Recovery Factor (RF) and Incremental Recovery Factor (IRF) Effect of number of cycles: 0 cycles: **RF=20%** 1 cycle: **RF=22%** 2 cycles: **RF=23.5%** 3 cycles: **RF=24%**

				Effect of fracture half-length: 110 ft: **RF= 16.5%**, **IRF=0%** 210 ft: **RF=22%**, **IRF=2%** 310 ft: **RF= 26%**, **IRF=3%**
Sun et al. [48]	Unstructured Discrete fracture network	In-house	CO_2 huff-n-puff	Initial reservoir pressure: 3000 psi. Effect of producer BHP: 1000 psi: **IRF=10%** 1300 psi: **IRF=3.56%** 1550 psi: **IRF=1.57%** 2000 psi: **IRF=1.68%**
Alharthy et al. [49]	Dual porosity and dual perm	GEM	NGL/CO_2 huff-n-puff	Experiment: The experiments recovered 90% oil from several Middle Bakken cores and nearly 40% from Lower Bakken cores. Simulation: Primary depletion: **RF=7.5%** Effect of CO_2 injection rate and soaking time: Injection: 200 Mscf/D; soaking: 15 days: **RF=12%** Injection: 200 Mscf/D; soaking: 30 days: **RF=12%** Injection: 400 Mscf/D; soaking: 15 days: **RF=14.5%** Injection: 400 Mscf/D; soaking: 30 days: **RF=14.5%** Effect of molecular diffusion: CO_2 injection without diffusion: **RF=11%** CO_2 injection with diffusion: **RF=11.5%** NGL injection without diffusion: **RF=12%** NGL injection with diffusion: **RF=12.5%**

2.2.4 Limitations of previous CO_2 EOR studies

Experimental work is fundamental to understanding and evaluating the performance of any new EOR technology in the oil and gas industry. The main limitations of most of the previous CO_2 EOR experimental studies can be summarized as follows:

- Several CO_2 injection tests were conducted under non-realistic reservoir conditions.
- Multiple studies used non-representative oil and rock samples as synthetic oil or rock samples with relatively high porosity and permeability.
- Most of the previous lab work studies used very small samples, which might not represent the heterogeneity in the formation and the complexity of fluid flow mechanistic in tight formations.

Also, there is no agreement in the literature regarding the oil mechanisms using CO_2 injection in unconventional plays. Some studies indicated that concentration driven molecular diffusion is the key mechanism, while others concluded that it had a minimal effect on oil recovery in tight formations.

Despite the considerable amount of modeling work related to the Bakken EOR [18,19,36,50–53], such results need to be viewed with cautious optimism for the following reasons:

- Modeling programs have been developed primarily for conventional reservoirs and may not adequately address the additional complexities of a “tight oil” reservoir.
- Numerical models rely on relatively simple and non-realistic assumptions, which can affect their capacity to capture the multiple phases, complexities, and heterogeneities of a “real” reservoir situation.

CO_2 EOR modeling in unconventional reservoirs such as the Bakken requires the input of additional variables to adequately address the complexities of the reservoir.

2.3 Previous EOR Pilot Tests in Bakken

Several EOR pilot tests were performed in Bakken using water and gas injection. The objectives included testing the injectivity into the sub-millidarcy reservoir rocks and evaluating the performance of different EOR agents. Table 2 lists the different EOR pilot tests that were performed in the U.S portion of the Bakken and reported to public domain.

Table 2 List of EOR pilot tests performed in the U.S portion of the Bakken

Well ID	Operator	Formation	Test year	Injected fluid	Avg. inj. rate	Max. inj. Pres. (psi)	Cum. Inj. Volume	Type
#9660	Meridian	UBS	1994	Water	200 bpd	5000	13082 bbl	Flood
#16713	EOG	MB	2008	CO_2	580 bpd	1500	30.7 MMscf	HnP
#17170	EOG	MB	2012	Water	1500 bpd	4000	38177 bbl	HnP
#16986	EOG	MB	2014	Water / Produced gas	1500 Mscfd	5000	88.7 MMscf	Flood
#24779	Whiting	MB	2014	CO_2	500 Mscfd	3500	3.4 MMscf	Flood
#11413	XTO	MB	2017	CO_2	9 gpm	9480	1.7 MMscf	HnP
#32937	Hess	MB	2017	C3	105 Mscfd	5500	20 MMscf	-

2.3.1 Water injection tests

An early EOR pilot test was performed in 1994 by Meridian Oil Company. The operator used an existing horizontal well drilled into the UBS to test freshwater injection. The selected well was in production status before converting it to water injector to evaluate the feasibility of water flood in the Bakken shale. The injection began on March 8, 1994, for 50 days with an average injection rate of 200 bpd. On April 27, 1994, the well was shut-in for approximately 1-2 months to evaluate its performance. The monitored data were not reported, and the test was found to be unsuccessful (NDIC, well file 9660).

Another water injection test was conducted in 2012 by EOG Resources, Inc. They used a fractured horizontal well that was taken off production on April 22, 2012, then converted it to an injector for water flood. The injection operations started on May 3, 2012, using a HnP schedule with 30-day injection and 10-day soaking. Well returned to production on June 21, 2012, until October 12, 2012. A second injection cycle was performed from October 12, 2012, to November 11, 2012. The well returned to production on December 25, 2012. The test was deemed uneconomical, and the operator declared no intention to continue on water injection (NDIC, well file 17170).

2.3.2 CO_2 injection tests

In 2008, EOG Resources used a fractured horizontal well to perform HnP injection test using food-grade CO_2. The selected well was actively producing from the MB before starting the injection. The operating company was licensed for only one HnP injection scheme with 30 days of injection and 60 days of soaking. The injection started on September 15, 2008, until October 14, 2008, with a cumulative injection volume of 30.7 MMscf of CO_2. After 11 days of injection, CO_2 breakthrough was detected in an offset well located over a mile away from the injector. The operator continued the injection and completed the planned 30 days injection period. Then the well was shut-in for 50 days and reopened for production on December 3, 2008. The production history is presented in Fig. 2.6. The well was allowed to naturally flow for the first six months of the producing life. At this point, the well had a cumulative oil production of 133,152 bbl of oil before the decision was made to place the well on artificial lift using an electronic submersible pump. Right after injection, a slight increase in oil production was observed; however, it quickly declined after one month (see Fig. 2.6).

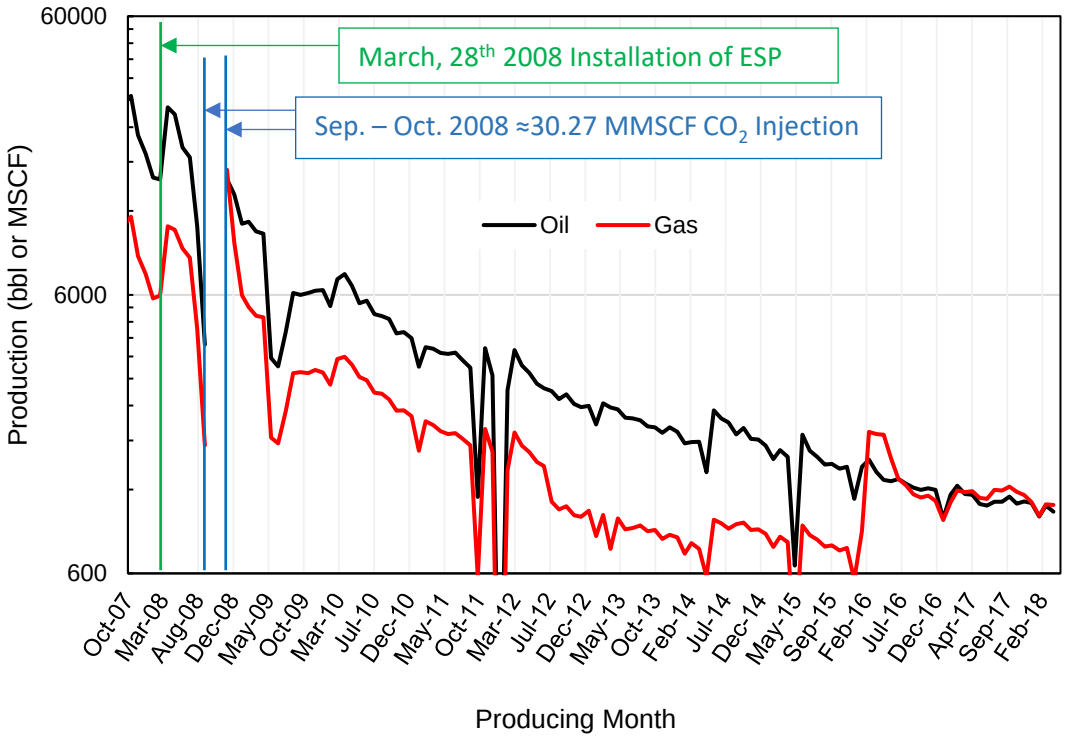

Fig. 2.6. Oil production history of well # 16713 (data from NDIC website under well file #16713)

In 2014, Whiting Oil & Gas Corporation used a vertical non-fractured well completed in the MB to conduct a CO_2 injection test. The objective of the test was to evaluate the injectivity of CO_2 into the MB rock matrix. They planned to conduct one HnP cycle with an injection period of 20 days and an average injection flow rate of 500 Mscf per day. The production records of MB wells located within a quarter-mile radius were monitored (Red circle in Fig. 2.7). Also, to further understand the potential for CO_2 propagation into the underlying Three Forks formation, three TF producers were also monitored for increased CO_2 production (green rectangles in Fig. 2.7).

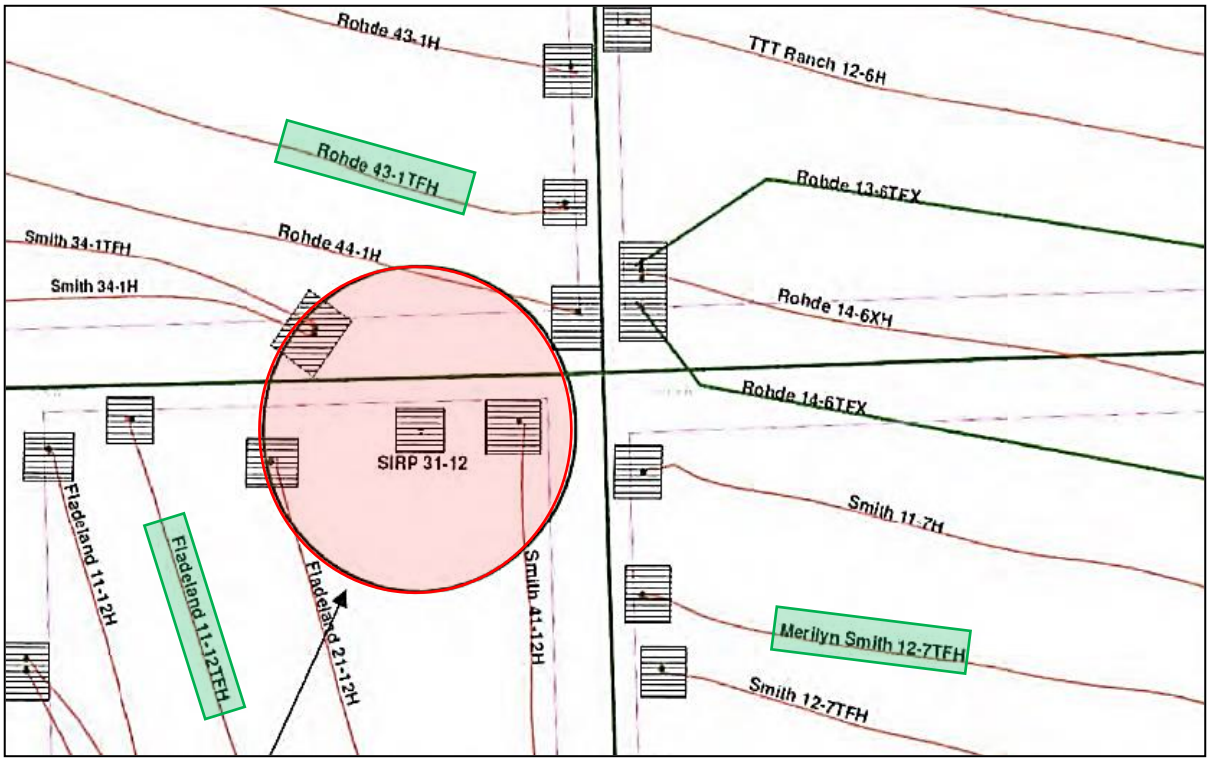

Fig. 2.7. Well 24779 quarter-mile radius of interest in monitoring Bakken CO_2 production changes during CO_2 injection (NDIC, well file 24779)

The test started on February 2, 2014, and after four days, the injection was ceased due to a CO_2 breakthrough that was detected in the offset MB well Fladeland 21-12H. The test was stopped, and only a small volume of CO_2 was injected. No substantial influence was observed on oil production from the offset MB wells. Whiting stated that the test was “less than optimal” and would re-evaluate the injection operation before attempting another field trial with CO_2 EOR in the Bakken. Another CO_2 pilot test in a vertical MB well was performed by XTO and the EERC in 2017. Similar to the test performed by Whiting Corporation, the objective was to evaluate the injectivity of CO_2 into a non-stimulated reservoir volume. The test was motivated by the results of previous numerical simulations and experiments that showed a recovery factor of nearly 100% after CO_2 injection. They performed one HnP cycle with four days of injection and a soak period of 15 days.

A total of 1.7 MMscf of CO_2 was injected into the MB. After soaking, the well flowed to produce 9 bbl of oil over the first 45 minutes, then stopped. The hydrocarbon composition was analyzed, and the results suggested that CO_2 successfully penetrated and displaced oil from the rock matrix.

2.3.3 Hydrocarbons gas injection tests

A produced gas pilot test performed by EOG Resources was conducted in 2014. They used a horizontal well producing from the MB. The well was first taken off production on March 30, 2012, and converted to an injection well on April 6, 2012, for produced water flood pilot project. The produced water injection continued until February 17, 2014, and the well returned to production in March 2014. There are no available details on the injection schedule or the outcome of the water flood test. On June 27, 2014, the well was used to inject a mixture of field gas and produced water. The injected produced gas consisted mainly of nitrogen, methane, ethane, and propane with a mole percent of 10.3, 52, 19, and 12.7%, respectively. The test goal was to evaluate the technical feasibility and production performance results after injecting produced gas into the MB for the purpose of secondary recovery. The mixture of water and gas was used to manage the surface injection pressure, increase the viscosity of the injected steam to manage the gas mobility in the fracture system, and build system pressure with less gas volume. It appeared that there was no communication with the production well, and the injection ended on August 16, 2014.

In 2017, Hess conducted an EOR pilot test to evaluate propane injection. They used a vertical hydraulically fractured well that was producing from the MB. The test plan state that propane will be injected in the vertical fractured well and four offset wells were monitored to track oil and gas production changes. The injection scheme was not clearly stated; however, based on the injection and pressure data, the test was conducted for approximately one year and a half and consisted of

two propane injection cycles (see Fig. 2.8). Fig. 2.9 presents the oil production of the offset wells monitored during this pilot test.

After two months of injection, one offset well had a sharp increase of oil production from 22 to 54 bbl per operated day. The production gradually decreased to stabilize at the previous baseline. Hess considered this test as a demonstration of the feasibility of miscible EOR in Bakken, while requiring further evaluation for future larger-scale tests.

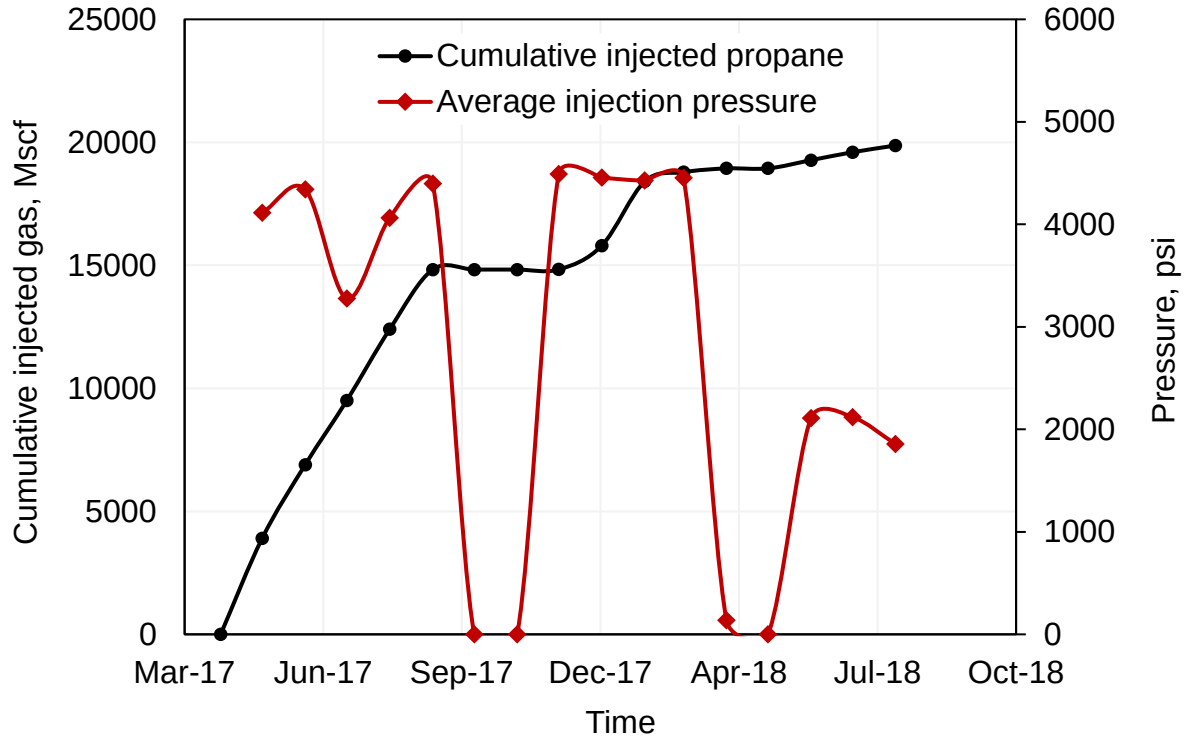

Fig. 2.8. Hess pilot test cumulative injected gas and injection pressure history (data from NDIC website under well file #32937)

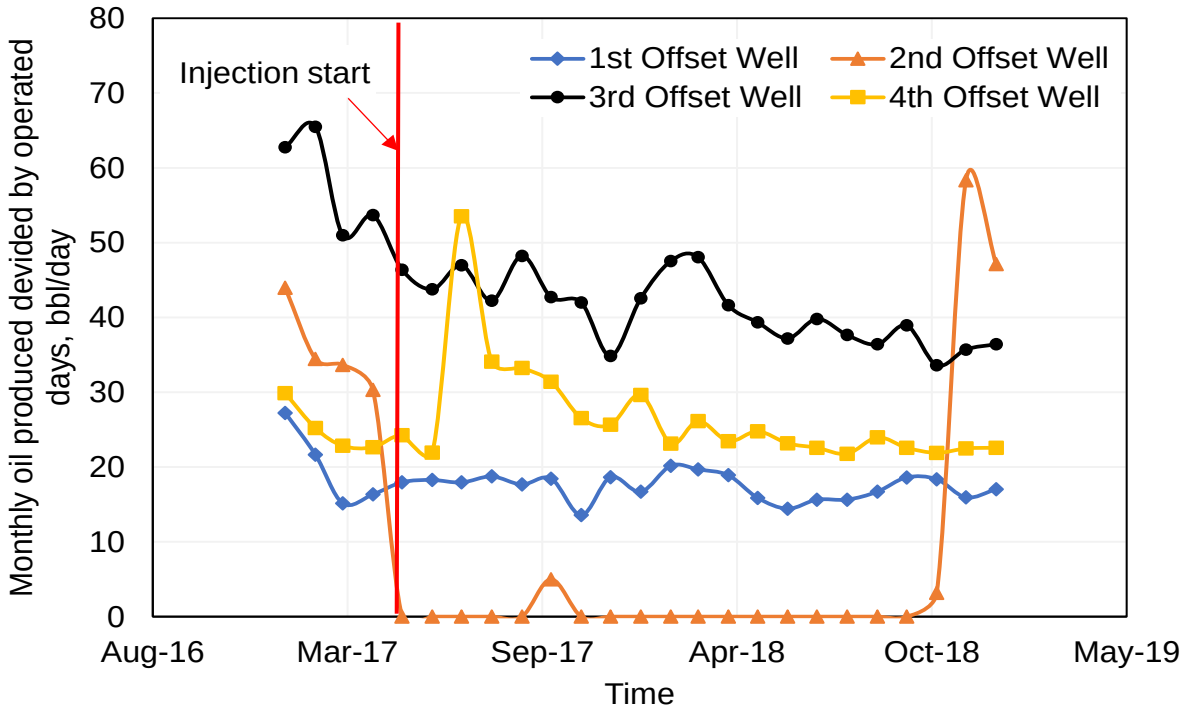

Fig. 2.9. Offset well production during propane pilot test performed by Hess (data from NDIC website under well file #32937)

2.3.4 Lessons learned from pilot scale EOR tests

The main lessons that can be learned from the previous pilot tests can be summarized as follow:

- Both water injection tests (fresh water and produced water) confirmed the non-viability of this technique in Bakken due to the low injectivity.
- The pilot-scale injections were performed separately with little to no collaboration between the operating companies. Better coordination in the future can reduce the cost and lead to obtaining more valuable outcomes.
- The results of CO_2 injection pilot tests revealed that the simulation studies in the literature were too optimistic, and the previous core-scale injection tests overestimated CO_2 potential.

- Some tests had promising outcomes; however, no clear consensus has been reached. The reported results have revealed that CO_2 EOR mechanisms in unconventional reservoirs are still poorly understood.
- Almost all the gas EOR pilot tests were concluded with a recommendation of further evaluation of oil recovery mechanisms under miscible EOR conditions.

2.4 Summary

In this Chapter, we presented an overview of the BPS and a review of the previous CO_2 EOR research studies in tight formations. Also, we summarized and discussed the results of previous pilot-scale EOR tests in Bakken. It was mentioned that the results of various CO_2 EOR experimental studies were highly variable. Furthermore, the injection tests that were conducted in the Bakken between 2008 and 2014 did not produce the same robust results as some of the previous modeling and laboratory work.

Also, it was indicated that further CO_2 EOR evaluation efforts are required to bridge the gap between the results of previous research studies and field pilot tests.

In the next Chapter, we present the samples used to represent the oil producing units in Bakken and describe the different experimental designs used in this study.

Chapter 3

Experimental Designs

In this Chapter, we present the methods and materials used in this study. The properties of the samples used in this study are presented in this section. Also, a description of the different equipment used for the experimental work is provided. This Chapter comprises of two sections related to materials and experimental setups description.

3.1 Materials

3.1.1 Sampling location

In five out of the seven EOR pilot tests performed by different operators in the U.S portion of the Bakken, the selected wells are located in Mountrail County, ND (see Fig. 3.1). This highlights the interests of operating companies in that region of the basin. To be able to compare and correlate

our experimental results with the outcomes of the field pilot tests, two wells located in Mountrail County, ND were selected for sampling in this study (see Fig. 3.1).

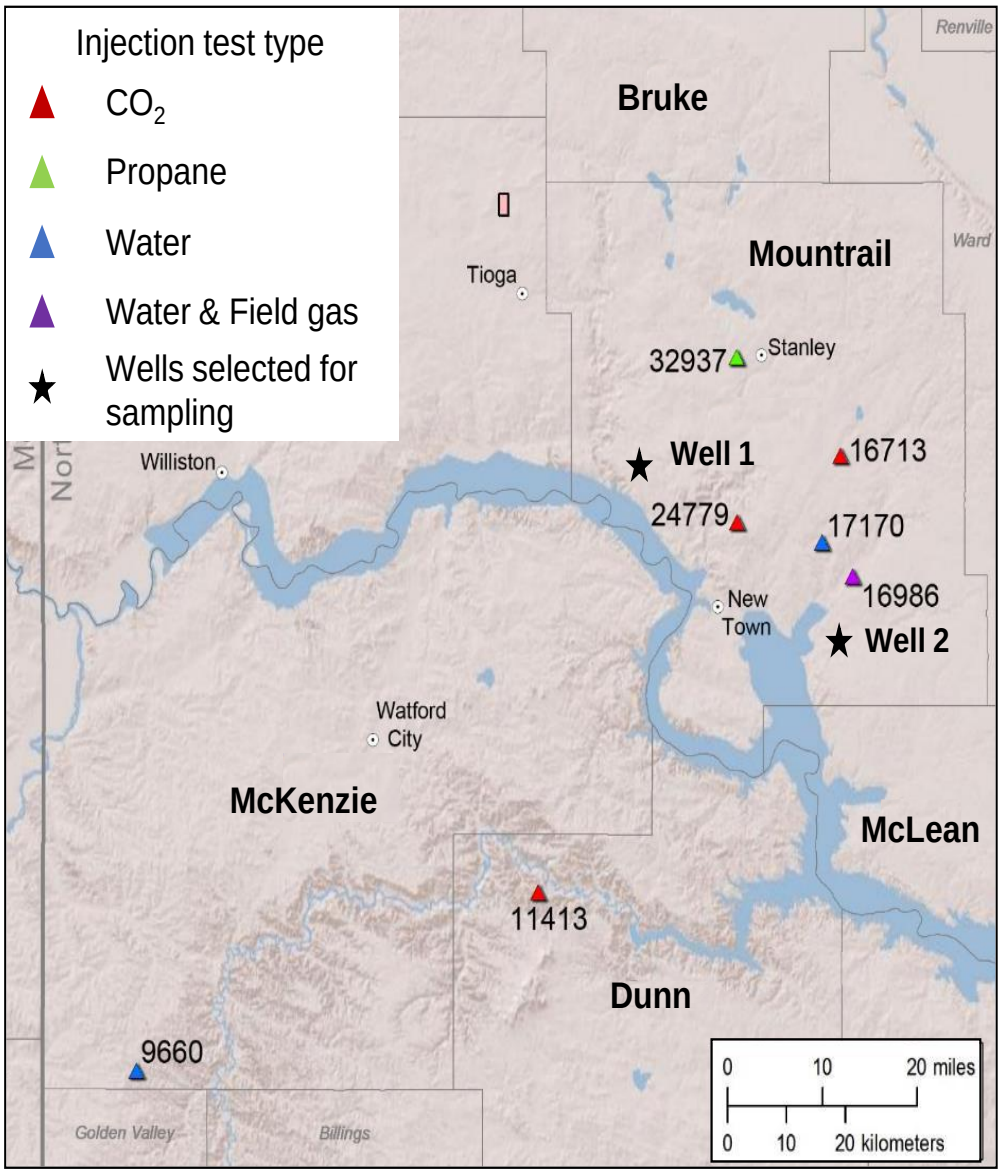

Fig. 3.1 Map location of the wells used for EOR pilot Bakken and the wells selected for sampling in this study

It is important to mention that the availability of well-data in the public domain and the availability of core samples in the targeted reservoir intervals had a major impact on wells selection in this study. Table 3 lists the producing units of both wells and the corresponding cumulative production.

Table 3 producing units and production data of the wells selected for sampling

Well ID	Well NDIC number	Field	Producing unit	Cum oil production (bbl)	Cum water production (bbl)	Gas production (Mscf)
Well 1	25688	Robinson Lake	Middle Bakken Member	270,886	420,943	313,447
Well 2	18101	Parshall	Three Forks Formation	258,922	114,018	164,572

3.1.2 Samples

3.1.2.1 Rock samples

A total of 20 rock samples were retrieved from both wells for the different experiments performed in this study. The samples were drilled from both Middle Bakken Member and the Three Forks Formation. The properties of the tested rock samples will be presented in each corresponding Chapter.

3.1.2.2 Oil properties

Crude oil samples were collected from each sampled well. Table 4 illustrates the reservoir conditions and the properties of Bakken crude oil. PVT analysis was performed to measure the different properties of a bottomhole oil sample retrieved from a similar location of the selected wells. A detailed PVT analysis of a Bakken crude oil sample is included in Appendix A.

Table 4 Bakken crude oil properties and reservoir conditions

Reservoir temperature (°F)	213
Reservoir pressure (psi)	6555
Oil density at reservoir conditions (g/cc)	0.668
API gravity (°)	39.3
Viscosity at reservoir conditions (cp)	0.37
Bubble point pressure (psi)	2198
Formation Volume Factor at reservoir conditions	1.609

3.2 Experimental Setups

3.2.1 Samples preparation

Depending on the experimental design, some samples were tested as-received while others were cleaned then re-saturated. After drilling the plugs from the original core slab, cleaning and drying were performed following the recommended best practice of McPhee et al. [54]. Samples saturation with oil was performed at reservoir pressure and temperature (see Table 4). The schematic of the saturation setup used in this work is illustrated in Fig. 3.2. The apparatus can withstand a pressure of 10,000 psi and a temperature of 315 °F. It is composed of a vacuum pump, a saturation chamber equipped with a pressure gauge, a floating piston accumulator, a water syringe pump, and an air bath thermostat that keeps the saturation process at a constant temperature.

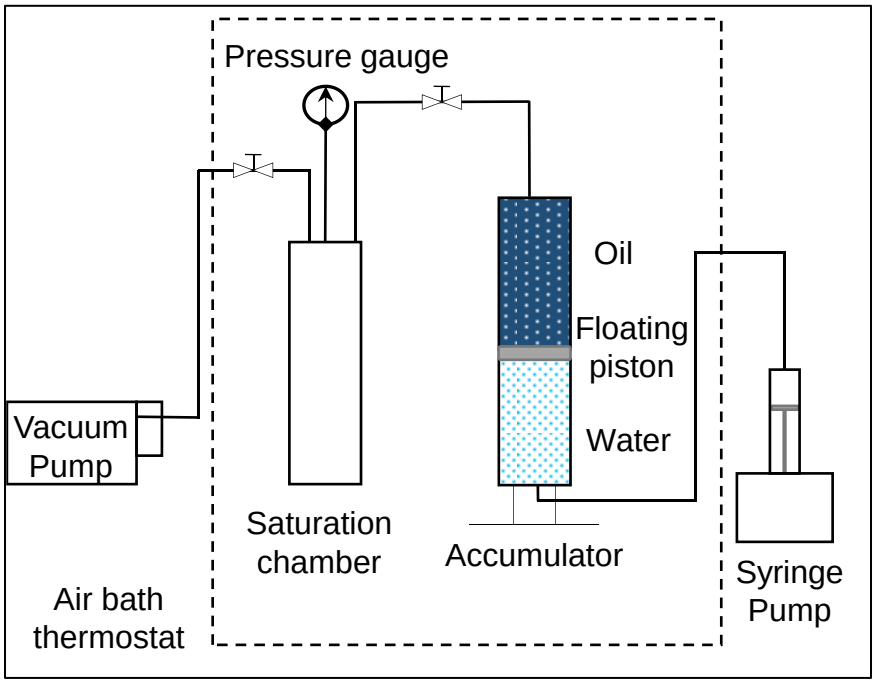

Fig. 3.2 Schematic of the saturation setup

3.2.2 Mineralogical composition

The bulk mineralogical composition of two MB and two TF samples was examined using X-ray diffraction (XRD). The samples were crushed and pulverized to be analyzed with a RIGAKU Smartlab XRD equipment and results were interpreted with a PDXL software. Each sample was analyzed at 5 degrees to 90 degrees, two theta (5º-90º 2θ) in order to identify the entire mineral assemblage and distributions.

3.2.3 CO_2 injection

Fig. 3.3 illustrates the experimental setup used to run the CO_2 Huff-n-Puff experiments. It consists of two floating piston accumulators used to pressurize CO_2, where each piston is connected to a water syringe pump, a Hassler-type core holder with a maximum pressure of 10,000 psi connected to a pressure transducer that monitors the CO_2 injection pressure, a back pressure regulator, an air bath thermostat, and a data acquisition system.

The OOIP and the recovered oil volume are expected to be very small for samples with very low porosity. The produced oil might be smaller than the dead-volume of the experimental setup. Therefore, we recommend using the difference in core weights to accurately determine the recovery factor. We measured the core weight difference before and after saturation to determine the OOIP before each injection cycle (Equation (1)). We then measured the core weight after CO_2 injection and calculated the oil recovery factor using Equation (2).

$$OOIP = W_2 - W_1 \quad (1)$$

$$RF = \frac{W_3 - W_2}{OOIP} \times 100\% \quad (2)$$

Where $OOIP$ is the original oil in place, W_1, W_2, and W_3 are the core weights before saturation, after saturation, and after CO_2 injection, respectively, and RF is the oil recovery factor.

We used the same apparatus with a modified core holder assembly for CO_2 flooding experiments (Fig. 3.4). The core sample was placed in a rubber sleeve and a manual pump was used to apply a confining pressure, which was 500 psi higher than the desired injection pressure to prevent CO_2 slippage between the core and the sleeve. The backpressure regulator (BPR) was used to control the injection pressure during the flooding process. The produced oil volume was collected in a graduated pipette and recorded over time.

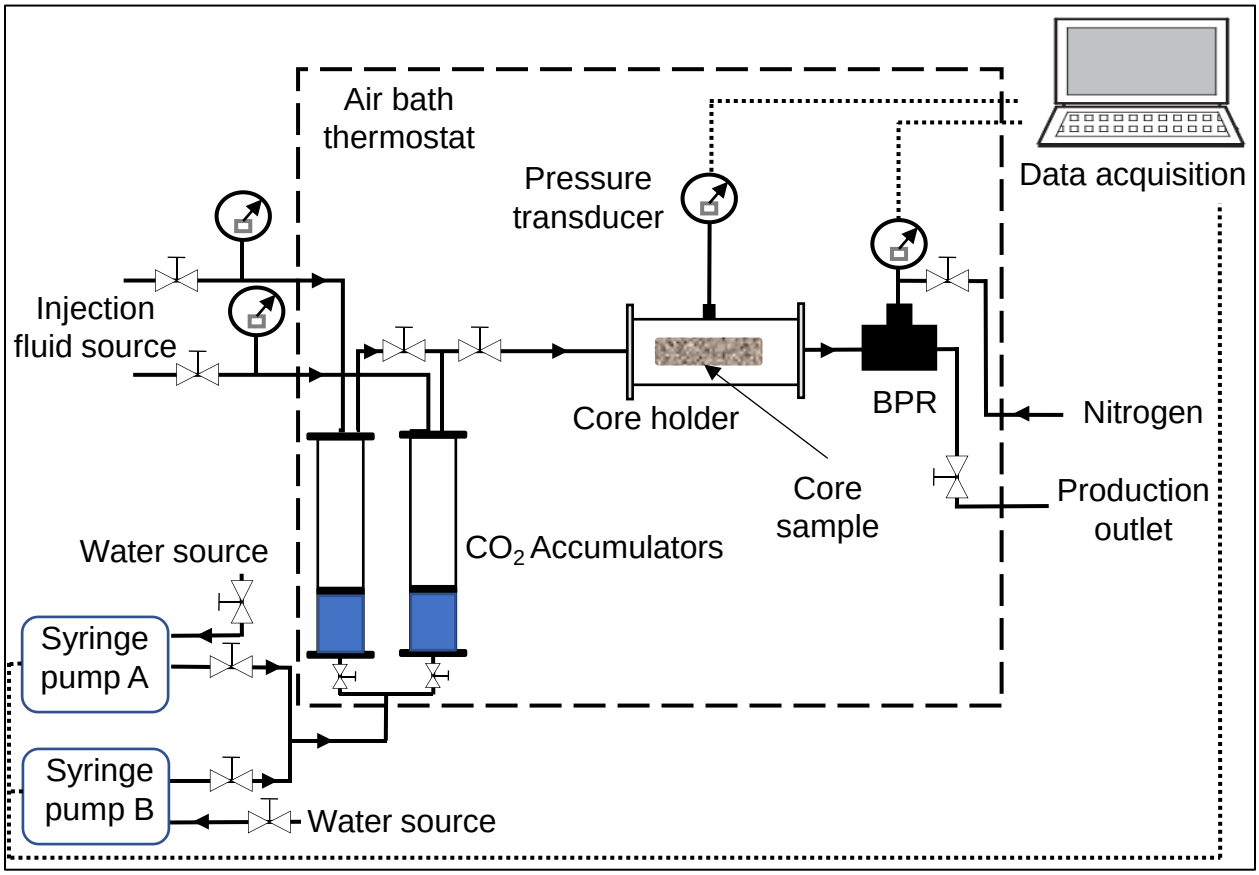

Fig. 3.3 Schematic of the CO_2 injection experimental design

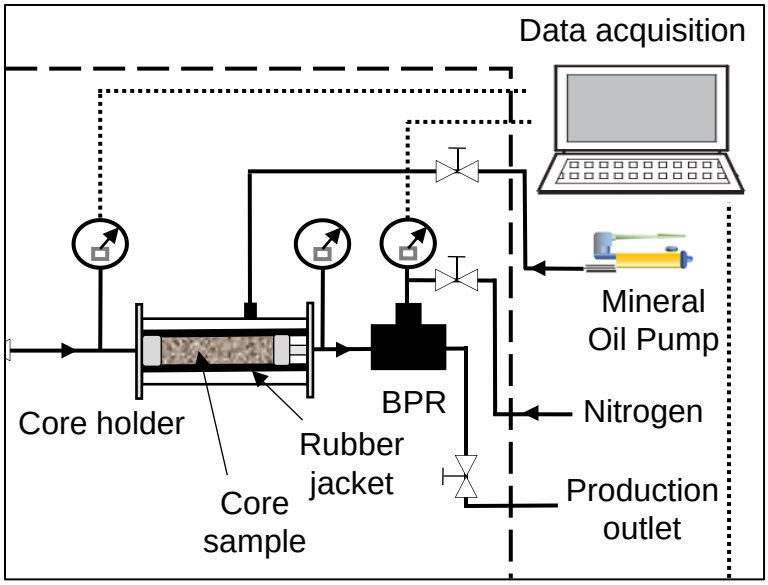

Fig. 3.4 Schematic of the core holder assembly for HnP in fractured samples and CO_2 flooding experiments

3.2.4 Wettability

Fig. 3.5 depicts the schematic of the Core Lab IFT-10 model we used in our experiments, which was designed to measure both interfacial tension and contact angle under high pressure, up to 10,000 psi, and high temperature, up to 315°F. The key components of this apparatus are a manual pump, two floating piston accumulators used to pressurize and inject the surrounding phase and the droplet phase, a visual cell in which we placed the core chunk and injected the fluids, a thermocouple to set the desired temperature, a camera with a light source, and a PC with droplet image analysis software.

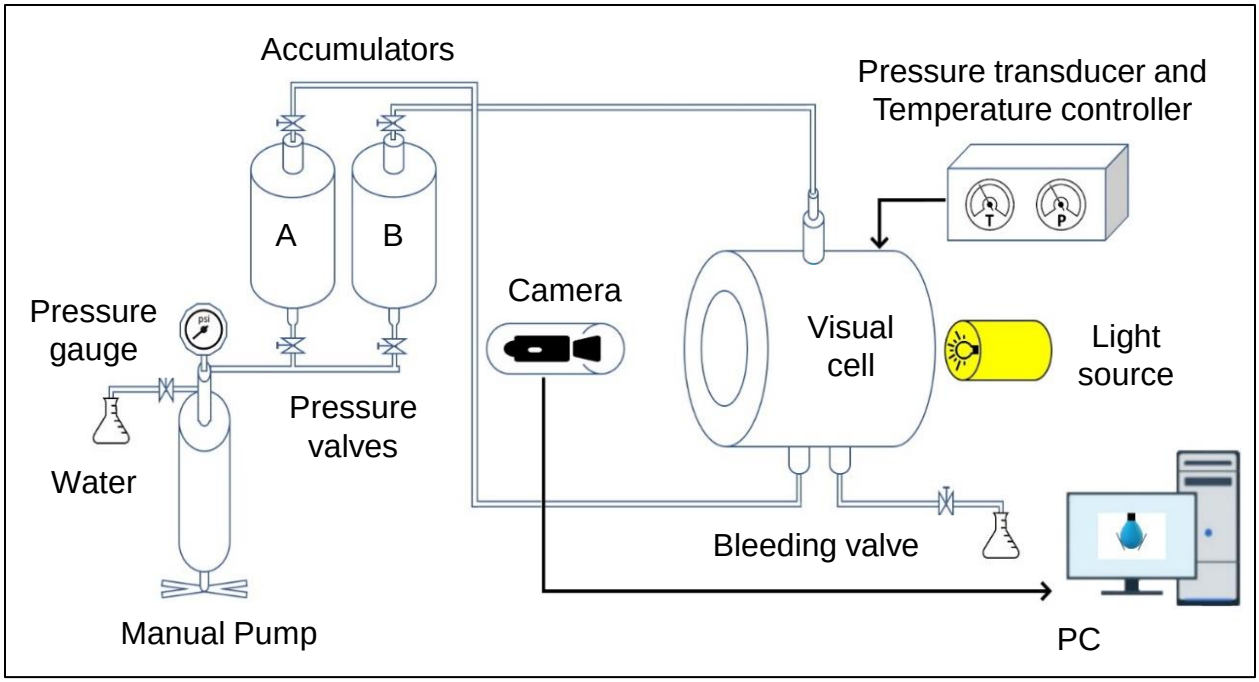

Fig. 3.5 Schematic of the contact angle measurement equipment

3.2.5 Nuclear Magnetic Resonance

Nuclear magnetic resonance (NMR) was used to characterize pore fluid distribution within the rocks. An Oxford Instruments GeoSpec2 core analyzer coupled with Green Imaging Technology software was used to acquire the NMR transverse relaxation measurements. Porosity geometry and pore sizes distribution were acquired from NMR transverse relaxation (T_2) analysis. NMR T_2 results were used to estimate pore size distributions and to classify them into micropore, mesopore, and macropore, based on unconventional T_2 cut-off.

3.3 Summary

In this Chapter, we presented the sampling location and depicted the different experimental designs used in this study.

In the next Chapter we present the evaluation of the effect of cyclic CO_2 injection parameters on oil recovery from MB and TF samples.

Chapter 4

Optimization of CO_2 Huff-n-Puff Parameters

Several research studies and pilot tests reported that the Huff-n-Puff injection technique helps overcome the limitations of continuous gas injection in gas EOR applications in unconventional reservoirs. As described in the previous chapters, the HnP cycle consists of three fundamental steps: 1) gas injection to reach a set downhole pressure, 2) shut-in period to allow the injected gas to soak, and 3) reopening for production. Therefore, in cyclic injection, a single well is used to perform a preset number of HnP cycles.

In this Chapter, we evaluate the effect of CO_2 Huff-n-Puff injection parameters (injection pressure, soaking time, and the number of cycles) on oil recovery using MB and TF rock samples. We first introduce the methodology used in this work, then present and discuss the experimental results

obtained using different injection pressures and multiple soaking times. Finally, the effect of increasing the number of cycles on oil recovery is investigated and discussed.

4.1 Methodology

Four rock samples were selected to represent the target formations in Mountrail County, ND. They were retrieved from two different wells in Parshall and Robinson Lake fields. Two samples from each well were collected to represent the Middle Bakken member and Three Forks formation, respectively. The oil samples were also collected from the same location of the selected wells. The properties of the selected rock samples are listed in Table 5.

Table 5 Properties of rock samples used to investigate the effect of CO_2 HnP parameters

Sample ID	Well	Formation	Diameter (in)	Length (in)	Porosity (%)	Permeability (mD)
MB#1	W1	Middle Bakken	1	3.8	2.6	0.005
TF#1	W1	Three Forks	1	4	8.21	0.178
MB#2	W2	Middle Bakken	1	4	7	0.0017
TF#2	W2	Three Forks	1	3.25	8.3	1.83

Fluid properties and interactions can be strongly affected by temperature. All CO_2 injection and saturation experiments were performed at the actual reservoir temperature of 213 °F. The experimental setup used to conduct CO_2 HnP experiments is illustrated in Fig. 3.3.

In this part of the study, we performed several CO_2 injection tests to evaluate the effect of injection pressure, soaking time, and the number of HnP cycles on oil recovery from MB and TF rock samples. The rock samples were initially cleaned and saturated with crude oil. After each experiment, the tested rock plugs were re-cleaned and re-saturated with oil before starting the next

CO_2 injection test. First, the samples MB#1 and TF#1 were used to measure the oil recovery after CO_2 HnP using a soaking time of 24 hours and different injection pressures of 880, 1500, 3300, 3750, and 4500 psi. The same samples were used to assess the effect of soaking time on oil recovery. Five HnP tests were performed at the same injection pressure of 3750 psi and soaking times of 3, 10, 17, 31, and 38 hours. After selecting the optimum injection pressure and soaking time, the samples MB#1, MB#2, TF#1, and TF#2 were re-cleaned re-saturated and to conduct six successive CO_2 HnP cycles for each sample.

4.2 Effect of Injection Pressure

Different studies have estimated the CO_2 MMP in the Bakken, and the values can vary from 2600 to 3300 psi, depending on the location of the oil sample used and the measuring method [3,35,55,56]. Fig. 4.1 presents the measured oil recovery factor using CO_2 HnP below, Near, and above MMP.

The tests performed at 880 psi and 1500 psi are considered below MMP and yielded recovery factors of 5.3% and 12.4% for the MB sample and 6.8% and 19.2% for the TF sample, respectively. CO_2 injection at miscible conditions is represented using an injection pressure of 3300 psi, which resulted in recovering 23.9% from the MB sample and 35.7% from the TF sample. To study the effect of increasing the pressure above MMP, CO_2 was injected at 3750 psi and 4500 psi, which tremendously increased the oil recovery to 41.2% and 46.1% for the MB sample and 48.4% and 57.9% for the TF sample, respectively.

Our results indicate that the injection pressure considerably impacts oil mobilization in tight formations. Also, it highlights the importance of achieving miscibility between CO_2 and reservoir fluids. Furthermore, the results suggest that increasing the pressure above MMP leads to incremental oil recovery. Previous experimental studies performed on Eagle Ford and Barnett

shales reported similar observations [30,31,33]. The authors indicated that increasing the pressure above MMP can promote the vaporizing gas drive mechanism and multiple contact miscibility. Menzie [57] performed oil CO_2 multi-exposure experiments at different pressure conditions and found that increasing the injection pressure leads to increasing the capacity of CO_2 to dissolve oil. Another possible explanation is the increase of the contribution of viscous forces to oil recovery when the injection pressure is increased above MMP. It enables CO_2 to sweep more pore volume and promotes its access to the micro-pores, which are the most dominant in this type of rock.

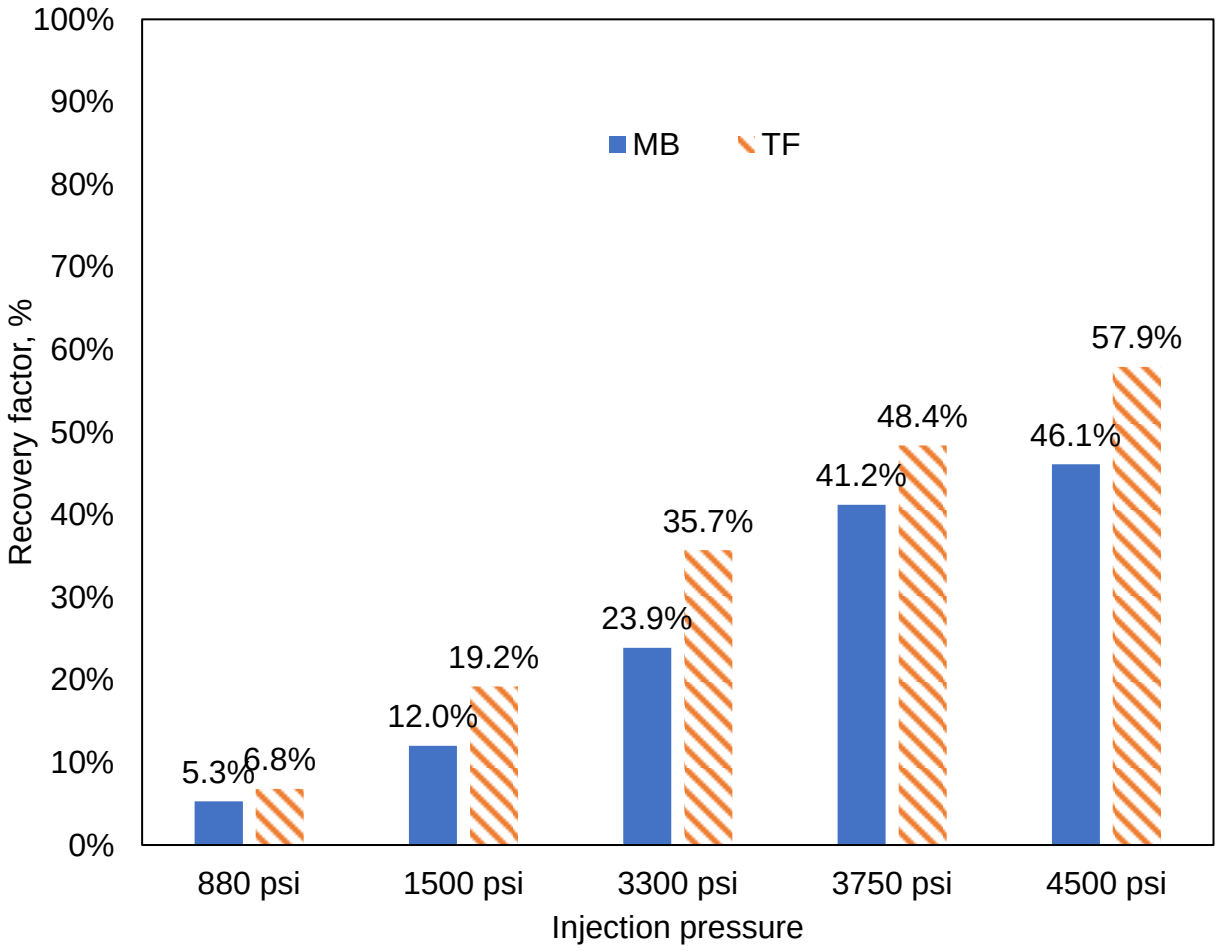

Fig. 4.1 Recovery factors of MB and TF samples after on CO_2 HnP cycle at different injection pressures and using the same soaking period of 24 hours

4.3 Effect of Soaking Time

There are different concepts proposed in the literature to describe the oil recovery mechanism in tight formations; however, it is clear that the injected CO_2 could not permeate a rock matrix with nano-Darcy permeability via convective flux [58,59]. Several researchers suggested that concentration-driven molecular diffusion can control the oil recovery at some stages of oil mobilization using CO_2 injection [58,60–63]. Thereby, the soaking time during a HnP injection is a key parameter that needs to be optimized. Fig. 4.2 presents the oil recovery factors from MB and TF samples after a CO_2 HnP cycle at 3750 psi and different soaking times.

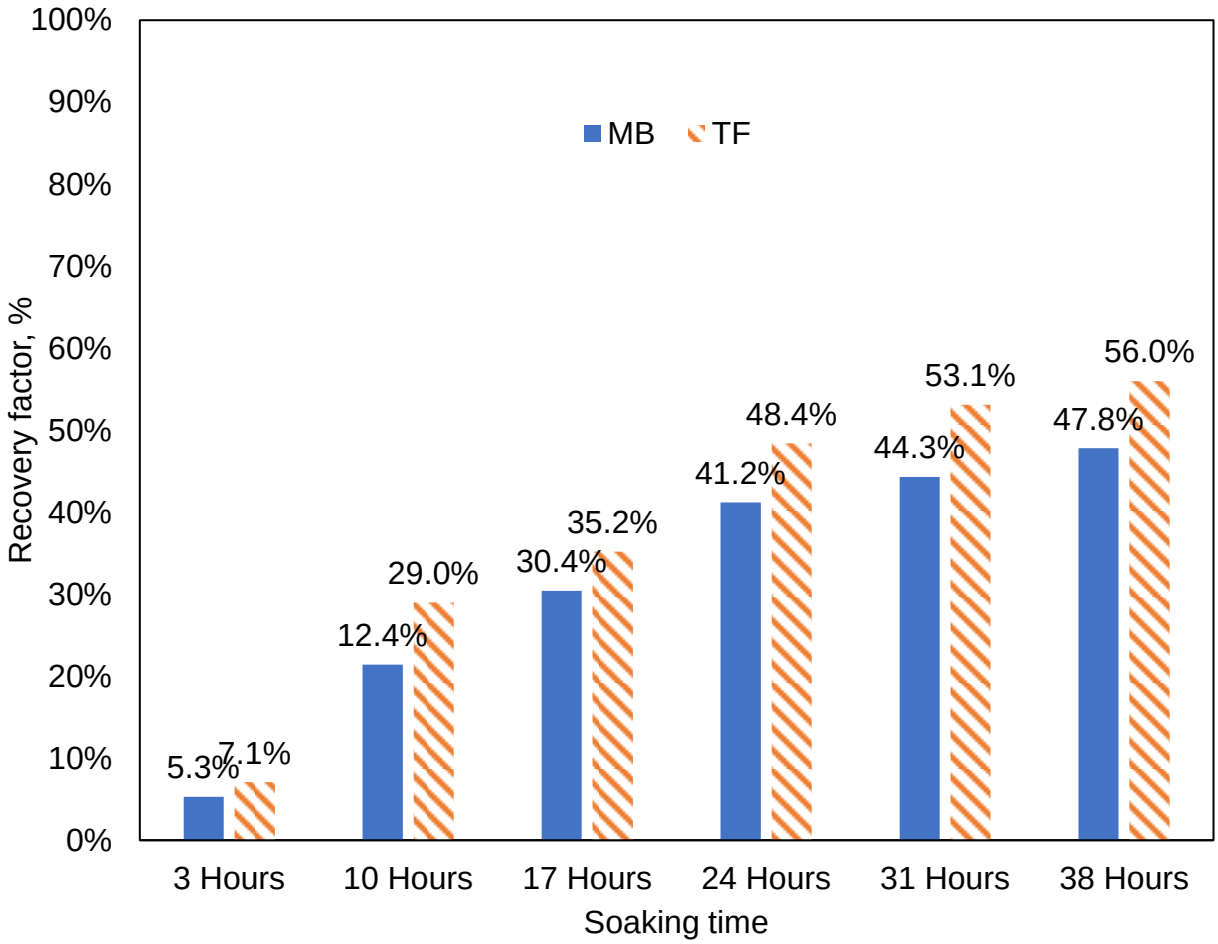

Fig. 4.2 Recovery factors of MB and TF samples after one CO_2 HnP cycle at different soaking periods and using the same injection pressure of 3750 psi

The results clearly suggest that increasing the soaking time to a specific threshold can exceedingly increase the oil recovery from ultra-tight rock samples. For a soaking time of 3, 10, 17, 24, 31, and 38 hours CO_2 recovered 5.3, 12.4, 30.4, 41.2, 44.3, 47.8% of the OOIP for the MB sample and 7.1, 29.0, 35.2, 48.4, 53.1, and 56.0% for the TF sample, respectively.

Increasing the soaking time from 3 to 24 hours resulted in an incremental oil recovery of 35.9% and 41.3 % of the OOIP from the MB and TF samples, respectively, which reflects the kinetics of molecular diffusion that is known as a relatively slow process. Nevertheless, increasing the soaking time beyond 24 hours did not result in remarkable additional oil recovery. Only 6.6% and 7.6% of the OOIP were incrementally recovered by increasing the soaking time from 24 to 38 hours. These results indicate that the concentration gradient between the sample surface and near-surface zone decreases drastically after approximately 24 hours of soaking, which slows further the CO_2 diffusion in the rock, and consequently reduces the oil recovery efficiency.

4.4 Effect of Number of Injection Cycles

After identifying the optimum injection pressure and soaking time for CO_2 HnP in MB and TF samples, we studied the performance of multicyclic CO_2 injection by performing six successive HnP cycles for each MB and TF sample. Prior to CO_2 injection tests, all the rock samples were cleaned and re-saturated with oil. Fig. 4.3 illustrates the cumulative oil recovery factors after six CO_2 HnP cycles performed at 3750 psi and 24 hours of soaking for each cycle. As mentioned above, all the experiments were performed at the reservoir temperature of 213°F. The ultimate oil recovery factors after the sixth cycle for the samples MB#1, MB#2, TF#1, and TF#2 were 61.3, 64.8, 73.0, and 68.3%, respectively. The permeability of the TF samples is two to three degrees of

magnitude higher than the MB samples, which might explain the slightly larger oil recovery factors obtained for those samples.

The results show that the oil recovery performance of the injected CO_2 diminishes after each cycle and the oil recovery curves exhibit a plateau after the second cycle for all the tested samples. Most of the cyclic CO_2 injection studies in the literature reported similar observations, where the CO_2 oil recovery capacity significantly decreases after each HnP cycle [16,28,32,37–39,64,65]. The equilibrium partitioning mechanism controls oil solubility in the injected gas, and the dissolved oil concentration in the gas-dominated phase diminishes after each sequential exposure to the injected CO_2. This fundamental limitation of cyclic CO_2 injection will be further discussed in Chapter 7.

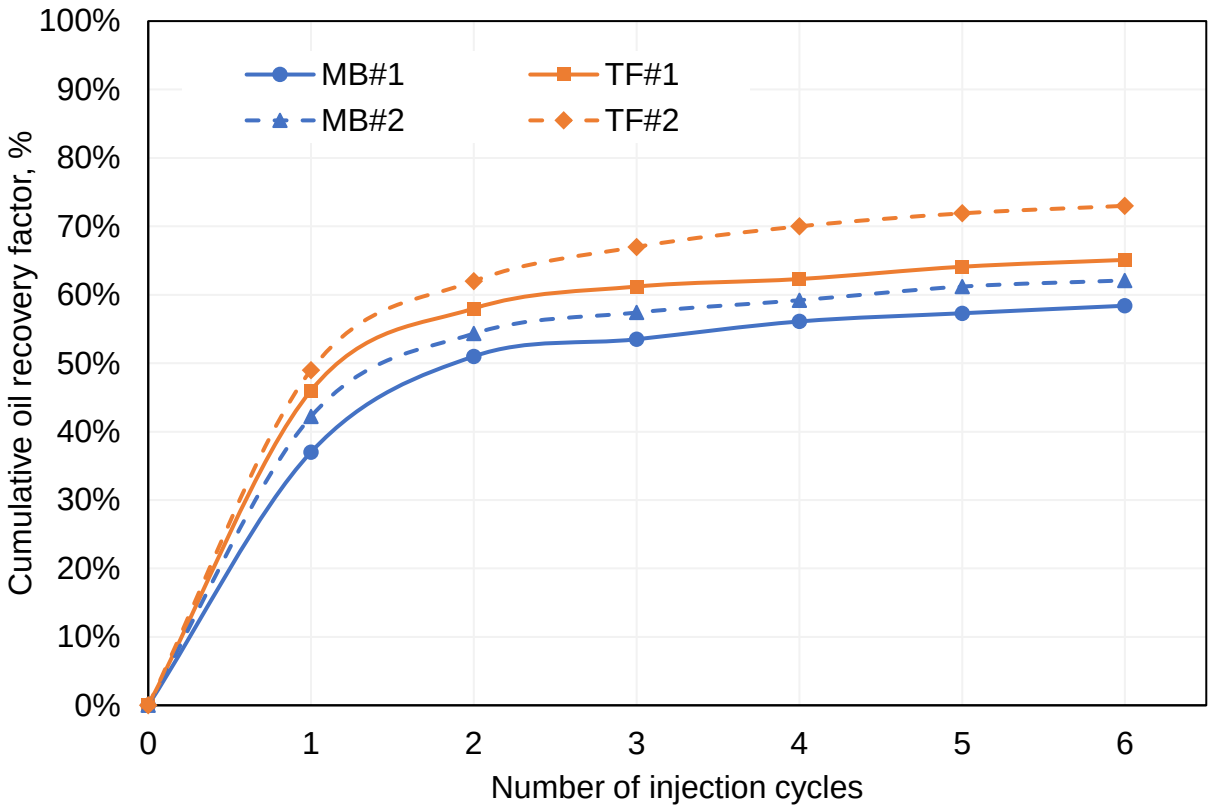

Fig. 4.3 Cumulative oil recovery factors of MB and TF samples after six successive CO_2 HnP cycles at 3750 psi and 24 hours soaking

4.5 Summary

The effect of injection pressure and soaking time was evaluated in this Chapter. The experimental results showed that increasing the injection pressure above MMP can help recover more oil from tight rock samples. Also, a soaking time of 24 hours was determined as the optimum value for one CO_2 HnP cycle using MB and TF samples. The results of multicyclic CO_2 injection indicate that the CO_2 performance decreases drastically after the second HnP cycle.

In the next Chapter, we present the results of the experimental parametric study that was conducted to understand the effect of different parameters on oil recovery using CO_2 HnP.

Chapter 5

Experimental Parametric Study in The Bakken

Very little work has been performed to investigate the difference between field results and the antecedent simulation and experimental studies despite the disappointing results from the different CO_2 pilot tests in the Bakken. Alfarge et al. [34] investigated oil recovery delay after CO_2 pilot tests in unconventional reservoirs by combining production data analysis for different pilot tests with numerical simulation to identify the controlling mechanisms of oil recovery. The authors determined that molecular diffusion is the governing mechanism in shale formations, which causes a delayed response in incremental oil recovery after CO_2 injection. To the best of our knowledge no previous work has examined the effect of water presence in the fractures, nor the effect of fracture size on CO_2 performance in tight formations, even though these effects are key factors in hydraulically fractured unconventional reservoirs. In this Chapter, we have addressed the gap

between the results of the recent pilot tests and previous research studies in the Bakken by conducting an extensive parametric study to examine and understand the effects of a series of key parameters, such as sample size, water presence, fracture size, and CO_2 injection scheme, on CO_2 EOR in unconventional reservoirs.

5.1 Methodology

To expand our understanding of CO_2 performance in MB and TF, in this study, we examined the effect of other parameters on oil recovery by comparing the recovery factor obtained after each experiment. Table 6 lists the properties of the core plugs used in this study. Fig. 5.1 and Fig. 5.2 illustrate the experimental workflow used to perform the parametric study. We cut two plugs with different dimensions from the same Middle Bakken core slab: MB#3 and MB#4 (Fig. 5.1). Similarly, TF#3 and TF#4 were cut from the same Three Forks core.

Table 6 Properties of rock samples used in the CO_2 parametric study

Sample Number	Formation/Member	Length (in)	Diameter (in)	Porosity (%)	Permeability (md)
MB#3	Middle Bakken	3.35	1.0	4	0.001
MB#4	Middle Bakken	3.35	1.5	4	0.001
TF#3	Three Forks	3.35	1.0	5	0.930
TF#4	Three Forks	3.35	1.5	5	0.930
MB#5	Middle Bakken	3.00	1.5	4	0.006
TF#5	Three Forks	3.00	1.5	9	1.040

MB#3 and MB#4 were placed simultaneously in the core holder after cleaning and saturation, then we performed one CO_2 HnP cycle to determine the recovery factor. The same steps were repeated

to measure the oil recovery for TF#3 and TF#4. We compared the recovery factors obtained in this step to examine the effect of sample size on CO_2 performance.

The MB and TF samples with the highest recovery factor after Test (I) were re-saturated then placed in the core holder. We filled 30% of the fracture space, or the void volume in the core holder, with Bakken brine collected from the field before injecting CO_2. We compared the recovery factors measured after Test (II) with the previous experiment to investigate the effect of water-presence in the fracture space.

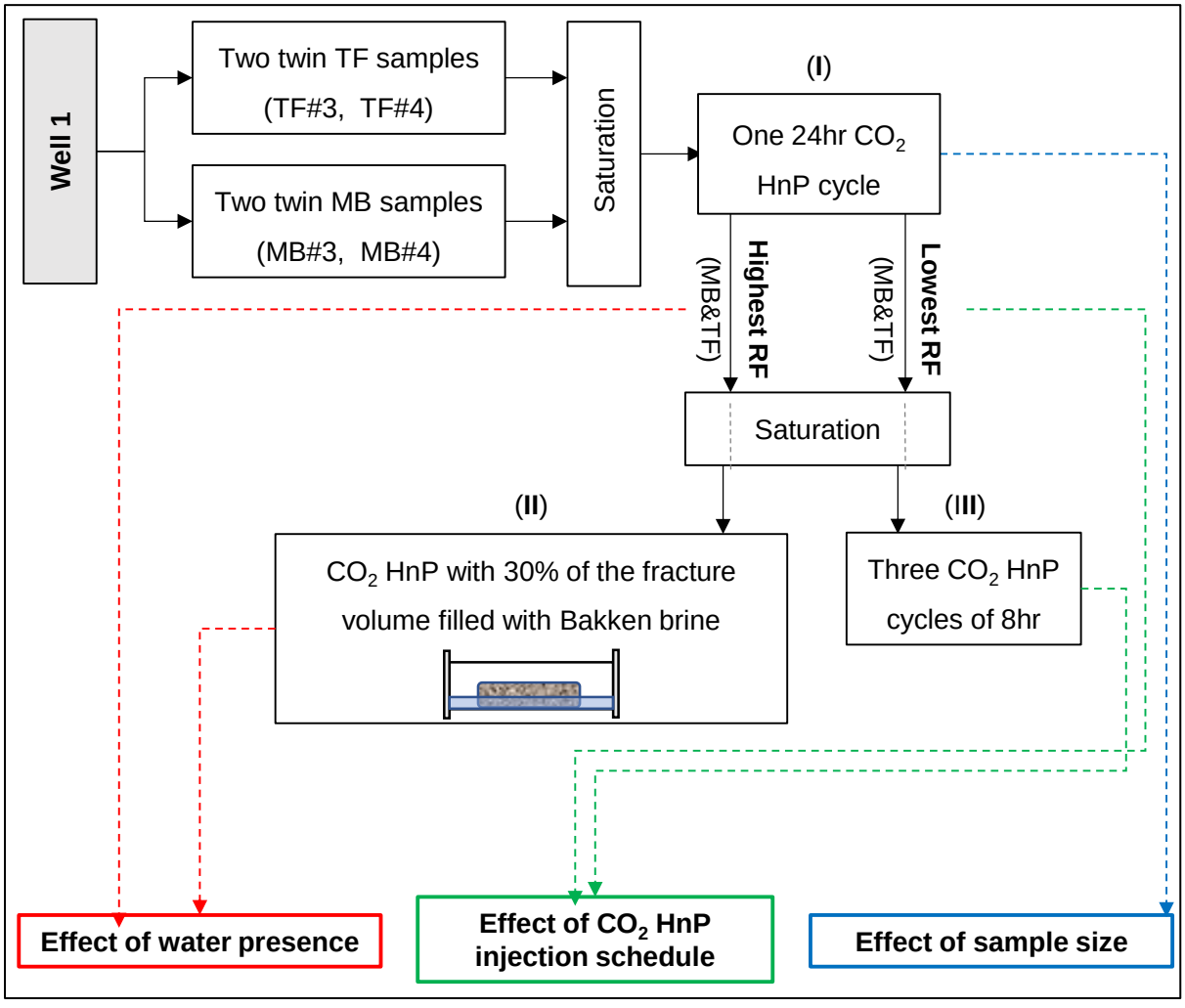

Fig. 5.1 Experimental workflow schematic part 1: investigation of the effects of sample size, water presence, and CO_2 HnP injection schedule

We present the experimental workflow of the second part of this parametric study in Fig. 5.2. CO_2 was injected in relatively large volumes around samples to simulate fracture/matrix systems in almost all previous HnP shale experiments that can be found in the literature [20]. Large amounts of CO_2 around the sample surface might not represent the conditions in unconventional reservoirs, where the fracture volume limits the amount of CO_2 that can sweep and interact with the rock matrix during the EOR process. Therefore, we examined the effect of reducing the CO_2 volume that surrounds the sample during the HnP experiment.

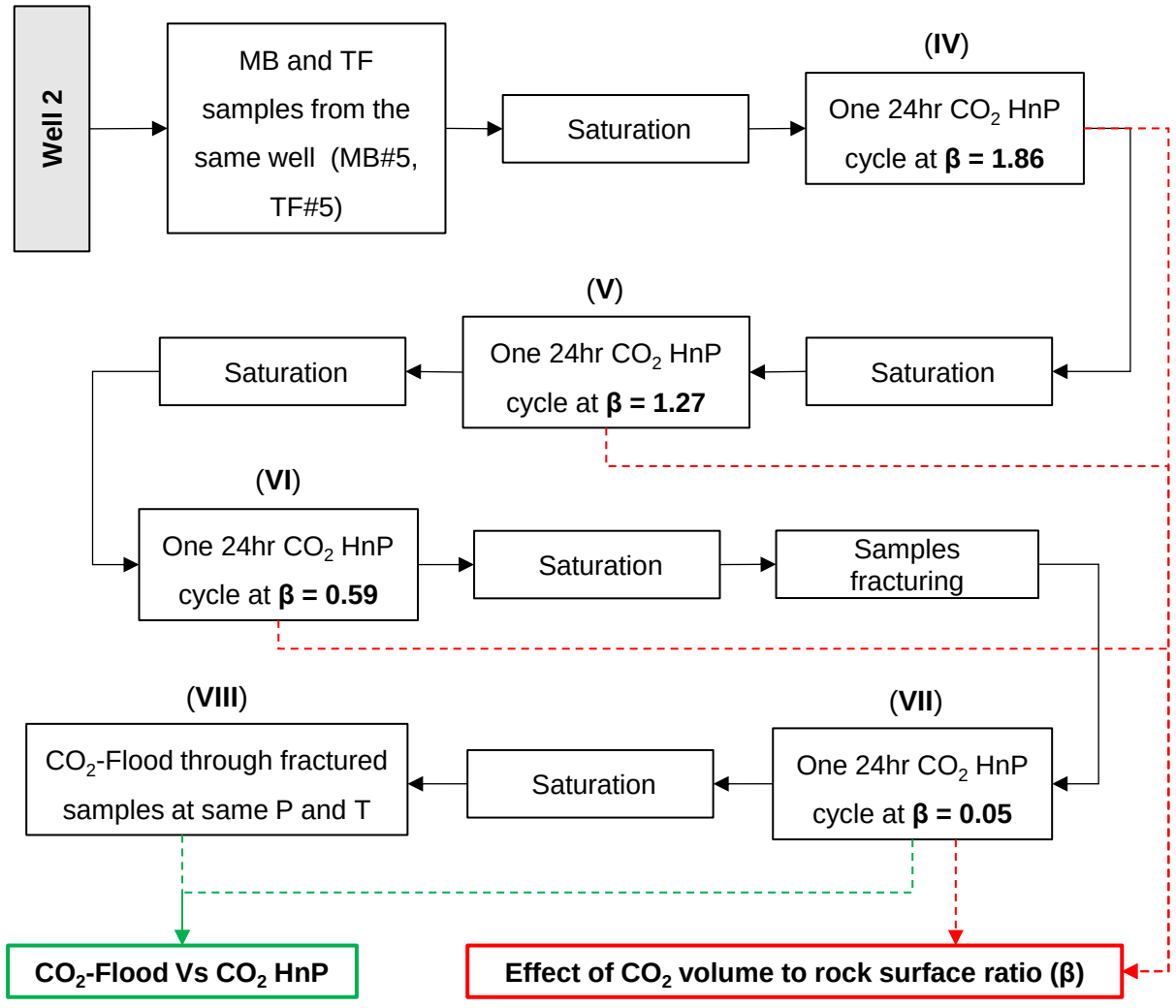

Fig. 5.2 Experimental workflow schematic part 2: investigation of the effect of CO_2 volume to rock surface ratio and comparing CO_2 flood to CO_2 HnP

We used the ratio of the volume available in the core chamber for the permeation of CO_2 into the rock matrix to the rock sample surface, or the Beta ratio (β), as an indicator for each experiment. The samples MB#5 and TF#5 were cut from the MB and TF core slabs of the second well, respectively. Each sample was subjected to one CO_2 HnP cycle with a soaking time of 24 hours (Test (IV)) after cleaning and saturation. We continued to reduce the Beta ratio and subject the cores to a CO_2 HnP cycle to measure the recovery factor for Tests (V) and (VI) (Fig. 5.2). We then fractured the rock samples (see Fig. 5.3) to reach a lower value of the Beta ratio. The oil recovery factors for CO_2 HnP (Test (VII)) and CO_2 flooding (Test (VIII)) were measured and compared. HnP and continuous flooding tests were performed at the same temperature, injection pressure, and CO_2 exposure time.

Fig. 5.3 Photos of the fractured MB#5 and TF#5 samples

5.2 Effect of Sample Size

Unconventional reservoirs are typically characterized by ultra-small pore sizes [66,67], which may lead to the assumption that small samples can represent the pore sizes distribution. Reducing the experimental time and targeting a quicker oil recovery response are other reasons to use samples with relatively small sizes for CO_2 EOR experimental studies in tight formations [37,39].

Jin et al. [39] measured the oil recovery factor using CO_2 HnP for MB and TF samples with similar properties to those used in this study. The tested cores had a bulk volume of 3.8 cc, and the recovery factor was measured after seven hours of soaking time with an injection pressure of 5,000 psi. Hawthorne et al. [37] used the same experimental parameters to test Middle Bakken cores with three different sizes and shapes: cylindrical rods (3.14 cc), square rods (2.43 cc), and small rock

chips (0.24 cc). We used twin samples with bulk volumes of, 97.01 cc and 43.11 cc, from each target formation to investigate the effect of sample size and measured the recovery factor after one CO_2 HnP at 3,750 psi and 24 hours of soaking. Fig. 5.4 illustrates the recovery factor under similar conditions for the MB and TF samples, including the cores tested in this study and results found in the literature.

MB#3 had a recovery factor of 59.8%, while MB#4 had a factor of 35.5% after soaking for 24 hours. We recovered 68.5% from the smaller TF sample, TF#3, and 54.6% from TF#4. Jin et al. [39] obtained recovery factors of 81.5% and 95% for MB and TF cores, respectively, with seven hours of soaking time. Hawthorn et al. (2013) had high oil recovery factors of 87%, 91%, and 97% for MB samples with bulk volumes of 3.14 cc, 2.4 cc, and 0.24 cc, respectively, with the same soaking time. The results indicate that the use of smaller samples leads to an overestimation of CO_2 performance in the lab. The portion of the oil adsorbed on the core surface might be higher than the oil volume imbibed in the pores after saturation for samples with relatively small bulk volumes, such as chicklets or small diameter rods, which explains previous lab results that reported high recovery factors after just a few hours of CO_2 exposure.

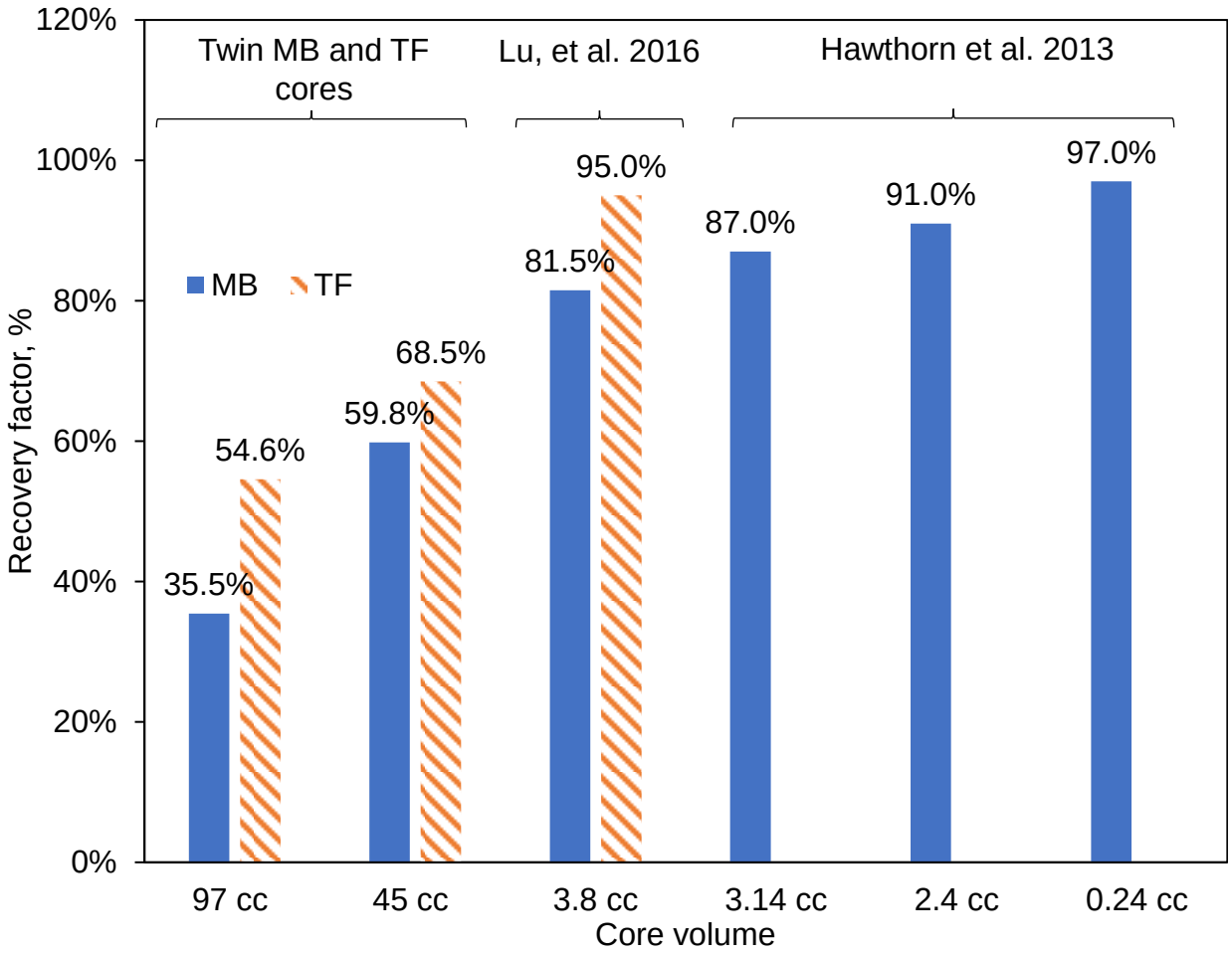

Fig. 5.4 Oil recovery factors for MB and TF samples of different sizes

5.3 Effect of CO_2 HnP Injection Schedule

We used samples MB#4 and TF#4, which had the lowest recovery factors after the previous injection test, for Test (II) to investigate the effect of changing the injection schedule on CO_2 HnP performance. MB#4 and TF#4 had recovery factors of 35.5% and 54.6%, respectively, after one HnP cycle with 24 hours of soaking time. The samples were re-saturated, then subjected to three successive HnP cycles each with eight hours of soaking time.

The solid blue line curve in Fig. 5.5 represents the recovery factor for MB#4 after one HnP cycle with 24 hours of soaking time, and the dashed blue line represents the recovery factor after HnP

cycles with eight hours of soaking in CO_2. CO_2 HnP yielded a recovery of 28% after the first eight hours, then after the second and third cycles the recovery increased to 36% and 45%, respectively. 54.6% was recovered from sample TF#4 after one cycle with 24 hours of soaking (solid orange line), while the recovery factor after the first, second, and third HnP cycles, with eight hours of soaking, were 41%, 56%, and 71%, respectively (dashed orange line).

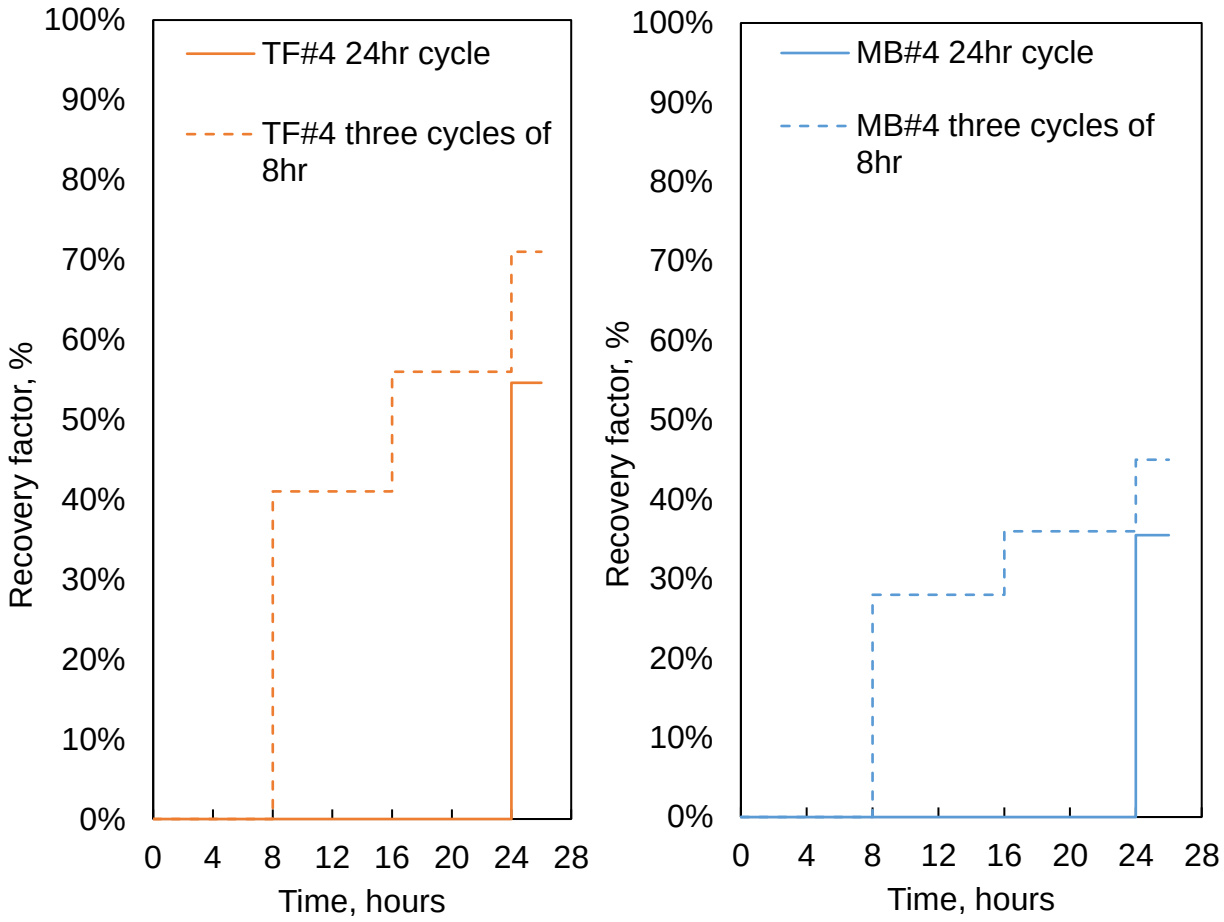

Fig. 5.5 Oil recovery factors for MB#4 (right) and TF#4 (left) after one CO_2 HnP with 24 hours of soaking (solid lines) and three cycles with eight hours of soaking time (dashed line).

The total CO_2 exposure time was the same for Tests (I) and (II); however, Test (II) was subdivided into three different cycles, resulting in recovering 9.5% more oil for sample MB#4 and 16.4% for TF#4 compared to the one soaking cycle of 24 hours in Test (I).

Several researchers reported that diffusion is the primary mechanism for oil recovery using CO_2 injection in tight formations [35,59,63,68,69]. Our results suggest that the pressure gradient drives the rock permeation of the injected CO_2 in the early stages of the soaking period, causing the rock to swell and mobilizing some of the oil toward the bulk CO_2 surrounding the sample. The CO_2 pressure gradient subsequently declines, and concentration gradient diffusion drives oil production from the pores into the fractures filled with CO_2. Molecular diffusion is a slow process and becomes slower as the concentration gradient gets smaller once a portion of the oil is extracted near the fracture. Splitting the 24 hours of soaking into three HnP cycles, that were eight hours long each, resulted in exposing the rock to new pressure and concentration gradients. This new exposure allowed us to recover more oil compared to the oil recovered when the core was allowed to soak in CO_2 for 24 hours, where diffusion drove the oil production for an extended period at a slow rate.

5.4 Effect of Water Presence

Different factors may contribute to an increase of the water cut in Bakken wells, such as expanding the production area, which leads to drilling wells in regions with relatively higher water saturation, and massive fracturing activities. We simulated the accumulation of the mobile water in the lower portion of the fracture that may occur in such reservoirs for Experiment (III). We performed a CO_2 HnP test using samples MB#3 and TF#3, which had the highest recovery factor after Experiment (I). We filled a portion of the fracture space, or void volume, with formation brine before starting CO_2 injection after loading the sample in the core holder.

The results presented in Fig. 5.6 indicate that the oil recovery factor for MB#3 decreased from 59.8% in Test (I) to 18.6% when brine was present in the fracture, and from 68.5% to 39.8% for the Three Forks sample TF#3. The significant decrease in oil recovery indicates that water

presence can severely impact CO_2 EOR performance. The water accumulating in the fracture can cover a portion of the rock and impede its contact with the injected gas, reducing oil recovery.

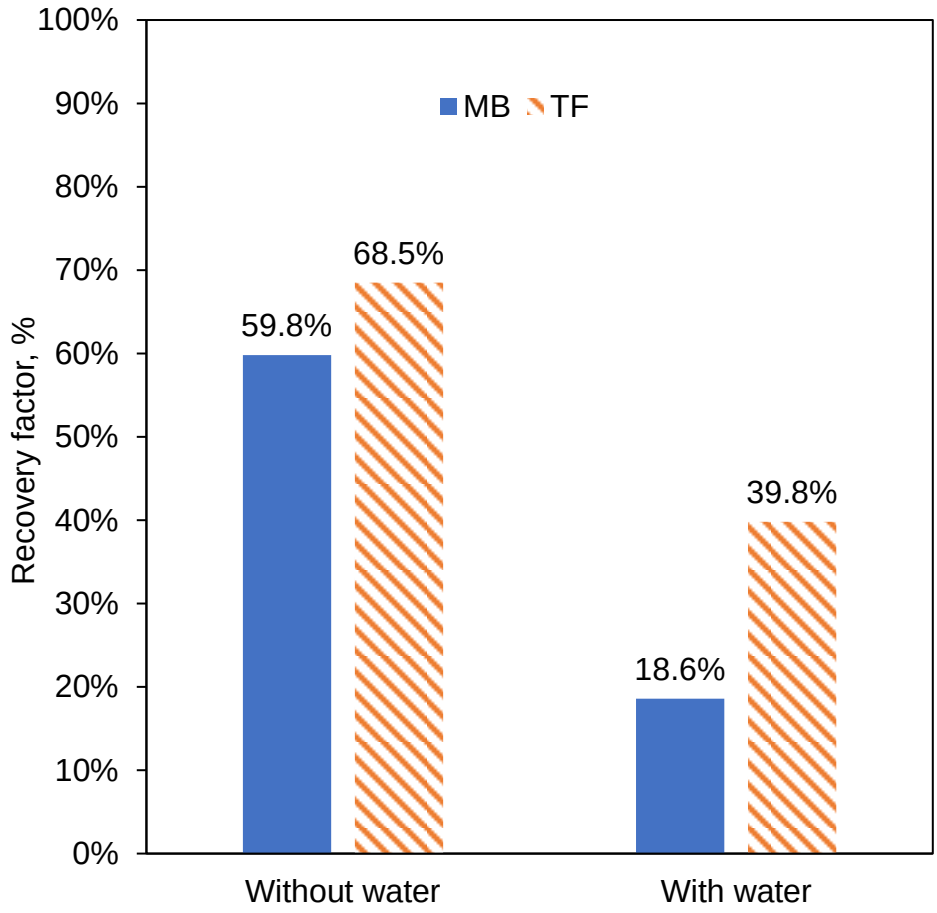

Fig. 5.6 Oil recovery factors for MB#3 and TF#3 with and without water presence

5.5 Effect of CO_2 Volume to the Exposed Rock Surface

The common practice in CO_2 HnP lab studies consists of placing a core sample in a vessel to inject a certain amount of CO_2 specified by the design of the apparatus in use. In tight formations, the rock matrix is characterized by an ultralow permeability, and the injected fluid is limited to the volume of the fractures to permeate the rock surfaces; therefore, the CO_2 abundance around the sample can be an important parameter that affects the reliability of the experimental results. We

continued to reduce the void volume in the core chamber for Experiments (IV) through (VI) to evaluate the impact of reducing the CO_2 volume surrounding the sample with cyclic injection experiments. At the final stage, in experiment (VII), we created a longitudinal fracture through the sample to reach lower volume to surface ratios and simulate the reservoir conditions (see Fig. 5.3). Fig. 5.7 presents the change in oil recovery for samples MB#5 and TF#5 at different β values. The results indicate that reducing β after each experiment resulted in decreased CO_2 performance in the same samples. The recovery factor of the TF plug was 56%, 49.7%, 35.1%, and 25.7% for CO_2 volume to rock surface ratios of 1.86, 1.27, 0.6, and 0.05, respectively. The oil recovery for the MB sample was also negatively impacted, and the recovery factor decreased from 35.5% to 31.3%, 23%, and 13.6% for the same β ratios used in the TF sample experiments.

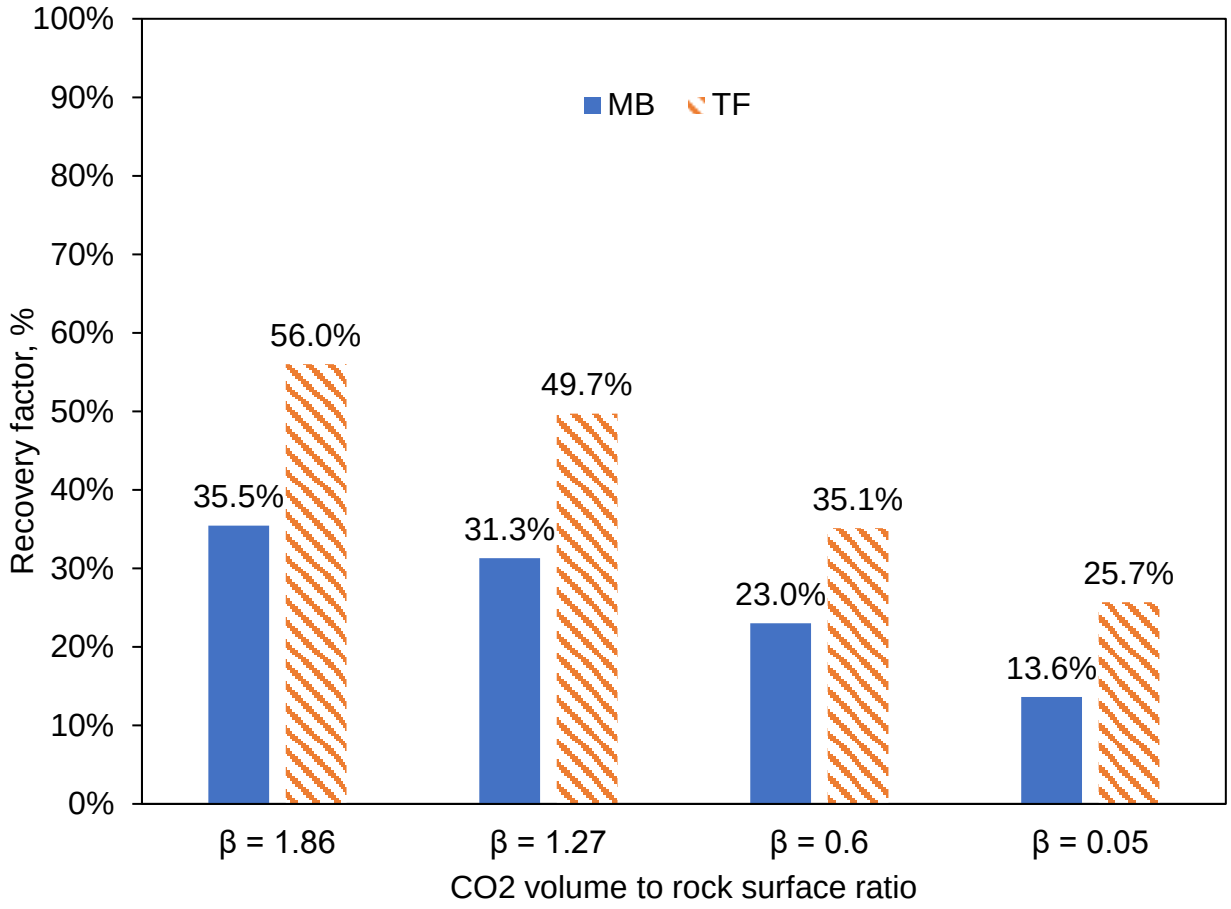

Fig. 5.7 Oil recovery factors with different CO_2 volume to exposed rock surface ratios for the MB#5 and TF#5 samples

This test illustrates that the performance of a CO_2 EOR application is related to the amount of CO_2 that can permeate the rock sample and interact with the fluids in place, which is consistent with the results of previous experiments in this study. Reducing the volume of CO_2 in contact with the rock surface while keeping the same injection pressure in each scenario will have two main consequences: 1) quicker depletion of the CO_2 concentration gradient that leads to a less effective molecular diffusion, and 2) less CO_2 to maintain the pressure in the fracture, which limits the contribution of viscous forces to CO_2 imbibition and oil mobilization.

The outcomes of this test suggest that the standard experimental procedure used to evaluate cyclic injection, which consists of submerging the core sample into a relatively large volume of CO_2 [28,37,38,65,70], can lead to optimistic results and an oil recovery overestimation.

5.6 CO_2 Flooding Vs HnP in Fractured Samples

CO_2 flooding in consolidated MB and TF samples can be very challenging and impossible in some cores. In this work, it was possible to perform a CO_2 flood experiment and compare the results with the previous HnP test for the same samples after they were fractured during Test (VII).

The results displayed in Fig. 5.8 indicate that HnP outperforms the flooding technique in both MB and TF fractured plugs. The recovery factor for the fractured TF and MB samples after CO_2 HnP was 25.7% and 13.6%, respectively. We recovered 13.1% and 5.2% of the OOIP during the CO_2 flood test for the TF and MB samples, respectively, after re-saturating them. The high contrast in permeability between the fractures and rock matrix in both samples causes poor sweep and displacement efficiency. A CO_2 breakthrough was detected during the flood experiment: after 15 minutes for the MB sample and 38 minutes for the TF sample. On the other hand, the HnP injection schedule provided more time for the injected CO_2 to permeate the rock matrix.

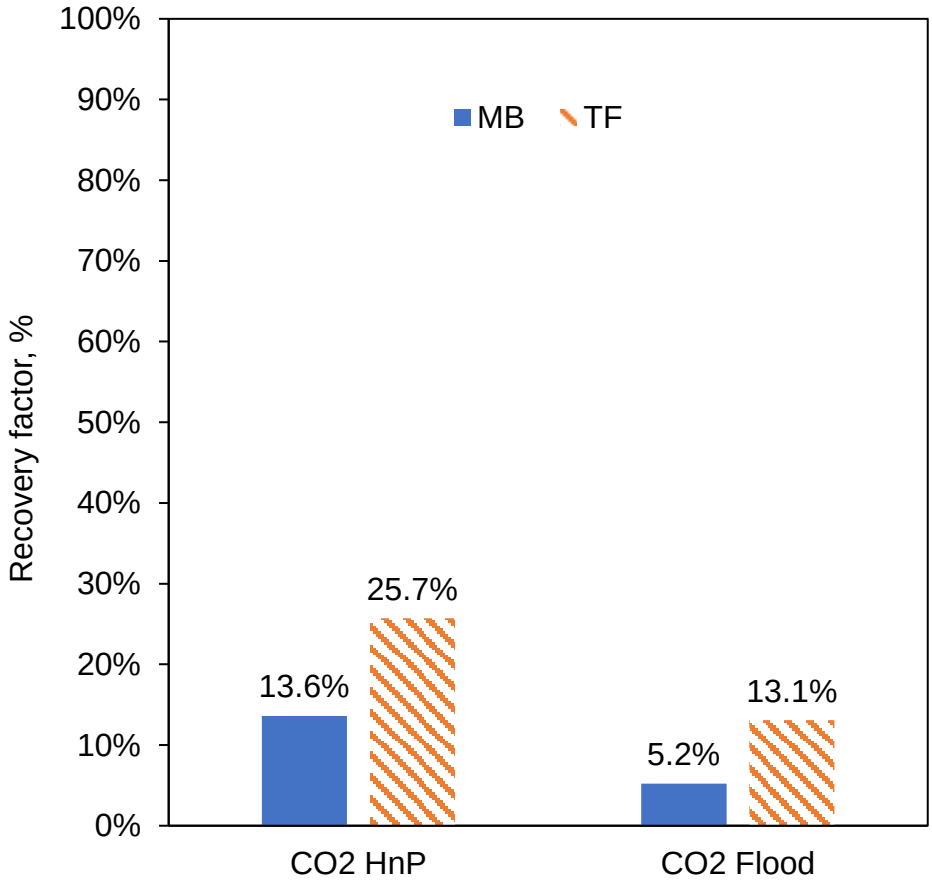

Fig. 5.8 Oil recovery factors after CO_2 HnP and flood through fractured MB and TF samples

5.7 Summary

We evaluated the effects of different parameters on oil recovery using CO_2 injection experiments in Middle Bakken and Three Forks samples. This comprehensive study provides a better understanding of how to enhance oil recovery in the Bakken effectively. Several observations were revealed by the experimental results, which could be used to enlighten future EOR design:

- The size of the tested samples has an important impact on EOR experiments. The selection of smaller samples can lead to overestimating the potential of CO_2 EOR and oil recovery. We recommend using samples that are large enough to represent fluid flow in the reservoir and represent its heterogeneity.

- Splitting one HnP cycle into three successive cycles allowed us to recover 10 % and 17% more oil from the same MB and TF samples, respectively. These results suggest that both viscous forces and molecular diffusion control oil recovery. The pressure gradient initially pushes CO_2 into larger pores and promotes its penetration, then diffusion controls oil extraction toward the bulk CO_2 volume surrounding the rock.
- Water accumulated in the fracture can impede the contact between CO_2 and the reservoir rock, which results in reduced oil recovery. Water presence significantly impacted CO_2 performance: the measured recovery factor decreased from 59.8% to 18.6% for the MB sample and from 68.5% to 39.8% for the TF sample.
- The ratio of the volume surrounding the sample to the sample surface needs to be considered carefully and should represent reservoir conditions for cyclic injection experiments in tight samples. The experimental results indicated that submerging a core sample in a relatively large CO_2 volume can overestimate subsequent oil recovery.
- It became possible to test a CO_2 flooding scheme and compare its performance to HnP under similar conditions using fractured tight formation samples. Cyclic injection outperformed the flooding process, which was limited by low sweep efficiency and early breakthrough.

In the next Chapter, we present the effect of CO_2 injection on different reservoir attributes in unconventional plays.

Chapter 6

Evaluation of CO_2 Injection Side Effects

This Chapter aims to provide insight into property alteration in unconventional reservoirs that might occur due to CO_2 injection and to improve the understanding of those mechanisms. We present the evaluation of the potential side effects of CO_2 injection related to rock wettability, pore size distribution, and effective porosity. Two Middle Bakken (MB) and two Three Forks (TF) formation samples were tested to investigate changes in rock wettability, Pore Size Distribution (PSD), and effective porosity before and after exposure to CO_2. We used the contact angle technique to measure the wettability state with and without CO_2 exposure. The Nuclear Magnetic Resonance (NMR) spectroscopy technique was used to determine fluid distribution before and after CO_2 injection.

6.1 Background

As depicted in previous Chapters, CO_2 injection can assist with extracting residual oil and overcoming injectivity problems in tight formations [71]; however, its interactions with the *in-situ* reservoir fluids and rock minerals can affect some reservoir attributes and must be evaluated. The interaction of the injected CO_2 with the oil in place can result in asphaltene precipitation, which can cause pore plugging and reduce reservoir permeability [72,73]. Some chemical reactions may also occur when CO_2 is in contact with brine and rock minerals [74]. The possible reactions that can take place in water-containing oil reservoirs include [74–80]:

$$CO_2+H_2O \leftrightarrow H_2CO_3 \quad (1)$$

$$H_2CO_3 \leftrightarrow H^+ + HCO_3^- \quad (2)$$

$$2H^+ + CaMg(CO_3)_2(\text{dolomite}) \leftrightarrow Mg^{2+} + Ca^{2+} + 2HCO_3^- \quad (3)$$

$$H^+ + CaCO_3(\text{Calcite}) \leftrightarrow Ca^{2+} + HCO_3^- \quad (4)$$

$$2KAlSi_3O_8(\text{Potash feldspar}) + 2H^+ + 9H_2O \rightarrow Al_2Si_2O_5(OH)_4(\text{Kaolinite}) + 2k^+ + 4H_4SiO_4 \quad (5)$$

$$2NaAlSi_3O_8(\text{Albite}) + 3H_2O + 2CO_2 \rightarrow Al_2Si_2O_5(OH)_4 + 4SiO_2 + 2Na^+ + 2HCO_3^- \quad (6)$$

$$CaAlSi_3O_8(\text{Anorthite}) + H_2CO_3 + H_2O \rightarrow CaCO_3 + Al_2Si_2O_5(OH)_4 \quad (7)$$

The injected CO_2 can dissolve into the formation brine and form a weak acid solution (Equation (1)), which will decompose into bicarbonate and hydrogen ions (Equation (2)). The acid solution can dissolve some of the existing minerals (Equations (3) to (7)) such as dolomite, calcite, and feldspar. New pores may be created as a result of these reactions, and others might be plugged by formed precipitates, such as carbonate and kaolinite [79,80].

Previous studies have been conducted to evaluate possible CO_2-induced petrophysical property changes in oil reservoirs. The impact of these CO_2-rock-fluid interactions on oil reservoir attributes

can vary based on the characteristics of the reservoir of interest, the tested oil's properties, and the experimental conditions. Contradictory results have been reported: some studies reported that CO_2 can negatively affect the petrophysical properties of the reservoir [76,78,79,81–83], while others observed an improvement in porosity and permeability [77,80,84–88].

Numerous studies have been performed to evaluate the effect of CO_2 injection and asphaltene deposition on rock permeability, however, the CO_2 induced changes of wettability, PSD, and effective porosity are seldomly discussed. Very little research has been performed to investigate those changes in unconventional plays compared to conventional reservoirs, and no previous work has investigated the side effects of CO_2 injection into the Bakken to the best of our knowledge.

An alteration of the wettability state can have a huge impact on oil displacement in the reservoir [89,90]. A change of the PSD or the porosity can impact future field development plans and needs to be assessed in advance. Thus, a thorough understanding of the side effects of CO_2 injection on those parameters is fundamental for evaluating the performance of CO_2 EOR applications. In this work, we compared the wettability state of the rock before and after CO_2 exposure, and investigated the possible changes in fluid distribution and PSD after CO_2 Huff-n-Puff (HnP). Since there is no agreement in the literature regarding the effect of CO_2 injection on the pore volume of the rock, we evaluated the porosity changes before and after CO_2 exposure using representative MB and TF rock samples. This study aims to provide insight into property alteration in unconventional reservoirs that might occur due to CO_2 injection and improve the understanding of those mechanisms. The reported results help understand the potential side effects of CO_2 injection in tight formations and can be used to enlighten future EOR projects.

6.2 Methodology

6.2.1 Materials

We retrieved two twin MB and TF samples (MB#6, MB#6*, TF#6, and TF#6*) from the first well. We used one more MB and TF sample (MB#7 and TF#7) from the second well for experiment repeatability purposes. The brine and dead oil samples were collected from each sampled well. Table 7 lists the properties of the cores as received. We cut two identical disc-shaped chunks (Ca. 1*1*0.3 cm) from each sample for the contact angle measurements, denoted as MB#6c1, MB#6c2, MB#7c1, MB#7c2, TF#6c1, TF#6c2, TF#7c1, and TF#7c2.

We used the X-Ray Diffraction (XRD) technique to determine the mineralogical composition of each sample so we could analyze the results of the experiments performed in this study and understand the effect of the CO_2 reactions with the core minerals. The XRD results, summarized in Table 8, indicate that carbonate minerals such as calcite and dolomite, feldspar, quartz, and clays are the dominant minerals in our samples. The MB samples have a higher calcite content than dolomite, while the latter is the primary component of both TF samples.

Table 7 Properties of rock samples used to investigate CO_2 injection side effects

Sample ID	Formation	Length (in)	Diameter (in)	Permeability (mD)	Oil Saturation (%)	Water Saturation (%)
MB#6 / MB#6*	Middle Bakken	4.0	1.0	0.009	30.8	28.4
TF#6 / TF#6*	Three Forks	4.2	1.0	0.130	30.9	26.4
MB#7	Middle Bakken	4.2	1.0	0.002	51.5	22.7
TF#7	Three Forks	4.0	1.0	0.183	59.9	11.4

Table 8 Mineralogical composition of the MB and TF samples

Sample ID	Calcite (%)	Dolomite (%)	Feldspar (%)	Clays (%)	Anhydrite (%)	Quartz (%)	Pyrite (%)
MB#6	20.20	8.43	13.80	7.30	10.90	37.42	2.00
TF#6	1.10	53.00	0.40	23.00	1.00	19.80	3.40
MB#7	48.90	10.80	14.70	3.53	1.30	20.63	0.10
TF#7	2.60	46.30	21.70	5.60	6.00	17.60	0.73

6.2.2 Wettability assessment

Wettability is a reservoir attribute that defines the degree of adhesion of a fluid to the rock surface when other immiscible fluids are present, dictating the tendency of that fluid to occupy smaller pores and how much rock surface it can contact [91]; therefore, it is an important parameter that can control fluid flow and distribution in the reservoir, and its evaluation is critical for the success of any EOR technique. Several methods have been proposed to determine wettability, including USBM, Amott cell, and contact angle [91–93]. The wettability state can be determined directly by measuring the contact angle of a brine droplet on a rock surface using the contact angle method, which makes it the most appropriate technique for unconventional reservoirs due to ultralow permeability and porosity; therefore, we used this method to determine the wettability state of the MB and TF samples. Different contact angle thresholds have been proposed in the literature to determine the wetting state. We adopted the repartition in carbonate reservoirs introduced by Chilingar and Yen [94] for our experiments (see Fig. 6.1). The rock can be considered water-wet

if the contact angle of a brine droplet is between 0° and 80°, mixed-wet for values between 80° and 100°, and oil-wet when the contact angle is higher than 100°.

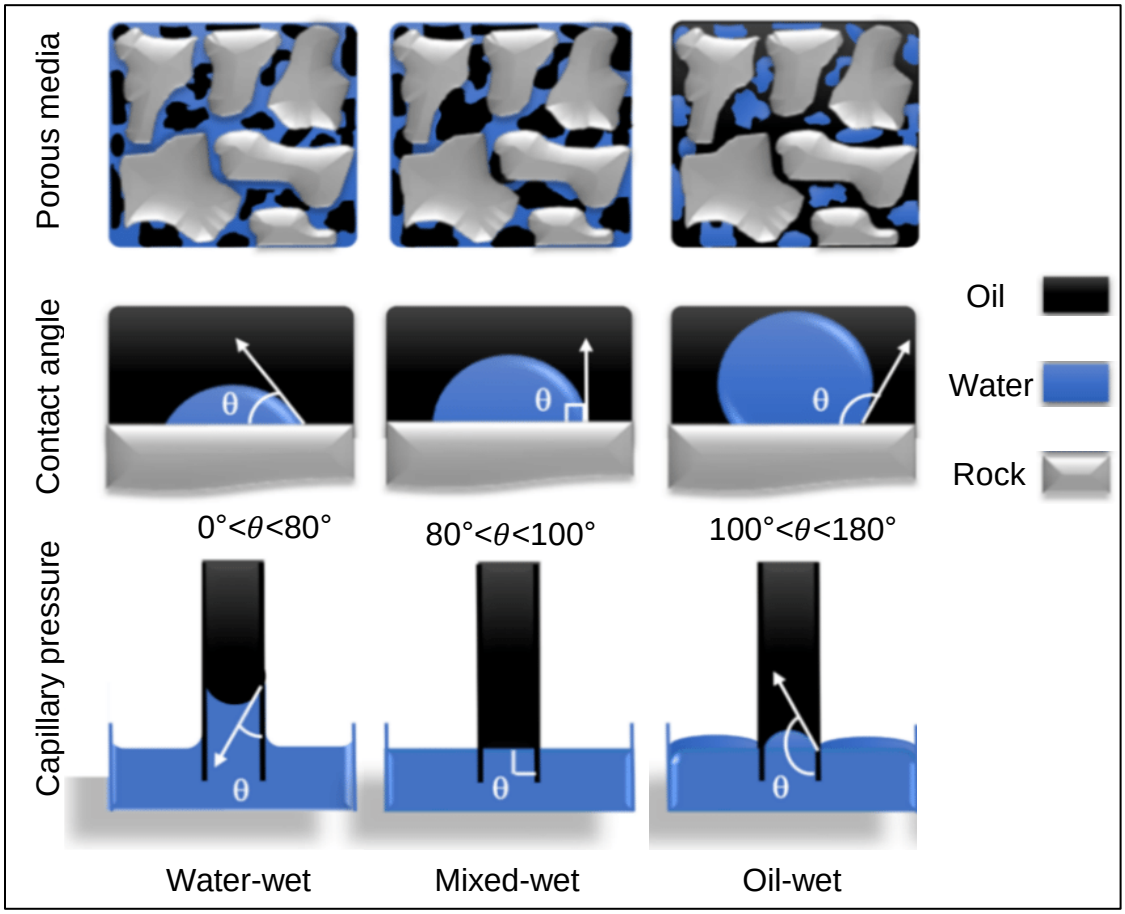

Fig. 6.1 Display of the different wettability states based on the contact angle of a water droplet (modified based on [95])

The apparatus used to measure the contact angle at different experimental conditions is presented in Fig. 3.5.

6.2.2.1 Oil brine rock system

We placed the samples MB#6c1, TF#6c1, MB#7c1, and TF#7c1 in the visual cell at the beginning of the experiment. Oil was then injected to fill the chamber and displace the existing air. The temperature was set to match the reservoir temperature of 213°F, and the system was allowed to

stabilize. The pressure was set to approximately 3,800 psi, and the brine was steadily injected through a capillary needle to generate a droplet on the rock surface, which was then allowed to stabilize before taking the final contact angle measurement. Instead of taking the contact angle measurement at a preset time, we used a different approach to ensure the stabilization of the system. The bubble shape was monitored, and the contact angle was measured every 30 minutes. The contact angle was considered stable when there was no variance among the last three values, and the final measurement was acquired.

6.2.2.2 CO_2 brine oil-saturated-rock system

We pre-saturated the samples MB#6c2, TF#6c2, MB#7c2, and TF#7c2 with oil before placing each one of them in the visual cell for this set of experiments. We then injected CO_2 into the cell and evacuated the existing air. We used the same procedure for the oil-brine system to increase the temperature to 213°F, the pressure to 3,800 psi, and generate the brine droplet on the rock surface. Several contact angle measurements were taken before obtaining the final value to make sure the system stabilized.

6.2.3 Nuclear magnetic resonance technique

Nuclear Magnetic Resonance is a technique used to detect the distribution of pore fluids in a porous media. Nuclear magnetic resonance can occur due to the oscillating magnetic field when hydrogen-containing fluids are exposed to a static magnetic field [96]. The measured transverse time (T_2) is generally affected by bulk relaxation, diffusion in magnetic gradients, and surface relaxation [96,97]; however, the diffusion relaxation can be neglected in tight formations, and the surface relaxation is correlated with the specific area of the core, which represents the ratio of the surface of the pore to the total pore volume of the sample. Transverse relaxation time T_2 is expressed as [80,98]:

$$\frac{1}{T_2}=\frac{1}{T_{2B}}+\frac{1}{T_{2S}}=\frac{1}{T_{2B}}+\rho\frac{S}{V} \qquad (8)$$

where T_2 is the transverse relaxation time (ms), T_{2B} is the transverse relaxation time due to bulk relaxation, T_{2S} is the transverse relaxation time due to surface relaxation, ρ is the relaxation rate (μm/ms), and $\frac{S}{V}$ represents the surface to volume ratio of the pore system (1/μm).

The NMR results can be used to evaluate the movable fluid porosity in low permeability reservoirs and determine the distribution of pore size across the samples. The relationship between the pore radius and T_2 spectrum can be defined as [99]:

$$r=CT_2 \qquad (9)$$

where r is the pore throat radius (μm), and C is a dimensionless proportional constant that should be determined to convert the T_2 spectrum to pore distribution.

The pore sizes can be classified into three categories: micro, meso, and macro using the unified pore size classification proposed by Zdravkov et al. [100]. The pores are considered of a macro, meso, and micro size when the pore diameter (d) >50nm, 50>d>3nm, and d < 3nm, respectively.

6.2.3.1 PSD before and after CO_2 injection

An Oxford Instruments GeoSpec2 core analyzer coupled with Green Imaging Technology software was used to acquire the NMR transverse relaxation measurements. The MB#6, TF#6, MB#7, TF#7 samples were saturated with oil and placed in the NMR instrument to measure the T_2 spectrum and determine the fluid distribution in the core. We then performed one CO_2 HnP cycle for each plug. The sample was placed in the NMR machine again to evaluate the PSD change after CO_2 injection.

6.2.3.2 Effective porosity measurement

Samples MB#6* and TF#6* were cleaned and saturated with brine to measure the change in effective porosity, then saturated with oil under high pressure to ensure that each core was 100% saturated. More details regarding the core preparation and saturation procedure can be found in our previous publications [101,102]. The cores were placed in the NMR machine to determine the initial effective porosity after saturation, then we performed a CO_2 injection cycle followed by re-saturation. The core was placed into the NMR instrument to measure the effective porosity after one HnP cycle (24 hours of soaking). The process was repeated, and four injection cycles followed by re-saturation were performed for each sample. We used the same procedure to remeasure effective porosity. These experiments are costly and are relatively time-consuming; therefore, we only tested one sample each from MB and TF.

6.3 Wettability Alteration Due to CO_2 Exposure

Fig. 6.2 and Fig. 6.3 illustrate the results of the contact angle experiments performed on the MB and TF samples with and without CO_2 exposure. The contact angle of the brine droplet submerged in oil and introduced on the MB samples MB#6c1 and MB#7c1 was 134° and 133°, respectively (Fig. 6.2 (A) and Fig. 6.3 (A)). The contact angle was 143° and 142° for the TF samples TF#6c1 and TF#7c1, respectively. These results demonstrate that both reservoirs can be characterized as oil-wet to strongly oil-wet prior to CO_2 exposure (see reservoir wettability classification in Fig. 6.1).

Fig. 6.2 (B) and Fig. 6.3 (B) illustrate that the contact angle of the brine droplet on the oil-saturated MB samples MB#6c2 and MB#7c2 dropped to 69° and 85°, respectively, after CO_2 exposure. The contact angle was 82° and 89° for the TF samples TF#6c2 and TF#7c2, respectively. These results indicate that CO_2 increased the hydrophilicity of the MB and TF samples and shifted the wettability from strongly oil-wet towards neutral- and water-wet.

Chen et al. [103] observed a contact angle shift when they introduced an oil droplet on calcite substrates in non-carbonated and carbonated brine solutions. They observed that the system became more water-wet using the carbonated brine.

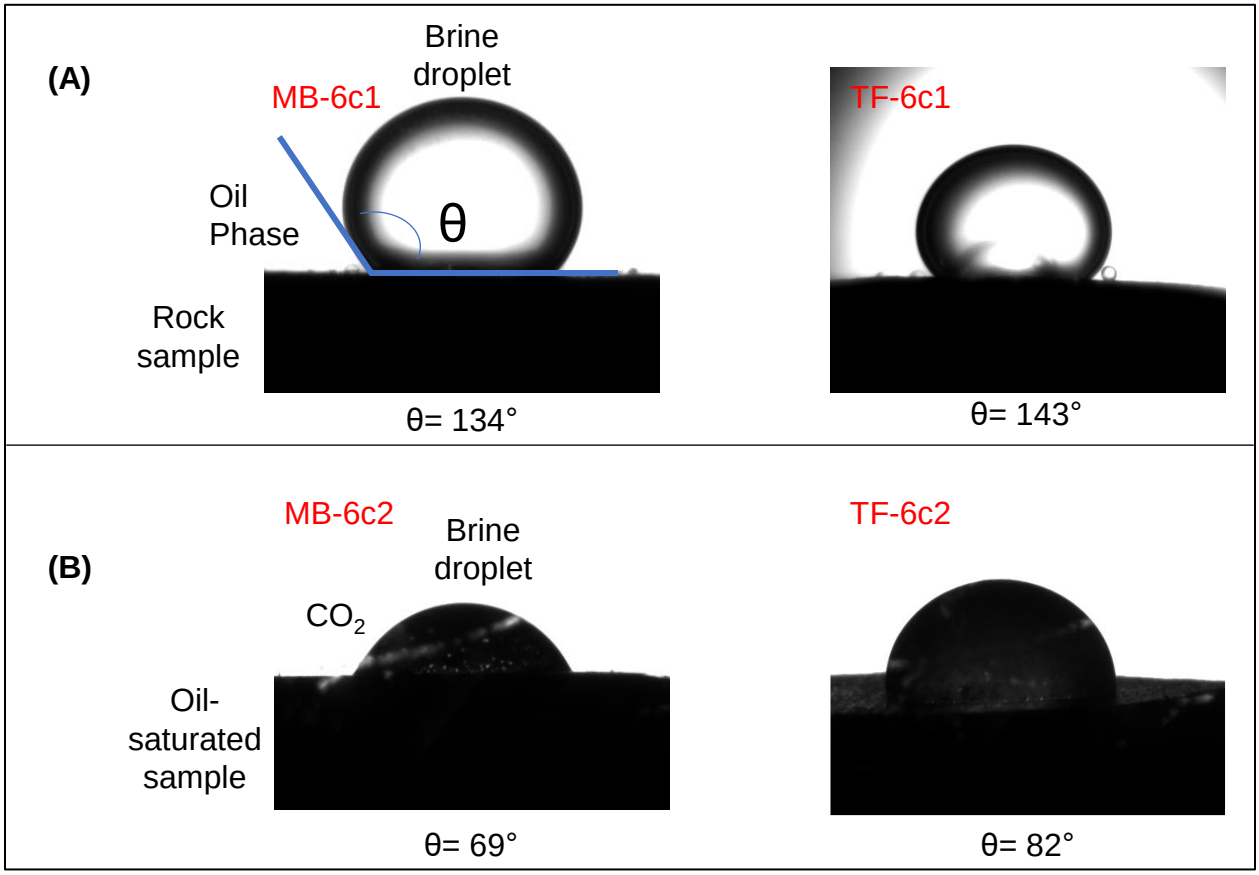

Fig. 6.2 Contact angle measurements in MB and TF samples from the first well, (A) oil/brine/rock system, and (B) CO_2/brine/oil-saturated-rock

Teklu et al. [104] used a seawater/oil/Three-Forks-sample system and found that the rock's wettability preference switched from oil-wet to water-wet when they used a mixture of seawater and CO_2. The contact angle measurements can yield important observations and determine the reservoir sample's wettability state under different conditions; however, it may not capture the complexity of the surface-fluid interactions. Closer examinations of the complex nature of wettability are needed to better understand the CO_2-induced wettability shift. Chen et al. [103]

developed a geochemical model, which coupled CO_2 dissolution, mineral dissolution, and oil and calcite surface chemistry to understand how dissolved CO_2 increases hydrophilicity. They used a quantitative measure of electrostatic attraction named the Bond Product Sum (BPS) to reflect the electrostatic force change between fluid-fluid and fluid-rock interfaces with and without CO_2. The authors determined that the BPS change after carbonate-calcite equilibrium can increase hydrophilicity, which explains the dramatic drop of the contact angle. Another possible reason for the increase of the hydrophilicity, is the CO_2 capacity to dissolve the hydrocarbons. Considering the pressure and temperature conditions of our test CO_2 is in the supercritical state, and it can dissolve the oil in place, thereby rendering the surface of the rock sample more water-wet. Adel et al., 2018 and Tovar et al., 2018 showed that CO_2 can volatilize a large portion of the hydrocarbons via gas drive mechanism. Hawthorne and Miller, 2020 indicated that when CO_2 is injected at miscible conditions, it can dissolve large volumes of the oil in place. The capacity of supercritical CO_2 to dissolve the crude oil from the interstitial pores of the rock matrix has been proven in several studies [8,29,31,106]. Displacing the oil from the rock surface toward the CO_2-dominated phase via molecular diffusion or vaporizing gas drive will expose more pores to the brine bubble, which might explain the increase of hydrophilicity after CO_2 exposure.

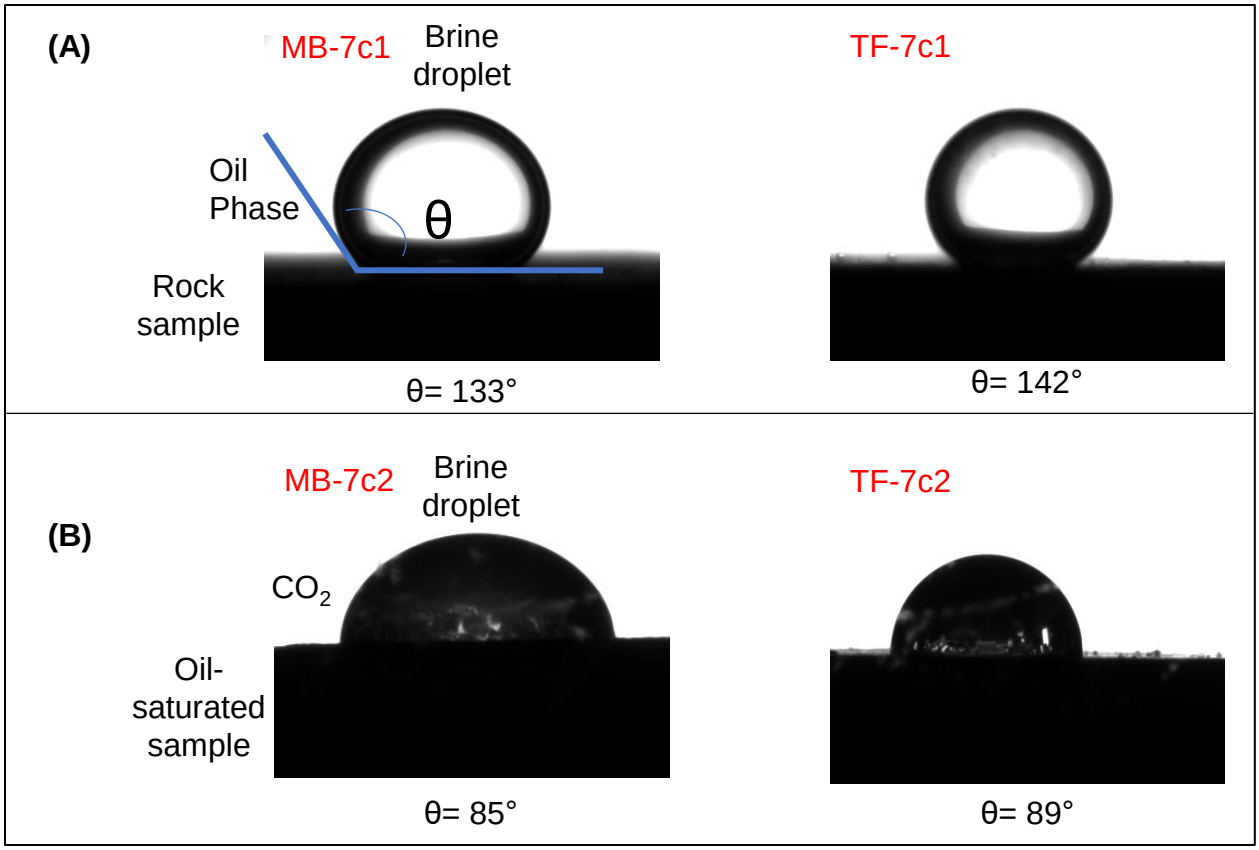

Fig. 6.3 Contact angle measurements in MB and TF samples from the second well, (A) oil/brine/rock system, and (B) CO_2/brine/oil-saturated-rock

6.4 T_2 Spectrum Change After CO_2 Injection

The NMR technique can be used to detect the distribution of hydrogen-containing fluids in a reservoir rock sample that contains water and hydrocarbons. The generated data can then be used to determine the movable fluid porosity in low-permeability reservoirs and evaluate the pore size distribution. Fig. 6.4 and Fig. 6.5 depict the T_2 spectrum of the saturated MB and TF samples before and after one CO_2 HnP cycle. The difference in the areas below the curves before and after CO_2 injection, the straight lines and squared lines, reflect the total amount of displaced fluids after the HnP cycle.

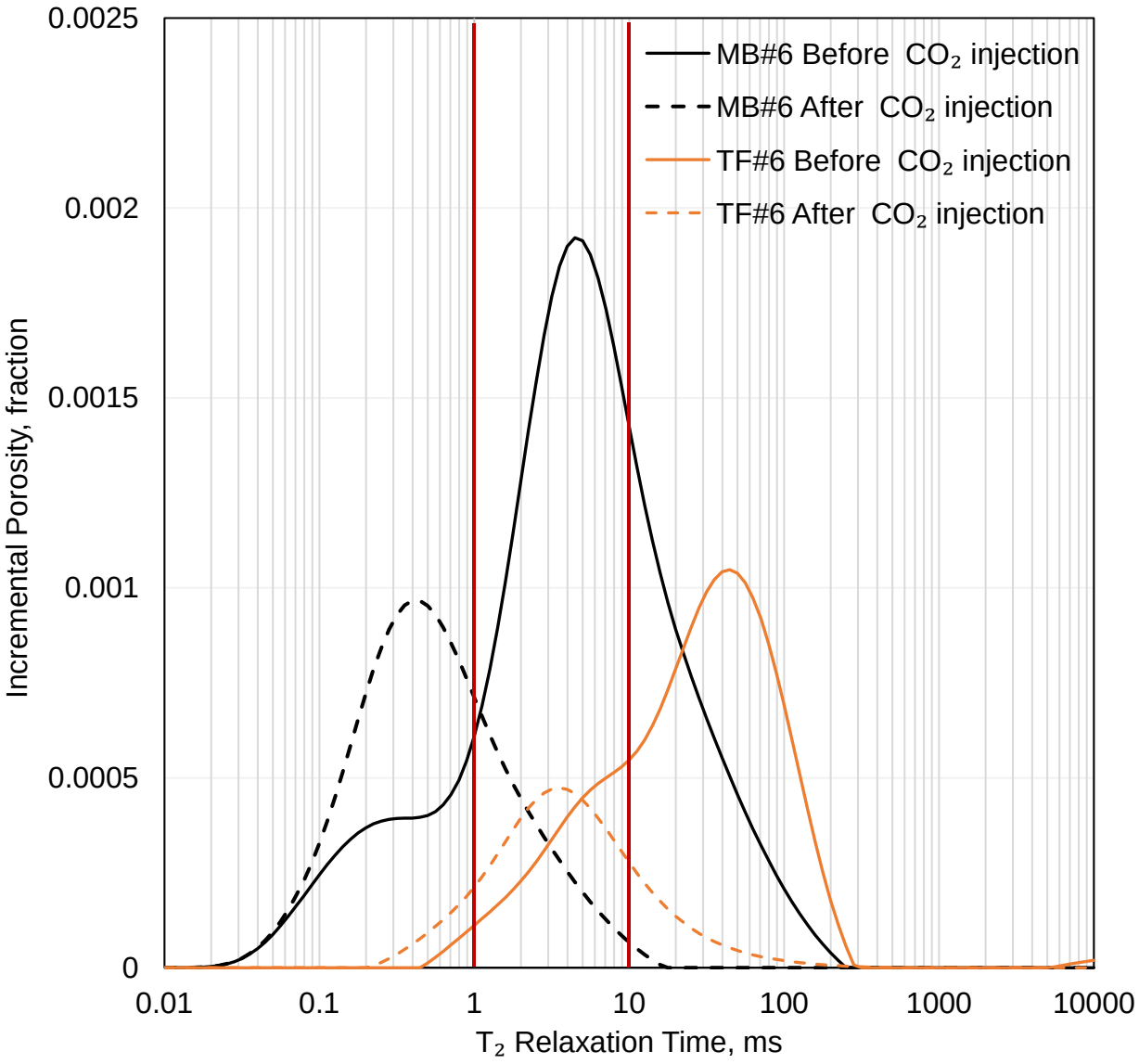

Fig. 6.4 Incremental porosity vs. T_2 Relaxation, straight black line: sample MB#6 before CO_2 injection, black-squared line: sample MB#6 after one CO_2 HnP cycle, straight orange line: sample TF#6 before CO_2 injection, orange-squared line: sample TF#6 after one CO_2 HnP cycle

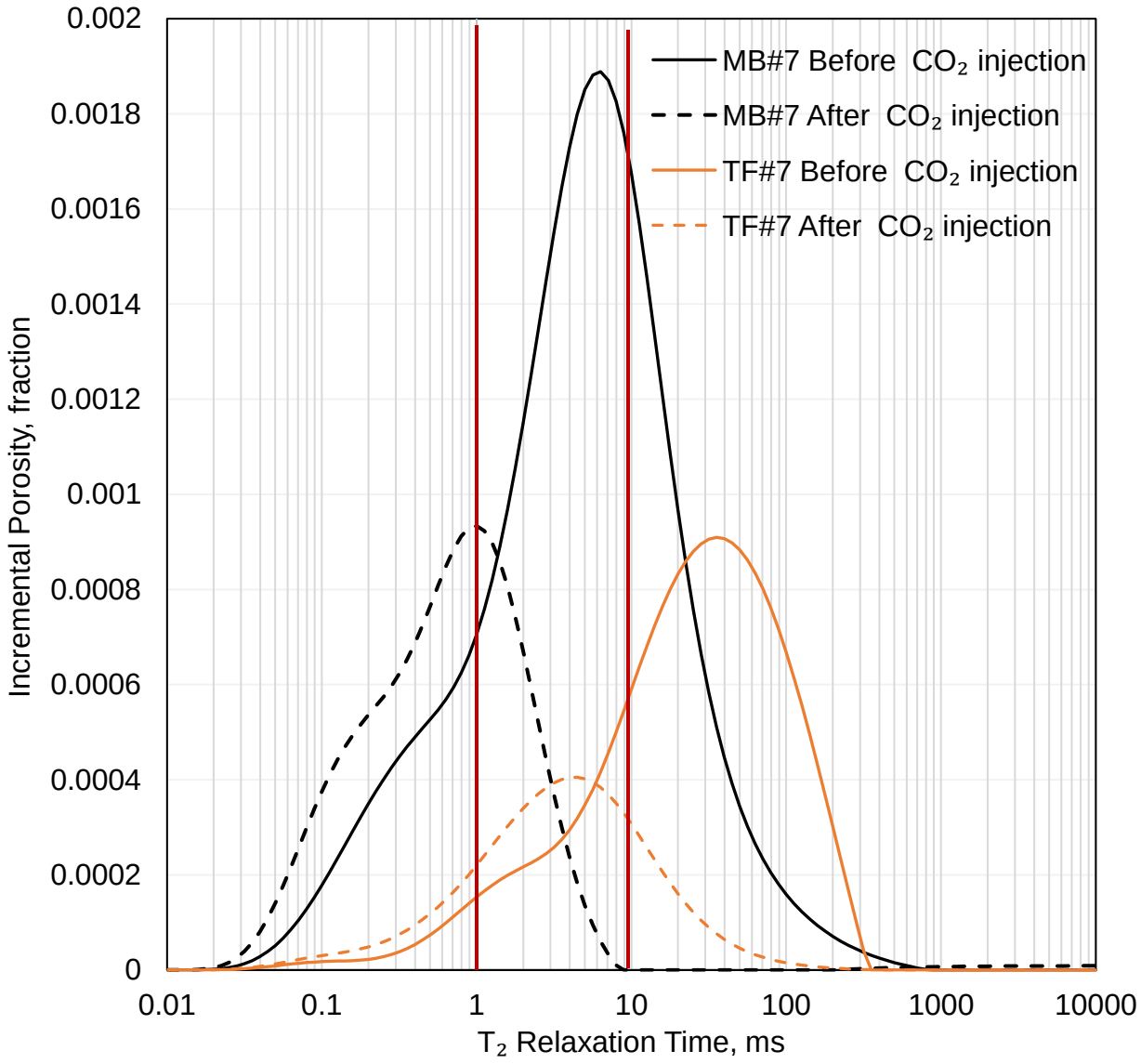

Fig. 6.5 Incremental porosity vs. T_2 Relaxation, straight black line: sample MB#7 before CO_2 injection, black-squared line: sample MB#7 after one CO_2 HnP cycle, straight orange line: sample TF#7 before CO_2 injection, orange-squared line: sample TF#7 after one CO_2 HnP cycle

All curves shifted towards smaller T_2 values after CO_2 exposure. The curve shift reflects a PSD change, and new small pore volumes were detected after CO_2 injection. We used the T_2 cutoff repartition of the different pore sizes adopted by Onwumelu et al. [67] to analyze the PSD change and partition the micro-, meso-, and macro-porosity in the Bakken samples (see Fig. 6.6).

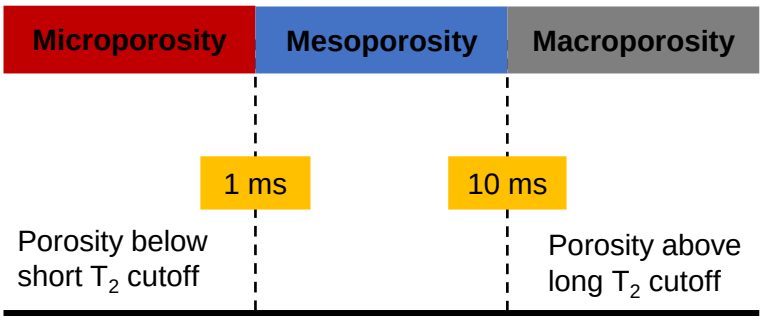

Fig. 6.6 NMR porosity partitioning in Bakken samples based on T_2 cutoffs (modified based on [67])

We calculated the percentage of each porosity type, before and after the CO_2 test, by summing the incremental porosity that falls between the corresponding T_2 cutoffs and dividing it by the initial cumulative porosity when the core was 100% saturated. Fig. 6.7 illustrates the PSD changes in our samples based on the NMR data before and after the HnP cycle. Nearly all of the fluids in the macropores were displaced and the macro-porosity decreased from 26% to 0.2 % for MB#6, 15% to 3% for MB#7, 73% to 7% for TF#6, and 27% to 1% for TF#7 after CO_2 injection. The mesopore distribution decreased for samples MB#6, MB#7, and TF#7 by 44%, 37%, and 21%, respectively. We expect that CO_2 will displace a portion of the fluids in place and "clean" some pores. Those empty pores will not be detected in the NMR after the injection test, explaining the decrease in macro- and meso-porosity; however, the meso-porosity of sample TF#7 increased by 2% after CO_2 exposure and the total volume of the micropores increased for all tested samples. The micro-porosity increased by 14%, 25%, 3%, and 8% for samples MB#6, MB#7, TF#6, and TF#7, respectively. The initial NMR results before CO_2 injection reflect the total pore volume initially saturated with brine and hydrocarbons. The increase in micro-porosity after CO_2 HnP is the result of pushing a portion of the fluids in place toward those pores instead of displacing it toward the fracture volume.

The XRD results (Table 8) indicate that calcite and dolomite are the primary mineral constituents of our samples. The acid solution generated from the reaction of the injected CO_2 with the brine in the core can dissolve some of those minerals, resulting in the creation of new tiny-pore volumes (Equations (1(1) through (7)).

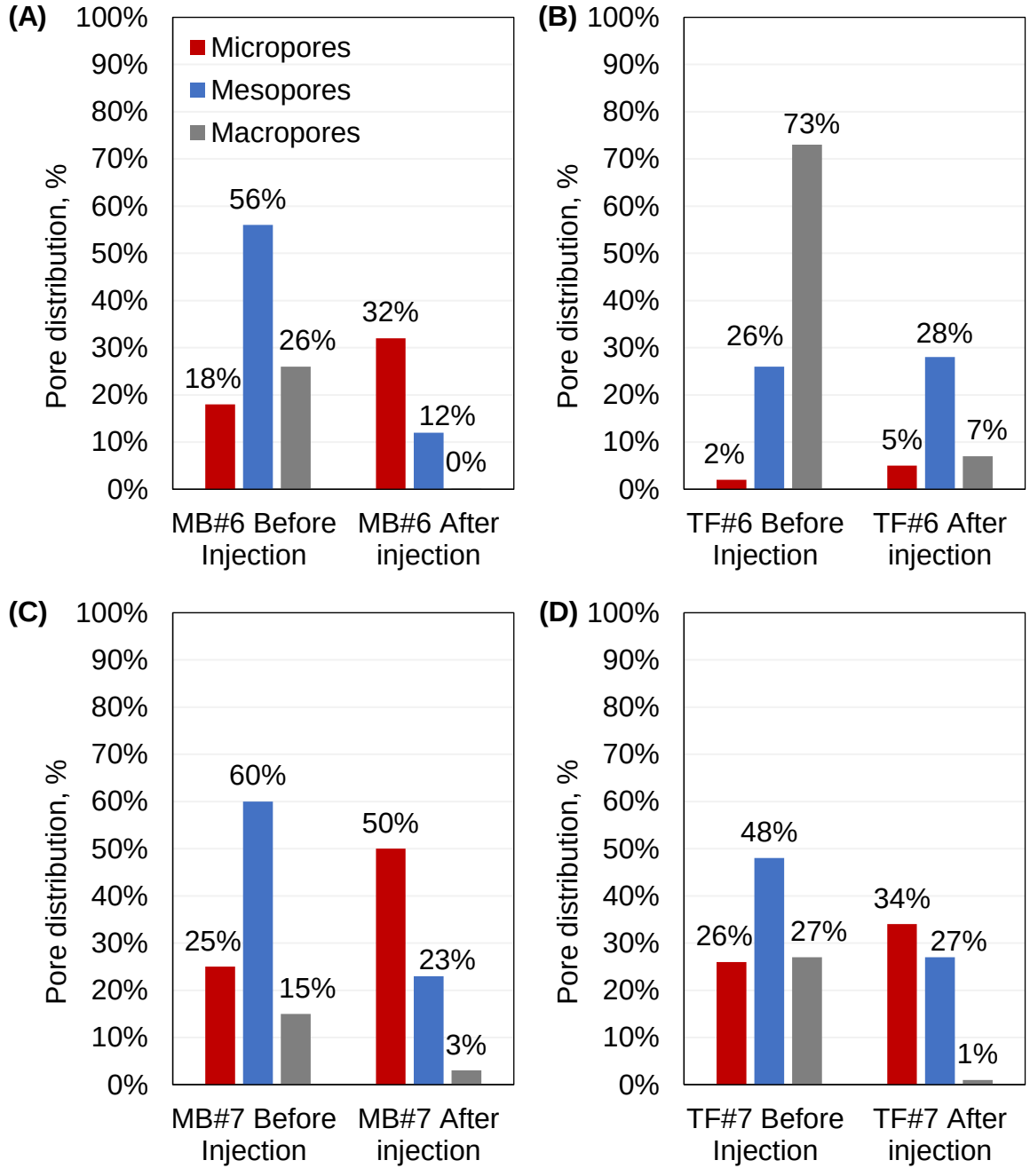

Fig. 6.7 Distribution of pore sizes before and after one CO_2 HnP, (A): MB#6, (B): TF#6, (C): MB#7, (D) TF#7

The "new" pores must be filled with hydrogen-containing fluids to be detected in the NMR, which confirms that the injected CO_2 displaced a portion of the reservoir fluids toward the rock matrix. A closer examination using a high-resolution Computed Tomography Scanner (CT-Scan) is recommended to characterize the pore microstructure change after CO_2 exposure better, even though the NMR results were very informative.

6.5 Variation of Effective Porosity After CO_2 HnP

We used the NMR technique to determine the initial cumulative porosity of each sample after cleaning and saturation with oil and brine. Four CO_2 HnP cycles were performed, and the core was re-saturated with oil after each cycle to remeasure the effective porosity before the next injection test. Fig. 6.8 illustrates the effective porosity changes after multiple CO_2 HnP cycles. The effective porosity of the MB sample was reduced from 5.3% to 4.8%, 4.4%, 4.2, and 3.8% after the 1^{st}, 2^{nd}, 3^{rd}, and 4^{th} injection cycles, respectively. The TF samples' effective porosity was reduced from 7.6% to 7%, 6.9 %, 6.7%, and 6.3%. Equations (5),(6), and (7) describe the different precipitates, kaolinite and calcite, that can form when dissolved CO_2 reacts with the core minerals; therefore, the minerals on the pore walls can react with carbonic acid to form precipitates, reducing pore volume. These precipitates may consequently plug some of the pore volumes, resulting in a decrease of the total pore volume of the core. Moreover, the alternative change of the effective stress induced by cyclic CO_2 injection can result in damaging a portion of the pore volume.

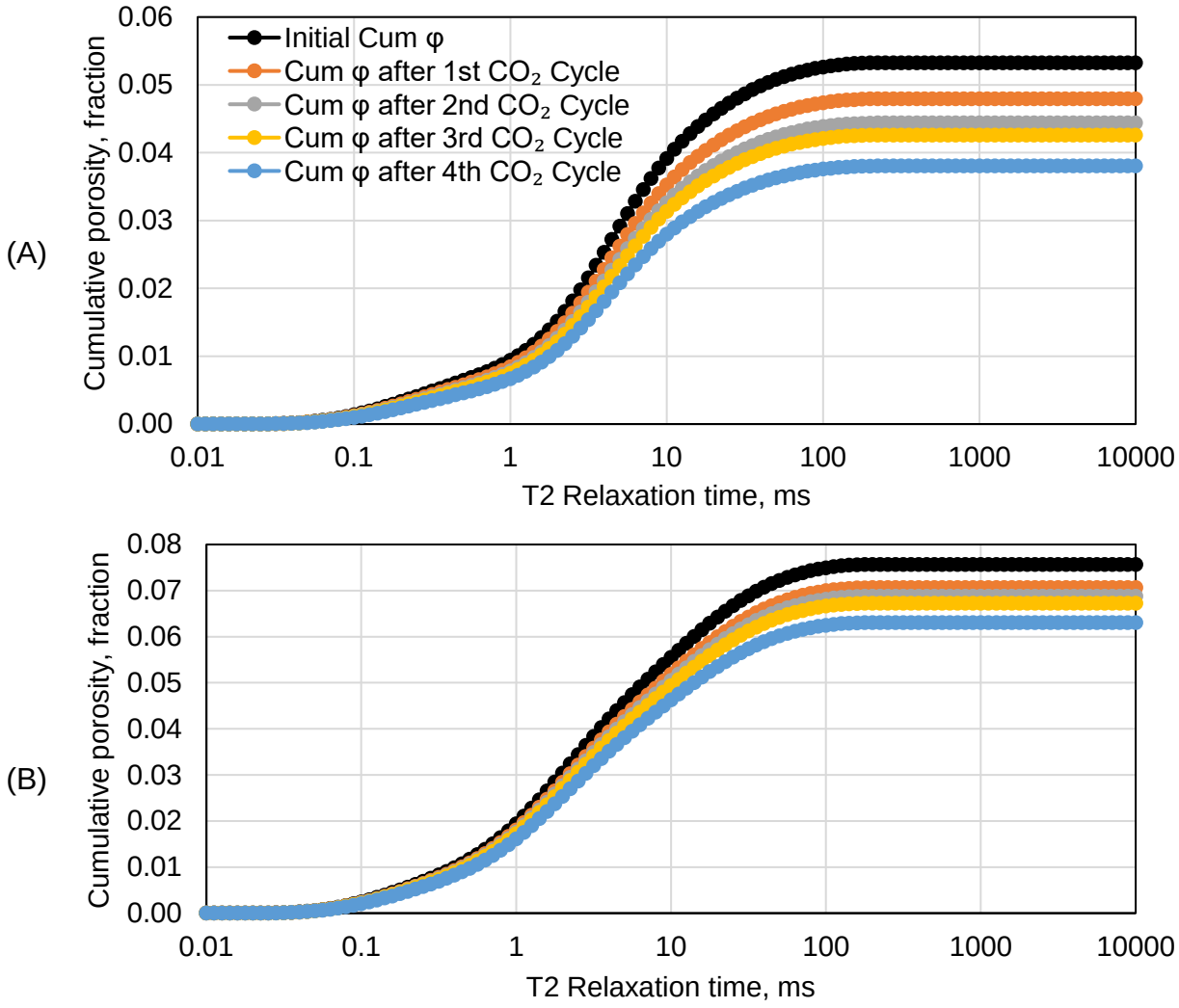

Fig. 6.8 Change in cumulative porosity (Cum φ) after each CO_2 HnP cycle, (A): MB#6*, (B): TF#6*

6.6 Summary

We investigated the different side effects that could result from CO_2 exposure in the Middle Bakken member and the Three Forks formation to optimize the prediction and management of CO_2 EOR and storage operations in unconventional reservoirs. We evaluated the CO_2-induced wettability shift using the contact angle method and the NMR technique to investigate pore size distribution and effective porosity changes before and after CO_2 HnP. The findings can be summarized as follows:

- The contact angle measurements indicate that MB and TF samples were originally strongly oil-wet. CO_2 exposure resulted in a rock hydrophilicity increase. When we used a CO_2/brine oil-saturated-rock system, the tested sample wettability preference became mix-wet to water-wet.
- The NMR results indicated a change in T_2 spectrum before and after CO_2 injection. The curve shifted towards small transverse time values after CO_2 injection, reflecting the PSD changes caused by the interaction of injected CO_2 with some minerals present in the tested cores.
- The microporosity increased in all samples, indicating that new tiny pores can be created after the dissolution of calcite and dolomite into the carbonic acid that forms when CO_2 is in contact with formation brine.
- The increase of the micropores volume after CO_2 HnP indicated that some hydrocarbons were displaced towards the small pores of rock sample, which might complicate their recovery in the future.
- CO_2 chemical reactions with rock minerals can form precipitates that block a portion of the existing pore volume. The effective porosity decreased by 28.7% for the MB sample and 16.6% for the TF sample after four CO_2 HnP cycles.

In the next Chapter, we compare the EOR performance of CO_2 and several hydrocarbon gases. Also, a combination of different gases into one EOR scheme is discussed.

Chapter 7

Novel EOR Scheme Using CO_2 and Hydrocarbon Gases

In this Chapter, we introduce a novel EOR scheme by alternating the type of the injected gas in each cycle to further improve the EOR performance of cyclic gas injection in tight formations. A comparison of the performance of multiple gases is presented based on the MMP, capacity to vaporize oil hydrocarbons, and molecular weight selectivity of each gas. After selecting the most promising gases, we present the results of several HnP injection tests that were performed to compare the oil recovery factor using MB and TF rock samples. Then the results are compared with a HnP test that was performed by combing CO_2 and hydrocarbon gases.

7.1 Background and Motivations

In 2019, 19% of the produced gas from the Bakken was flared due to the inadequate pipeline and production infrastructure, resulting in the emission of about 1.5 million metric tons of CO_2 equivalents [107]. The mutual goals of increasing oil production and reducing the emission of greenhouse gases have led to growing interest in gas EOR, which are epitomized in several pilot-scale injection tests in Bakken. These pilot tests suggested that gas injection can help overcome the injectivity concern in Bakken, and it is a promising solution to enhance oil recovery. The results also showed that gas flooding in densely fractured unconventional reservoirs might result in an early breakthrough, resulting in poor performance [15] . Cyclic injection scheme so-called Huff and Puff (HnP) method can be used to mitigate these issues [16,29]. In a HnP scheme, the gas is injected into the reservoir until reaching a predesigned pressure. After that, the well is shut-in to allow the injected gas to soak for a given period, the system is opened for production [101]. The common HnP procedure consists of repeating the same steps for a set number of cycles using the same gas. Although cyclic injection can help overcome continuous flooding challenges in unconventional reservoirs, the injected gas capacity to mobilize crude oil hydrocarbons decreases tremendously after each cycle. Regardless of the type of gas used, previous simulation and experimental studies that evaluated the HnP technique under realistic reservoir conditions indicated that oil production reaches a plateau at a relatively low cumulative recovery factor after a few cycles [108]. Both results in the literature and our study show that CO_2 capacity to recover oil diminishes after each cycle and becomes less and less efficient.

As presented in Fig. 4.3, the results of multicyclic CO_2 injection showed a tremendous decrease in the CO_2 performance after a few HnP cycles. After the second cycle, only 7% OOIP, on average, was incrementally recovered for samples MB#1 and TF#1, respectively. The oil recovery curve exhibited a plateau after the first two cycles for all the samples we tested. Similar observations can

be found elsewhere in the literature. For example, Adel et al. [31] performed seven successive CO_2 HnP tests using rock samples from the Eagle Ford shale. Fig. 7.1 presents the oil recovery factor for each cycle using an injection pressure of 3500 psi and a soaking time of 10 hours. The results show that 25% of the OOIP was recovered after the first cycle and only 6% after the second cycle. The oil recovery decreased continuously after each cycle to reach less than 1% after the seventh cycle.

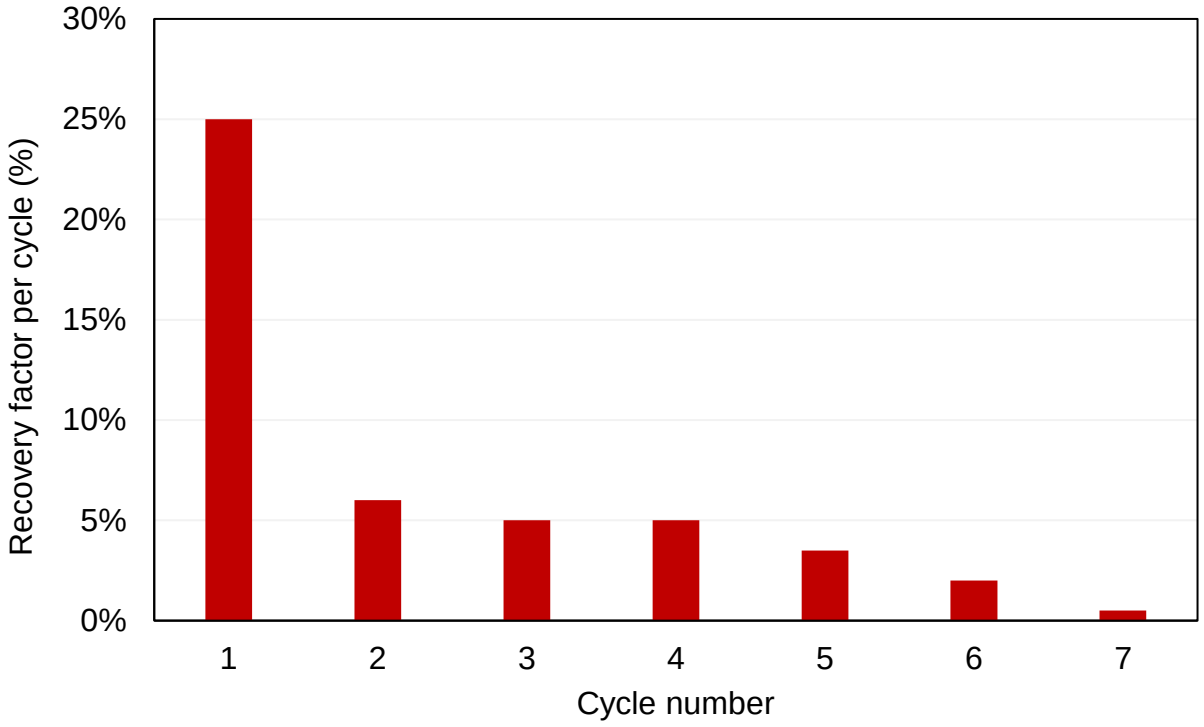

Fig. 7.1 Recovery factor per cycle during CO_2 HnP on Eagle Ford shale core plug at 3500 psi and soaking time of 10 hours ([31])

Menzie [57] and Hawthorne and Miller [106] performed oil gas multi-exposure experiments using different gases to investigate crude oil hydrocarbons mobilization by vaporizing gas drive. The tests were performed by partially filling a chamber with crude oil then the tested gas was injected to reach the desired pressure. After reaching equilibrium, the gas-dominated phase was collected

to measure the dissolved oil, and a new injection cycle took place. Both studies indicated that the equilibrium partitioning mechanism controls oil solubility in the injected gas, and the dissolved oil concentration in the gas-dominated phase diminishes after each sequential exposure. These findings help understand the tremendous decrease of oil mobilization efficiency after each HnP cycle.

Alternating the type of the injected gas after each cycle can be a solution to boost the oil recovery and hydrocarbons mobilization using cyclic injection in tight formations. Although several studies evaluated the performance of different gases separately, combining them into one EOR scheme is seldom discussed. In this work, we used the data available in the literature to compare the EOR performance of CO_2 and multiple gas hydrocarbons (methane, ethane, propane, and produced gas mixture). After determining the most effective gases, several HnP tests were conducted to measure their oil recovery limit. Then we introduced a novel gas EOR scheme to boost oil mobilization and achieve higher recovery factors.

7.2 Evaluation of Different Gases

As stated in the previous sections, the oil recovery mechanisms in tight formations are different than EOR floods in highly permeable reservoirs [15,16,29]. Oil recovery using gas injection in conventional reservoirs relies on viscosity reduction after mixture with the injected gas, oil swelling, and generating a stable oil-gas front [13,57]. For unconventional reservoirs, molecular diffusion driven by the concentration gradient seems to control the oil recovery [35,60,109]; therefore, the success of gas EOR applications relies on the ability of the injected gas to mix with the reservoir fluids, efficiently dissolve the residual oil in the interstitial pores, and displace the hydrocarbons toward the fractures.

7.2.1 Minimum miscibility pressure

In the previous Chapters, we indicated that reaching miscible conditions between the injected gas and the reservoir fluids is crucial for gas EOR applications in tight formations. Different gases can be used for miscible EOR processes, which include CO_2, methane, ethane, propane, and produced rich gas. Hawthorne et al. [110] used the vanishing interfacial tension technique to measure the Minimum Miscibility Pressure (MMP) of those gases with MB and TF crude oil samples. The produced rich gas was simulated by mixing methane, ethane, and propane with a composition of 69.5%, 21%, and 9.5%, respectively. The results presented in Table 9 show that the gases can be arranged based on their MMP values from highest to lowest as follow: methane, CO_2, produced gas, ethane, and propane.

It has been shown that increasing the injection pressure above the MMP can result in an incremental oil recovery [33,101]; therefore, the gases with lower MMP requirements limit the need to over-pressure the reservoir and are expected to have better EOR performances at relatively low reservoir pressures.

Table 9 MMP values of different gases with MB and TF crude oil

Solvent	Methane	CO_2	Ethane	Propane	Produced gas
MMP with MB crude oil (psi)	4238	2521	1330	554	2435
MMP with TF crude oil (psi)	4461	2696	1453	614	2345

7.2.2 Oil solubility in different gases

The capacity of the injected gas to dissolve crude oil is an important parameter that needs to be evaluated in order to compare the EOR performance of different gases. Harthorne and Miller [105] used oil-gas contact experiments to measure Bakken crude oil solubility in the gases listed in Table 9. A visual cell was filled with 10 ml of Bakken crude oil. Then the test gas was injected in the remaining 10 ml through the oil sample at different pressures of 1450 psi (below MMP), 3000 psi

(near MMP), and 5000 psi (above MMP). The system was allowed to equilibrate then the upper gas-dominated phase was collected and analyzed. The steps were repeated until four sequential injections were performed for each gas. Methane and produced gas had the poorest performance at all pressure conditions. At 5000 psi, the oil solubility expressed in mg of dissolved oil per ml of injected gas for methane, produced gas, CO_2, ethane, and propane was 67 mg/ml, 145 mg/ml, 254, mg/ml, 228 mg/ml, and 277 mg/ml, respectively. The results showed that CO_2, ethane, and propane had the highest capacity to dissolve Bakken crude oil at all pressure conditions; therefore, only these three gases will be considered in this work.

7.2.3 Molecular weight selectivity

Another important characteristic of the gas EOR agent is its Molecular Weight Selectivity (MWS), which needs to be considered to design an appropriate EOR scheme for the targeted formation. The MWS can be defined as the bias of the injected gas to dissolve and mobilize hydrocarbons within a specific molecular weight window. Hawthorne et al. [105,111,112] compared the MWS of different gases using gas-oil contact experiments and HnP injection tests. They used oil and rock samples retrieved from a similar location to our rock and oil samples. Fig. 7.2 shows the similarity between the composition of our Bakken oil sample (black line) and the oil sample they used in their experiments (blue line). The same carbon numbers are present in our oil sample with similar compositions.

In a first step, Hawthorne et al. [105] evaluated the viscosity change after sequential exposure to different gases. The test consists of filling a 20 ml cell with 10 ml of Bakken crude oil then injecting the test gas from the bottom of the cell at 5000 psi and 230°F. The fresh oil viscosity was 2.2 cp, and the change of the Bakken crude oil viscosity after contact with the gases selected in this study is presented in Fig. 7.3.

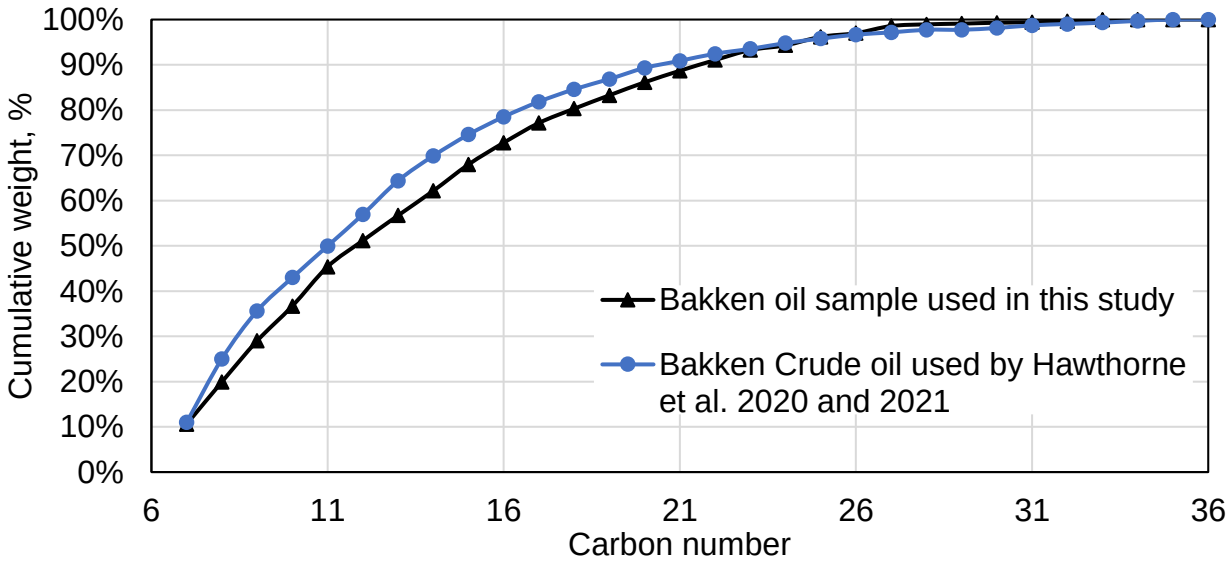

Fig. 7.2 Oil composition of the crude oil sample used in our work (black line) and the oil samples used by Hawthorne et al. 2020 and 2021([105,111]) to study the MWS of different gases.

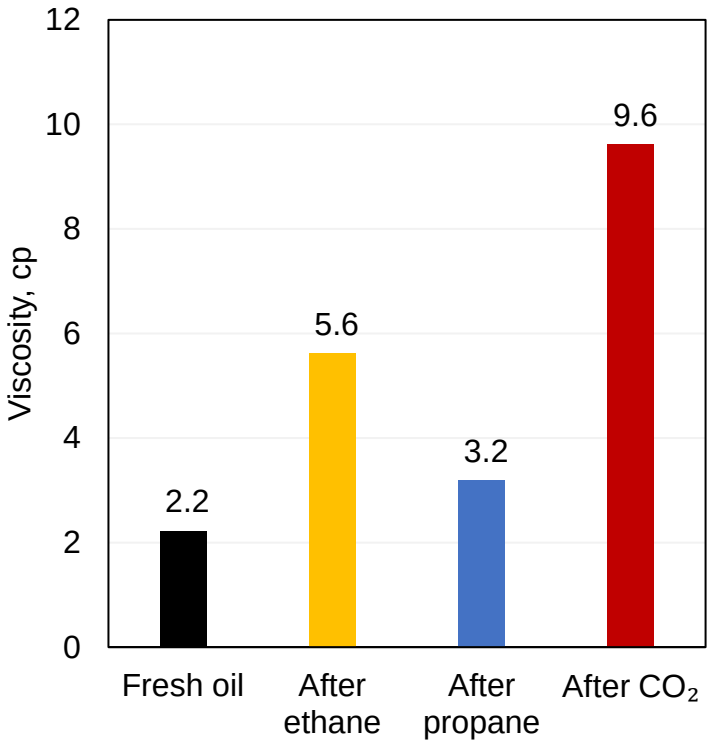

Fig. 7.3 Bakken oil viscosity change after exposure to CO_2, ethane, and propane [105]

Changes in the oil viscosity after contact with the injected gas are directly related to the changes in hydrocarbon distribution. The increase of oil viscosity to 9.6 cp after CO_2 injection reflects the high selectivity of CO_2 towards Light Weight Hydrocarbons (LWH). The oil that was exposed to ethane had a viscosity of 5.6 cp, which indicates that ethane has a larger MWS window than CO_2 that includes LWC and Medium Weight Components (MWC). Also, the results suggest that propane has the most uniform MWS. The oil viscosity after propane injection was 3.2 cp which is the closest value to the original viscosity of the Bakken crude oil.

In a recent study, Hawthorn et al. [111] performed a series of HnP tests using MB rock samples and analyzed the composition of the displaced oil using Gas Chromatography (GC). Fig. 7.4 depicts the recoveries of C8, C16, C22, and C28 after CO_2, ethane, and propane HnP injection tests using an injection pressure of 5000 psi, temperature of 230°F, and 24 hours of soaking. The results of these tests confirm the findings of oil viscosity change (Fig. 7.3). CO_2 recovered 98.0, 66.7, and 13.0 % of the C8, C16, and C22 fractions in the crude oil, respectively. Also, the GC results show that the oil displaced by CO_2 didn't contain any C28 faction, which confirms the CO_2 bias against higher molecular weight hydrocarbons. After ethane injection, 96.0, 85.7, 66.8, and 27.6% of the C8, C16, C22, and C28 fractions were recovered from the rock sample, respectively. As expected, propane had the most uniform recovery and displaced 95.0, 75.0, 60.0, and 40.0% of the C8, C16, C22, and C28 fractions, respectively.

In conclusion, CO_2 recovered the highest amount of LWH and couldn't mobilize Heavy Weight Hydrocarbons (HWH). Ethane had the best performance in recovering MWH, and the MWS of propane covers the widest range of hydrocarbons.

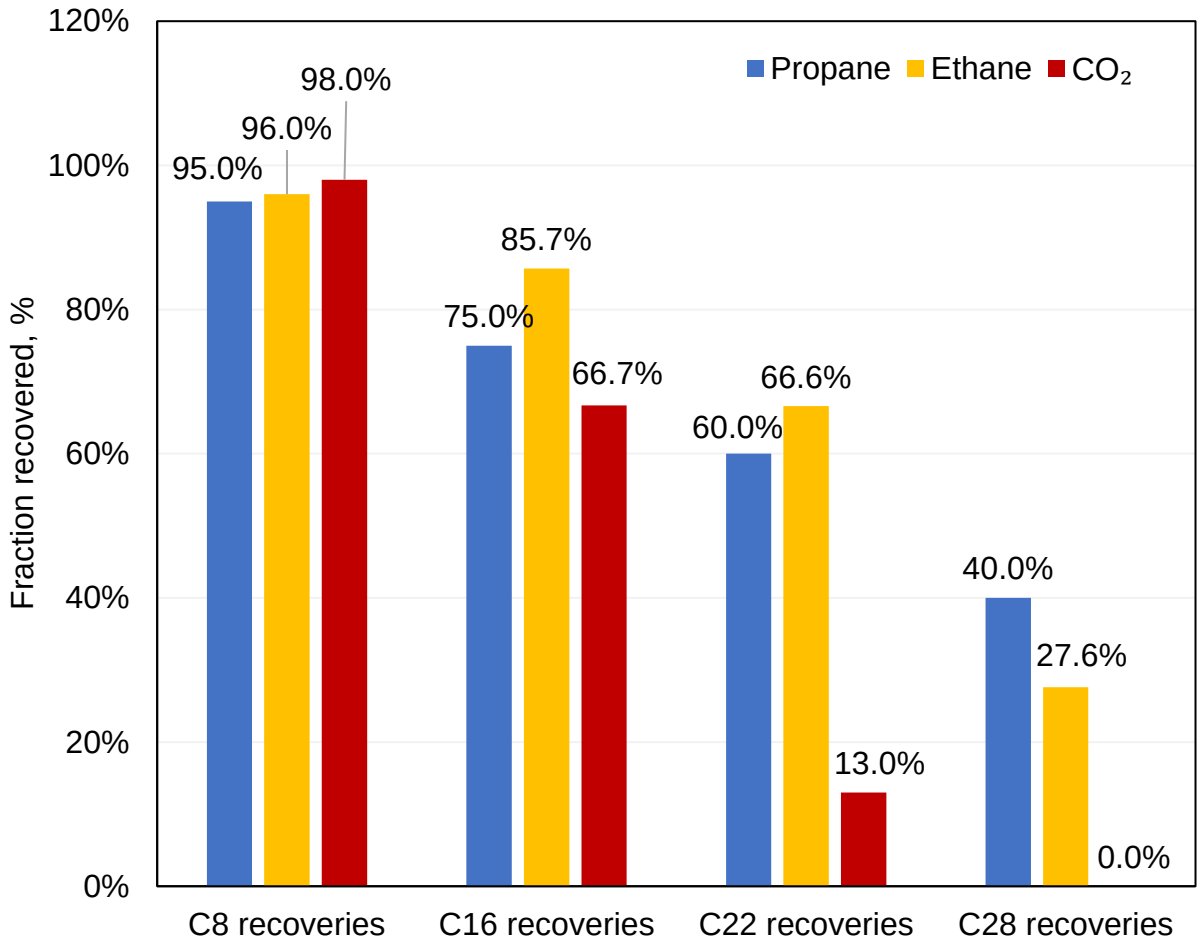

Fig. 7.4 Recoveries of C8, C16, C22, and C28 from MB rock samples after 24 h exposure to CO_2, ethane, and propane ([111])

7.3 Comparing EOR Performance of CO_2, Ethane, and Propane

As discussed in the previous sections of this Chapter, CO_2, ethane, and propane are the most promising gases for EOR in tight formations. Hawthorne et al. [111] compared the oil recovery performance of these gases using cylindrical MB rods (0.44 in diameter * 1.75 in length) and LBS rock cuttings (see Fig. 7.5). They performed HnP tests at different pressures, including 1500, 2500, and 5000 psi. In this study, we focus on comparing the EOR performance above MMP. Fig. 7.6

presents the oil recovery factors from the MB rods after cyclic injection of CO_2, ethane, and propane at 5000 psi.

Fig. 7.5 Geometries of the rock samples used by Hawthorn et al. [111] for gas HnP experiments, 0.44 in diameter * 1.75 in length rods to represent the MB (left) and 0.04-0.13 in cuttings for the LBS (right)

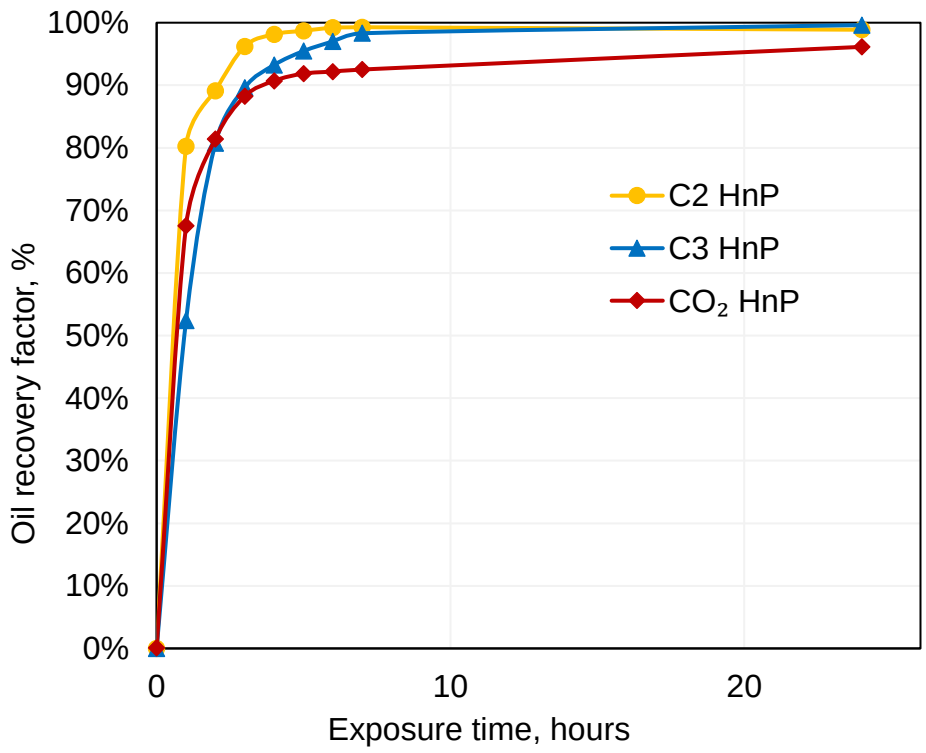

Fig. 7.6 Oil recovery from MB rods after CO_2 (red line), ethane (yellow line), and propane (blue line) HnP at 5000 psi and 230°F

The reported results didn't clearly display the difference between the tested gases. In fact, the usage of very small rock samples resulted in recovering over 90% of the OOIP after two to three hours of soaking for all the gases. Therefore, we used larger MB and TF samples to compare the oil recovery of each gas using multicyclic injection at typical reservoir conditions. Four twin MB and four twin TF rock samples (1.5 in diameter * 4 in length) were selected for this study. The permeability and porosity of the MB and TF samples were 0.009 mD, 6.4%, 0.145 mD, and 8.4%, respectively. After cleaning and saturating the rock samples, we first performed two CO_2 HnP cycles using an injection pressure of 4000 psi, a temperature of 213 °F, and a soaking time of 24 hours. As expected (see section 7.1), the results illustrated in Fig. 7.7 show that the EOR performance of all the tested gases diminishes after each cycle and the oil recovery reaches a

plateau after a few HnP cycles. The oil recovery after the second cycle of CO_2 injection was 32.3% and 38.1% for the TF and MB samples, respectively. However, the ultimate oil recovery factor after six HnP cycles was 38.3% and 44.7% for the TF and MB samples, respectively. For ethane and propane injection, the oil recovery factor after the second cycle was 34.0% and 38.9% for the MB samples and 41.5% and 48.1% for the TF samples, respectively. Similar to CO_2 HnP, the incremental oil recovery from the second to the sixth cycle of ethane and propane injections was between 6 and 8% of the OOIP for the MB and TF samples.

To overcome this limitation, we proposed an EOR scheme that consists of alternating the test gas based on the MWS. We first injected CO_2 for its preference to dissolve and mobilize the light hydrocarbons. Then, ethane injection was performed to efficiently mobilize the medium-weight components, followed by propane injection to displace the remaining heavy hydrocarbons. After cleaning and saturating the rock samples, we first performed two HnP cycles using CO_2, followed by two ethane and propane cycles. All the tests were performed at similar experimental conditions of 4000 psi, 213°F, and 24 hours of soaking.

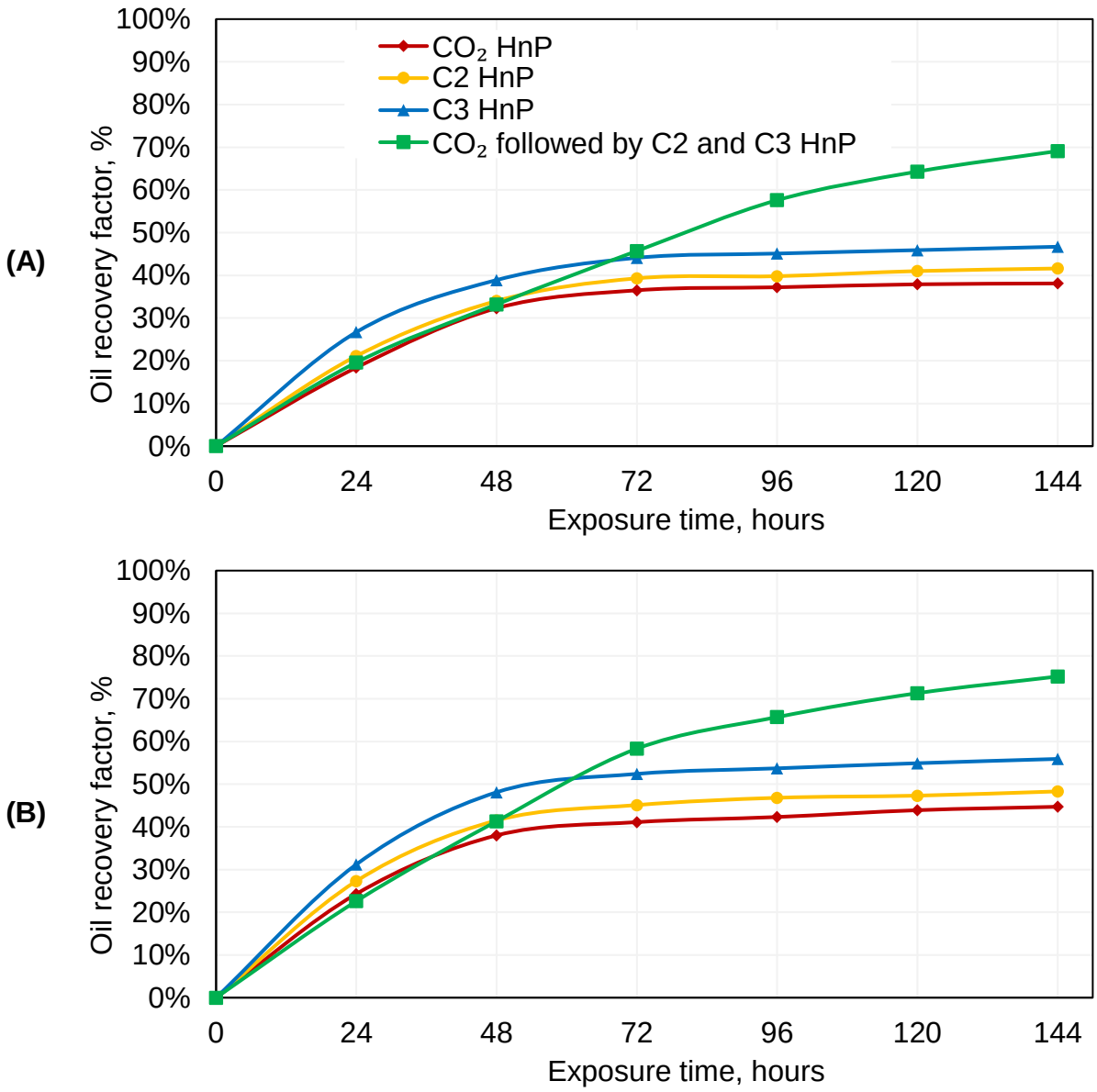

Fig. 7.7 Oil recoveries from MB samples (A) and TF samples (B) using CO_2, ethane and propane

The green line curves in Fig. 7.7 (A) and (B) represent the oil recovery using the alternating gas injection method in MB and TF samples, respectively. Alternating the injection gas resulted in an incremental oil recovery of 31.2, 27.5, and 22.4 % of the OOIP from the MB sample compared to multicyclic injection of CO_2, ethane, and propane, respectively. Similarly, 24.4, 20.8, and 13.2% of the OOIP were incrementally recovered from the TF sample compared to CO_2, ethane, and

propane HnP, respectively. The composition of the oil in the interstitial pores changes after gas injection; therefore, alternating the type of the injected gas can help mobilize most of the hydrocarbons in place better than re-injecting the same gas for multiple cycles.

7.4 Summary

In this Chapter, we compared the EOR performance of CO_2 and gas hydrocarbons then evaluated the oil recoveries using multicyclic and alternating gas injection schemes. The findings can be summarized as follow:

- In cyclic gas injection, the capacity of the injected gas capacity to mobilize crude oil hydrocarbons decreases tremendously after each cycle. The equilibrium partitioning mechanism controls oil solubility in the injected gas, and the dissolved oil concentration in the gas-dominated phase diminishes after each sequential exposure.
- The ability of the injected gas to reach the miscibility with the reservoir fluids, efficiently dissolve the residual oil in the interstitial pores, and displace the hydrocarbons toward the fractures are important factors for the success of gas EOR applications in unconventional reservoirs.
- CO_2, ethane, and propane had the lowest MMP with Bakken crude oil compared to methane and produced rich gas mixture. Also, Oil-gas contact experiments showed that CO_2, ethane, and propane dissolved the highest volumes of hydrocarbons from Bakken oil.
- The GC analysis of the oil displaced using CO_2, ethane, and propane suggested that CO_2 can efficiently displace the light hydrocarbons, while ethane has a better performance in mobilizing the medium weight components, and propane has the most uniform recovery and the best performance in recovering the heavy hydrocarbons.

- Multicyclic injection tests in MB and TF rock samples showed that using an injection pressure of 4000 psi and a soaking time of 24 hours, all the three gases had similar EOR performance.
- Each gas can dissolve and mobilize hydrocarbons within a specific molecular weight window; therefore, alternating the type of the injected gas based on their MWS instead of multicyclic injection of the same gas led to increasing the oil recovery.

Chapter 8

Conclusions and Recommendations

The main conclusions driven from this work are summarizedin the first section of this Chapter and the second section presents some of the future work that is recommended as continuation of this study.

8.1 Conclusions

In this study, we evaluated the performance of CO_2 EOR in unconventional reservoirs. We first studied the influence of HnP injection parameters on oil recovery using representative MB and TF rock and fluid samples. Then, we investigated the gap between the results of CO_2 EOR field tests and the antecedent research studies. We conducted an extensive parametric study to examine and understand the effects of a series of key parameters, such as sample size, water presence, fracture size, and CO_2 injection scheme, on CO_2 EOR in unconventional reservoirs. After that, we studied the potential side effects of CO_2 injection in tight formations and evaluated the possible CO_2-induced alteration of reservoir properties. The effect of CO_2 injection on rock wettability, pore size

distribution, and effective porosity was assessed and discussed. Finally, we compared the EOR performance of CO_2 and different hydrocarbon gases to determine the most promising gases. Then the selected gases were combined into one EOR scheme to overcome the oil recovery limits of multicyclic gas injection.

The main findings of this work can be summarized as follow:

- Increasing the injection pressure above MMP can help recover more oil from tight rock samples and the results of multicyclic CO_2 injection indicate that the CO_2 performance decreases drastically after the second HnP cycle.
- The size of the tested samples has an important impact on EOR experiments. The selection of smaller samples can lead to overestimating the potential of CO_2 EOR and oil recovery. We recommend using samples that are large enough to represent fluid flow in the reservoir and represent its heterogeneity.
- The results suggest that both viscous forces and molecular diffusion control the oil recovery. The pressure gradient initially pushes CO_2 into larger pores and promotes its penetration, then diffusion controls oil extraction toward the bulk CO_2 volume surrounding the rock.
- Water accumulated in the fracture can impede the contact between CO_2 and the reservoir rock, which results in reduced oil recovery.
- Submerging a core sample in a relatively large CO_2 volume can result in overestimating the oil recovery. The ratio of the volume surrounding the sample to the sample surface areas needs to be considered carefully and should represent reservoir conditions for cyclic injection experiments in tight samples.

- Using fractured tight formation samples, cyclic injection outperformed the flooding process, which was limited by low sweep efficiency and early breakthrough.
- The contact angle measurements indicate that MB and TF samples were originally strongly oil-wet. CO_2 exposure resulted in a rock hydrophilicity increase. When we used a CO_2/oil/brine system, the tested sample wettability preference became mix-wet to water-wet.
- The NMR results indicated a change in T_2 spectrum before and after CO_2 injection. The curve shifted towards small transverse time values after CO_2 injection, reflecting the PSD changes caused by the interaction of injected CO_2 with some minerals present in the tested cores.
- The microporosity increased in all samples, indicating that new tiny pores can be created after the dissolution of calcite and dolomite into the carbonic acid when CO_2 is in contact with formation brine.
- The increase of the micropore volumes after CO_2 HnP indicated that some hydrocarbons were displaced towards the small pores of rock sample, which might complicate their recovery in the future.
- CO_2 chemical reactions with rock minerals can form precipitates that block a portion of the existing pore volume, which might result in decreasing the effective porosity after CO_2 exposure.
- In cyclic gas injection, the capacity of the injected gas capacity to mobilize crude oil hydrocarbons decreases tremendously after each cycle. The equilibrium partitioning mechanism controls oil solubility in the injected gas, and the dissolved oil concentration in the gas-dominated phase diminishes after each sequential exposure.

- The ability of the injected gas to reach the miscibility with the reservoir fluids, efficiently dissolving the residual oil in the interstitial pores, and displacing the hydrocarbons toward the fractures are important factors for the success of gas EOR applications in unconventional reservoirs.
- CO_2, ethane, and propane had the lowest MMP with Bakken crude oil compared to methane and produced rich gas mixture. Also, Oil-gas contact experiments showed that CO_2, ethane, and propane dissolved the highest volumes of hydrocarbons from Bakken oil.
- The GC analysis of the oil displaced using CO_2, ethane, and propane suggested that CO_2 can efficiently displace the light hydrocarbons, while ethane has a better performance in mobilizing the medium weight components, and propane has the most uniform recovery and the best performance in recovering the heavy hydrocarbons.
- Each gas can dissolve and mobilize hydrocarbons within a specific molecular weight window; therefore, alternating the type of the injected gas based on their MWS instead of multicyclic injection of the same gas led to increasing the oil recovery.

8.2 Recommendations

Below are some recommendations for future gas EOR related work in unconventional reservoirs:

- Coupling the gas injection experiments with CT-scanner or NMR measurements can help understand gas penetration into the rock matrix.
- The CO_2-induced pore structure change can be further investigated using SEM and CT-scan images comparison before and after CO_2 exposure.

- The experimental results can be used to calibrate analytical models and numerical simulations for a better prediction performance of EOR applications in tight formations in the future.
- A mixture of different gases such as CO_2 and hydrocarbon gases can be studied and compared to pure gas injection results. We recommend measuring the MMP of different mixtures and analyze the produced oil composition using different gas mixtures.

Appendix

Compositional Analysis of Bakken Bottomhole Sample

Component	MW	Flashed Gas		Flashed Liquid		Reservoir Fluid	
	g/mol	wt%	mole %	wt%	mole %	wt%	mole %
CO_2	44.01	0.55	0.39	0.00	0.00	0.13	0.24
H_2S	34.08	0.00	0.00	0.00	0.00	0.00	0.00
N_2	28.01	2.88	3.19	0.00	0.00	0.65	1.98
C_1	16.04	23.35	45.26	0.00	0.00	5.29	28.14
C_2	30.07	20.31	21.01	0.00	0.00	4.60	13.04
C_3	44.10	22.86	16.13	0.27	1.06	5.39	10.41
i-C_4	58.12	3.51	1.88	0.14	0.42	0.90	1.32
n-C_4	58.12	12.33	6.60	0.86	2.57	3.46	5.07
i-C_5	72.15	3.01	1.30	0.63	1.52	1.17	1.38
n-C_5	72.15	4.48	1.93	1.31	3.15	2.03	2.39
C_6	84.00	3.15	1.17	2.88	5.96	2.94	2.98
Mcyclo-C_5	84.16	0.72	0.27	1.04	2.15	0.97	0.98
Benzene	78.11	0.07	0.03	0.09	0.20	0.08	0.09
Cyclo-C_6	84.16	0.20	0.07	0.39	0.81	0.35	0.35
C_7	100.21	1.43	0.45	4.70	8.15	3.96	3.37
Mcyclo-C_6	98.19	0.22	0.07	1.06	1.88	0.87	0.75
Toluene	92.14	0.08	0.03	0.33	0.62	0.27	0.25
C_8	114.23	0.55	0.15	5.97	9.04	4.74	3.54
C_2-Benzene	106.17	0.02	0.01	0.26	0.43	0.21	0.16
m&p-Xylene	106.17	0.03	0.01	0.61	1.00	0.48	0.38
o-Xylene	106.17	0.01	0.00	0.20	0.33	0.16	0.13
C_9	128.26	0.18	0.04	4.73	6.41	3.70	2.46
C_{10}	134.00	0.05	0.01	5.80	7.52	4.50	2.86
C_{11}	147.00	0.01	0.00	4.89	5.78	3.79	2.19
C_{12}	161.00	0.00	0.00	4.68	5.05	3.62	1.92

C_{13}	175.00	0.00	0.00	4.59	4.56	3.55	1.73
C_{14}	190.00	0.00	0.00	3.98	3.64	3.08	1.38
C_{15}	206.00	0.00	0.00	3.96	3.34	3.06	1.27
C_{16}	222.00	0.00	0.00	3.53	2.76	2.73	1.05
C_{17}	237.00	0.00	0.00	3.30	2.42	2.55	0.92
C_{18}	251.00	0.00	0.00	3.10	2.15	2.40	0.81
C_{19}	263.00	0.00	0.00	2.99	1.98	2.31	0.75
C_{20}	275.00	0.00	0.00	2.67	1.69	2.07	0.64
C_{21}	291.00	0.00	0.00	2.51	1.50	1.94	0.57
C_{22}	305.00	0.00	0.00	2.32	1.32	1.80	0.50
C_{23}	318.00	0.00	0.00	2.14	1.17	1.66	0.44
C_{24}	331.00	0.00	0.00	1.98	1.04	1.53	0.39
C_{25}	345.00	0.00	0.00	1.86	0.94	1.44	0.36
C_{26}	359.00	0.00	0.00	1.70	0.82	1.31	0.31
C_{27}	374.00	0.00	0.00	1.67	0.78	1.29	0.29
C_{28}	388.00	0.00	0.00	1.53	0.69	1.18	0.26
C_{29}	402.00	0.00	0.00	1.43	0.62	1.11	0.23
C_{30+}	532.59	0.00	0.00	13.90	4.53	10.73	1.72

Single Stage Flash of Bottomhole Sample Standard Conditions (15 psia and 60.0 °F)

GOR (SCF/STB)	STO API Gravity (API)	Measured STO Density (g/cm^3)	Vapor Gravity
1037	39.3	0.828	1.074

Gas Chromatogram of Flashed Liquid

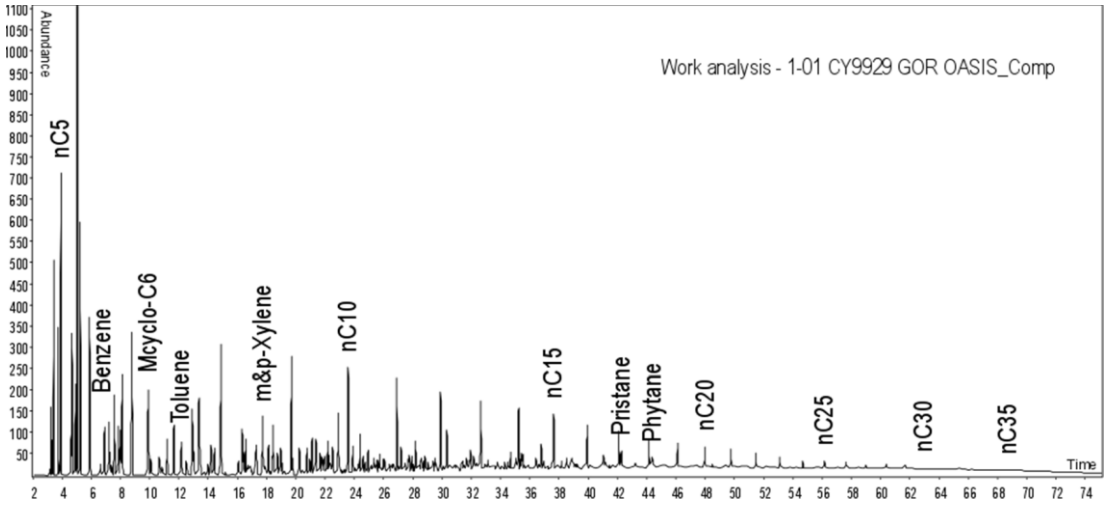

Fluid Properties at Reservoir Conditions

Density	0.668	g/cm^3
Viscosity	0.29	cP
Formation Volume Factor (B_o)	1.609	vol/vol
Oil Compressibility Coefficient (C_o)	12.425	10^{-6}/psia

Fluid Properties at Saturation Conditions

Bubble Point Pressure	2198	psia
Density	0.623	g/cm^3
Viscosity[1]	0.19	cP
Formation Volume Factor (B_o)	1.724	vol/vol
Oil Compressibility (C_o)	19.132	10-6/psia
Solution GOR	1184	SCF/STB

Stock Tank Fluid Properties

Density	0.828	g/cm3
API Gravity	39.3	API

References

[1] U.S. Energy Information Administration. How much shale (tight) oil is produced in the United States? Freq Asked Quest 2019. https://www.eia.gov/tools/faqs/faq.php?id=847&t=6 (accessed May 18, 2020).

[2] Flannery J. Integrated analysis of the Bakken petroleum system, US Williston Basin 2006.

[3] Kurtoglu B. Integrated Reservoir Characterization and Modeling in Support of Enhanced Oil Recovery for Bakken. Colorado School of Mines, 2013.

[4] Wang L, Yu W. Mechanistic simulation study of gas Puff and Huff process for Bakken tight oil fractured reservoir. Fuel 2019;239:1179–93. https://doi.org/https://doi.org/10.1016/j.fuel.2018.11.119.

[5] Hejazi SH, Assef Y, Tavallali M, Popli A. Cyclic CO2-EOR in the Bakken Formation: Variable cycle sizes and coupled reservoir response effects. Fuel 2017;210:758–67. https://doi.org/10.1016/j.fuel.2017.08.084.

[6] Yang J, Wang X, Peng X, Du Z, Zeng F. Experimental studies on CO2 foam performance in the tight cores. J Pet Sci Eng 2019;175:1136–49. https://doi.org/10.1016/j.petrol.2019.01.029.

[7] Smith SA, Kurz B, Sorensen J, Beddoe C, Mibeck B, Azenkeng A, et al. Laboratory Investigation of CO2 Injectivity and Adsorption Potential Within the Bakken Formation. SPE/AAPG/SEG Unconv Resour Technol Conf 2019. https://doi.org/10.15530/urtec-2019-967.

[8] Wang L, Yu W. Mechanistic simulation study of gas Puff and Huff process for Bakken tight oil fractured reservoir. Fuel 2019;239:1179–93. https://doi.org/10.1016/j.fuel.2018.11.119.

[9] Yu W, Lashgari HR, Wu K, Sepehrnoori K. CO2 injection for enhanced oil recovery in Bakken tight oil reservoirs. Fuel 2015;159:354–63. https://doi.org/10.1016/j.fuel.2015.06.092.

[10] Dechongkit P, Prasad M. Recovery Factor and Reserves Estimation in the Bakken Petroleum System (Analysis of the Antelope, Sanish and Parshall fields). Can Unconv Resour Conf 2011:15. https://doi.org/10.2118/149471-MS.

[11] Clark AJ. Determination of Recovery Factor in the Bakken Formation, Mountrail County, ND. SPE Annu Tech Conf Exhib 2009. https://doi.org/10.2118/133719-STU.

[12] Tang X, Zhang J, Wang X, Yu B, Ding W, Xiong J, et al. Shale characteristics in the southeastern Ordos Basin, China: Implications for hydrocarbon accumulation conditions and the potential of continental shales. Int J Coal Geol 2014;128:32–46.

[13] Aryana SA, Barclay C, Liu S. North Cross Devonian Unit - A Mature Continuous CO2 Flood Beyond 200% HCPV Injection. SPE Annu Tech Conf Exhib 2014. https://doi.org/10.2118/170653-MS.

[14] Todd HB, Evans JG. Improved Oil Recovery IOR Pilot Projects in the Bakken Formation. SPE Low Perm Symp 2016. https://doi.org/10.2118/180270-MS.
[15] Alfarge D, Wei M, Bai B, Alsaba M. Lessons learned from IOR pilots in Bakken formation by using numerical simulation. J Pet Sci Eng 2018;171:1–15. https://doi.org/10.1016/j.petrol.2018.07.025.
[16] Wan T, Yu Y, Sheng JJ. Experimental and numerical study of the EOR potential in liquid-rich shales by cyclic gas injection. J Unconv Oil Gas Resour 2015;12:56–67. https://doi.org/10.1016/j.juogr.2015.08.004.
[17] Alfarge D, Wei M, Bai B. Data analysis for CO2-EOR in shale-oil reservoirs based on a laboratory database. J Pet Sci Eng 2018;162:697–711. https://doi.org/10.1016/j.petrol.2017.10.087.
[18] Lashgari HR, Sun A, Zhang T, Pope GA, Lake LW. Evaluation of carbon dioxide storage and miscible gas EOR in shale oil reservoirs. Fuel 2019;241:1223–35. https://doi.org/10.1016/j.fuel.2018.11.076.
[19] Pankaj P, Mukisa H, Solovyeva I, Xue H. Enhanced Oil Recovery in Eagle Ford: Opportunities Using Huff-n-Puff Technique in Unconventional Reservoirs. SPE Liq Basins Conf - North Am 2018. https://doi.org/10.2118/191780-MS.
[20] Jia B, Tsau JS, Barati R. A review of the current progress of CO2 injection EOR and carbon storage in shale oil reservoirs. Fuel 2019;236:404–27. https://doi.org/10.1016/j.fuel.2018.08.103.
[21] Mba K, Prasad M. Mineralogy and its contribution to anisotropy and kerogen stiffness variations with maturity in the Bakken Shales. SEG Annu Meet 2010. https://doi.org/doi:10.1190/1.3513383.
[22] Nesheim TO. Examination of downward hydrocarbon charge within the Bakken-Three Forks petroleum system – Williston Basin, North America. Mar Pet Geol 2019;104:346–60. https://doi.org/10.1016/j.marpetgeo.2019.03.016.
[23] Gaswirth SB, Marra KR. U.S. Geological Survey 2013 assessment of undiscovered resources in the Bakken and Three Forks Formations of the U.S. Williston basin province. Am Assoc Pet Geol Bull 2015;99:639–60. https://doi.org/10.1306/08131414051.
[24] U.S. Energy Information Administration. Maps: Oil and Gas Exploration, Resources, and Production - Energy Information Administration 2011. https://www.eia.gov/maps/maps.htm (accessed February 16, 2022).
[25] U.S. Energy Information Administration. North Dakota Field Production of Crude Oil 2015. http://www.eia.gov/dnav/pet/hist/LeafHandler.ashx?n=PET&s=MCRFPND1&f=M (accessed February 16, 2022).
[26] Sorensen J, Hawthorne SB, Jin L, A.Torres J, Bosshart NW, Azzolina NA, et al. Bakken CO2 Storage and Enhanced Recovery Program. 2015.
[27] Irena Agalliu;Curtis Smith;Mohammad, Tavallali;Min, Rao; Stephen, Adams;Aube, Montero; Leslie, Levesque;Cody, Coughlin;Dennis, Yang;Shawn G. CO2 EOR Potential in North Dakota. 2016.
[28] Gamadi TD, Sheng JJ, Soliman MY, Menouar H, Watson MC, Emadibaladehi H. An Experimental Study of Cyclic CO2 Injection to Improve Shale Oil Recovery. SPE Improv Oil Recover Symp 2014. https://doi.org/10.2118/169142-MS.
[29] Song C, Yang D. Experimental and numerical evaluation of CO2 huff-n-puff processes in Bakken formation. Fuel 2017;190:145–62. https://doi.org/10.1016/j.fuel.2016.11.041.

[30] Tovar FD, Barrufet MA, Schechter DS. Gas Injection for EOR in Organic Rich Shale. Part I: Operational Philosophy. SPE Improv Oil Recover Conf 2018:25. https://doi.org/10.2118/190323-MS.
[31] Adel IA, Tovar FD, Zhang F, Schechter DS. The Impact of MMP on Recovery Factor During CO2 – EOR in Unconventional Liquid Reservoirs. SPE Annu Tech Conf Exhib 2018:D021S022R004. https://doi.org/10.2118/191752-MS.
[32] Tovar FD, Eide O, Graue A, Schechter DS. Experimental Investigation of Enhanced Recovery in Unconventional Liquid Reservoirs using CO2: A Look Ahead to the Future of Unconventional EOR. SPE Unconv Resour Conf 2014. https://doi.org/10.2118/169022-MS.
[33] Tovar FD, Barrufet MA, Schechter DS. Gas Injection for EOR in Organic Rich Shales. Part II: Mechanisms of Recovery. SPE/AAPG/SEG Unconv Resour Technol Conf 2018. https://doi.org/10.15530/URTEC-2018-2903026.
[34] Alfarge D, Wei M, Bai B. CO2-EOR mechanisms in huff-n-puff operations in shale oil reservoirs based on history matching results. Fuel 2018;226:112–20. https://doi.org/https://doi.org/10.1016/j.fuel.2018.04.012.
[35] Alfarge D, Wei M, Bai B, Almansour A. Effect of Molecular-Diffusion Mechanism on CO2 Huff-n-Puff Process in Shale-Oil Reservoirs. SPE Kingdom Saudi Arab Annu Tech Symp Exhib 2017. https://doi.org/10.2118/188003-MS.
[36] Zhang F, Adel IA, Saputra IWR, Chen W, Schechter DS. Numerical Investigation to Understand the Mechanisms of CO2 EOR in Unconventional Liquid Reservoirs. SPE Annu Tech Conf Exhib 2019. https://doi.org/10.2118/196019-MS.
[37] Hawthorne SB, Gorecki CD, Sorensen JA, Steadman EN, Harju JA, Melzer S. Hydrocarbon Mobilization Mechanisms from Upper, Middle, and Lower Bakken Reservoir Rocks Exposed to CO2. SPE Unconv Resour Conf Canada 2013. https://doi.org/10.2118/167200-MS.
[38] Jin L, Hawthorne S, Sorensen J, Pekot L, Kurz B, Smith S, et al. Advancing CO2 enhanced oil recovery and storage in unconventional oil play—Experimental studies on Bakken shales. Appl Energy 2017;208:171–83. https://doi.org/10.1016/j.apenergy.2017.10.054.
[39] Jin L, Sorensen JA, Hawthorne SB, Smith SA, Bosshart NW, Burton-Kelly ME, et al. Improving Oil Transportability Using CO2 in the Bakken System – A Laboratory Investigation. SPE Int Conf Exhib Form Damage Control 2016. https://doi.org/10.2118/178948-MS.
[40] Song C, Yang D. Performance Evaluation of CO2 Huff-n-puff Processes in Tight Oil Formations. SPE Unconv Resour Conf Canada 2013:SPE-167217-MS. https://doi.org/10.2118/167217-MS.
[41] Chen K. Evaluation of EOR Potential By Gas and Water Flooding in Shale Oil Reservoirs. Texas Tech University, 2013.
[42] Pu W, Hoffman T. EOS Modeling and Reservoir Simulation Study of Bakken Gas Injection Improved Oil Recovery in the Elm Coulee Field, Montana. Proc. 2nd Unconv. Resour. Technol. Conf., Tulsa, OK, USA: American Association of Petroleum Geologists; 2014. https://doi.org/10.15530/urtec-2014-1922538.
[43] Fai-Yengo VA, Rahnema H, Alfi M. Impact of Light Component Stripping During CO2 Injection in Bakken Formation. Proc. 2nd Unconv. Resour. Technol. Conf., Tulsa, OK, USA: American Association of Petroleum Geologists; 2014. https://doi.org/10.15530/urtec-

2014-1922932.
[44] Chen C, Balhoff M, Mohanty KK. Effect of Reservoir Heterogeneity on Primary Recovery and CO2 Huff 'n' Puff Recovery in Shale-Oil Reservoirs. SPE Reserv Eval Eng 2014;17:404–13. https://doi.org/10.2118/164553-PA.
[45] Sanchez-Rivera D. Reservoir simulation and optimization of CO2 Huff-and-Puff operations in the Bakken Shale. The University of Texas at Austin, 2014.
[46] Yu W, Lashgari H, Sepehrnoori K. Simulation Study of CO2 Huff-n-Puff Process in Bakken Tight Oil Reservoirs. SPE West. North Am. Rocky Mt., vol. 2, Denver, Colorado: SPE; 2014. https://doi.org/10.2118/169575-MS.
[47] Yu W, Lashgari HR, Wu K, Sepehrnoori K. CO2 injection for enhanced oil recovery in Bakken tight oil reservoirs. Fuel 2015;159:354–63. https://doi.org/10.1016/j.fuel.2015.06.092.
[48] Sun J, Zou A, Sotelo E, Schechter D. Numerical simulation of CO2 huff-n-puff in complex fracture networks of unconventional liquid reservoirs. J Nat Gas Sci Eng 2016;31:481–92. https://doi.org/10.1016/j.jngse.2016.03.032.
[49] Alharthy N, Teklu T, Kazemi H, Graves R, Hawthorne S, Braunberger J, et al. Enhanced oil recovery in liquid-rich shale reservoirs: Laboratory to field. SPE Reserv Eval Eng 2018;21:137–59. https://doi.org/10.2118/175034-pa.
[50] Yu W, Lashgari H, Sepehrnoori K. Simulation Study of CO2 Huff-n-Puff Process in Bakken Tight Oil Reservoirs. SPE West North Am Rocky Mt Jt Meet 2014:16. https://doi.org/10.2118/169575-MS.
[51] Kim TH, Cho J, Lee KS. Modeling of CO2 Flooding and Huff and Puff Considering Molecular Diffusion and Stress-Dependent Deformation in Tight Oil Reservoir. SPE Eur Featur 79th EAGE Conf Exhib 2017. https://doi.org/10.2118/185783-MS.
[52] Song C, Yang D. Performance Evaluation of CO2 Huff-n-Puff Processes in Tight Oil Formations. SPE Unconv Resour Conf Canada 2013. https://doi.org/10.2118/167217-MS.
[53] Joslin K, Abraham AM, Thaker T, Pathak V, Kumar A. Viability of EOR Processes in the Bakken Under Geological and Economic Uncertainty. SPE Canada Unconv Resour Conf 2018. https://doi.org/10.2118/189779-MS.
[54] McPhee C, Reed J, Zubizarreta I. Chapter 4 - Core Sample Preparation. In: McPhee C, Reed J, Zubizarreta IBT-D in PS, editors. Core Anal., vol. 64, Elsevier; 2015, p. 135–79. https://doi.org/10.1016/B978-0-444-63533-4.00004-4.
[55] Sorensen JA, Braunberger JR, Liu G, Smith SA, Hawthorne SA, Steadman EN, et al. Characterization and Evaluation of the Bakken Petroleum System for CO2 Enhanced Oil Recovery. SPE/AAPG/SEG Unconv Resour Technol Conf 2015. https://doi.org/10.15530/URTEC-2015-2169871.
[56] Adekunle O, Hoffman BT. Minimum Miscibility Pressure Studies in the Bakken. SPE Improv Oil Recover Symp 2014:SPE-169077-MS. https://doi.org/10.2118/169077-MS.
[57] Holm LW, Josendal VA. Mechanisms of Oil Displacement By Carbon Dioxide. JPT, J Pet Technol 1974;26:1427–38. https://doi.org/10.2118/4736-PA.
[58] Eide Ø, Fernø MA, Alcorn Z, Graue A. Visualization of Carbon Dioxide Enhanced Oil Recovery by Diffusion in Fractured Chalk. SPE J 2016;21:112–20. https://doi.org/10.2118/170920-PA.
[59] Sun R, Yu W, Xu F, Pu H, Miao J. Compositional simulation of CO2 Huff-n-Puff process in Middle Bakken tight oil reservoirs with hydraulic fractures. Fuel 2019;236:1446–57.

https://doi.org/10.1016/j.fuel.2018.09.113.
[60] Eide O, Ersland G, Brattekas B, Haugen A, Graue A, Ferno M. CO2 EOR by Diffusive Mixing in Fractured Reservoirs. Petrophysics 2015;56:23–31.
[61] Wang L, Yu W. Gas Huff and Puff Process in Eagle Ford Shale: Recovery Mechanism Study and Optimization. SPE Oklahoma City Oil Gas Symp 2019. https://doi.org/10.2118/195185-MS.
[62] Song Y-Q, Kausik R. NMR application in unconventional shale reservoirs – A new porous media research frontier. Prog Nucl Magn Reson Spectrosc 2019;112–113:17–33. https://doi.org/https://doi.org/10.1016/j.pnmrs.2019.03.002.
[63] Moh DY, Zhang H, Wang S, Yin X, Qiao R. Soaking in CO2 huff-n-puff: A single-nanopore scale study. Fuel 2022;308:122026. https://doi.org/10.1016/j.fuel.2021.122026.
[64] Peng X, Wang Y, Diao Y, Zhang L, Yazid IM, Ren S. Experimental investigation on the operation parameters of carbon dioxide huff-n-puff process in ultra low permeability oil reservoirs. J Pet Sci Eng 2019;174:903–12. https://doi.org/10.1016/j.petrol.2018.11.073.
[65] Mohammad RS, Zhang S, Zhao X, Lu S. An Experimental Study of Cyclic CO2-Injection Process in Unconventional Tight Oil Reservoirs. Oil Gas Res 2018;04:1–9. https://doi.org/10.4172/2472-0518.1000150.
[66] Liu K, Ostadhassan M, Zhou J, Gentzis T, Rezaee R. Nanoscale pore structure characterization of the Bakken shale in the USA. Fuel 2017;209:567–78. https://doi.org/10.1016/j.fuel.2017.08.034.
[67] Onwumelu C, Nordeng S, Adeyilola A, Nwachukwu F, Azenkeng A, Smith S. Microscale Pore Characterization of Bakken Formation. 53rd US Rock Mech Symp 2019:10.
[68] Chen C, Gu M. Investigation of cyclic CO2 huff-and-puff recovery in shale oil reservoirs using reservoir simulation and sensitivity analysis. Fuel 2017;188:102–11. https://doi.org/10.1016/j.fuel.2016.10.006.
[69] Tang M, Zhao H, Ma H, Lu S, Chen Y. Study on CO2 huff-n-puff of horizontal wells in continental tight oil reservoirs. Fuel 2017;188:140–54. https://doi.org/10.1016/j.fuel.2016.10.027.
[70] Pu W, Wei B, Jin F, Li Y, Jia H, Liu P, et al. Experimental investigation of CO2 huff-n-puff process for enhancing oil recovery in tight reservoirs. Chem Eng Res Des 2016;111:269–76. https://doi.org/10.1016/j.cherd.2016.05.012.
[71] Yu W, Lashgari HR, Wu K, Sepehrnoori K. CO2 injection for enhanced oil recovery in Bakken tight oil reservoirs. Fuel 2015;159:354–63. https://doi.org/https://doi.org/10.1016/j.fuel.2015.06.092.
[72] Fakher S, Imqam A. Asphaltene precipitation and deposition during CO2 injection in nano shale pore structure and its impact on oil recovery. Fuel 2019;237:1029–39. https://doi.org/10.1016/j.fuel.2018.10.039.
[73] Mullins O, Sheu E, Hammami A, Marshall A. Asphaltenes, Heavy Oils, and Petroleomics. 2007. https://doi.org/10.1007/0-387-68903-6.
[74] Fatah A, Mahmud H Ben, Bennour Z, Hossain M, Gholami R. Effect of supercritical CO2 treatment on physical properties and functional groups of shales. Fuel 2021;303:121310. https://doi.org/https://doi.org/10.1016/j.fuel.2021.121310.
[75] Sanguinito S, Goodman A, Tkach M, Kutchko B, Culp J, Natesakhawat S, et al. Quantifying dry supercritical CO2-induced changes of the Utica Shale. Fuel 2018;226:54–64. https://doi.org/https://doi.org/10.1016/j.fuel.2018.03.156.

[76] Shiraki R, Dunn TL. Experimental study on water–rock interactions during CO2 flooding in the Tensleep Formation, Wyoming, USA. Appl Geochemistry 2000;15:265–79. https://doi.org/10.1016/S0883-2927(99)00048-7.
[77] Khather M, Saeedi A, Rezaee R, Noble RRP, Gray D. Experimental investigation of changes in petrophysical properties during CO2 injection into dolomite-rich rocks. Int J Greenh Gas Control 2017;59:74–90. https://doi.org/10.1016/j.ijggc.2017.02.007.
[78] Hemme C, van Berk W. Change in cap rock porosity triggered by pressure and temperature dependent CO2–water–rock interactions in CO2 storage systems. Petroleum 2017;3:96–108. https://doi.org/10.1016/j.petlm.2016.11.010.
[79] Saeedi A, Delle Piane C, Esteban L, Xie Q. Flood characteristic and fluid rock interactions of a supercritical CO2, brine, rock system: South West Hub, Western Australia. Int J Greenh Gas Control 2016;54:309–21. https://doi.org/10.1016/j.ijggc.2016.09.017.
[80] Zhao J, Wang P, Zhang Y, Ye L, Shi Y. Influence of CO2 injection on the pore size distribution and petrophysical properties of tight sandstone cores using nuclear magnetic resonance. Energy Sci Eng 2020;8. https://doi.org/10.1002/ese3.663.
[81] Bacci G, Korre A, Durucan S. An experimental and numerical investigation into the impact of dissolution/precipitation mechanisms on CO2 injectivity in the wellbore and far field regions. Int J Greenh Gas Control 2011;5:579–88. https://doi.org/10.1016/j.ijggc.2010.05.007.
[82] Soroush S, Pourafshary P, Vafaie-Sefti M. A Comparison of Asphaltene Deposition in Miscible and Immiscible Carbon Dioxide Flooding in Porous Media. SPE EOR Conf Oil Gas West Asia 2014:10. https://doi.org/10.2118/169657-MS.
[83] Srivastava RK, Huang SS. Asphaltene Deposition During CO2 Flooding: A Laboratory Assessment. SPE Prod Oper Symp 1997:19. https://doi.org/10.2118/37468-MS.
[84] Jin C, Liu L, Li Y, Zeng R. Capacity assessment of CO2 storage in deep saline aquifers by mineral trapping and the implications for Songliao Basin, Northeast China. Energy Sci Eng 2017;5:81–9. https://doi.org/10.1002/ese3.151.
[85] Gharbi O, Bijeljic B, Boek E, Blunt MJ. Changes in Pore Structure and Connectivity Induced by CO2 Injection in Carbonates: A Combined Pore-Scale Approach. Energy Procedia 2013;37:5367–78. https://doi.org/10.1016/j.egypro.2013.06.455.
[86] Rosenbauer RJ, Koksalan T, Palandri JL. Experimental investigation of CO2–brine–rock interactions at elevated temperature and pressure: Implications for CO2 sequestration in deep-saline aquifers. Fuel Process Technol 2005;86:1581–97. https://doi.org/10.1016/j.fuproc.2005.01.011.
[87] Zhu W, Ma Q, Song Z, Lin J, Li M, Li B. The effect of injection pressure on the microscopic migration characteristics by CO 2 flooding in heavy oil reservoirs. Energy Sources, Part A Recover Util Environ Eff 2019:1–9. https://doi.org/10.1080/15567036.2019.1644399.
[88] Ross GD, Todd AC, Tweedie JA. The effect of simulated CO2 flooding on the permeability of reservoir rocks. Enhanc Oil Recover Elsevier, Amsterdam 1981:351–66.
[89] Haghighi OM, Zargar G, Khaksar Manshad A, Ali M, Takassi MA, Ali JA, et al. Effect of Environment-Friendly Non-Ionic Surfactant on Interfacial Tension Reduction and Wettability Alteration; Implications for Enhanced Oil Recovery. Energies 2020;13. https://doi.org/10.3390/en13153988.
[90] Nazarahari MJ, Manshad AK, Ali M, Ali JA, Shafiei A, Sajadi SM, et al. Impact of a novel biosynthesized nanocomposite (SiO2@Montmorilant@Xanthan) on wettability shift and

interfacial tension: Applications for enhanced oil recovery. Fuel 2021;298:120773. https://doi.org/https://doi.org/10.1016/j.fuel.2021.120773.
[91] Anderson WG. Wettability Literature Survey- Part 1: Rock/Oil/Brine Interactions and the Effects of Core Handling on Wettability. J Pet Technol 1986;38:1125–44. https://doi.org/10.2118/13932-PA.
[92] McPhee C, Reed J, Zubizarreta I. Chapter 7 - Wettability and Wettability Tests. In: McPhee C, Reed J, Zubizarreta IBT-D in PS, editors. Core Anal., vol. 64, Elsevier; 2015, p. 313–45. https://doi.org/10.1016/B978-0-444-63533-4.00007-X.
[93] Anderson W. Wettability Literature Survey- Part 2: Wettability Measurement. J Pet Technol 1986;38:1246–62. https://doi.org/10.2118/13933-PA.
[94] Chilingar G V, Yen TF. Some notes on wettability and relative permeabilities of carbonate reservoir rocks, II. Energy Sources 1983;7:67–75.
[95] Mousavi Moghadam A, Baghban Salehi M. Enhancing hydrocarbon productivity via wettability alteration: a review on the application of nanoparticles. Rev Chem Eng 2019;35:531–63. https://doi.org/doi:10.1515/revce-2017-0105.
[96] McPhee C, Reed J, Zubizarreta I. Chapter 11 - Nuclear Magnetic Resonance (NMR). In: McPhee C, Reed J, Zubizarreta IBT-D in PS, editors. Core Anal., vol. 64, Elsevier; 2015, p. 655–69. https://doi.org/10.1016/B978-0-444-63533-4.00011-1.
[97] Coates GR, Peveraro RCA, Hardwick A, Roberts D. The Magnetic Resonance Imaging Log Characterized by Comparison With Petrophysical Properties and Laboratory Core Data. SPE Annu Tech Conf Exhib 1991. https://doi.org/10.2118/22723-MS.
[98] Gao H, Liu Y, Zhang Z, Niu B, Li H. Impact of Secondary and Tertiary Floods on Microscopic Residual Oil Distribution in Medium-to-High Permeability Cores with NMR Technique. Energy & Fuels 2015;29:4721–9. https://doi.org/10.1021/acs.energyfuels.5b00394.
[99] Fang T, Zhang L, Liu N, Zhang L, Wang W, Yu L, et al. Quantitative characterization of pore structure of the Carboniferous–Permian tight sandstone gas reservoirs in eastern Linqing depression by using NMR technique. Pet Res 2018;3:110–23. https://doi.org/10.1016/j.ptlrs.2018.06.003.
[100] Zdravkov B, Čermák J, Šefara M, Janků J. Pore classification in the characterization of porous materials: A perspective. Open Chem 2007;5:385–95. https://doi.org/doi:10.2478/s11532-007-0017-9.
[101] Badrouchi N, Badrouchi F, Tomomewo OS, Pu H. Experimental Investigation of CO2-EOR Viability in Tight Formations: Mountrail County Case Study. 54th US Rock Mech Symp 2020.
[102] Badrouchi N, Pu H, Smith S, Badrouchi F. Evaluation of CO2 enhanced oil recovery in unconventional reservoirs: Experimental parametric study in the Bakken. Fuel 2022;312:122941. https://doi.org/https://doi.org/10.1016/j.fuel.2021.122941.
[103] Chen Y, Sari A, Xie Q, Brady P V, Hossain MM, Saeedi A. Electrostatic Origins of CO2-Increased Hydrophilicity in Carbonate Reservoirs. Sci Rep 2018;8:17691. https://doi.org/10.1038/s41598-018-35878-3.
[104] Teklu TW, Alameri W, Graves RM, Kazemi H, AlSumaiti AM. Low-salinity water-alternating-CO2 EOR. J Pet Sci Eng 2016;142:101–18. https://doi.org/10.1016/j.petrol.2016.01.031.
[105] Hawthorne SB, Miller DJ. Comparison of CO2 and Produced Gas Hydrocarbons to

Dissolve and Mobilize Bakken Crude Oil at 10.3, 20.7, and 34.5 MPa and 110 °C. Energy & Fuels 2020;34:10882–93. https://doi.org/10.1021/acs.energyfuels.0c02112.
[106] Hawthorne SB, Miller DJ. A comparison of crude oil hydrocarbon mobilization by vaporization gas drive into methane, ethane, and carbon dioxide at 15.6 MPa and 42 °C. Fuel 2019;249:392–9. https://doi.org/https://doi.org/10.1016/j.fuel.2019.03.118.
[107] North Dakota Drilling and Production Statistics 2012. https://www.dmr.nd.gov/oilgas/stats/statisticsvw.asp (accessed January 28, 2022).
[108] Mahzari P, Mitchell TM, Jones AP, Oelkers EH, Striolo A, Iacoviello F, et al. Novel laboratory investigation of huff-n-puff gas injection for shale oils under realistic reservoir conditions. Fuel 2021;284:118950. https://doi.org/https://doi.org/10.1016/j.fuel.2020.118950.
[109] Eide, Fernø MA, Karpyn Z, Haugen Å, Graue A. CO2 injections for enhanced oil recovery visualized with an industrial CT-scanner. 17th Eur Symp Improv Oil Recover IOR 2013 - Saint Petersburg, Russ Fed 2013. https://doi.org/10.3997/2214-4609.20142641.
[110] Hawthorne SB, Miller DJ, Grabanski CB, Jin L. Experimental Determinations of Minimum Miscibility Pressures Using Hydrocarbon Gases and CO2 for Crude Oils from the Bakken and Cut Bank Oil Reservoirs. Energy & Fuels 2020;34:6148–57. https://doi.org/10.1021/acs.energyfuels.0c00570.
[111] Hawthorne SB, Grabanski CB, Jin L, Bosshart NW, Miller DJ. Comparison of CO2 and Produced Gas Hydrocarbons to Recover Crude Oil from Williston Basin Shale and Mudrock Cores at 10.3, 17.2, and 34.5 MPa and 110 °C. Energy & Fuels 2021;35:6658–72. https://doi.org/10.1021/acs.energyfuels.1c00412.
[112] Hawthorne SB, Miller DJ, Jin L, Azzolina NA, Hamling JA, Gorecki CD. Lab and Reservoir Study of Produced Hydrocarbon Molecular Weight Selectivity during CO2 Enhanced Oil Recovery. Energy & Fuels 2018;32:9070–80. https://doi.org/10.1021/acs.energyfuels.8b01645.